

AN ATLAS OF SECCHI DISC TRANSPARENCY
MEASUREMENTS AND FOREL-ULE COLOR CODES
FOR THE OCEANS OF THE WORLD

By

Margaret Anne Frederick

DUDLEY KNOX LIBRARY
NAVAL POSTGRADUATE SCHOOL
MONTEREY, CA 93943

DUDLEY KNOX LIBRARY
NAVAL POSTGRADUATE SCHOOL
MONTEREY, CALIFORNIA 93943

United States
Naval Postgraduate School



THESIS

AN ATLAS OF SECCHI DISC TRANSPARENCY
MEASUREMENTS AND FOREL-ULE COLOR CODES FOR THE
OCEANS OF THE WORLD

by

Margaret Anne Frederick

September 1970

*This document has been approved for public re-
lease and sale; its distribution is unlimited.*

T137263

An Atlas of Secchi Disc Transparency Measurements and Forel-Ule
Color Codes for the Oceans of the World

by

Margaret Anne Frederick
Lieutenant, United States Navy
B. S., in Chemistry, Marquette University, 1965

Submitted in partial fulfillment of the
requirements for the degree of

MASTER OF SCIENCE IN OCEANOGRAPHY

from the

NAVAL POSTGRADUATE SCHOOL
September 1970

ABSTRACT

An investigation was made of the global distribution of Secchi disc water transparency measurements and Forel-Ule water color codes which were on file at the National Oceanographic Data Center prior to June 1969. Charts were constructed for 17 major areas of the world's oceans to show the horizontal distributions of transparency and/or color. Data generally were presented as mean distributions. Charts were prepared showing the overall mean transparency and Forel-Ule color distribution for all of the data considered, except for the Sea of Japan, for which monthly mean charts were constructed. Plots of transparency measurements against the corresponding color codes were also drawn for five selected areas.

Transparency showed marked variations in each area considered. Generally it is greater in the central basins and decreases in coastal regions. Reduced transparency readings and discolored waters were noted for areas affected by river runoff, for areas of high organic productivity, and where standing plankton crops were found. Seasonal variations in transparency and color were not noted except for the Sea of Japan and the Indian Ocean (winter and summer). No simple relation between transparency and color was apparent.

TABLE OF CONTENTS

I.	INTRODUCTION	11
A.	GENERAL	11
B.	PURPOSE	13
C.	BACKGROUND ON THE SECCHI DISC	15
D.	BACKGROUND ON THE COLOR OF THE SEA	20
E.	FOREL-ULE COLOR SCALE	21
F.	PREVIOUS INVESTIGATIONS	22
G.	TREATMENT OF DATA	24
II.	DISCUSSION OF CONTOURS	26
A.	BERING SEA	26
B.	SEA OF OKHOTSK	28
C.	SEA OF JAPAN	29
D.	YELLOW SEA AND EAST CHINA SEA	32
E.	GULF OF TONKIN	34
F.	SOUTH CHINA SEA AND GULF OF THAILAND	35
G.	GULF OF ALASKA	38
H.	NORTH PACIFIC OCEAN	39
I.	EASTERN SOUTH PACIFIC OCEAN	40
J.	NORTH ATLANTIC OCEAN	41
K.	CARIBBEAN SEA	43
L.	EAST SIBERIAN SEA, CHUKCHI SEA, AND BEAUFORT SEA	45
M.	BARENTS SEA AND KARA SEA	47
N.	BLACK SEA	49
O.	MEDITERRANEAN SEA	50
P.	INDIAN OCEAN	52

Q.	SOUTHERN OCEAN	55
III.	RELATIONSHIP BETWEEN SECCHI DISC DEPTH AND FOREL-ULE COLOR CODE	58
IV.	CONCLUSIONS	60
V.	SUGGESTIONS FOR FURTHER RESEARCH	62
	DATA DISTRIBUTION CHARTS	64-67
	TRANSPARENCY AND COLOR CODE CONTOURS	68-153
	SECCHI DISC DEPTHS PLOTTED AGAINST FOREL-ULE COLOR CODES	154-158
APPENDIX A.	CHART OF MEAN TRANSPARENCY OF THE ATLANTIC OCEAN BY R. R. DICKSON	159
APPENDIX B.	RELATIVE TRANSPARENCY AND COLOR CHARTS OF BERING SEA BY ARSEN'YEV AND VOYTOV	162
APPENDIX C.	SEASONAL CHARTS OF TRANSPARENCY OF UPPER AND LOWER CALIFORNIA COASTAL WATERS BY ROBERT OWEN	163
APPENDIX D.	CHART OF TRANSPARENCY OF THE WESTERN SOUTH ATLANTIC OCEAN	168
	FORTRAN PROGRAM TO AVERAGE DATA OBSERVATIONS AND COMPUTE MEAN DEVIATIONS	172
	BIBLIOGRAPHY	176
	INITIAL DISTRIBUTION LIST	180
	FORM DD 1473	187

LIST OF TABLES

TABLE

- I. Vertical Extinction Coefficients and Their
Reciprocals Computed from Secchi Disc Depths 169
- II. Forel-Ule Color Scale, Proportions of
Component Chemical Solutions and Color Shades 170
- III. Monthly Minimum and Maximum Transparency
and Color Code Values for the Sea of Japan 171

LIST OF FIGURES

FIGURE

1A	Secchi Disc Transparency Observations Between 100 E and 90 W Longitude	64
1B	Secchi Disc Transparency Observations Between 100 W and 100 E Longitude	65
2A	Forel-Ule Color Code Observations Between 100 E and 90 W Longitude	66
2B	Forel-Ule Color Code Observations Between 100 W and 100 E Longitude	67
3-4	Transparency and Color Code Contours for the Bering Sea	68-69
5-6	Transparency and Color Code Contours for the Sea of Okhotsk	70-71
7-19	Transparency Contours for the Sea of Japan	72-84
20-32	Color Code Contours for the Sea of Japan	85-97
33-45	Mean Transparency Deviations for the Sea of Japan	98-110
46-58	Mean Color Code Deviations for the Sea of Japan	111-123
59-60	Transparency and Color Code Contours for the Yellow and East China Seas	124-125
61-62	Transparency and Color Code Contours for the Gulf of Tonkin	126-127
63-64	Transparency and Color Code Contours for the South China Sea and the Gulf of Thailand	128-129
65	Transparency Contours for the Gulf of Alaska	130
66A	Transparency Contours for the North Pacific Ocean Between 110 E and 170 W Longitude	131
66B	Transparency Contours for the North Pacific Ocean Between 170 E and 100 W Longitude	132
67A	Color Code Contours for the North Pacific Ocean Between 100 E and 170 W Longitude	133
67B	Color Code Contours for the North Pacific Ocean Between 170 E and 100 W Longitude	134

68	Transparency Contours for the Eastern South Pacific Ocean	135
69	Color Code Contours for the North Atlantic Ocean . . .	136
70-71	Transparency and Color Code Contours for the Caribbean Sea	137-138
72	Transparency Contours for the East Siberian, Chukchi and Beaufort Seas	139
73-74	Transparency Contours for the Barents and the Kara Seas	140-141
75	Transparency Contours for the Black Sea	142
76-77	Transparency Contours for the Western and Eastern Basins of the Mediterranean Sea	143-144
78-79	Color Code Contours for the Western and Eastern Basins of the Mediterranean Sea	145-146
80-81	Transparency and Color Code Contours for the Summer Monsoon Season for the Indian Ocean	147-148
82-83	Transparency and Color Code Contours for the Winter Monsoon Season for the Indian Ocean	149-150
84-85	Transparency and Color Code Contours for the Southern Ocean	151-152
86	Transparency Contours for the Ross Sea	153
87-91	Scatter Diagrams of Secchi Depths vs. Forel-Ule Color Codes	154-158

ACKNOWLEDGEMENTS

I would like to express my appreciation to my thesis advisor, Assistant Professor Robert S. Andrews, Department of Oceanography, and to Department Oceanographer Stevens P. Tucker, under whose direct supervision the data analyses were initiated when he was an assistant professor (1968-70). Mr. Tucker's enthusiasm for this project and his assistance, particularly in providing reference material, greatly aided in the completion of the project. I am also indebted to Mr. Henry Odum of the National Oceanographic Data Center for providing the data tape. The assistance of the Postgraduate School library staff and Mr. Alan Baldridge of Hopkins Marine Station in locating and making available reference material is greatly appreciated. I would also like to thank Miss Sharon D. Raney of the computer facility for her assistance in adapting the data tape for use on the Postgraduate School computer. Lastly, I would like to thank Mr. Robert Owen for his composite transparency charts and Dr. Robert R. Dickson for his kind permission to include his transparency chart for the North Atlantic Ocean in this work.

I. INTRODUCTION

A. GENERAL

Although sea water has an optical character as well as biological and chemical characters the properties which constitute its optical character have not been examined as extensively as other oceanographic parameters. Nevertheless a knowledge of optical conditions in the sea has a number of applications, suggesting that detailed investigations are desirable. For example, photosynthetic activity in the ocean is a function of light intensity, and studies of the effect of light intensity on photosynthetic rates of plankton are necessary in investigations of primary productivity. Also, the ecological niches occupied by biological organisms involve many factors, including light levels, the wavelength, and the polarization of the ambient light field.

It has been noted by Uda (44) that transparency measurements are often useful in corroborating the productivity indicated by the relative values of the dissolved oxygen content found in the upper layers of the ocean. The transparency of sea water is also related to the abundance of plankton present in the surface layers of the sea and can provide at least a qualitative measure of the geographical distribution of planktonic life. The color of sea water can sometimes be used as a measure of the abundance of planktonic organisms.

Jerlov (22) and others have suggested that optical data may be used in various ways to obtain useful information about oceanographic conditions since the optical properties of the water are dependent on the physical, chemical, and dynamical conditions of the sea, and the distribution of optical parameters may be useful in the characterization of water masses.

Although optical measurements are by no means numerous on a world wide basis, a compilation of available data is a useful starting point in the examination of the optical "structure" of the world's oceans.

On a global basis, the optical properties of sea water that have been examined and measured most extensively are transparency and color, as determined by use of the Secchi disc and the Forel-Ule color scale, or some modification of these. It is recognized that both determinations are at their best only semi-quantitative. Nevertheless, despite their shortcomings as precise quantitative descriptions of optical conditions, such measurements represent the only available indication of the optical character of the sea in many areas.

The Naval Oceanographic Office (NOO), formerly the United States Navy Hydrographic Office (H.O.), has published many oceanographic atlases presenting oceanographic environmental information. These atlases have summarized available knowledge of many ocean properties in several principal ocean areas of the world. Among the most familiar properties that have been charted and analyzed are sea surface temperature, salinity, density, sound velocity, ice distribution, tides and currents, marine geology, sea and swell, and wind. Some H. O. atlases have considered also the distributions of marine biological species, both plant and animal, as well as biological phenomena such as bioluminescence and the deep scattering layer. These atlas charts have been prepared on an annual and seasonal basis, and, where a sufficiently high number of observations were available, monthly analyses were prepared. Other atlases, prepared by individuals and institutions other than NOO, have shown the distribution of some of the above properties (1, 27).

Only one of these recent NOO atlases has included any of the optical properties of the ocean (46). Properties which indicate the optical character of a water mass include transparency, the beam attenuation coefficient, Forel color, and the vertical extinction coefficient (diffuse attenuation coefficient)¹. Some transparency and color contours were included in three other atlases published by H.O. in 1951 for Western Pacific coastal regions, including the waters off Indochina, Korea, and Japan (47-49). These contours were prepared from only a few measurements and have not been updated. It is believed that there exists no current atlas of Forel color data or transparency measurements as determined by Secchi disc.

B. PURPOSE

The purpose of this investigation is to examine the global distribution of Secchi disc (transparency) measurements and color measurements which have been collected and reported to the United States National Oceanographic Data Center (NODC, which has also been designated World Data Center A). The transparency values reported to NODC presumably were obtained with a white

¹In this paper the terms transparency, visibility, Forel color, beam attenuation coefficient, vertical extinction coefficient, and diffuse attenuation coefficient have the following definitions:

a. Transparency, sometimes called visibility, as measured by a Secchi disc is the average of the depths at which the disc disappears and reappears.

b. Forel color is water color described by comparison with the Forel color scale or some modified scale such as the Forel-Ule Scale.

c. Beam attenuation coefficient is the measure of the attenuation of a collimated light beam through a fixed path length.

d. Vertical extinction coefficient, also called diffuse attenuation coefficient, is a measure of the exponential attenuation of downwelling radiation in the sea.

Secchi disc and the water colors were measured according to the code based on the Forel-Ule scale. These measurements have been reported along with the surface environmental information on the physical and chemical data forms for oceanographic stations. The data tape provided by NODC contained records having transparency measurements on Forel-Ule color codes or both. On these records there were 67,257 transparency measurements and 23,482 color codes, representing NODC's holdings to June 1969.

Figures 1A, 1B, 2A, and 2B give the distribution by Marsden square of the Secchi disc measurements and color codes. The number in the upper half of each square indicates the number of the Marsden square; the number in the lower half indicates the number of observations in that Marsden square. The observations were reported by many countries as well as by different vessels and institutions of specific countries. It is seen from the distribution charts that observations are most numerous in the oceanic and coastal regions off Japan and China. These observations represent nearly 59 percent of the available transparency measurements and 69.5 percent of the available color determinations recorded in NODC's files.

In general, the best area coverage was in the Northwest Pacific Ocean between the 180th meridian and the Asian coast. Significantly fewer measurements were on record for the Northeast Pacific Ocean between the 180th meridian and the western coast of the North American continent. Data for the South Pacific Ocean were almost non-existent, except for three Marsden squares immediately adjacent to the coasts of Ecuador and Peru in South America. NODC coverage in the Atlantic Ocean was sparse but has been used by Dickson (10), along with additional unpublished data and data on file outside NODC, to construct a chart showing the major transparency features for that area. His chart is presented in Appendix A. Data coverage in the

Indian Ocean was also limited; however, a chart showing the transparency and color trend for both monsoon seasons was constructed. Data for the Southern Ocean were most numerous in the vicinity of the Ross Sea and the Weddell Sea. The number of data points was still insufficient to give more than a general trend. This was also true for the Arctic Ocean. Data for the European Mediterranean, the American Mediterranean, and the Black Sea were again not numerous enough to indicate more than general trends.

C. BACKGROUND ON THE SECCHI DISC

The Secchi disc has been widely used to measure water transparency. Named for Professor Secchi, who first described its properties and use, the Secchi disc has never really been standardized with respect to its physical properties. However, considerable research has been devoted to the investigation of its utility as a practical instrument for the measurement of submarine daylight. Collier (8), in his translation of some remarks on sea water transparency made by Secchi and Commander Cialdi on the cruise during which the first Secchi disc experiments were performed, lists the experimental considerations of Secchi. These included the influences of the size and color of the disc, shade from direct sunlight, height of observer above the water, altitude of the sun and clearness of the sky. The experiments in the Mediterranean were designed to determine the visibility of discs of different sizes and materials as influenced by the factors above. It was found that the depth of visibility increased with whiteness of the disc and with the altitude of the sun.

Tyler (42) described the theory and use of the Secchi disc and demonstrated that the sum of the beam and diffuse attenuation coefficients could be calculated using a Secchi disc reading. He stated that only an average value of the coefficients could be found, and these only in the upper 70 m

of the ocean. He listed some operational criteria which should be followed while taking measurements if the readings are to yield useful information.

Holmes (19), in a paper reporting field observations designed to help answer some of the questions and problems proposed by Tyler, used a Secchi disc in turbid coastal waters and determined a statistically significant relationship between the Secchi depth and beam transmittance for the green region of the spectrum. He also examined the effect of different diameter discs in the turbid waters and found no significant variation in the depths at which the various discs disappeared from view. The use of a viewer placed below the surface of the water did not increase the depth of disappearance. He determined values of the beam and diffuse attenuation coefficients from Secchi depths and from the Duntley-Preisendorfer equation of contrast reduction and found these values to have moderately large standard errors. He commented that these errors might be acceptable in some studies.

Further, biologists have established some useful relations between Secchi disc depths and the vertical extinction or diffuse attenuation coefficient for downwelling irradiance. This coefficient is the sum of the coefficients of the absorption and scattering properties of a water mass. The determination of the extinction coefficient by Secchi disc measurement is useful in spite of the imprecise nature of the instrument. Poole and Atkins (31) have shown from data gathered in the English Channel that extinction coefficients for visible rays can be approximated by the equation:

$$K = \frac{1.7}{Z_s} \quad (\text{m}^{-1}) \quad ,$$

where K is the vertical extinction coefficient, and Z_s is the depth in

meters at which the Secchi disc disappears from view.¹ This relation has been found useful in the investigation of the ecology of fishes as reported by Murphy (29) and in the investigation of the primary organic productivity of the oceans by Ryther and Yentsch (36) among others. Holmes (19) suggested that the constant 1.7 in the Poole and Atkins equation be replaced by a value 1.44 for determining the extinction coefficient in turbid water.

Graham (17), in his investigation in the Central and Eastern North Pacific Ocean, found excellent agreement between disc observations and extinction coefficients. His estimate of the extinction coefficient involved the Forel-Ule color scale index and the reciprocal of the Secchi disc depth and was corroborated by use of a submarine photometer. The photometer measured illumination intensities which were then used in the equation

$$I(z) = I(o) e^{-Kz},$$

where $I(o)$ and $I(z)$ are the illumination intensities at the surface and at depth z respectively; K is the vertical extinction coefficient; and z is the depth in meters. Although Graham found good comparison between the extinction coefficients determined by the different methods, he observed that extrapolation of the relationship between Secchi disc observations and extinction coefficients should be done cautiously when comparing one oceanic environment to another.

Emery (14) investigated the transparency of the waters off Southern California and showed that the Secchi disc readings taken there were closely

¹Extinction coefficients and reciprocal vertical extinction coefficients computed from this relation are given in Table I. For example, the vertical extinction coefficient, K , for a Secchi depth, Z_s , of 45 m is 0.038 m^{-1} . The reciprocal of K for this Secchi depth is 26.5 m.

related to the concentration of organic debris. He found low transparency readings in nearshore regions and attributed them to the presence of suspended inorganic sediment derived as erosion products. Upwelling in the general area was evidenced by reduced transparency measurements.

Postma (32) investigated the relation between suspended material and the visibility of a Secchi disc in the coastal and inland waters of the Netherlands. He derived an empirical relation between the amounts and particle size of the suspended materials and Secchi depth, i.e.

$$\frac{1}{D} = 0.34 \frac{V}{d} ,$$

where D is the Secchi depth in cm; V is the volume of the particles in cm^3 ; and d is the diameter of the particles in cm. His investigations considered the effects on visibility of organic and inorganic particulate matter as well as the suspension of matter under tidal and non-tidal influences.

Light attenuation in the North Sea and Dutch Wadden Sea in relation to Secchi disc visibility and suspended matter was examined by Otto (30), who gave relationships between Secchi disc depths and both the vertical extinction coefficient and the beam attenuation coefficient. His paper summarized the relations between the vertical extinction coefficient and Secchi depth determined by different authors. He also presented the relationships between Secchi depth and mean beam attenuation coefficient which were determined at different times in different areas.

An investigation of Secchi disc and color observations in the North Atlantic Ocean in 1964-1965 was made by Visser (52). He calculated the influence of wave-action on the visibility of the Secchi disc and found an empirical relation between the disc observation and the Forel color scale. This relation was given as:

$$\frac{100}{S} = 0.26 Y + 1.9 ,$$

where S is the mean Secchi depth in meters, obtained from two discs of diameter one meter and one foot, and Y is the percent yellow, according to the Forel scale, of the sea water. Visser observed that this empirical relation was valid only for the ocean area of study. He determined that the clearest (most transparent) water has the lowest yellow content.

Secchi depths and Forel-Ule color codes were plotted in Figures 87 through 91 in an attempt to examine a possible relation between disc observations and color codes. The observations plotted exhibited so much variability that no simple empirical relation could be determined. Certainly the data do not suggest the single-valued relation which is implied by Visser's equation. For comparison, Visser's empirical relation is plotted on Figure 90, which presents Secchi depths and Forel-Ule color codes for the Washington-Oregon coastal region.

Manheim and Meade (28) examined suspended matter in the surface waters off the Atlantic continental margin from New England to Florida. They evaluated a relation between concentrations of suspended matter and the transparency and color of the water using the relation

$$D = \frac{kd\rho}{w} ,$$

where D is Secchi disc visibility; d is the mean diameter of particles; ρ is the density of particles; w is weight of suspended matter; and k is a constant. They plotted suspended matter in milligrams per liter against Secchi depth in meters and found a strong, linear relation. A poorer relation between Forel color and weight concentration of particulates was found. The authors observed, however, that transitions in color of the water, when viewed from the air, are particularly striking and offer a potential method for estimating the suspended matter in surface waters over large areas if proper calibration techniques are used.

D. BACKGROUND ON THE COLOR OF THE SEA

A description of the color of sea water has both subjective and objective aspects. The chromatic sensitivity and visual acuity of the observer's eye contribute to the subjective aspect.

From the objective viewpoint, Kalle (24) concluded that the blue color of sea water is due to scattering of light by water molecules or by minute suspended particles, small with respect to the wavelength of light. The blue color of the water is thus due to Rayleigh scattering, somewhat comparable to the blue color of the sky. He also suggested that the presence of yellow substance (Gelbstoff) in combination with the blue water is responsible for the scale of green colors observed along coastal regions as well as in the open sea.

Shoulejkin (39) investigated the transmission of light through sea water and concluded that the color of the sea depends on four factors: selective absorption of light by water, scattering of light by tiny suspended particles such as small bubbles of air or other gas, selective reflections of light by other particles such as fine dust or plankton, and an admixture of the reflected light of the sky. He also derived from the Fresnel reflection formulae a relation between the intensity of the color and the inclination of waves moving over the surface of the sea. He asserted that the sea seems much more intensely colored from the lee side than from the weather side, where the surfaces of the waves are more steeply inclined.

Tyler (41) examined the color of the ocean within the framework of modern colorimetry. He specified the geometry of lighting and the measurement of spectral flux; and he considered the spectral distribution of light in Pacific coastal water and in a fresh water pond into which plankton and yellow substance had been added. Measurements of the radiance

were compared and plotted on a chromaticity diagram. Tyler concluded that major factors in the ocean color are the pigments and chlorophyll contained in the plankton.

A summary of recent color research was given by Jerlov (21) who summarized various investigations of the factors which influence the color of the sea. He presented an extensive review of various theories which have been advanced to explain both the color and the changes in color of the ocean.

E. FOREL-ULE COLOR SCALE

The color of the sea varies from a deep blue through an intense green to brown or brown-red. Prior to the development of the Forel scale, water color was described qualitatively in terms of color shades ranging from dark blue to bluish green. Forel (16) recognized that such a description lacks precision and is dependent on the physiological characteristics of the observer. He devised a numerical scale made up of mixtures of two chemical solutions, ammoniacal blue copper sulfate and yellow potassium chromate, in varying proportions. The resulting series of solutions had colors ranging from blue to yellow-green. The vials of solution were numbered, using the Roman numerals I to XI, and formed a scale of hues at regular intervals between the blue and yellow-green endpoints.

The scale was not adequate, however, for coastal waters, which may appear brown or brown-red as well. Ule (45) developed a scheme to provide a capability for measuring the brownish color of Baltic Sea waters. His scale similarly resulted from the combination of two chemical solutions, brown and green in color, in different amounts. The brown solution consisted of one-half gram of cobalt sulfate in strongly ammoniacal water

combined with distilled water to make a 100 ml solution. The green solution was made by combining 65 parts of a potassium chromate solution with 35 parts of the copper sulfate solution. The resulting series was numbered from XI to XXI, where the number XI of the Ule scale was identical to the number XI of the Forel scale. Table II gives the conversion from scale number to proportion of each component solution.

The combination of the two scales, the Forel-Ule scale, thus has a continuous sequence of number codes with which to report the estimation of sea water color in the deep oceanic regions and the transitions in color that occur as the depth diminishes into shallow coastal regions. Other modifications to the Forel scale have been developed, and a review and description of these modifications is given by Sower (40).

The color of sea water normally is determined with the Secchi disc at a depth of one meter providing the background against which a comparison is made between the sea water and the Forel-Ule scale. An attempt is made to match the color of the sea water against the Secchi disc with the color of one of the solution vials. The vials must be shielded from open sunlight while the determination is being made. When this is accomplished, the vial index is used to identify the proportions of the two colored water solutions. The number of the vial that blends most closely with the water color against the background of the disc is then recorded on the station data form.

F. PREVIOUS INVESTIGATIONS

On a global basis, optical measurements of the sea water were made as part of the investigation program of the Swedish Deep-Sea Expedition, which covered major ocean areas with the exception of the polar regions. However, measurements were made using a beam transmittance meter, not a

Secchi disc, and were used by Jerlov (20) optically to classify water masses. The number of stations in each major ocean was quite small, and the transmittance survey is little more than a description of localized optical conditions.

Dietrich (11) commented in a qualitative manner on the regional color and transparency characteristics of sea water. His comments on color and transparency were based largely on a consideration of the biological influences of each region.

Secchi disc and color observations have been made in specific areas by many independent investigators. For example, the transparency of the waters of the Western Pacific Ocean and Indian Ocean were presented in a series of reports by Russell and Clarke (7, 34, and 35).

Schott (38) constructed color contours of the Atlantic Ocean and the Mediterranean Sea. He expressed the color of the sea water in terms of the percent yellow solution according to the Forel scale.

Secchi disc transparency measurements were made along the coastal regions and in oceanic regions of the Northwestern Atlantic Ocean by Bumpus and Clarke (6) among others. Their report also included measurements taken by other investigators in regions north of 50 N Latitude. The authors used the Poole and Atkins (31) empirical relation to determine the extinction coefficient and expressed the transparency contours in the area of study in terms of calculated extinction coefficients.

In 1951 the U. S. Navy Hydrographic Office published three atlases on the marine geography, including water color and transparency contours, of the waters of the Sea of Japan, Korea, and Indochina (47-49).

The Hydrographic Office also prepared a transparency chart of the North Atlantic Ocean based on all available transparency observations available up to December 1950 (51). The observations used were either

Secchi disc depths or hydrophotometer readings which were converted to equivalent Secchi depths. Isolines on the chart indicate the maximum transparency of the water reported throughout the year, and no seasonal changes are shown.

Visser (personal communication) indicated that he has compiled many visibility measurements in the North Sea area but has not yet submitted his charts for publication. The number of his observations is considered to be far in excess of those available from NODC, and, for this reason, no contours of the NODC data were constructed for that region.

Arsen'yev and Voytov (2) charted the transparency of the Bering Sea water (Appendix B) and made a comparison between relative transparency and plankton biomass. They determined an inverse relationship between the two characteristics. In their paper it is reported that charts of water transparency and color for almost all of the marginal seas of the Soviet Union have been prepared.

As previously mentioned, Dickson (10) has constructed a chart of the mean ocean transparency of the Atlantic Ocean between 15 S and 60 N Latitudes. His chart (Appendix A) probably represents the most comprehensive and recent report of Secchi disc observations for this area.

G. TREATMENT OF DATA

In order to handle the quantity of data involved, individual observations were averaged in one-degree sub-squares within a Marsden square. A computer program was written to read the data, construct the one-degree sub-square grid, and sum and average all of the observations in a Marsden square. The averaged datum was rounded off to the next highest integer value if the fractional part was 0.5 or greater. These averaged values were plotted in the center of the one-degree square. This was done in all areas where the data density was very high. In other areas, where the

density of points was small, the data were plotted at the reported location of their measurement. Because the number of observations was insufficient to permit consideration on a monthly or seasonal basis, except for the Sea of Japan and the Indian Ocean, the data are presented as a mean distribution.

On each transparency and color chart the data points are indicated by a dot. On some charts, notably the Northeast Pacific Ocean transparency chart and the winter monsoon transparency chart for the Indian Ocean, data patches were contoured in a manner which might appear to be inconsistent with normal contouring procedures. Departures from normal procedures were made for areas where isolated observations were reported at some distance from other data. It was desired to show the relative value of the data groupings relative to the other data on the chart. Some contour lines were also terminated where no data were present to permit further extension.

In the discussions of the various charts the descriptions of surface circulation were based on The Encyclopedia of Oceanography (15), except where specifically noted, and in the discussion of each color chart, the qualitative terms used to describe water colors (e.g. "deep-blue", "bluish-green") correspond to the color shades given in Table II. These color descriptions corresponding to the Forel numbers are those given in the Oceanographic Atlas of the Polar Seas (46).

II. DISCUSSION OF CONTOURS

A. BERING SEA

Data observations for the Bering Sea were contributed by Canada, Japan, Russia, and the United States. They were obtained mainly during the months of May to September in the period 1932 to 1966; of these, most were reported during the period 1957 to 1966.

Figures 3 and 4 give the transparency and color for the Bering Sea. Minimum and maximum values of transparency were 6 and 29 m, respectively. Color codes ranged from 2 to 9.

Surface flow into the Bering Sea occurs mainly at Longitude 170 E, where the Alaskan Stream merges with the Western Subarctic Gyre with the formation of a cyclonic eddy in the western section of the Sea. Another cyclonic eddy exists over the deep basin, and cyclonic and anticyclonic eddies are also formed in the eastern part of the sea. Currents over the continental shelf off the Alaskan coast are mainly tidal currents, except adjacent to the coastline, where river runoff flows northward and is discharged into the Chukchi Sea through the Bering Strait.

Major river runoff comes from the Kuskokwim, Yukon, and Anadyr Rivers. The maximum plankton biomass occurs during the spring in surface waters over the continental shelf, followed by a reduction during the summer. A second bloom occurs during the fall. Zenkevitch (54) reports that the fall peak is less than that for the spring by an order of magnitude.

As previously mentioned, Arsen'yev and Voytov (2) constructed charts to show the relative transparency and color of the Bering Sea during the summer and winter seasons. Their charts are given for reference in Appendix B. Their summer chart shows a region of low transparency, less than 10 m,

extending from Longitude 180 to the eastern continental border. Two small areas with transparency greater than 10 m are shown within this region for the southeastern section of the Sea. A larger area, also within that region, whose transparency ranges from 10 to 15 m or greater, is shown for the region just south of the Bering Strait. Transparency values for the western side of the Sea are greater than 10 m, except for two coastal areas, where they are less than 10 m. A southern area has transparency values reported to be 15 m or greater.

Figure 3 shows a region of low transparency, 10 m or less, along the coast of Alaska and along the coast of the western section of the Sea. The main body of the Sea has transparency in the range of 10 to 15 m. Several regions having higher transparency readings, 15 m and greater, exist in the deeper portions of the Sea as well as over the shallow shelf region.

The color chart for summer, constructed by Arsen'yev and Voytov (Appendix B), shows considerably more variability than that shown in Figure 4. Their distribution indicates that the water over the shelf region is more discolored than that in the open basin. Figure 4, however shows no marked difference between the water color of the two regions. The Russian authors identified their color scale only as a "standard color scale," but did not specify it as the Forel-Ule scale.

Arsen'yev and Voytov stated that the data used for their charts were collected mainly during the years 1950 to 1956. Their Secchi data were less numerous, however, than those used to construct Figure 3, collected mainly during 1957 to 1966. Their color contours are based upon about twice the number of observations used in Figure 4.

B. SEA OF OKHOTSK

Data for the Sea of Okhotsk are largely of Japanese origin and were obtained during the period 1935 to 1966. A few observations were reported by Russia and the United States. The majority of the observations were made between the years 1935 and 1942.

Figures 5 and 6 give the transparency and water color for this region. Transparency values ranged between 3 and 25 m, and color codes ranged from 3 to 8.

The bulk of the water in the Sea of Okhotsk is of Pacific origin and enters the Sea through the various straits between the Kurile Islands. Surface waters circulate in a cyclonic gyre which occupies the entire Sea. In addition, three stationary, anticyclonic eddies exist in the area of the southern basin.

Numerous rivers empty into the Sea. Most of the river discharge comes from the Amur River west of the northern part of Sakhalin Island, but many rivers from the surrounding Russian territory empty into the north-western and northern sections of the Sea. Rivers from the Kamchatka Peninsula, the Kurile Islands, Sakhalin, and Hokkaido also discharge into the Sea.

The Sea of Okhotsk, according to Zenkevitch (54), has a high index of productivity with the highest concentration of plankton in the surface layers. A spring maximum concentration occurs throughout the whole body of water, but the autumn maximum occurs only in the southern portion of the Sea. The plankton population is distributed in varying proportions throughout the Sea. Transparency values would be expected to vary with the fluctuation, both seasonal and regional, in plankton population.

The transparency contours, Figure 5, show a region of low transparency, 10 m or less, around the periphery of the sea. Several patches

of low transparency also exist in the vicinity of the Kurile Islands. This area is very rich in species of sea weeds and has an abundance of micro-organisms in the water (54). These factors may contribute to the low transparency values found there.

Although the northern region is characterized by a luxuriant plankton growth, transparency values were not exceptionally low. A patch of relatively high transparency is shown to the north of Sakhalin Island. This may be attributed to the fact that these transparency measurements were taken mainly during the summer months when the plankton population is at a minimum. The low values near the coast are in regions where rivers discharge sediment-laden waters into the Sea.

The color contours, Figure 6, show that the main body of the Sea is blue-green, with the regions near the coast becoming increasingly green. Three isolated small patches of greenish-blue water are shown at various positions in the Sea. An isolated patch of green water is also shown in the southern part of the Sea.

C. SEA OF JAPAN

Japanese hydrographical data for the inland Sea of Japan far exceed additional data reported by South Korea and Russia. The observations were made during all months of the year between 1927 and 1964. A large portion of the data was obtained during the period 1933 to 1941, and the remainder was gathered from 1953 to 1964. Since the number of observations for this region is quite large, the data were charted on a monthly basis, and additional charts showing mean transparency and water color as an average for all months were constructed using all the available NODC data for the Sea. Figures 7 through 19 show the overall mean transparency and the distribution for each month, while Figures 20 through 32 show mean water color

during the same periods. The minimum and maximum transparency for the overall average were 8 and 23 m respectively, and the range of color codes was from 2 to 6. Table III gives the range of transparency and water color codes for each monthly chart. In addition the average deviations from the means of the observations for the one-degree squares within the area of the Sea were computed and are presented as the charts shown in Figures 33 through 58.

These deviations were computed to illustrate what relative uncertainties in data values might be expected elsewhere, when the number of observations becomes sufficiently large. The deviations also can be used to indicate the relative confidence with which the contours can be viewed.

The deep waters of the Sea of Japan are isolated from the trenches of the Pacific Ocean and adjacent seas. The main inflow into the Sea comes from the Korea Strait, through which the Tsushima Current enters and flows northward along the western coast of Honshu and Hokkaido. South of 47° N the Liman Current flows southward along the Siberian coast and completes the general counterclockwise circulation in the Sea of Japan.

According to Zenkevitch (54), the phytoplankton of the Sea have two periods of maximum bloom, one in the spring (March-April) and the other in autumn (September-October). He further states that the plankton population changes considerably, both qualitatively and quantitatively, with depth and with season. Cold-water plankton prevail in upper layers during the winter, but the plankton population changes sharply in summer. This population also has definite biogeographical zones within the Sea, the maximum development being for the open sea.

The variations in transparency to be expected throughout the Sea due to fluctuations in plankton population as well as other causes are shown in

Figures 7 through 19. April and May are shown to be the months of least transparency. The greatest transparency occurs during autumn and winter, although the fall season is not unproductive with respect to plankton growth. Greatest transparency generally occurs in the central sector of the Sea, and patches of water of relatively high transparency, greater than 25 m, appear in various places throughout the area.

Figures 2 through 32 give the color contours for the Sea of Japan and generally show the Sea to be greenish-blue in color in the central section and bluish-green in nearshore regions. Little correlation is seen between the color and transparency contours. The most variable color contours are those for April and May, which is a period of marked diatom growth. The bloom of September and October, however, is not sharply indicated in either the transparency or color charts.

Both transparency and water color contours were presented in the Marine Geography (49) prepared by the U. S. Hydrographic Office in 1951 using data that was available up to 1941. The contours for the Marine Geography were constructed to show seasonal variations in both properties. Figures 7 through 32 probably contain many of the same data as well as additional, more recent, observations. The general trend of both sets of contours is the same, although the marked seasonal changes suggested in the Geography's contours are not seen in Figures 7 through 32.

Uda (43) also discussed the transparency and color of the Sea of Japan and described the color as bluer (less than 3 on the Forel scale) in the warmer (eastern) sector than in the colder (western) sector and particularly green in the northern half of the Sea. He reported the transparency to be more than 25 m in the Tsushima Current area and less than 10 m in the colder sector. His descriptions of color and transparency are so general that comparisons with Figures 7 through 32 are not really meaningful.

D. YELLOW SEA AND EAST CHINA SEA

Data for the Yellow Sea and the East China Sea were contributed by Japan, Russia, and South Korea, but the majority of the measurements were taken by Japan. Observations of transparency and color were collected during all months of the year, and the collection period spanned the years 1932 to 1967, but most of the observations were obtained during the years 1932 to 1940.

Figures 59 and 60 indicate the transparency and color contours for these waters. In the Yellow Sea, including the Gulf of Pohai, the transparency measurements had minimum and maximum values of 2 and 15 m, respectively. The color codes ranged from 2 to 7. Transparency in the East China Sea ranged from 2 to 26 m, and the color codes ranged from 1 to 7.

The seasonal Asiatic monsoons influence the surface circulation of this region. The principal current, the Kuroshio, enters the East China Sea from the Pacific Ocean between Taiwan and Yazama Island and extends northward along the continental slope. A portion of the Kuroshio extends westward into the Yellow Sea. In the western part of the East China Sea water from the Yellow Sea passes along the mainland of China, gradually deviating eastward. The cyclonic gyre that exists in the East China Sea is formed from these main currents.

River runoff into the Yellow Sea and the East China Sea comes from several major rivers, including the Yellow River and the Yangtze River, as well as several smaller rivers along the Chinese coast. The mean transparency of the Yellow Sea is lowest, 2 m, at the mouth of the Yellow River. Transparency increases toward the middle basin of the Yellow Sea, while the color codes indicate light-green water for the regions of runoff and bluish-green water toward the same basin. Similarly, runoff from the Yangtze River

into the East China Sea was evidenced by low transparency values and color codes indicative of highly discolored waters.

Kharchenko (25) reported that there are several areas of upwelling in the East China Sea. The largest and most stationary one is an area of upwelling over the continental slope on the western side of the Sea. Three other areas of upwelling are associated with the divergence of the Kuroshio and in the eddies of cyclonic circulation. Deep water with a relatively high content of biogenous material is brought to the surface at this time. This feature of the East China Sea hydrography occurs mainly during the spring and summer seasons.

The combination of river runoff and upwelling on the western side of the East China Sea would seem to account for the reduced values of transparency observed in that region. The waters of the eastern region of the Sea, away from the influence of these two factors, are significantly more transparent, and the color codes of the eastern region indicate relatively blue water.

Contours of water color and transparency for a portion of this region were given in H. O. Publication No. 752 (47). This atlas, Marine Geography of Korean Waters, was published in 1951 and is based on unpublished Japanese data on file at the Hydrographic Office which was collected during the years 1931 to 1944. The atlas contours were constructed to show seasonal variations of the two properties. It is believed that much of the data used in their preparation was used in the construction of Figures 59 and 60. The general trend of these contours is not dissimilar to the trend shown in the atlas figures.

The atlas contours show seasonal structure, whereas Figures 59 and 60 are mean transparency and color charts for all seasons over many years. Figure 59 and the atlas contours show that the main body of the Yellow

Sea has transparency values of 10 to 15 m with considerably smaller values near the coast. The region of least transparent water appears in the coastal area, particularly near the mouths of the two major rivers which discharge into the Yellow Sea. The color contours of the atlas and Figure 60 show the water of the Yellow Sea to be quite variable, with the regions of greatest variability occurring at the mouths of the Yellow and Yangtze Rivers.

E. GULF OF TONKIN

Data for the Gulf of Tonkin are mostly Russian observations, with a much lesser number contributed by the United States and Japan. Most of the data were taken between April and October during the years 1935 to 1965, with the majority of observations reported during the period 1961 to 1965.

Figures 61 and 62 give the contours of transparency measurements and color codes. The transparency data range from 4 to 30 m, and the range of color codes was from 2 to 9.

The Gulf of Tonkin is fairly shallow, with the deepest part in the center having a depth of only 70 m. The Gulf is subject to the Asiatic monsoon wind system which influences the seasonal surface circulation pattern.

The most transparent area of the Gulf is to the west of Hainan Island. Farther south, in the channel between Hainan and the coast of North Vietnam, the waters become more transparent. The waters of least transparency appear along the mainland shelf. There is a zone of mud, characteristic of the Red River Delta, which contributes to the low transparency found in that region.

Contours of transparency and water color for the Gulf of Tonkin are given in H. O. Publication No. 745 (48). This atlas, Marine Geography of Indochinese Water, shows only a single chart for the season July through December. The general trend of these color and transparency contours is

not greatly dissimilar to the trend shown in Figures 61 and 62. The atlas indicated that the Gulf water was less transparent than suggested by Figure 61. The maximum Secchi depth range reported in the atlas is 15 to 20 m, whereas the data utilized in Figure 61 show a maximum range of 20 to 25 m in the same central area of the Gulf.

The atlas color contours indicate that the Gulf water varies from blue-green at the southern extreme to a mixture of yellow-green and green-yellow near the Red River delta and yellowish-green in the western and northwestern coastal regions. Along the northeastern and eastern coasts the water color varies from green to yellowish-green. Figure 62 shows that the central basin is greenish-blue in color and changes to a bluish-green toward the coast. The coastal water was coded to indicate that the water is primarily green with a region of greenish-yellow water near the Red River delta.

F. SOUTH CHINA SEA AND GULF OF THAILAND

Japan's data observations in this region are extremely numerous. Other countries which have made data contributions include Russia, the Republic of China, the Republic of Germany, Thailand, the United Kingdom, and the United States. Data have been collected during all months of the year for the period 1907 to 1967, but the majority of observations were made during the years 1930 to 1941.

Figures 63 and 64 give the transparency and color contours for this region. In the South China Sea the transparency measurements have minimum and maximum values of 4 and 42 m respectively. The range of color codes is 1 to 7. In the Gulf of Thailand, the transparency observations have a minimum value of 4 m and a maximum value of 28 m, and the color codes range from 3 to 7.

This region is subject to the seasonal monsoons that characterize the climate of Southeast Asia. As a result, the surface circulation is subject to seasonal variations which alter the direction of water flow through the area. The main interchange of surface water is through the Bashi Channel, north of Luzon, and Karimata Strait, southwest of Borneo. Weak counter-currents exist at the eastern side of the Sea during both monsoon seasons. Upwelling occurs off the coast of central South Vietnam in midsummer.

The major river runoff into the waters of the South China Sea comes from the Mekong River. The runoff is at a maximum during the summer monsoon season. Low transparency values were observed in this region, while higher values were found in the main basin of the Sea. Reduced values were found along the mainland shelf and in the waters over the Sunda Shelf. The color code distribution indicates that bluer water is found in the main basin of the Sea, and greenish-blue water is found near the coast and over the shallow Sunda Shelf region.

The Gulf of Thailand is a shallow arm of the South China Sea with a mean depth of 45.5 m. Four large rivers empty into the head of the Gulf, as do many smaller ones along both shores. Heavy precipitation and runoff dilute the surface waters considerably. Seasonal variation in the surface circulation occurs with the seasonal monsoons. The combined effects of variable winds, tidal currents, freshwater runoff, and excessive precipitation produce localized areas of divergence and convergence. Organic productivity in the Gulf is greater than that of the eastern side of the South China Sea due to vertical mixing and upwelling (15). The transparency of the Gulf water is less than that of the main basin of the South China Sea. The color of the Gulf water is nearly that of the coastal water of the Sea

except for an area at the head of the Gulf, where the color code index indicates considerable discoloration which might be attributed to the river runoff.

Contours of water color and transparency for the South China Sea and the Gulf of Thailand were given in H. O. Publication No. 754 (48). This atlas, Marine Geography of Indochinese Waters, referenced unpublished Japanese data on file at the Hydrographic Office which was obtained during the period 1931 to 1944 as well as oceanographic data collected by the Netherlands Meteorological Institute. These contours indicate seasonal variations in the two properties. Figures 63 and 64 probably contain some of the same data as well as additional, more recent data. Very little correlation seems to exist between the atlas contours and Figures 63 and 64.

Both sets of contours show the least transparent water of this region to be near the mouth of the Mekong River. The atlas shows the extent of this region of low transparency to fluctuate with season. Figure 63 shows only the mean transparency over an extended period of time. The atlas indicates that the Gulf of Thailand is more transparent than suggested by the data used in Figure 63. The main body of the Gulf is shown in Figure 63 to be less than 20 m except for a small isolated region in the southern area. The atlas contours show a large expanse of water having transparency of 20 m or greater. Both the atlas contours and Figure 63 show that the transparency in the South China Sea varies between values which are less than 10 m at the coast and 30 m or greater in the open sea basin.

The color of the main body of the Gulf of Thailand is shown in the atlas and in Figure 64 to be bluish-green. The main body of the South

China Sea is shown to be blue in the open sea and greenish-blue near the coast. The Mekong River is shown to have highly variable water in the atlas. Figure 64 does not show this variability due to a lack of data for that area.

G. GULF OF ALASKA

Canada and the United States have reported the largest number of observations for the Gulf of Alaska, but additional data have been contributed by Japan and Russia. Observations were taken during all months of the year during the years 1949 to 1968, with the majority of the data obtained during the period 1956 to 1966.

Figure 65 gives the transparency contours for the area. Minimum and maximum values of transparency are 5 and 30 m respectively. No color observations were available for the Gulf.

Subarctic waters which flow into the Gulf of Alaska circulate around the irregular coastline in a well-defined cyclonic gyre. The coast of the Gulf is indented and fringed with islands. Major river runoff into the Gulf comes from the Copper, Susitna, and Matanuska Rivers. The lack of data in the region of their discharge prevented the effect of river runoff on transparency of the Gulf water to be shown.

Uda (44), in his discussion of the oceanography of the Subarctic Pacific Ocean, showed four charts of transparency constructed from Secchi disc measurements which included the Gulf of Alaska for the summers of 1955 through 1958. His contours show a marked random variation in transparency and exhibit the same general features as Figure 65, constructed from much more recent data and not plotted by season. A direct comparison between the charts is not feasible. In general there are patches in the open Gulf water where transparency is 20 m or greater. The coastal waters shown in

Figure 65 as well as in Uda's charts generally have transparencies of less than 10 m. Uda attributes the patchiness of the summer transparency profiles to variations in plankton population throughout the region.

H. NORTH PACIFIC OCEAN

Excluding the marginal seas of the North Pacific Ocean, charts showing mean transparency and water color were prepared for this area between the latitudes 10 S to 55 N. The data utilized in these charts were obtained during the period 1907 to 1967 by the following countries: Canada, China, Germany, Japan, Russia, and the United States. Most of these observations were made during the last 30 years and are Japanese hydrographical data.

Figures 66 and 67 give the mean transparency and water color charts for this region. Transparency ranges from 2 to 60 m and color codes range from 1 to 13. Transparency was plotted at 5-m contour intervals until it reached a value of 30 m. The region enclosed by the 30-m contour contained data which were quite variable and a 35-m contour level was not practical unless some of the data were ignored. To avoid this, the 35-m level was not drawn; and slashed and dotted areas were drawn to indicate ranges of data greater than 30 m. The dotted regions indicate a range of 40 to 50 m, and the slashed area denotes a range of 50 to 60 m. On the color chart, the isolated patches of single observations which differed from the surrounding area by one unit, either above or below the color code of the adjoining area, were not drawn.

Surface currents in the Pacific are driven by the trade winds and the westerlies, and the surface flow is predominantly westward at low latitudes and eastward at high latitudes. At the continental borders, the zonal flows are diverted to form both north and south flowing currents at the

eastern and western boundaries, establishing cyclonic and anticyclonic gyres within the oceanic region.

As shown in Figure 66, the transparency contours, particularly in the western area, exhibit the productivity characteristics of the Pacific water masses. The region of greatest transparency is located in the lower latitudes where, due to the strong stratification of the water, depletion of nutrients in the photic zone occurs. The tropical plankton population is reduced below that of the subpolar regions. In 1954, Bogorov (4) reported productivity in the boreal regions to be 20 times that of the tropical regions. This is also the region of bluest water, as seen in Figure 66. The Kuroshio is notably less fertile than the Oyashio, and this distinction is seen on both the transparency and water color charts. The Kuroshio Current region is shown to have a transparency range of about 20 to 30 m and is deep blue to greenish-blue in color; the Oyashio has a transparency range of about 12 to 18 m and is bluish-green in color. These transparency ranges agree quite closely with those reported by Aruga and Monsi (3), who investigated the productivity in the region of the two currents in 1960 and 1961.

On the northeastern side of the Ocean, the coastal regions near the Columbia River are extremely discolored and have water of low transparency. Offshore the transparency increases to values comparable to those recorded at the same latitude on the western side of the Ocean.

I. EASTERN SOUTH PACIFIC OCEAN

Although transparency measurements in the South Pacific Ocean as a whole are rather limited, over 1000 observations were reported from the oceanic region adjoining the coasts of Ecuador and Peru. A chart was constructed for this region between 10 N and 40 S Latitude and between 70 W and 115 W Longitude.

Most of the observations for this area were reported by Peru, but additional data were contributed by Ecuador, Japan, Russia, and the United States. These observations were obtained during all months of the year between 1953 and 1967, but most of the data were recorded during the period 1963 to 1967. No Forcl-Ule color codes were reported for the area.

Figure 68 gives the transparency contours for this area. Transparency ranged from 3 to 38 m. The transparency distribution seems to be in good agreement with the surface circulation present in the area. Between latitudes of approximately 45 S, off the coast of Chile, and 4 S, off northern Peru, the prevailing surface currents flow northward parallel to the coast nearshore, with increasing westward motion farther offshore. At about 4 S, the current merges with the South Equatorial Current, leaves the coast and flows west.

The equatorward-flowing Peru (Humboldt) Current directly contributes to the abundance of marine life characteristic of the area. Upwelling off the coastal boundaries seems to occur during the whole year, but it is greater during the southern winter, since the wind intensity is greatest then. Upwelling brings to the surface a rich supply of nutrient elements and thus continually supports a high standing crop of phytoplankton and high rates of organic production. Coastal concentrations of organic material contribute to the cause for the low values of transparency shown in those areas on Figure 68. Transparency values increased offshore away from the coastal influences.

J. NORTH ATLANTIC OCEAN

Because of the recent work of Dickson (10), who compiled a chart showing the mean transparency of the Atlantic Ocean between latitudes of

15 S to 60 N (Appendix A), only the water color data reported for the Atlantic Ocean were used. These observations were contributed largely by Russia and the United States. A few color reports were submitted by Brazil, the Congo, Venezuela, Nigeria, and the Netherlands. These data were obtained between 1960 and 1968, with the majority of observations made during the period 1963 to 1968. Figure 69 gives the distribution of mean water color between latitudes 10 S and 50 N. Color codes ranged from 1 to 18.

As previously mentioned, Schott (38) constructed a color chart of the Atlantic Ocean based on the Forel scale. His chart shows a color distribution of deep blue in the Sargasso Sea to green or yellow-green water in equatorial regions, in nearshore areas, and in higher latitudes. Figure 69 utilizes much more recent data and shows a color distribution ranging from deep blue to yellowish-brown water. The main body of the Atlantic in the mid-latitude region is shown to be blue in color with several patches of deep blue water. The data in the Sargasso Sea does not seem to indicate the deep blue reported by Schott. However, the number of observations in that area is far too small to make an accurate determination.

Higher latitude regions are bluish-green to greenish-blue in color, and green water is shown south of Nova Scotia and in St. George's Channel near Ireland. Coastal waters off North America and Europe and Northwest Africa (above 5 N Latitude) are bluish-green and greenish-blue in color. The coastal waters off South America and Africa, south of 5 N Latitude, are markedly more discolored. The Niger and Congo Rivers empty into the Atlantic from Northwest Africa and make the African coastal water considerably more discolored than that off South America which is influenced by discharge from the Amazon and Orinoco Rivers. The oceanic region receiving the Niger and Congo River discharges is at the junction of the South

Equatorial Current and the Equatorial Counter Current. A small anticyclonic gyre is established in the Gulf of Guinea. Highly variable color conditions are shown in this region.

K. CARIBBEAN SEA

The United States and Venezuela contributed most of the data for this sea. Three measurements taken by two Russian vessels were also reported for the area north of Venezuela. The data were collected during all months of the year during the period 1953 to 1967, with most of the observations obtained during the years 1963 to 1967.

Figures 70 and 71 gives the contours of transparency and color for the region. Figure 70 shows average minimum and maximum Secchi depths of 10 and 35 m, respectively. The average minimum and maximum color codes are shown in Figure 71 to be 2 and 9, respectively.

The circulation in this area is from east to west in the upper 1500 m. The source of water entering the area is the wind-driven Guiana Current. Most of the water is forced through the central section of the Lesser Antillean Island chain, principally in the passages north and south of St. Lucia Island. Major river runoff enters the Caribbean Sea from the Magdalena River in the northern part of Colombia.

Secchi disc measurements were made in the Caribbean Sea by Curl (9), during his investigation of primary productivity in the northern coastal waters of South America during October and November 1958. His investigation covered the entire southern coastline from Trinidad to the Gulf of Darien. The Secchi disc data were used to establish the euphotic zone depth. Results of his investigation related transparency to primary production in the water in the vicinity of the Magdalena River. The lowest

transparency and production rates occurred at the mouth of the river. Greatest light penetration occurred in the eastern portion of the Gulf of Venezuela.

Figure 70 shows that the area of greatest transparency and bluest water in the Caribbean Sea is along the axis of the Caribbean Current. Lower values of transparency appear along the coastal regions. Upwelling exists along the eastern side of the Gulf of Venezuela, where low transparency would be expected. Another region of upwelling exists in the Gulf of Cariaco, which is also a region of relatively high biological productivity. Transparency values in the region of the Gulf of Cariaco were low in comparison with water transparency away from the Gulf. However, these values were obtained at different times of the year and may indicate the low transparency usually associated with coastal regions as well as the influences of upwelling. No transparency measurements were obtained in the region of the Gulf of Venezuela. Several isolated patches of highly transparent water, 30 m or greater, are shown in the northern part of the Sea.

The distribution of sea water color, Figure 71, shows that the coastal waters are bluish-green at the southwestern side of the Sea and greenish-blue at the southeastern side. A region of highly discolored water is shown northeast of the Gulf of Cariaco. Color codes of 7 to 9 were reported, indicating that the water is green to greenish-yellow. These measurements were taken in September, and the discoloration may be due to a high plankton concentration at that time. A region of green to light-green water is shown near the mouth of the Magdalena River, west of the Gulf of Venezuela. Curl (9) reported that the surface waters of this river flow eastward and the extent of this area of green water seems to be in agreement with the direction of that flow. A region of green water is

influenced by the inflow of surface water through the various channels between the island arc forming the eastern boundary to the Sea.

L. EAST SIBERIAN SEA, CHUKCHI SEA, AND BEAUFORT SEA

Data for this region were contributed largely by the United States, but a lesser number were also reported by Russia. The data were collected during the months of July, August, and September and were reported for the years 1933 to 1966. Most of the observations were obtained during the period 1957 to 1966.

Figure 72 gives the transparency contours for this region. A minimum value of 2 m was reported near the coast of Siberia, while a maximum value of 35 m was reported for the open ocean north of Alaska. No color observations were reported for this area, nor were transparency observations reported north of 75 N Latitude.

A small part of the eastern portion of the East Siberian Sea is shown on Figure 72. A region of low transparency, 10 m or less, exists along the coast of this shallow sea. Surface waters flow eastward along the coast into the Bering Strait. There are several rivers along the coast which discharge into the Sea, and the sediment-laden waters contribute to the low transparency values. The transparency of the deeper waters has a maximum value of 16 m.

The Chukchi Sea is the connection between the Arctic and Pacific Oceans. Surface waters from the Pacific are carried into the Sea, and the current flows northward along the Alaskan coast. Part of the current is deflected to the west, while the remainder continues to flow along the Alaskan coast. A cyclonic flow pattern is established across the Sea; this pattern is best developed during the summer months. The water coming into the Sea has been affected by the discharge from the Yukon River south of the Bering Strait.

This effect is seen in the low transparency, less than 10 m, of the shallow water of the Strait.

The circulation pattern of the Beaufort Sea is dominated by a well-defined anticyclonic gyre. Along the coast the currents depend on the local winds and are highly variable. Major river runoff into the Beaufort Sea is contributed by the Colville, MacKenzie, and Anderson Rivers as well as several smaller streams. A region of low transparency extends seaward along the Alaskan coast. Nearshore, the shelf has many gravel islands whose relief features are continually being modified by the action of strong offshore currents. The erosion products from this process and the sediment deposited by rivers provide a partial explanation for the reduced transparency found along the coast. The maximum value reported for the Beaufort Sea was 18 m in the water west of Banks Island.

Transparency and water color distributions are shown in the Oceanographic Atlas of the Polar Seas (46). These contours were constructed by the Hydrographic Office using all available data up to 1957. Figure 72 contains more recent data. The general trend of the atlas transparency contours and Figure 72 is the same, except for the eastern section of the Beaufort Sea near Banks Island. The atlas contours indicate that the average transparency of the open water in that locality is 10 m or less. Figure 72 shows the transparency to be between 10 and 20 m. Particularly good agreement is shown in the Bering Strait area and in the southern part of the Chukchi Sea. Transparency measurements in the East Siberian Sea indicate that the average transparency of the open water is between 10 and 20 m. The values in the coastal region agree with the atlas. The atlas contours did not extend into the open water area due to a lack of data at that time.

M. BARENTS SEA AND KARA SEA

Data for this area were contributed mainly by Russia, with a lesser number of observations reported by Germany, Norway, and the United States. The observations were obtained during the months May to September during the period 1926 to 1967. Approximately two-thirds of the data were recorded prior to 1958.

Figures 73 and 74 show transparency and water color for this region. In the Barents Sea transparency values ranged from a minimum of 7 m to a maximum of 39 m. Color codes ranged from 4 to 11. Transparency values for the Kara Sea had a minimum and maximum value of 3 and 24 m, respectively. The range of color codes was from 5 to 12.

A branch of the Gulf Stream flows into the Barents Sea and circulates in a cyclonic gyre around the main body of the Sea. Arctic water also enters the Sea from the north, and numerous eddies exist in the central basin. The Barents Sea is characterized by the presence of the polar front at the boundary between the cold Arctic and warm Atlantic waters. Major river runoff into the Sea comes from the Perchora and Mezen Rivers, which empty into the southeastern portion of the Sea.

At the polar front, vertical mixing occurs which brings to the surface a vast accumulation of nutrients which support a vast production of plankton. The Barents Sea is noted for its luxurious blooms of phytoplankton and a general abundance of organic life. The maximum development of both phytoplankton and zooplankton is during the summer months. Zenkevitch (54) reports a qualitative as well as quantitative variation in plankton composition throughout the Barents Sea on a seasonal and annual basis. Because of this, the transparency of the Sea varies seasonally.

The Oceanographic Atlas of the Polar Seas (46) presents contours of the average range of transparency and water color for the Barents and the Kara Seas. The data used for those contours were taken prior to 1957. The data used in Figures 73 and 74 were collected up to 1967. Approximately one-third of the transparency observations shown in the above figures are more recent than the latest data shown in the atlas. All of the color codes in Figure 74 were reported since 1960.

Figure 73 shows a region of relatively high transparency, 30 m or greater, due west of Novaya Zemlya. The central basin of the Sea surrounds this region with an area of water whose transparency is between 20 and 30 m. A considerable expanse is shown as well where the transparency is less than 20 m. This is in sharp contrast with the atlas which indicates that the entire central basin has a transparency range of 20 to 30 m.

The water color distribution (Figure 74) presents a marked difference from the atlas contours, which indicate that most of the entire basin of the Barents Sea has an average color range of from 2 to 3 on the Forel scale. The data used in Figure 74 indicates an average range of from 5 to 6. The latter range corresponds to colors from green to light-green in contrast to the blue to greenish-blue suggested by the atlas.

The Kara Sea is a shallow sea lying entirely over the continental shelf. A marked cyclonic gyre dominates the circulation pattern of the surface waters. A considerable amount of fresh water enters the Sea from the Ob and Yenisei Rivers in the southern portion of the Sea. Sand and silty-sand deposits are accumulated at the mouths of these rivers, and an abundance of fresh water flora are present there. The river discharge sets up a northward current, which diverges to the northeast, west, and southwest. Figures 73 and 74 show the effect of this river discharge. Very low transparency values were obtained in this region, and the Forel-Ule color codes indicate markedly discolored waters.

The deepest section of the Sea is located at the site of the Novaya Zemlya Trough. This region is relatively poor in marine life and has a low index of productivity. The highest transparency readings for the Sea were obtained in that area.

As in the case of the Barents Sea, seasonal and regional fluctuations occur in the plankton population of the Kara Sea. Variations in transparency values occur concomitant with these fluctuations.

Transparency and water color for the Kara Sea are shown in Figures 73 and 74 and have the same general trend as the figures shown in the atlas, although the atlas shows a much larger area of relatively highly transparent water in the central basin which extends farther north than indicated in the present work. Figure 73 shows the region of greatest transparency to be limited to the area over the deepest section of the Sea, while Figure 74 shows a pattern of more discolored water than that suggested by the atlas.

N. BLACK SEA

All of the data for the Black Sea is of Russian origin. Observations of transparency were made during all months of the year during the years 1923 to 1958. Most of the data were taken between 1923 and 1925. No reports of color measurements were given with the transparency data. Figure 75 shows the transparency distribution for the Black Sea. Minimum and maximum mean values were 4 and 25 m respectively.

A cyclonic surface circulation pattern exists along the shores of the Black Sea. Two cyclonic gyres exist in the eastern and western parts of the Sea. River runoff into the western portion of the Sea comes mainly from the Danube, Dniester, and Dniepper Rivers of eastern Europe. Transparency values in this area were low in comparison with the values in the central basin.

Redfield, et al. (33), reports that nutrients in the Black Sea have accumulated to an extreme degree and are brought to the surface by vertical mixing. The water column is very stable, preventing the discharge of these nutrient-rich waters out of the sea basin, and thus supports a high organic productivity. As a result the floral and faunal populations of the Black Sea are greater than those of the Mediterranean.

Zenkevitch (54) reports that portions of the Black Sea have both a temporary and permanent plankton population, and that marked changes, both seasonal and annual, are observed in the composition and quantity of plankton. Transparency measurements would then be expected to vary as the population fluctuates.

The maximum value of transparency coincides with the area of maximum depth of the Sea. The amount of plankton in the northwestern part of the Sea is reported by Zenkevitch to be always greater than that present in the open sea. This area also receives abundant river discharge. A combination of these two factors, abundant river discharge and high productivity, contributes to the low transparency for the shallow northwestern part of the Black Sea.

Zenkevitch reports, too, that the transparency of the open sea usually varies from 18 to 21 m and decreases near the coast. He stated that the maximum value observed in the Black Sea was 30 m. This corresponds to the maximum value reported in the data utilized in Figure 75.

O. MEDITERRANEAN SEA

Russian, Yugoslavia, and the United States have collected the data reported for this region. The most numerous contributions were made by Russia and Yugoslavia. These observations were obtained during all months of the year in a period spanning the years 1925 to 1960. Most of the data were taken during the period 1948 to 1958.

For charting purposes, the Mediterranean Sea was divided at 16 E Longitude. Figures 76 and 77 give the transparency contours for the western and eastern regions respectively, and Figures 78 and 79 give the color code contours. In the western basin transparency values had a minimum value of 17 and a maximum value of 47 m, and the range of color codes was from 2 to 4. In the eastern basin transparency measurements ranged from 9 to 51 m, while color codes ranged from 2 to 4.

Surface water from the North Atlantic enters the Mediterranean through the Strait of Gibraltar and follows the coast of North Africa. The waters spread out over the sea surface and generally flow in a cyclonic pattern. The major river runoff into the western basin of the Mediterranean comes mainly from the Rhone River at the northwest part of the basin. The Po River empties into the northern Adriatic Sea. The Nile River provides the main river discharge into the southeastern part of the eastern basin. Numerous small rivers along the African and European coasts discharge into the Mediterranean.

Nutrient concentrations are very small in this Sea, and the productivity is low. This lack of nutrients is in sharp contrast with the Black Sea, where nutrients tend to accumulate.

The transparency observations taken in the Mediterranean Sea show that the two basins tend to be fairly transparent at their centers, while lower values occur along the continental coasts. The Mediterranean Sea is considerably more transparent than the neighboring Black Sea. The greatest transparency, 51 m, reported for the Mediterranean Sea is nearly twice that of the maximum value, 30 m, observed in the Black Sea. No observations were taken in the immediate vicinity of the points of discharge of the major rivers, so the effect of river effluent on transparency is not seen.

Nearly all of the color codes reported for the eastern basin show the water to be nearly blue. The water of the Adriatic Sea is greenish-blue in comparison to the blue water of the eastern basin. The water of the western basin is blue in the central part of the basin, but that near the coast of Sicily is more greenish-blue, like Adriatic water.

P. INDIAN OCEAN

Data observations in the Indian Ocean were obtained largely by Japan. These were supplemented by data reported by India, Portugal, Russia, South Africa, and the United States. Measurements were taken during all months of the year between 1930 and 1966, but the majority were reported for the period 1963 to 1966.

To the north of 10 S Latitude the surface currents vary greatly in conjunction with the seasonal alteration in wind direction. The area then is characterized by a winter monsoon during which the winds blow offshore from the northeast and northwest and a summer monsoon during which the winds blow onshore from the opposite direction. Transparency and water color charts were constructed for both monsoon seasons, although the observations for the winter regime are far more numerous than those for the summer season. The winter monsoon encompasses the period November to April, and the summer monsoon prevails during May to September. These monsoon seasonal limits are those used by Dietrich (11).

Figures 82 and 83 present the transparency and color contours for the winter season*, and Figures 80 and 81 give the two distributions for the summer regime. During the winter monsoon transparency varies between a minimum of 6 m in the Persian Gulf and a maximum of 46 m at several locations in the open sea. Color codes ranged mainly from 1 to 4, although an isolated report of 13 was given off the tip of Somali. Transparency values

*After having completed our charts we received Voytov's paper (55) in which he presents his own chart for this season. The charts are in essential agreement.

during the summer season had a minimum of 4 m in the Bay of Bengal and a maximum of 45 m, which was reported for the Mozambique Channel and to the west of Sumatra. The range of color codes was from 1 to 10. As Figure 80 indicates, most of the transparency data taken during the summer monsoon were collected in three general areas: the northeast section of the Indian Ocean including the Bay of Bengal; the Red Sea and the Gulf of Aden; and the Mozambique Channel. Color determinations were made almost exclusively in the northeast section.

Upwelling between the island of Java and Australia occurs during the southwest monsoon, and the area is reported to be highly productive by Bogorov and Bass (5). However, the transparency data do not show the effect of plankton production to any great extent. Values along the Java and northwest Australian coasts indicate water of relatively high transparency, generally greater than 20 m. A small patch of reduced transparency is shown off northwest Australia, but the transparency is also shown to be increasing toward the coast.

Wyrтки (53) investigated summer season upwelling in this region and stated that the low transparency indicated a high concentration of suspended matter. He reported the transparency in terms of the vertical extinction coefficient and showed that the distribution of the extinction coefficient resembled closely that of the plankton biomass. Using the Poole and Atkins (31) empirical equation relating the vertical extinction coefficient to Secchi depth (Table I), Secchi depths were computed from Wyrтки's coefficients. A range of 8.5 to 11.3 m was computed from extinction coefficients which ranged from 0.15 to 0.20 m^{-1} or greater. These values are about one-half of the transparency values shown in Figure 80 which were obtained during the same months, although not necessarily during

the same years, as Wyrteki's data. Color determinations made in this region show the water to be deep blue to blue in most of the area. Northwest of Australia the water was greenish-blue to bluish-green. Neither water color nor transparency measurements in this area show the effect of high concentrations of plankton biomass.

There exists in the Red Sea a narrow trough in the central sector which is bordered by broad reef-studded shelves. This deep seaway has an inflow from the Gulf of Aden throughout much of the year. No rivers flow into the Red Sea and little water enters from the Suez Canal. Primary production in the Red Sea is generally low, although occasionally there are blooms of the algae from which the Red Sea supposedly derives its name, producing regions of discolored water of presumably low transparency. Figure 80 shows the transparency in the central basin of the Sea to be relatively high indicating the absence of river discharge and standing plankton crop. Reduced values, approximately 15 m, were reported over the shallow sill at the southern extreme of the Red Sea.

The Somali coast is also characterized by strong coastal upwelling during the summer monsoon season (38). Low transparency values and discolored water would be expected to be present in the area. Figures 80 and 81 indicate that neither transparency nor color show the effect of upwelling in the region. Both properties have values approximately equal to those reported in the upwelling region northwest of Australia.

The Mozambique Channel is described by Ryther, et al. (36), as being of intermediate productivity. A transparency range of 30 to 40 m is shown in Figure 80 for this region. These values are, somewhat unexpectedly, within the range reported for the highly productive regions in the northwestern part of the Sea.

A much more complete distribution of transparency and water color is presented for the winter monsoon season in Figures 82 and 83. Transparency shows marked variations throughout the Indian Ocean area. In areas where comparison was possible little difference is apparent between the two seasons in either transparency or water color.

During the winter monsoon season the main body of the Indian Ocean, as shown in Figure 82, generally has transparency between 20 and 30 m. Not unexpectedly, along some coastal regions, notably in the Arabian Sea, Gulf of Aden, and in the water off Somali, transparency is less than 20 m. Marked fluctuations in productivity were noted by Ryther, et al. (36), for the western section of the Indian Ocean, but the regions of very high productivity are not clearly indicated by the transparency data. Not much change in transparency is noted between the eastern and western sections of the Ocean. The winter color contours, Figure 83, show little change from that for the summer season. Water color is mainly blue with patches of deep blue and greenish-blue water occurring within the oceanic region.

Q. SOUTHERN OCEAN

Data observations for the Southern Ocean were contributed by six countries: Argentina, Germany, Japan, Russia, the United Kingdom, and the United States. Observations were obtained during 11 months of the year, but most were made during December through February. The collection period spanned the years 1912 to 1968, with the majority of data reported during the period 1958 to 1968.

Secchi disc measurements in the Southern Ocean were made largely in the Ross Sea and the Weddell Sea. There were also reported observations in the open seas of the Indian Ocean sector from 170 E to 10 E Longitude. Some

data were taken in the seas west of the Antarctic Peninsula between 60 W and 100 W Longitude. Nearly all of the data were reported in the seas south of 60 S Latitude. Figure 84 indicates the distribution of Secchi disc measurements. A transparency minimum of 3 m and a maximum of 41 m were reported.

The surface circulation pattern in the Southern Ocean is influenced by the East Wind Drift which prevails around the periphery of the Antarctic continent. It is separated from the West Wind Drift on the north by the Antarctic Divergence Zone which is an area of general upwelling. The configuration of the continent and the bottom topography influence the formation of eddies and countercurrents which deflect the surface flow across the divergence zone into the West Wind Drift. The water flow is from east to west across the Ross Sea and along the border of the continent from Victoria Land to Queen Maud Land. A well-defined clockwise gyre is present within the Weddell Sea. Another clockwise gyre is formed on the west side of the Antarctic Peninsula and the surface flow is deflected north. The West Wind Drift influences surface flow east and northeast around the continent.

The circulation has influenced the high fertility associated with the waters of the Southern Ocean. The euphotic layer is very stable, and high concentrations of phytoplankton are found in these waters. Phytoplankton concentrations were shown by Hart (18) to be at a maximum during the Antarctic summer. The geographic variation in transparency corresponds to the geographic variation in productivity.

The Weddell Sea exhibits regional variations in productivity according to El-Sayed and Mandelli (13), with the northern region more productive than either the eastern or southern areas. The eastern part is lower in

productivity than either the northern or southern parts. Transparency of the eastern water would thus be expected to be greater than that of the other regions, while the transparency of the northern region would be less. This regional trend in transparency is indicated by the data presented in Figure 84.

The coastal water west of the Antarctic Peninsula are reported by El-Sayed (12) to be highly productive, and a region of low transparency at the tip of the Peninsula was found corresponding to the areas of high productivity.

Regional variations in transparency in the Ross Sea and the Indian Ocean sector of Antarctica were not compared with regional variations in productivity because the productivity measurements in these areas seem to be limited to the investigation of plankton productivity under the sea ice. In general, regions of low transparency were found at the border of the continent, and higher transparency values were found farther away from the coast. Figure 86 shows the transparency distribution for the Ross Sea.

There were only 15 reports of Forel-Ule color codes throughout this area. Figure 85 indicates the position and value of these measurements. Three values at one location, south of the tip of Argentina, were averaged; hence 13 values appear on the chart. The color codes range in value from a minimum of 3 to a maximum of 13. The minimum and maximum values appeared in the Weddell Sea where most of the observations were made. The distribution of reported values in the Weddell Sea was random, and, due to the paucity of color data, no distinct color pattern is apparent.

III. RELATIONSHIP BETWEEN SECCHI DEPTHS AND FOREL-ULE COLOR CODES

In an attempt to examine a possible relationship between transparency and water color for the data presented, five graphs of Secchi disc depths vs. Forel-Ule color codes were plotted for five ocean regions. These regions were plotted showing the data from either a single Marsden square or as a combination of two or more Marsden squares. An area in each of the Atlantic, West Pacific, and Indian Oceans was chosen as being representative of open ocean areas. An area adjoining the Washington-Oregon coast was selected as representing a coastal region, and another coastal region, the Gulf of Tonkin, was selected to examine color and clarity in a shallow semi-enclosed area. The selection of the Marsden squares depended on the number of transparency and color observations available in each region to give a reasonable representation of their distribution. The results of plotting the two parameters are given as the scatter diagrams, Figures 87 through 91.

It was believed that water which is highly transparent would have a low Forel-Ule scale number, since the higher transparency generally indicates the absence of suspended materials. That is, water color is due to selective absorption by the water molecules themselves and the upward light emanation from multiple scattering by these molecules. According to Jerlov (21), this latter factor is responsible for the brilliant blue color of the ocean. He further states that in turbid waters the selective absorption by particles and yellow substance, sometimes called Gelbstoff, shifts to the longer portion of the spectrum, and a change in color is observed. Turbid waters generally have low transparency, and yellow substance decreases the blueness of the water, which would then be described by a larger scale code number relative to the scale code describing water without yellow substance. Thus an inverse relationship between transparency and water color was expected.

Joseph (25) made a comparison between transparency and a modified Forel color scale for two different bodies of water and showed the two properties to be inversely related. His graphs also suggest, for the data points considered, that the relation between transparency and water color is single-valued; that is, for each color scale value only one value of transparency exists. However, it should be noted that in the paper referred to only five pairs of values were plotted for one area and seven pairs for the other.

Jerlov (20) stated that the character of the upward-travelling light is intimately connected with the color of the sea, but he gave no specific quantitative reference to a transparency value and color scale number. Graham (17) referenced Jerlov's remarks in his paper and further stated that information provided by the Secchi disc and Forel-Ule color is not independent. He used both measurements in regression formulae to estimate extinction coefficients.

As shown in Figures 87 through 91, no such relationship appears to be verified by the data in any of the regions which were considered. Isolated instances of high transparency accompanied by a low color code, as well as water of low transparency with high color code, are certainly seen; however, the relationship between color codes and transparency generally is highly variable. It is seen in nearly all these figures, particularly at the low end of the color scale, that waters whose transparencies differ by as much as 20 m have been described by the same color code. At the higher end of the color scale a similar situation exists; however, the range between transparencies described by the same color code is somewhat smaller. This is seen most clearly in Figure 90. This lack of positive correlation between Secchi disc depth and Forel-Ule color code suggests the independent nature of these two parameters.

IV. CONCLUSIONS

Transparency and color of ocean regions are generally quite variable. Little correlation seems to exist between the transparency and water color contours.

Transparency generally is low in nearshore regions and increases seaward. Transparency in regions of river runoff sometimes reached the low value of 4 m. The highest transparency reading was 60 m in the tropical western North Pacific Ocean.

Water of low transparency generally is more discolored than water which is more transparent, although waters whose transparencies differed by as much as 20 m often were described by the same color code.

Regions characterized by regional trends in plankton production generally had regional trends in transparency corresponding to the areas of concentration of plankton. However, in the Indian Ocean regional trends in plankton production did not have corresponding trends in transparency measurements. Areas where productivity has been shown to be high had transparency values of the same magnitude of those found in relatively unproductive areas.

Upwelling, which occurs along the Peru and Ecuador coast during most of the year, was evidenced by low mean transparency readings along the whole coast. Seasonal upwelling in other regions was not specifically identified by low transparency readings. Except in the Indian Ocean where the conditions were noted as above, the charts for the other regions were not constructed on a seasonal basis, and fluctuations in transparency readings due to upwelling could not be determined.

Fluctuations in transparency or color due to variable factors associated with the Secchi disc or Forel-Ule color scale could not be determined in this study.

V. SUGGESTIONS FOR FURTHER RESEARCH

In those areas where data are lacking, investigations should be made to collect transparency and color information so that complete area coverage charts could be presented.

Data collection in areas already investigated should be continued so that seasonal and annual variations could be determined.

The temperature, salinity, oxygen, chlorophyll, and particulate data obtained with the transparency and color data used in this study should be analyzed to determine what correlation exists between transparency and color and each of those parameters.

Since correlations between transparency and color measurements and the geographical distributions and concentrations of plankton have been suggested, these investigations should be continued to determine if quantitative relationships can be derived.

Studies relating Secchi disc measurements to other ocean parameters such as the vertical extinction coefficient should be continued to check further the empirical relationships that have been formulated.

The Secchi disc and Forel-Ule color scale, as well as procedures for their use, should be standardized, so that fluctuations in the data due to variable factors associated with the disc, color scale, and field techniques could be eliminated.

Variable factors influencing data taken with the Secchi disc, such as the altitude of the sun, wire angle, and meteorological factors should be further investigated to determine quantitatively their effects on transparency.

Verification of the transparency and water color charts by means of more accurate techniques of data measurement is highly desirable. This might be achieved through the application of satellite photography, which was utilized by Lepley (26) to observe water clarity in coastal regions.

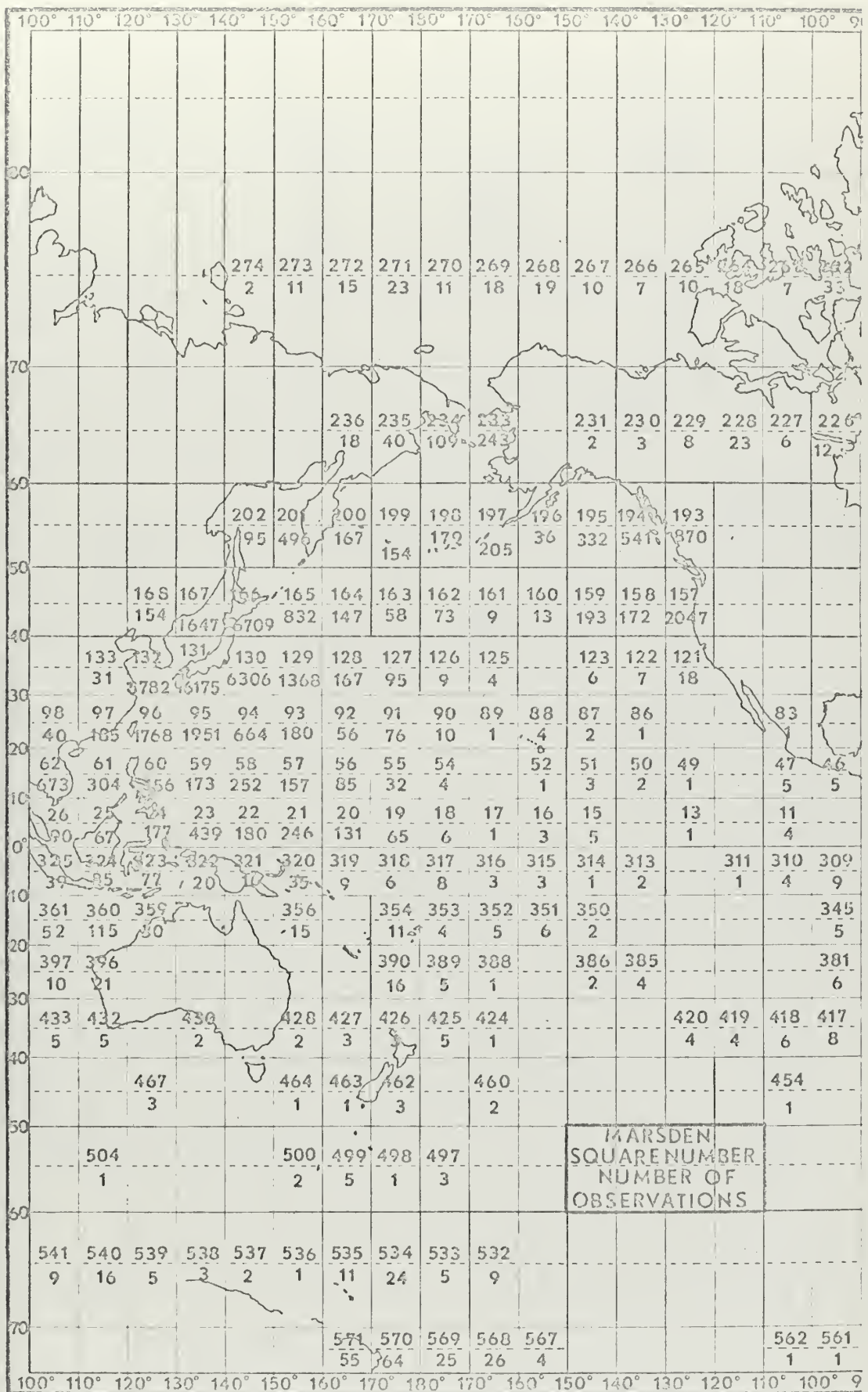


Figure 1A. Secchi Disc Observations between 100 E and 90 W Longitude

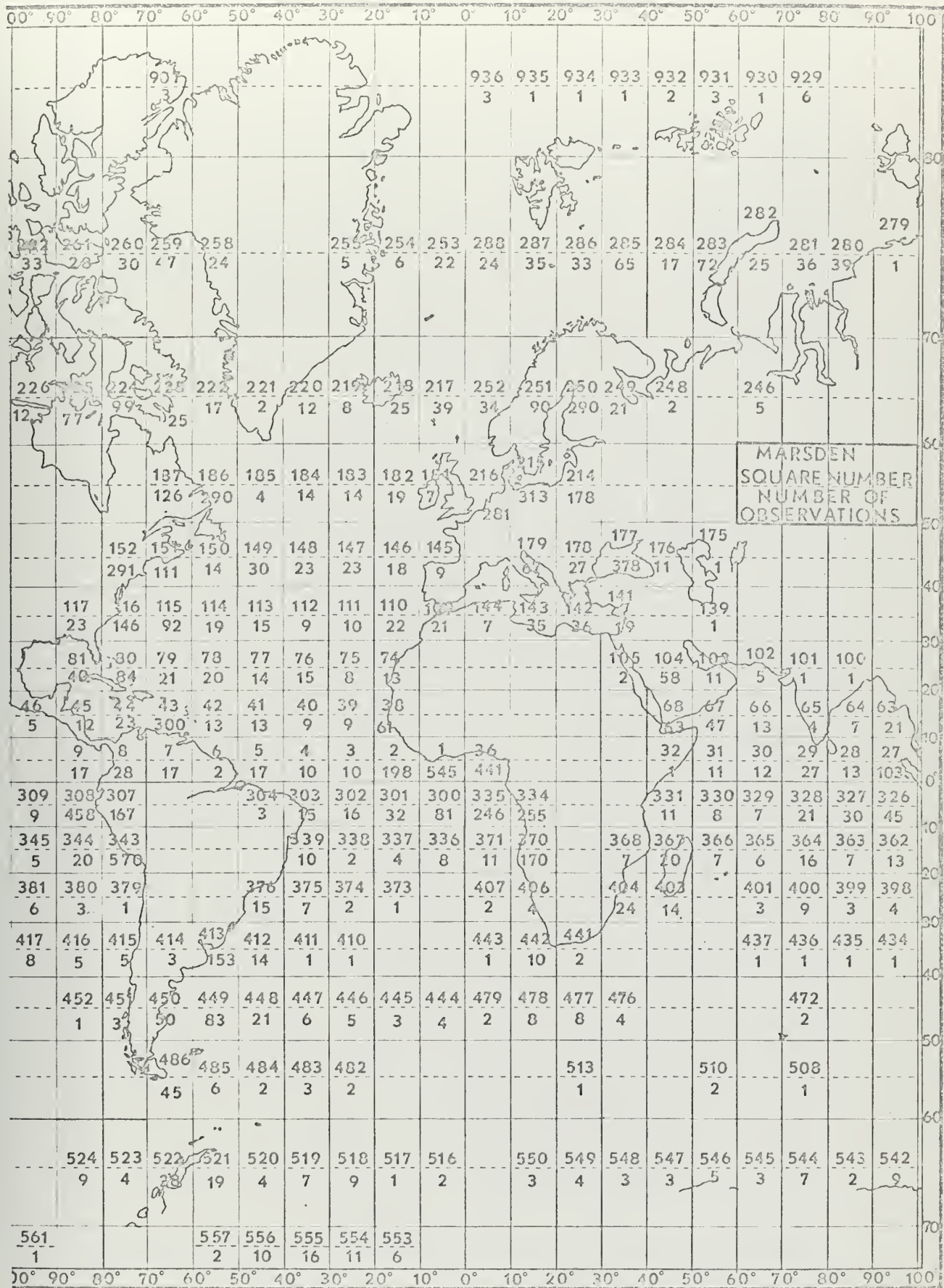


Figure 1B. Secchi Disc Observations between 100 W and 100 E Longitude

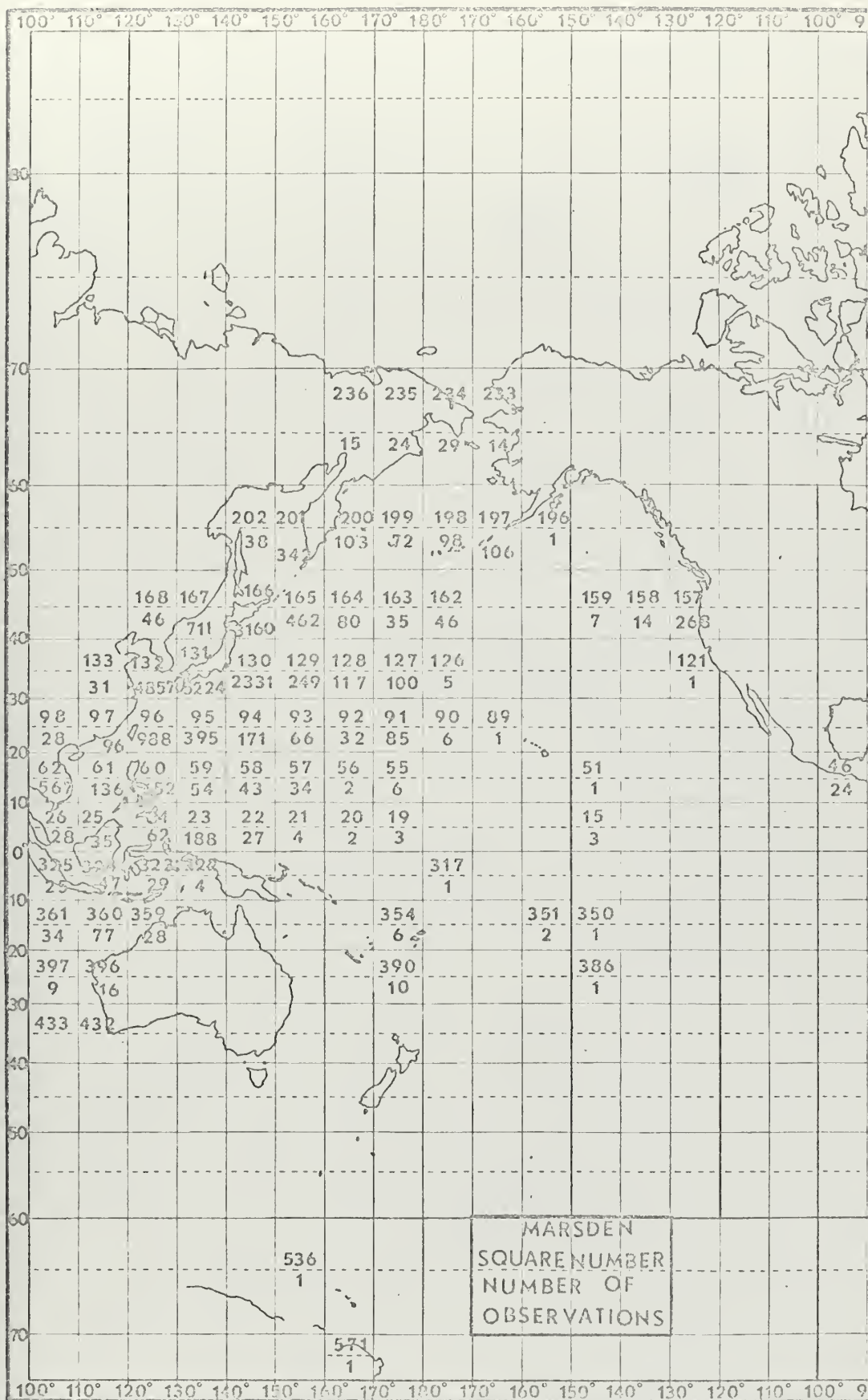


Figure 2A. Forel Color Code Observations between 100 E and 90 W Longitude

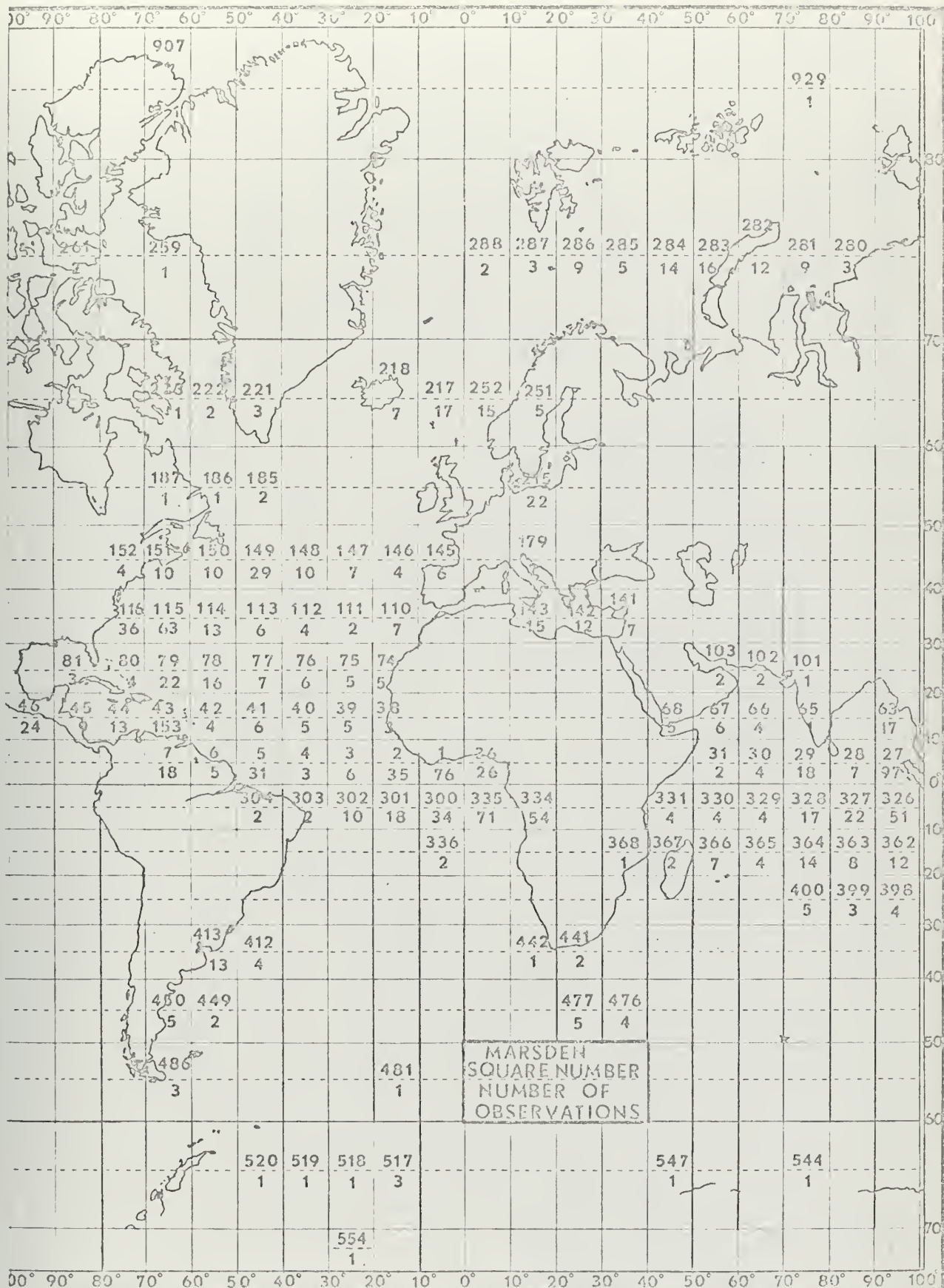


Figure 2B. Forel Color Codes between 100 W and 100 E Longitude

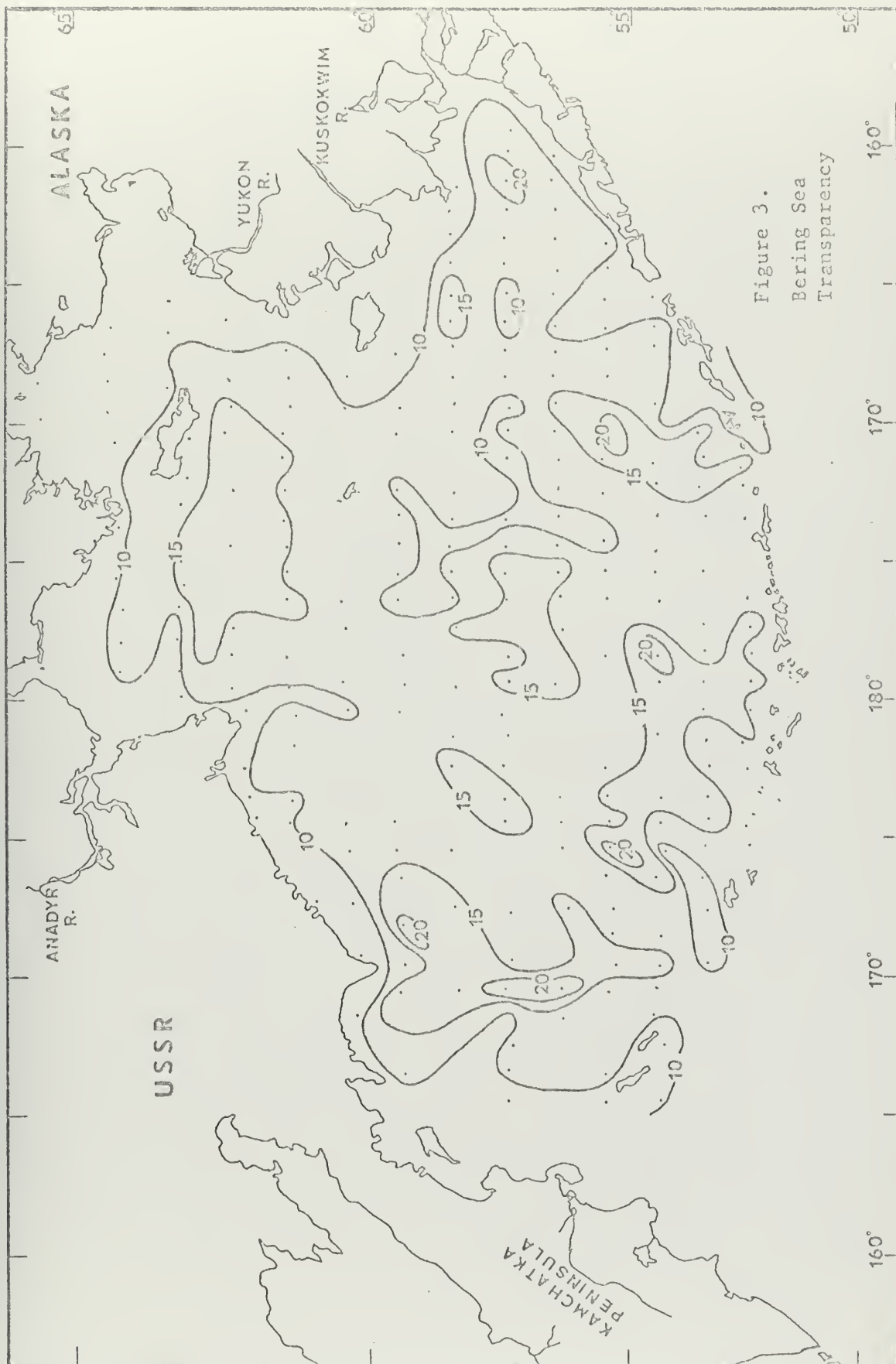


Figure 3.
Bering Sea
Transparency

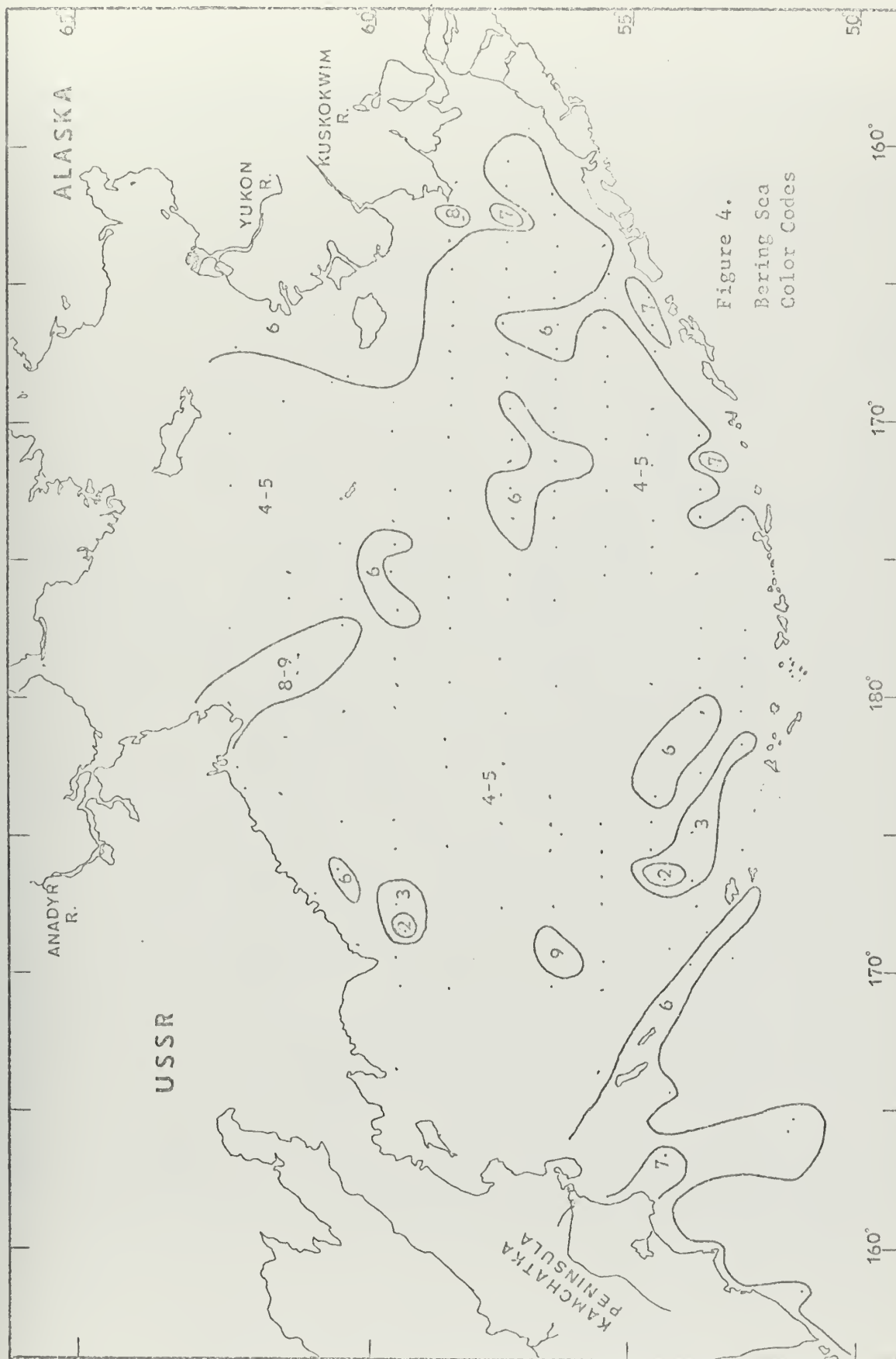


Figure 4.
Bering Sea
Color Codes

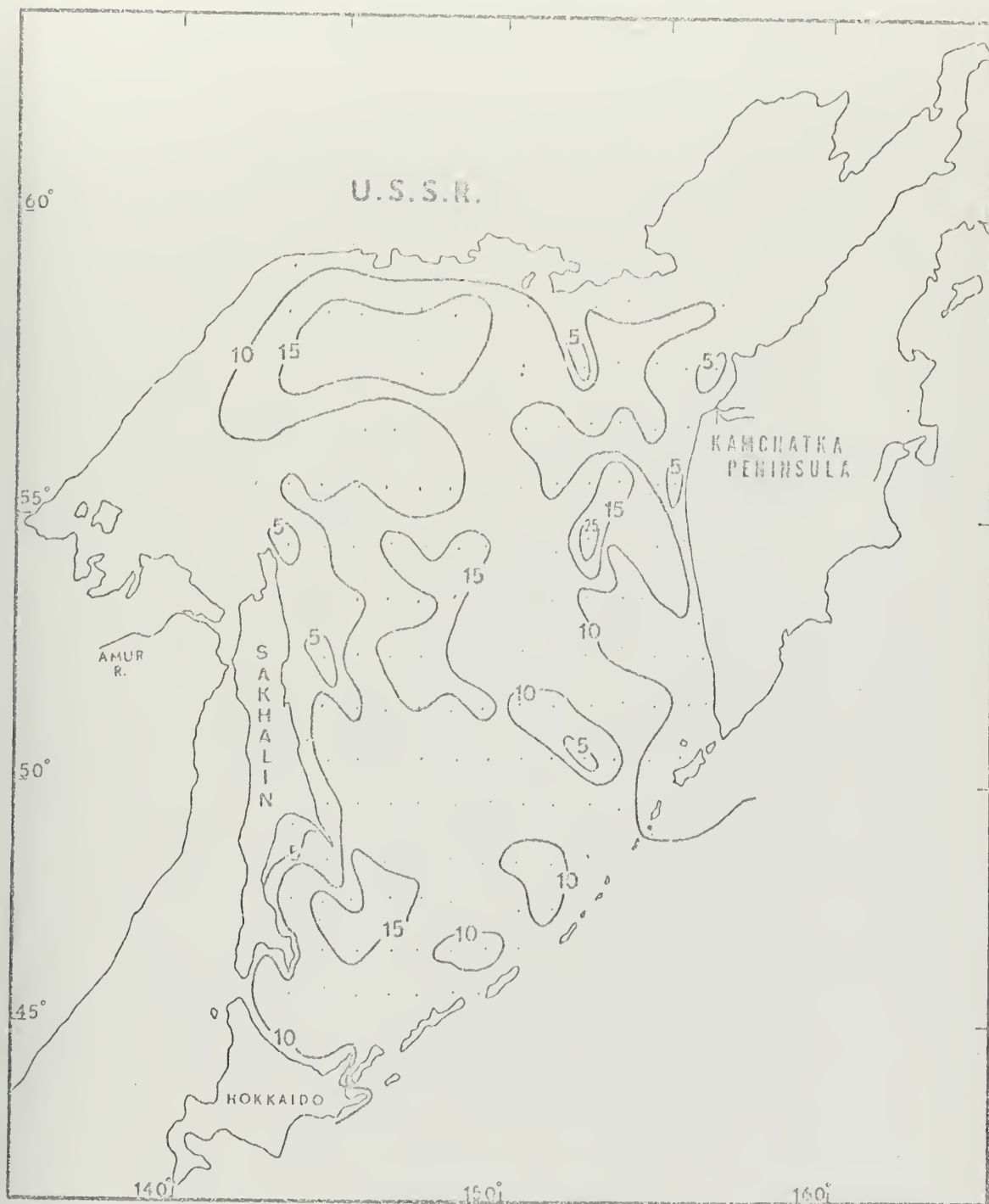


Figure 5. Sea of Okhotsk Transparency.

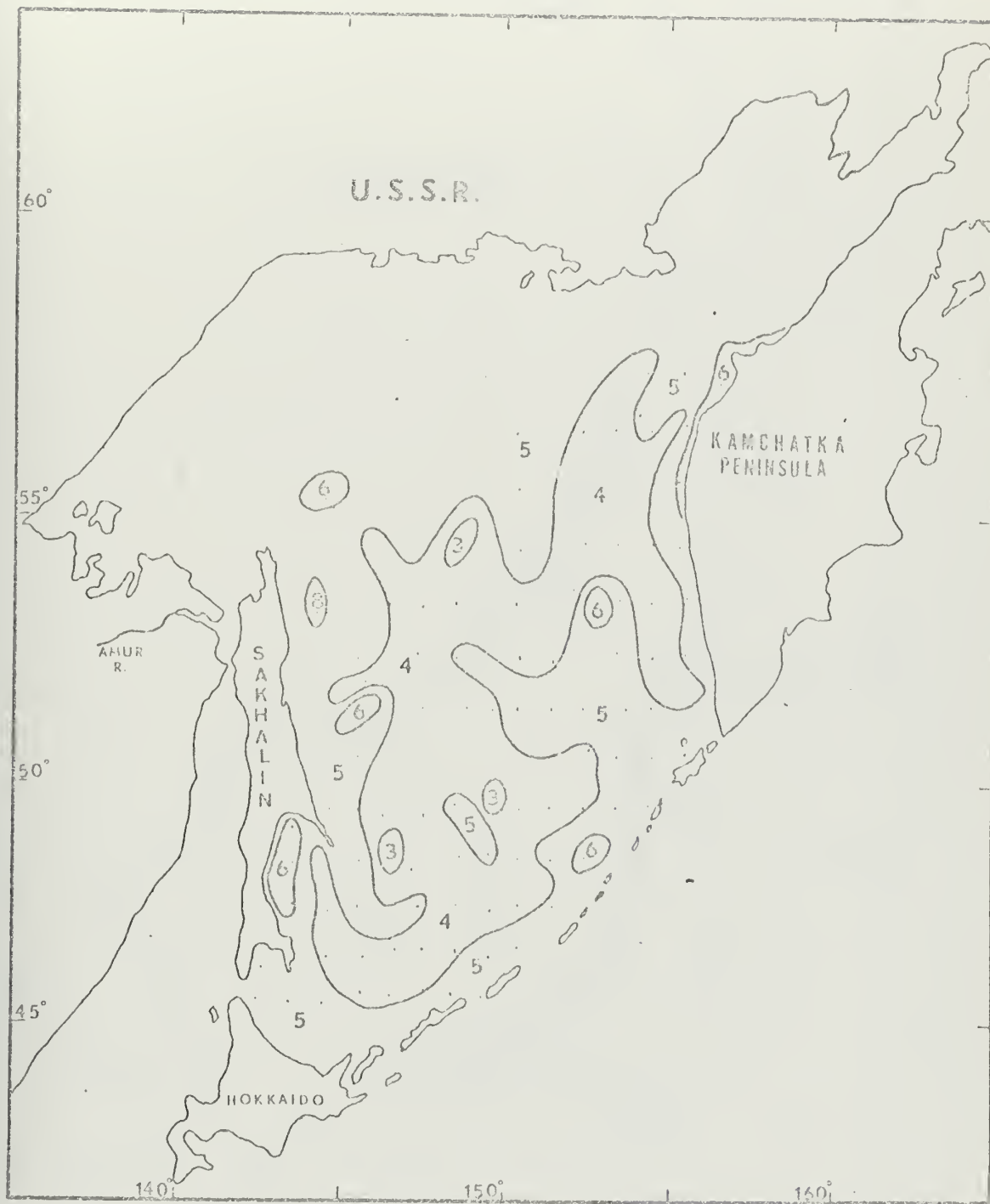


Figure 6. Sea of Okhotsk Color Codes.





Figure 8.
Sea of Japan
January Transparency

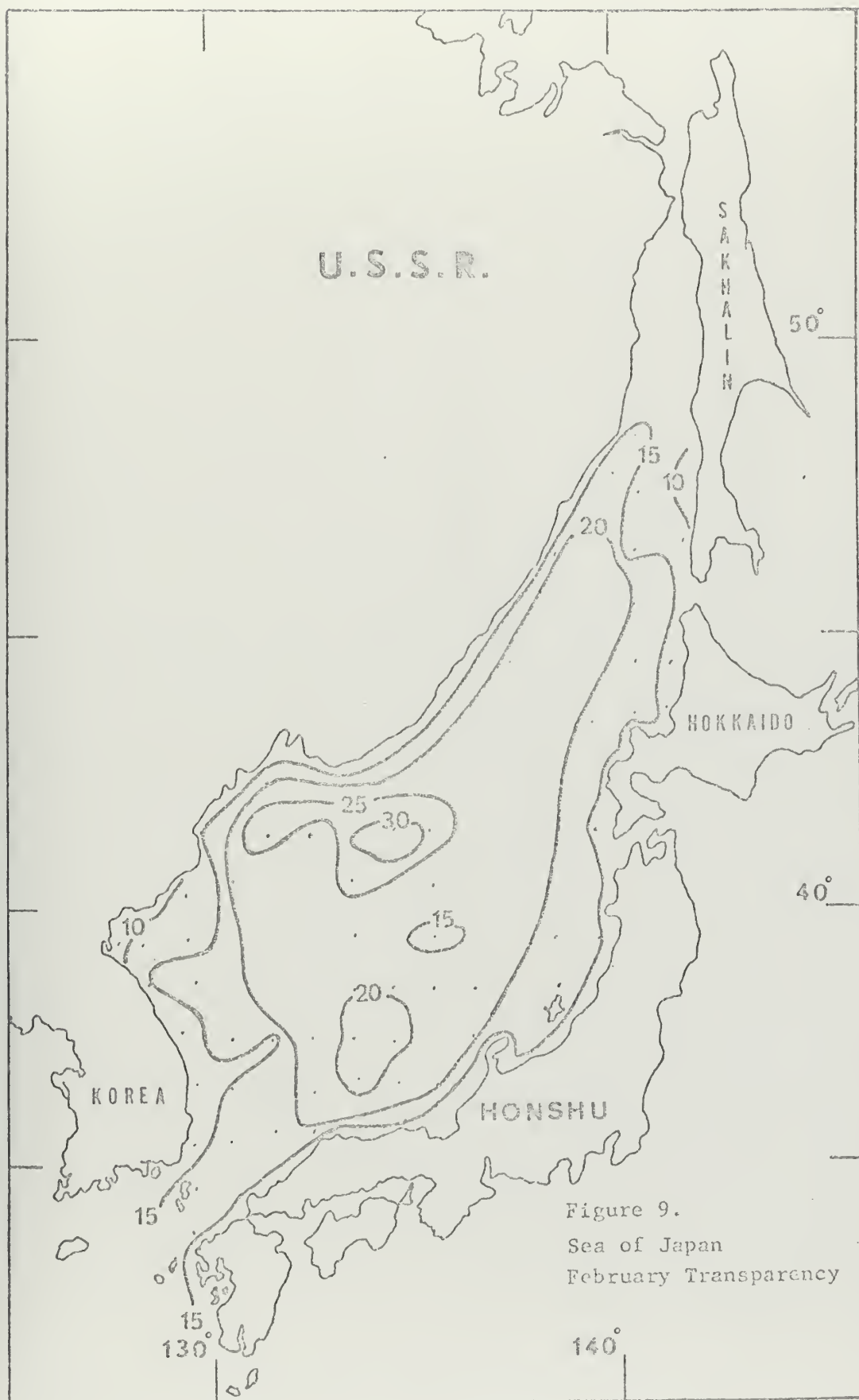


Figure 9.
Sea of Japan
February Transparency



Figure 10.
Sea of Japan
March Transparency



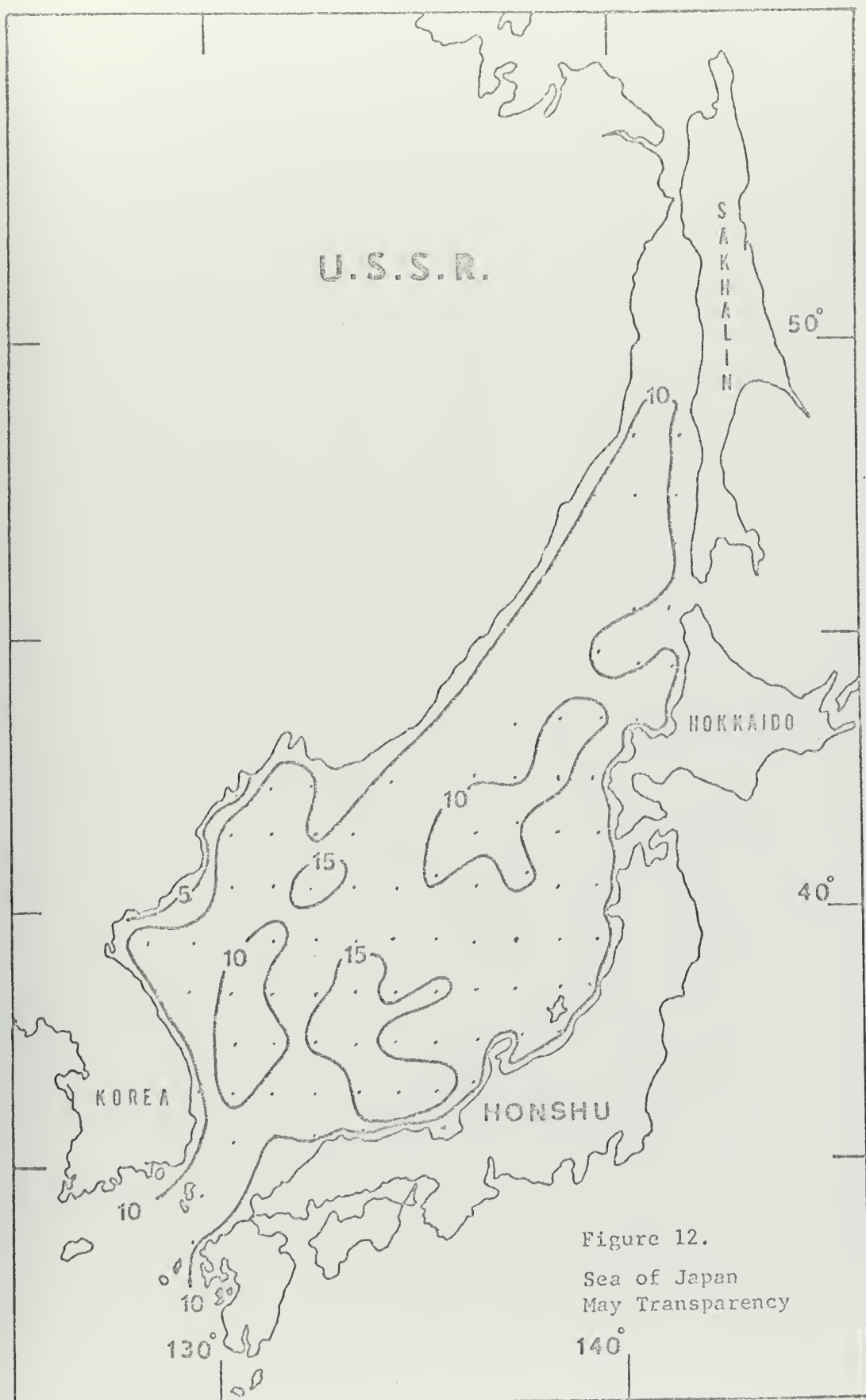


Figure 12.
Sea of Japan
May Transparency

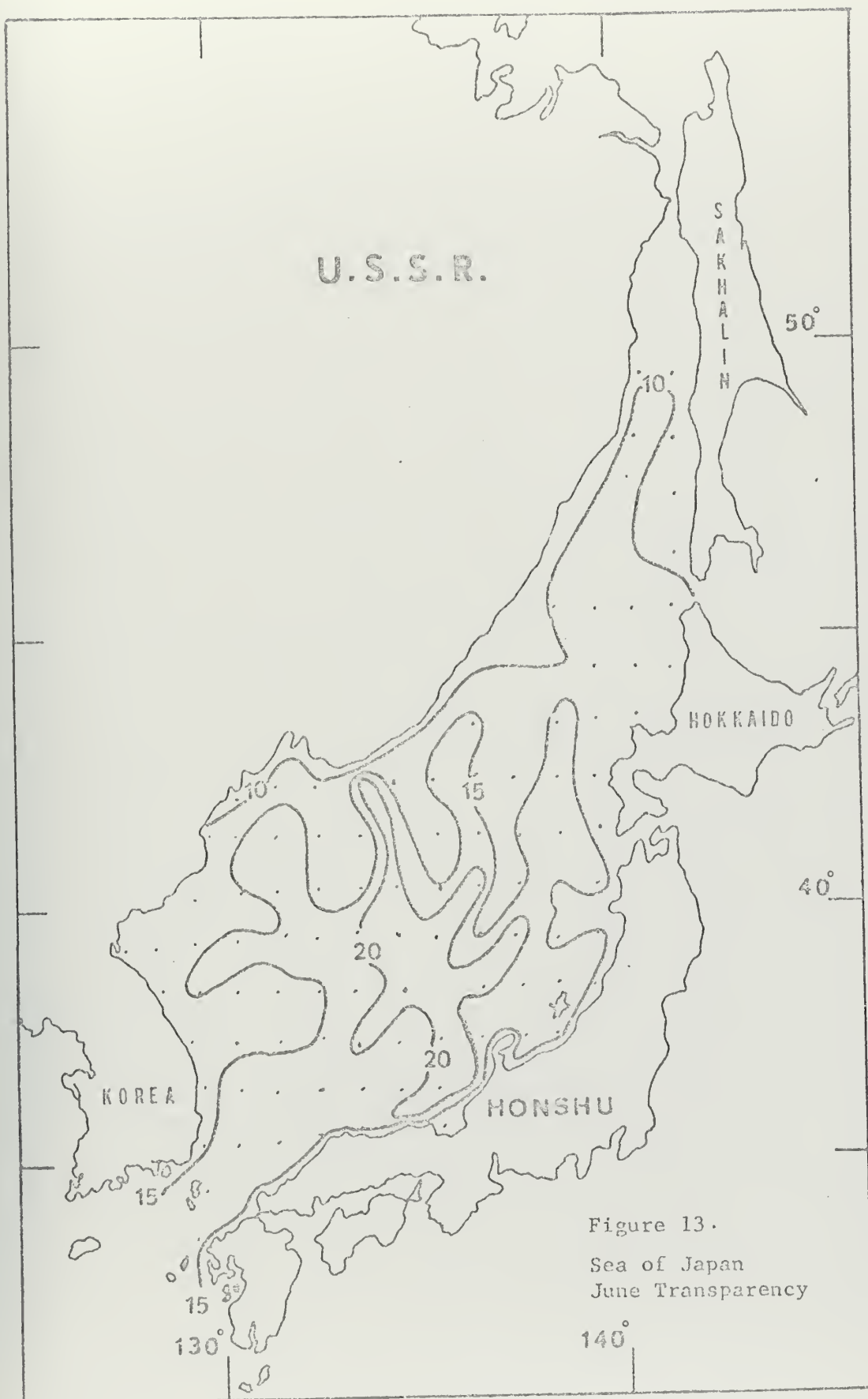


Figure 13.
Sea of Japan
June Transparency



Figure 14.
Sea of Japan
July Transparency

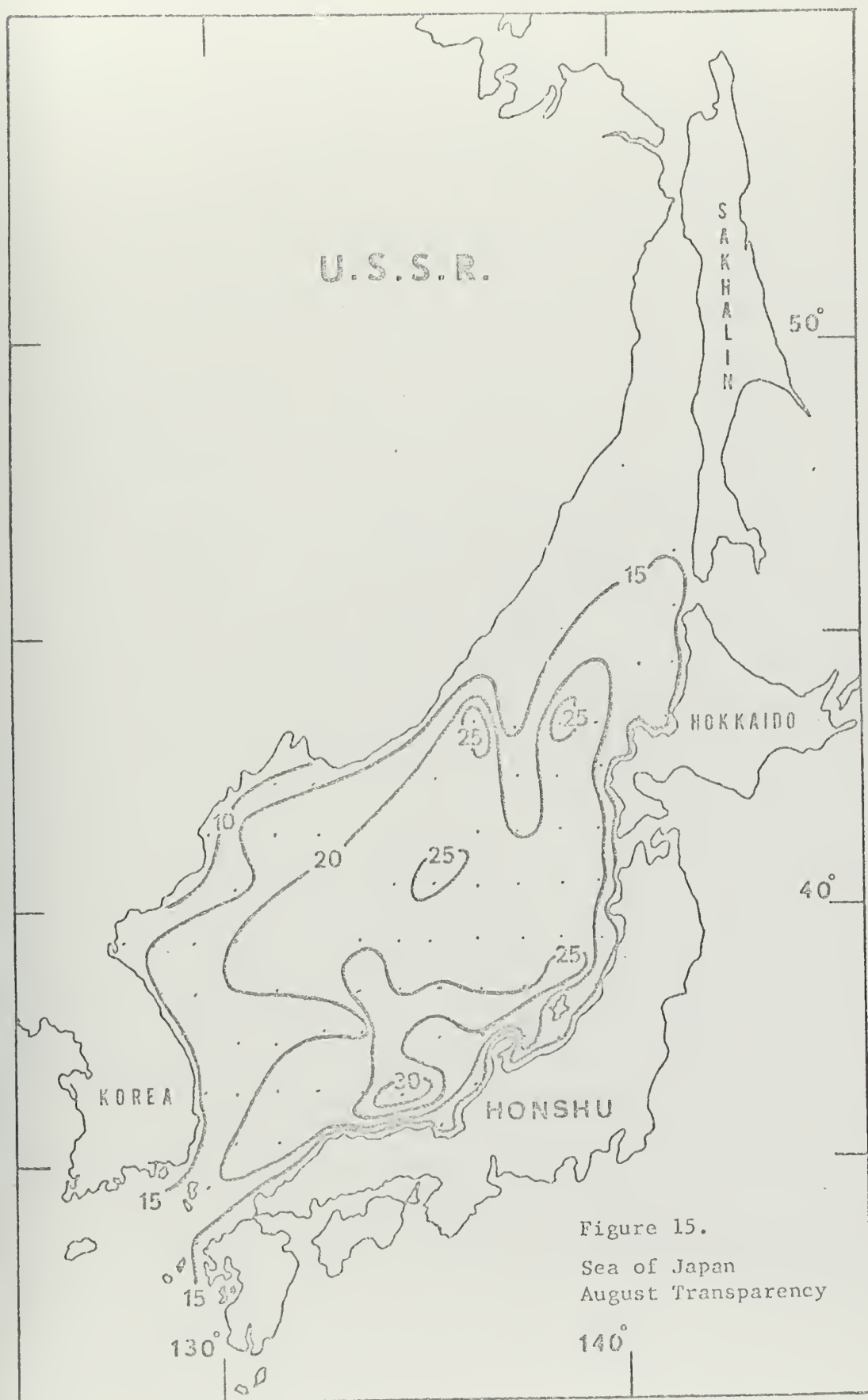


Figure 15.
Sea of Japan
August Transparency

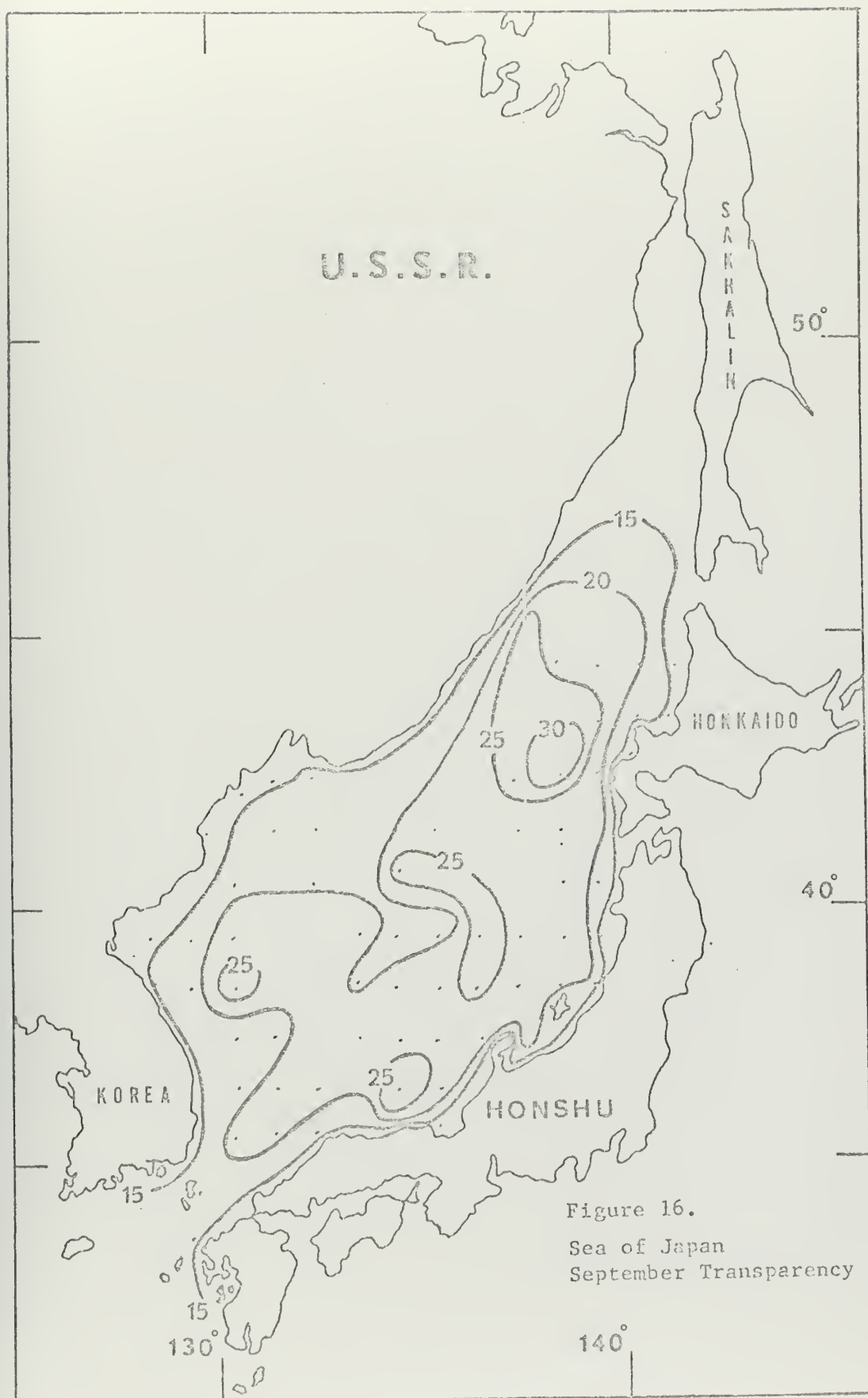


Figure 16.
Sea of Japan
September Transparency

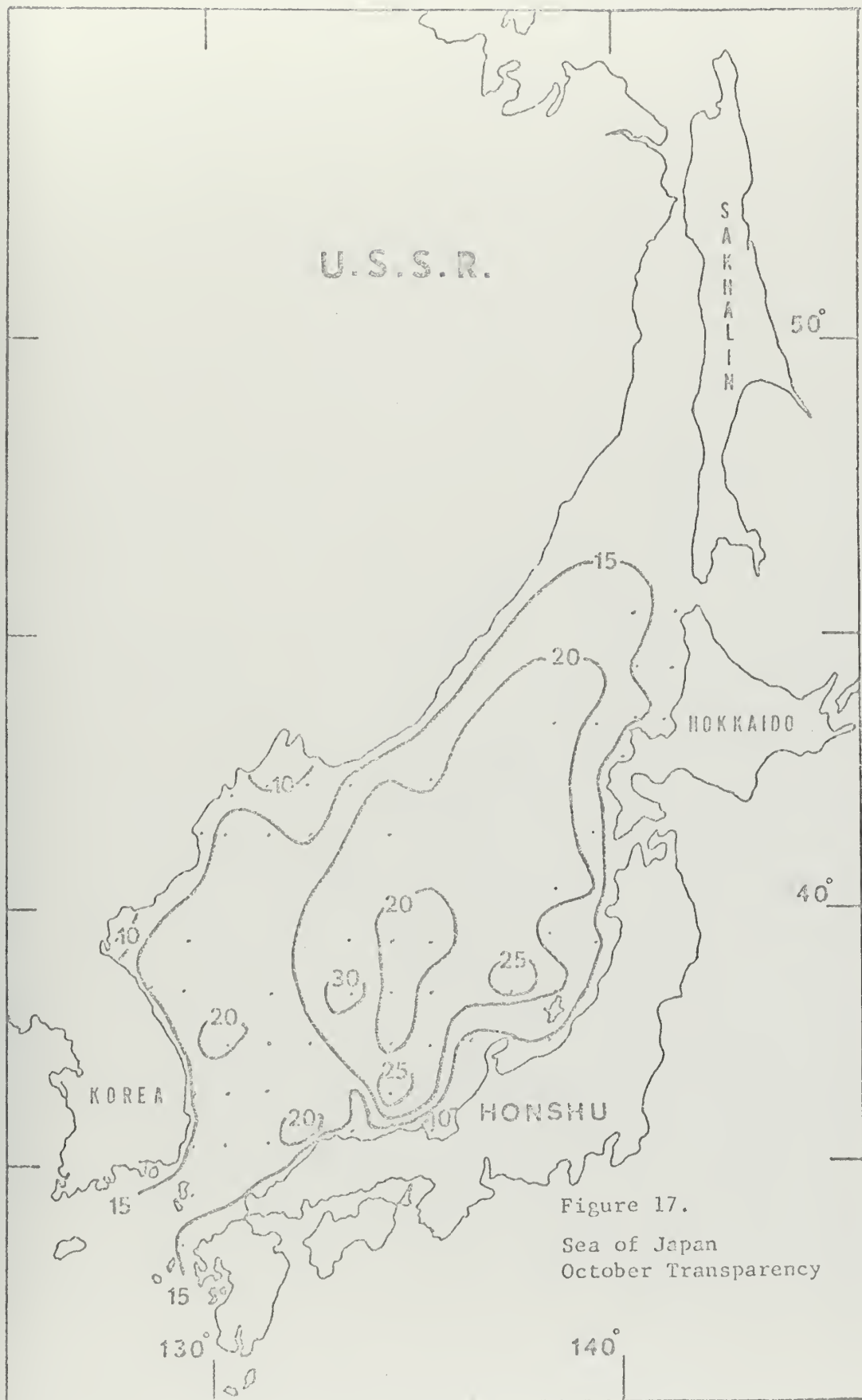


Figure 17.
Sea of Japan
October Transparency



Figure 18.
Sea of Japan
November Transparency



Figure 19.
Sea of Japan
December Transparency



Figure 20.
Sea of Japan
Color Codes,
Mean of all Data

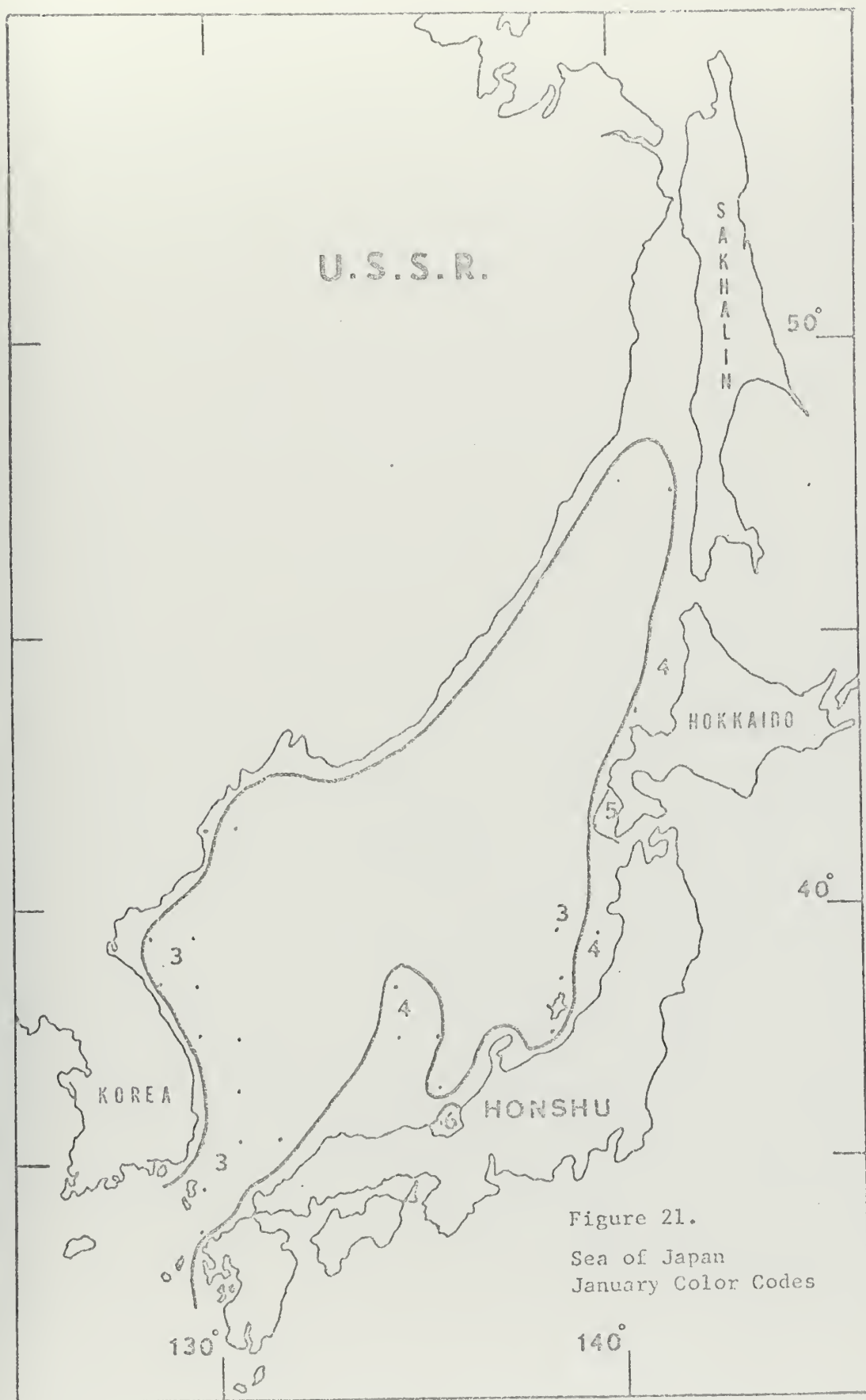


Figure 21.
Sea of Japan
January Color Codes

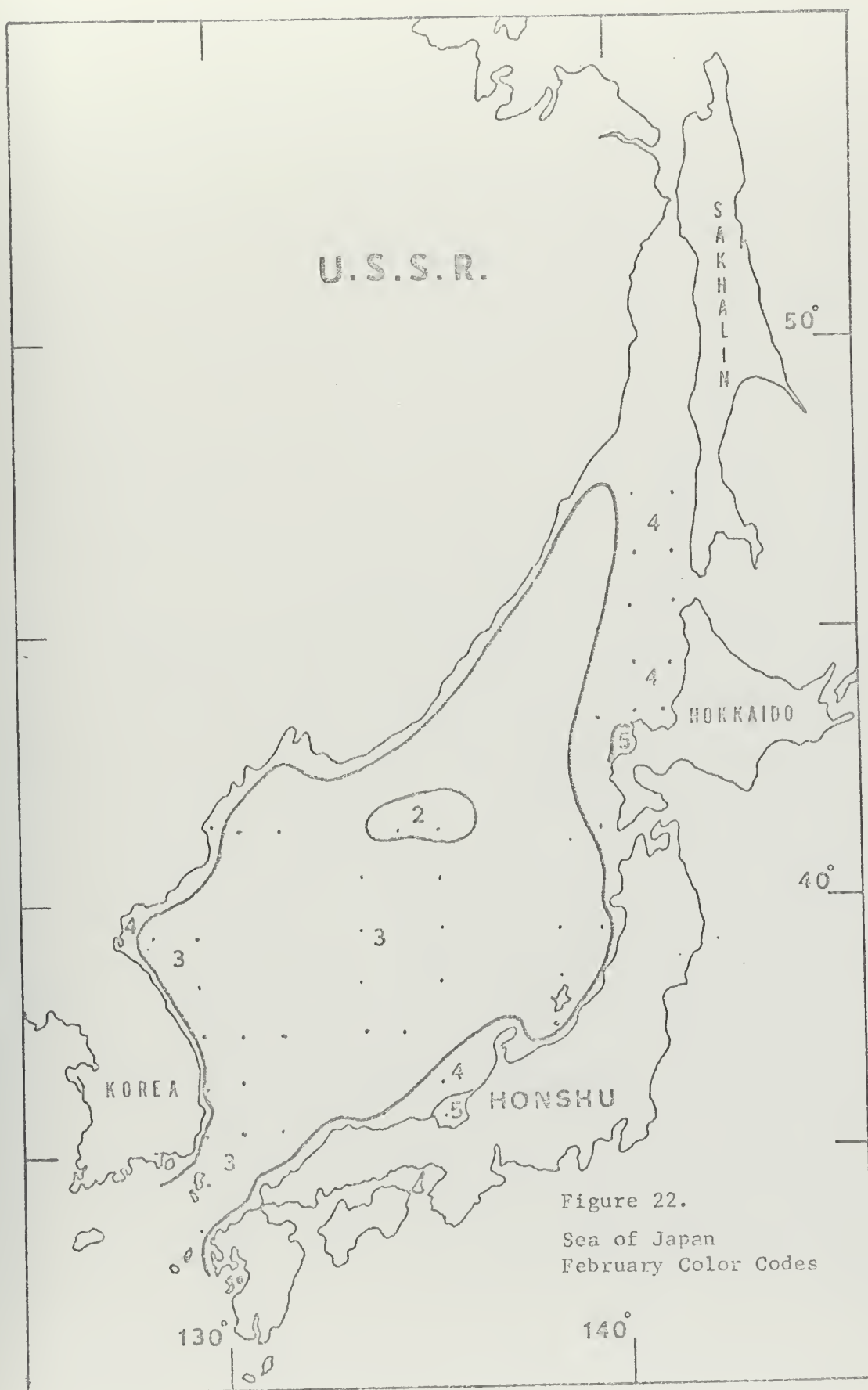


Figure 22.
Sea of Japan
February Color Codes

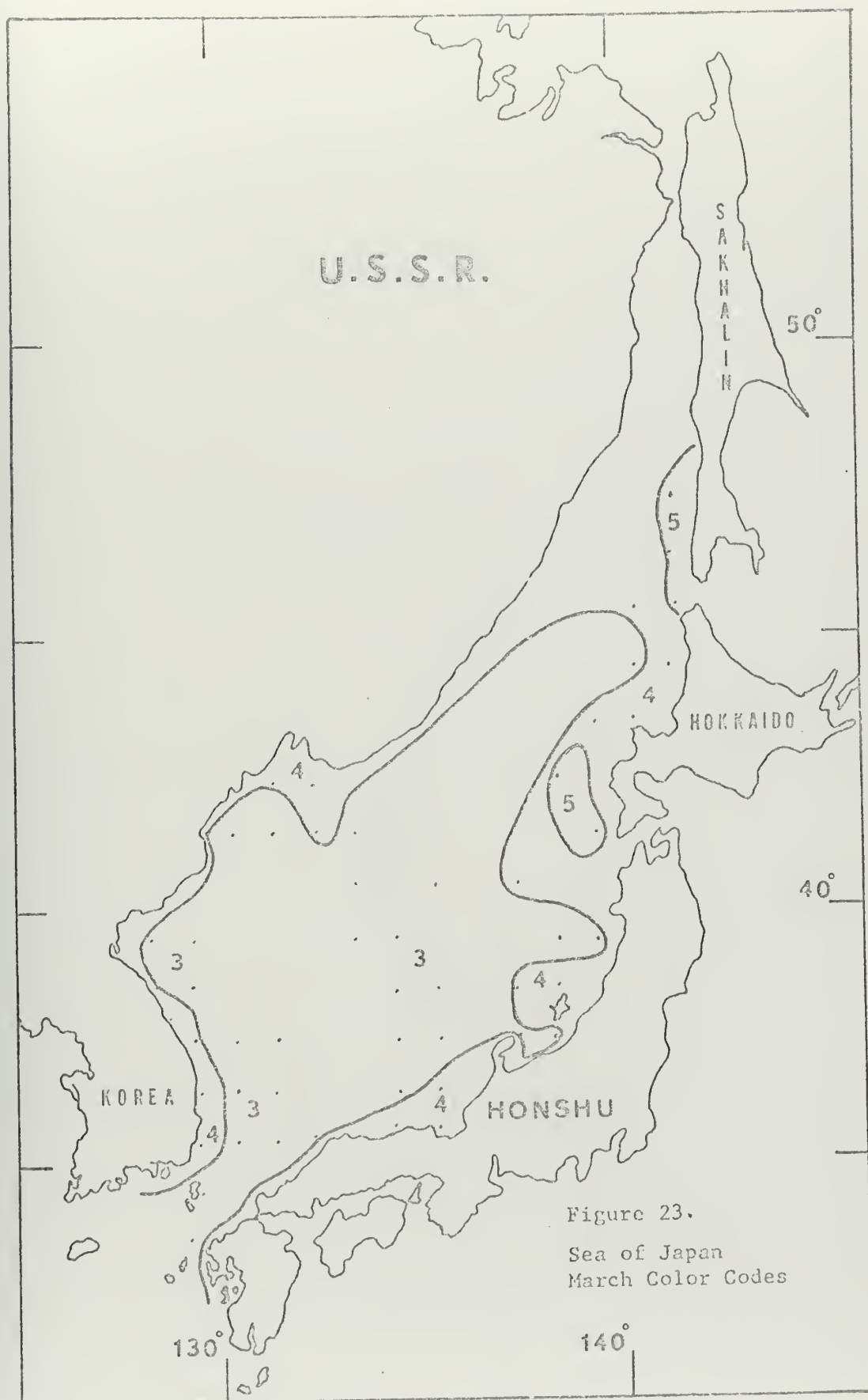


Figure 23.
Sea of Japan
March Color Codes

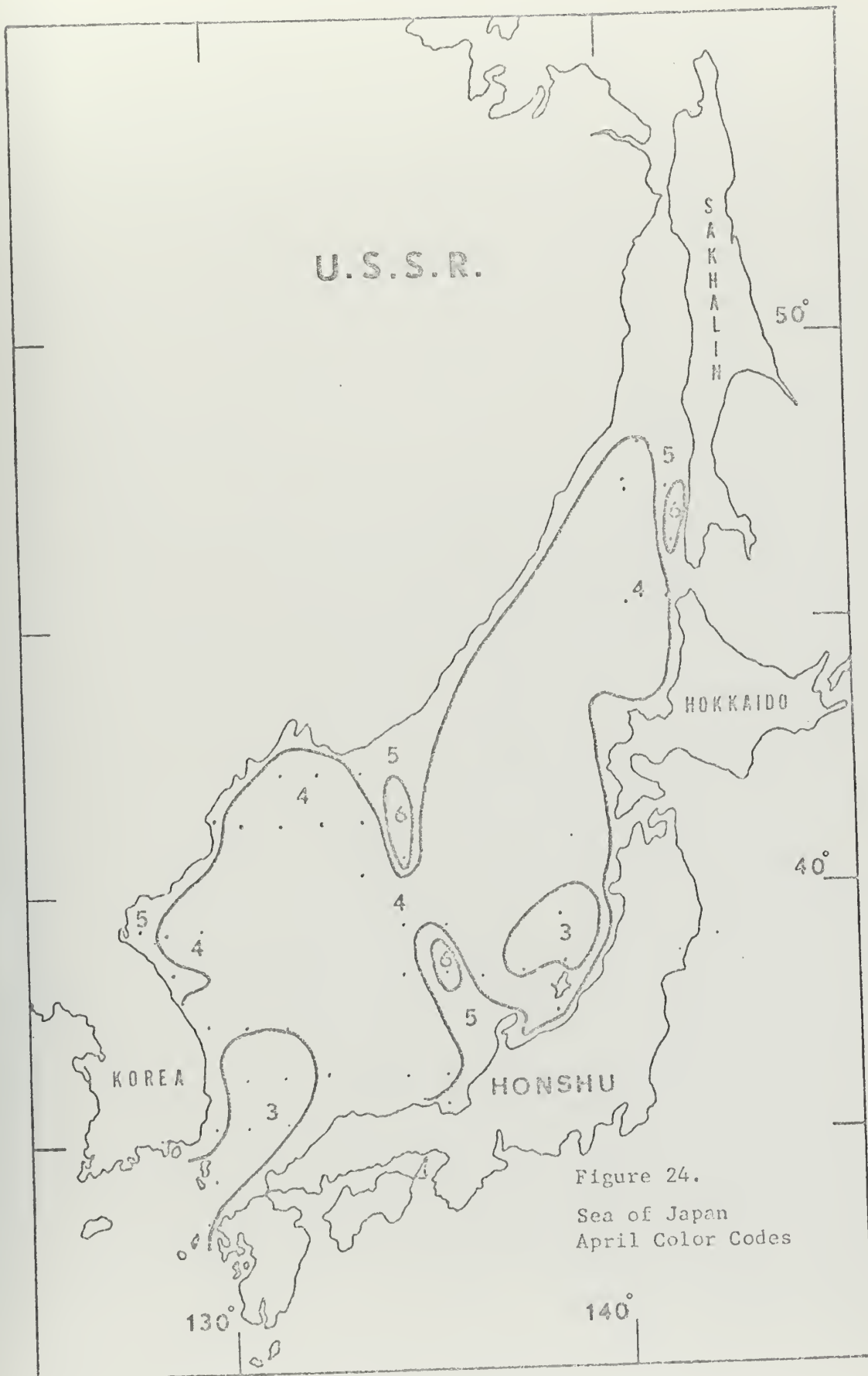


Figure 24.
Sea of Japan
April Color Codes

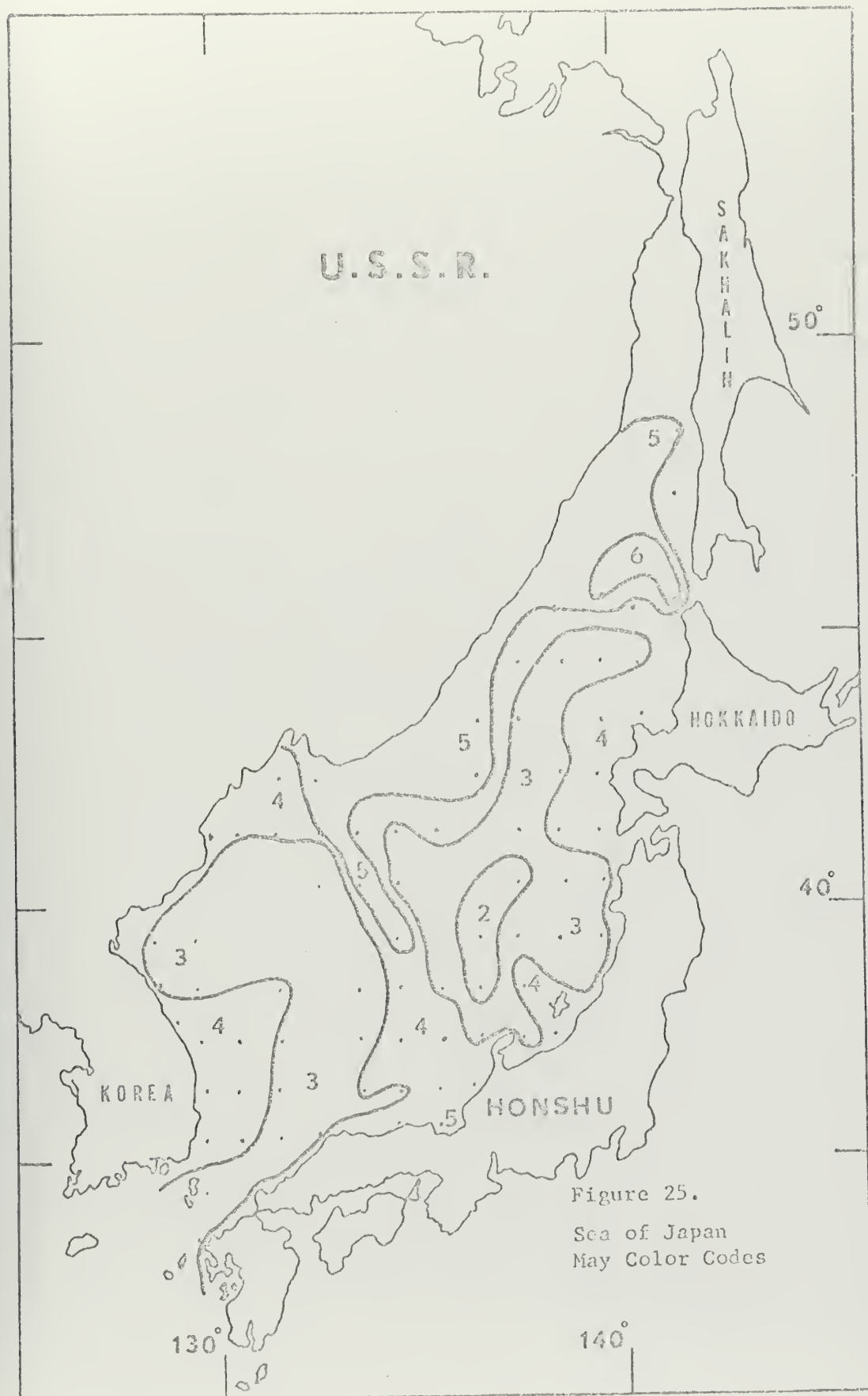


Figure 25.
Sea of Japan
May Color Codes

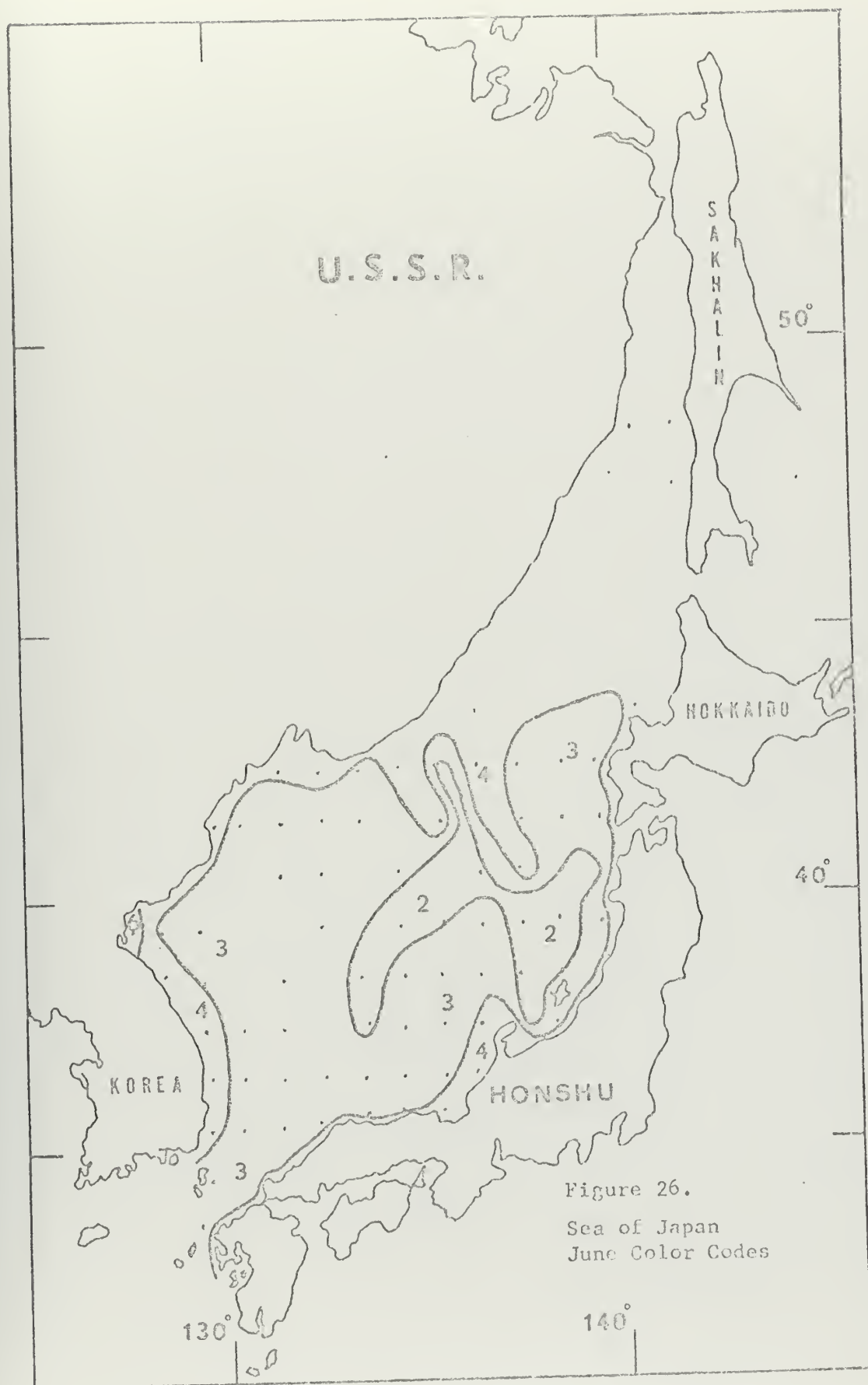
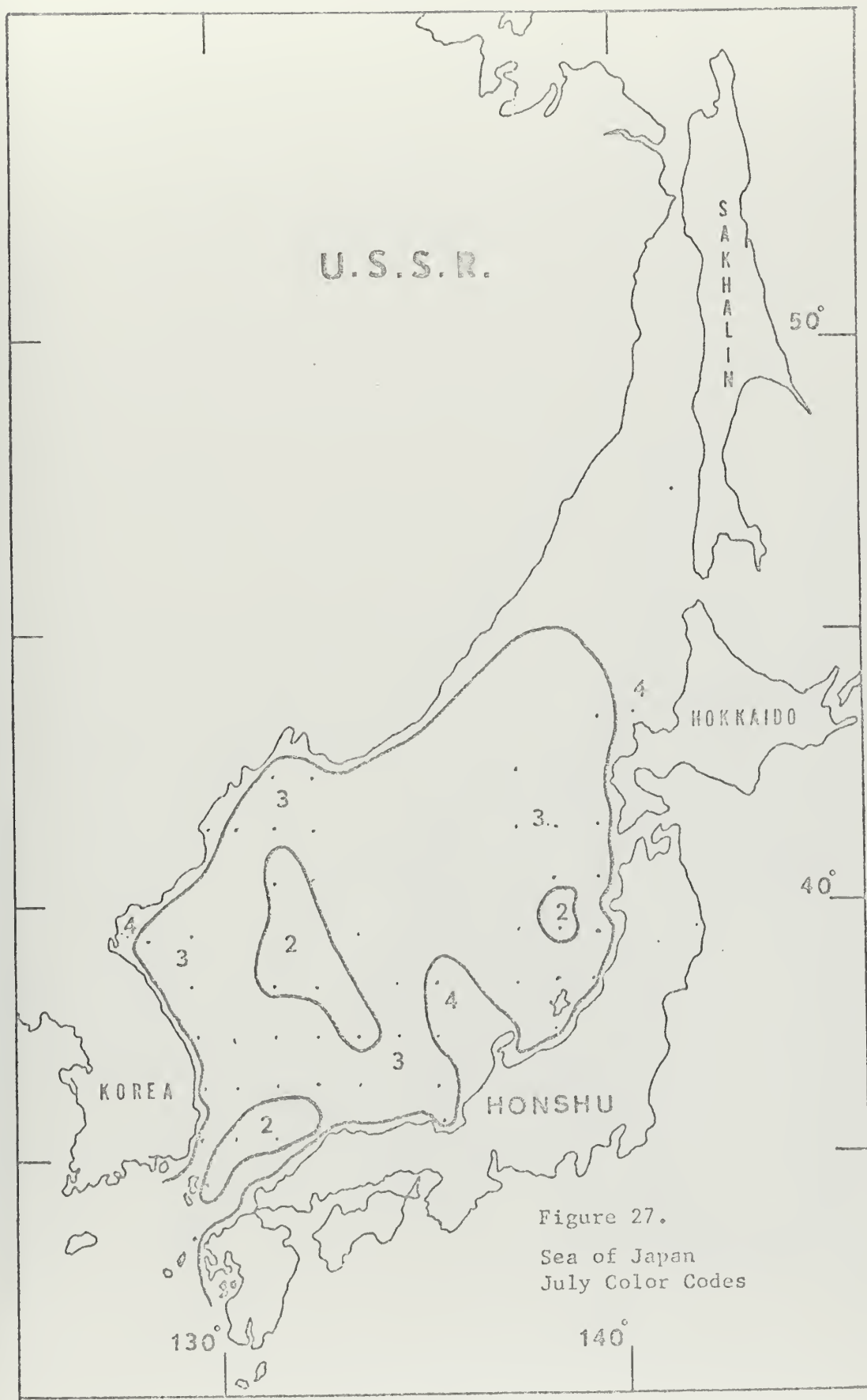


Figure 26.
Sea of Japan
June Color Codes



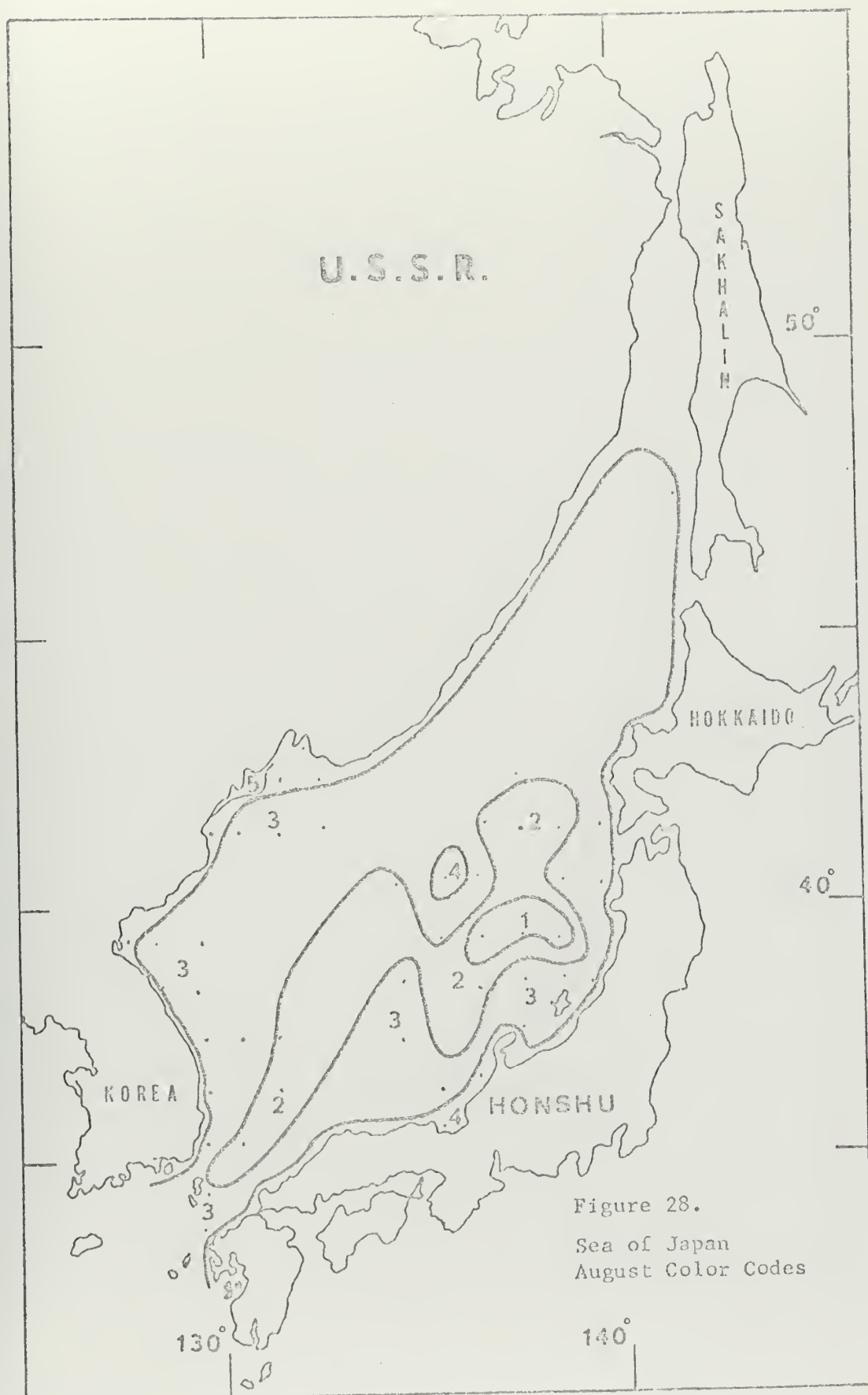


Figure 28.
Sea of Japan
August Color Codes

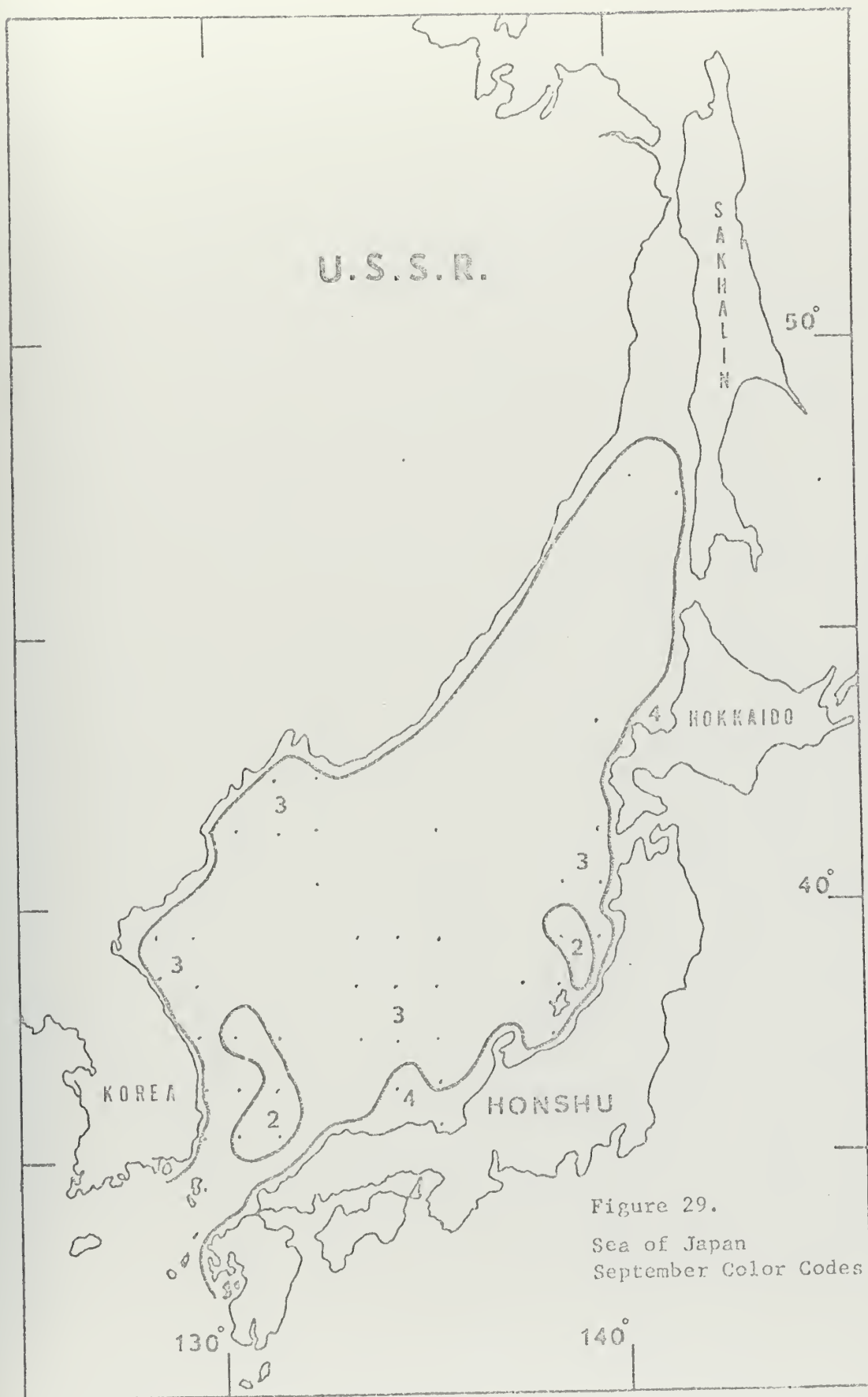


Figure 29.
Sea of Japan
September Color Codes

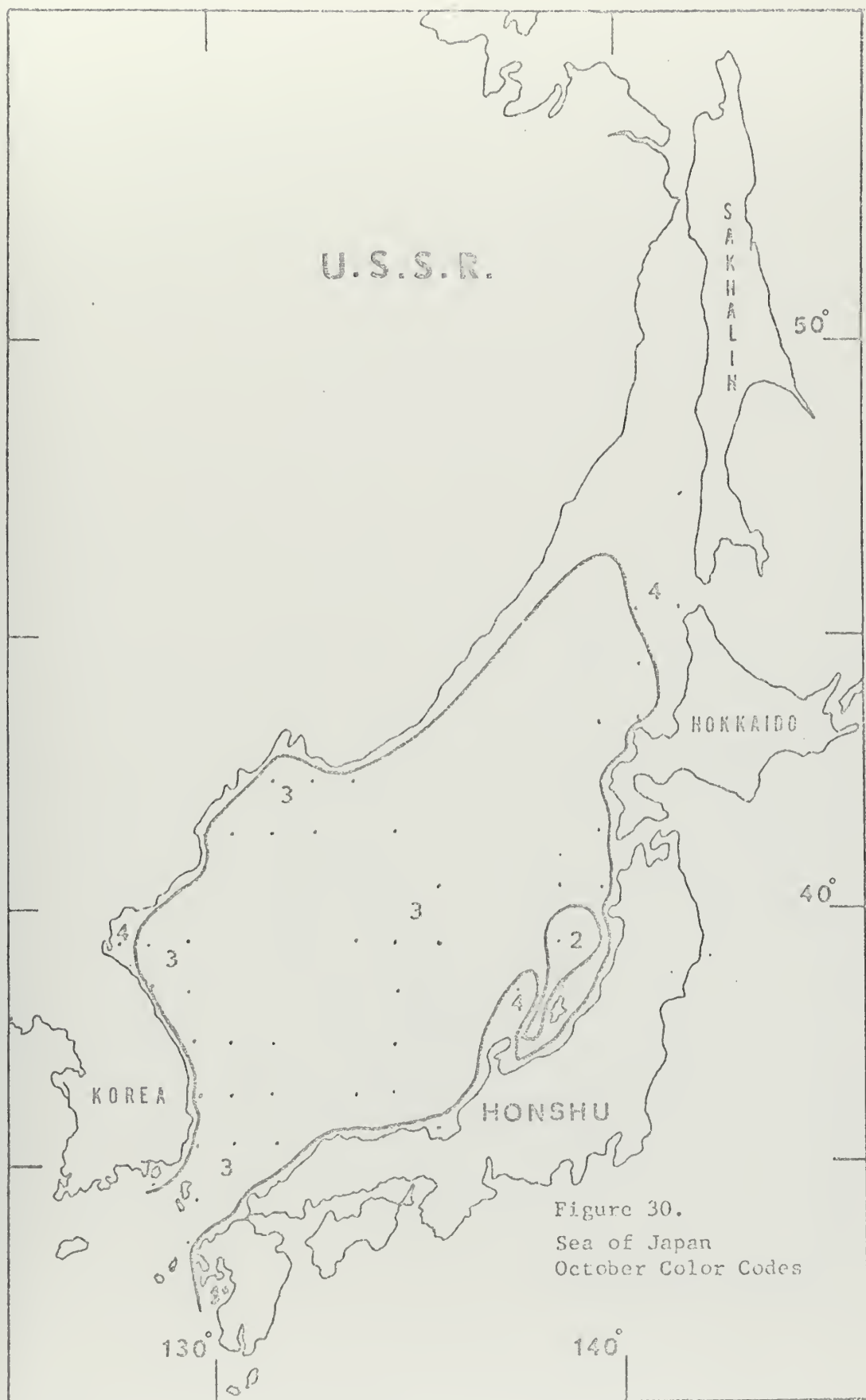


Figure 30.
Sea of Japan
October Color Codes

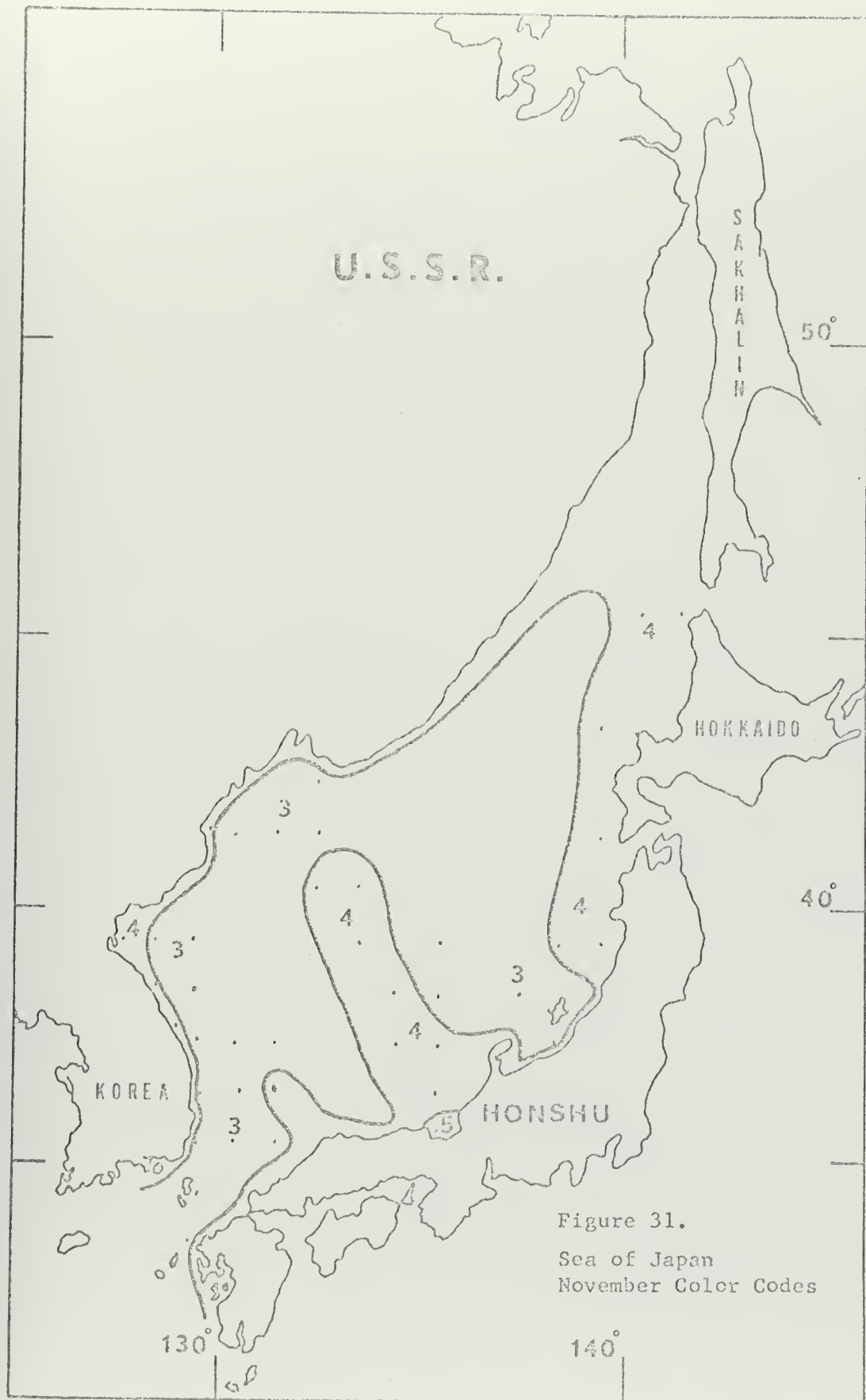


Figure 31.
Sea of Japan
November Color Codes

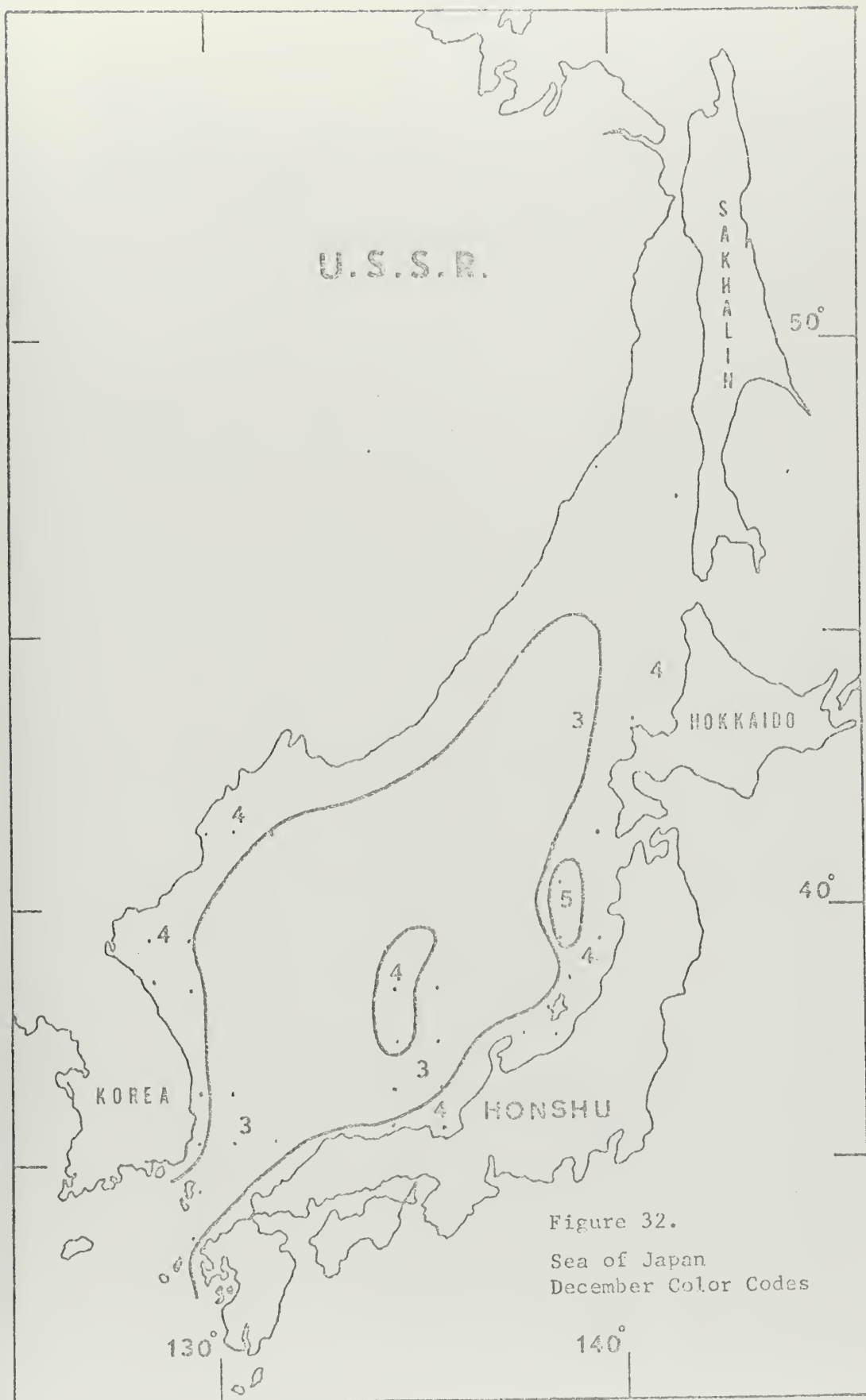


Figure 32.
Sea of Japan
December Color Codes

Figure 33.

Sea of Japan
Mean Deviation of all
Transparency Data

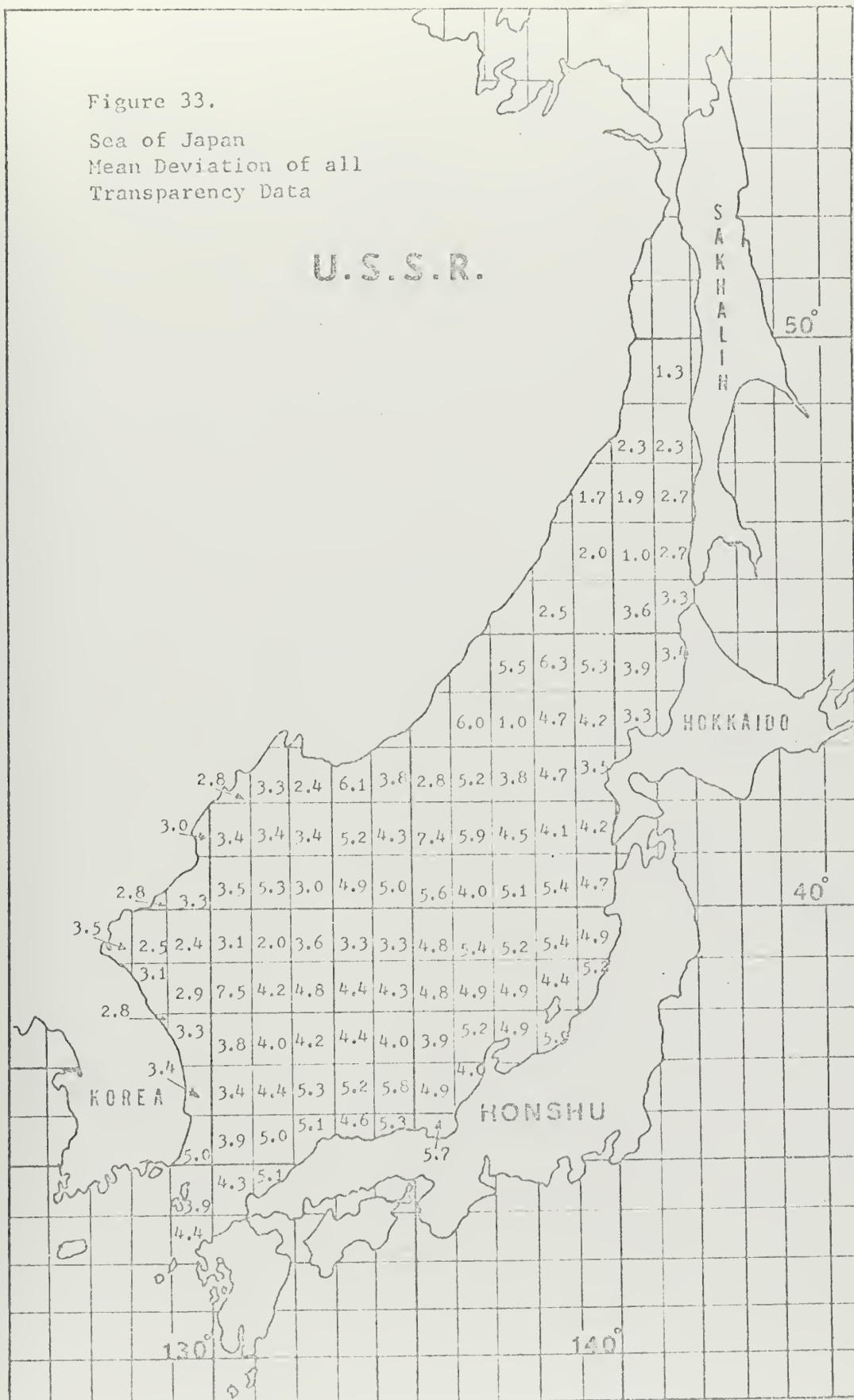


Figure 34.

Sea of Japan

Mean Transparency Deviation

January

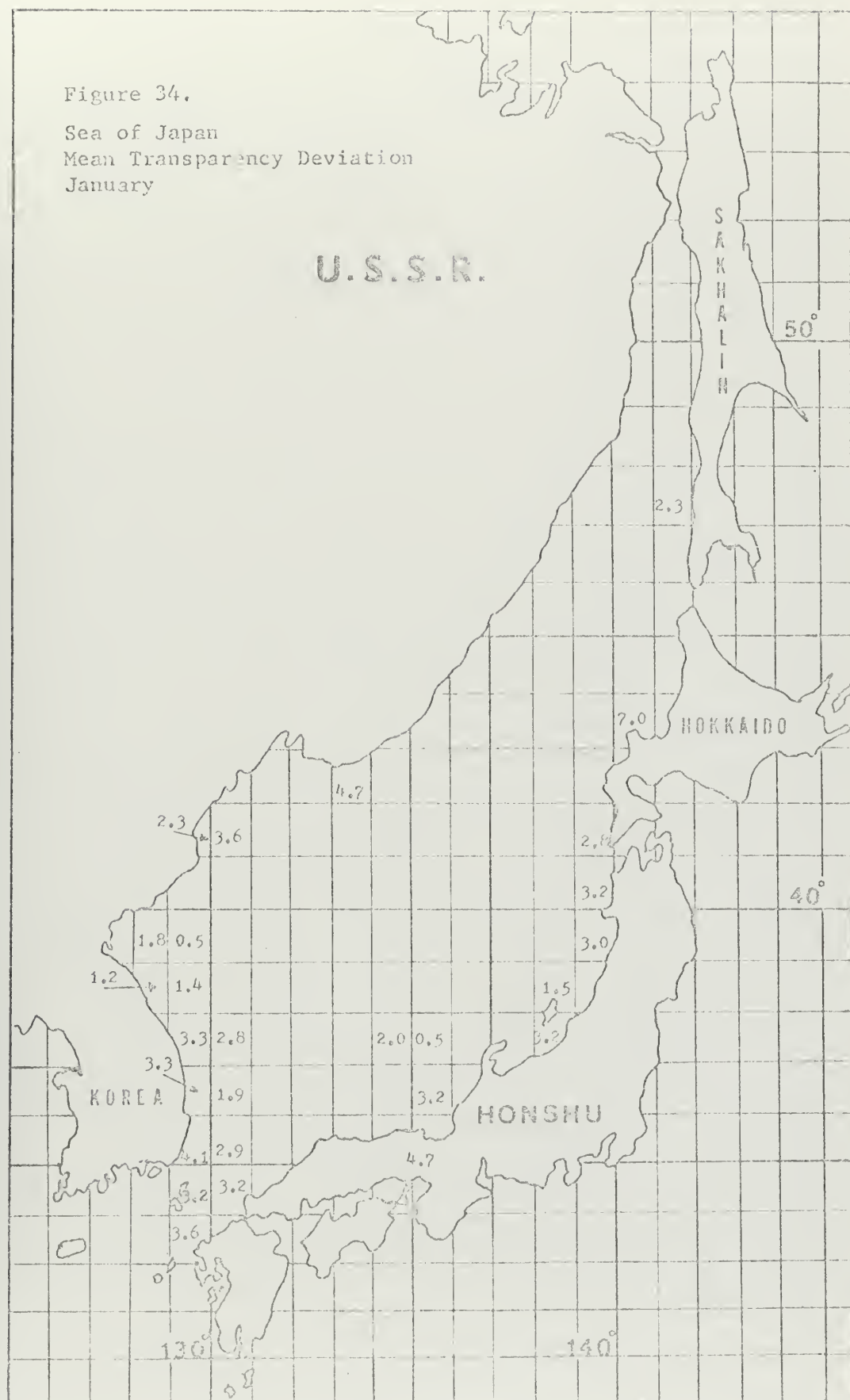


Figure 35.

Sea of Japan
Mean Transparency Deviation
February

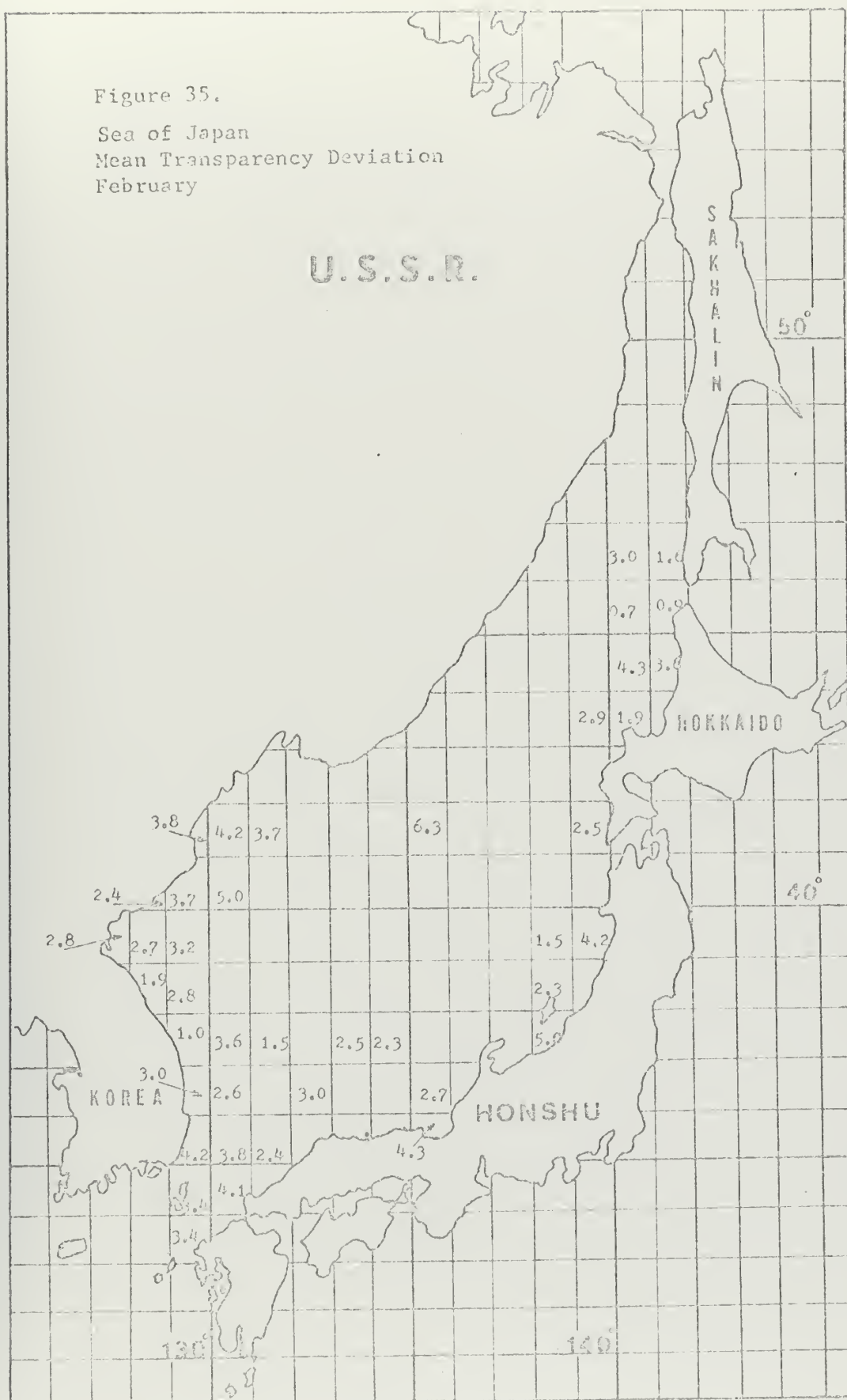


Figure 36.

Sea of Japan
Mean Transparency Deviation
March

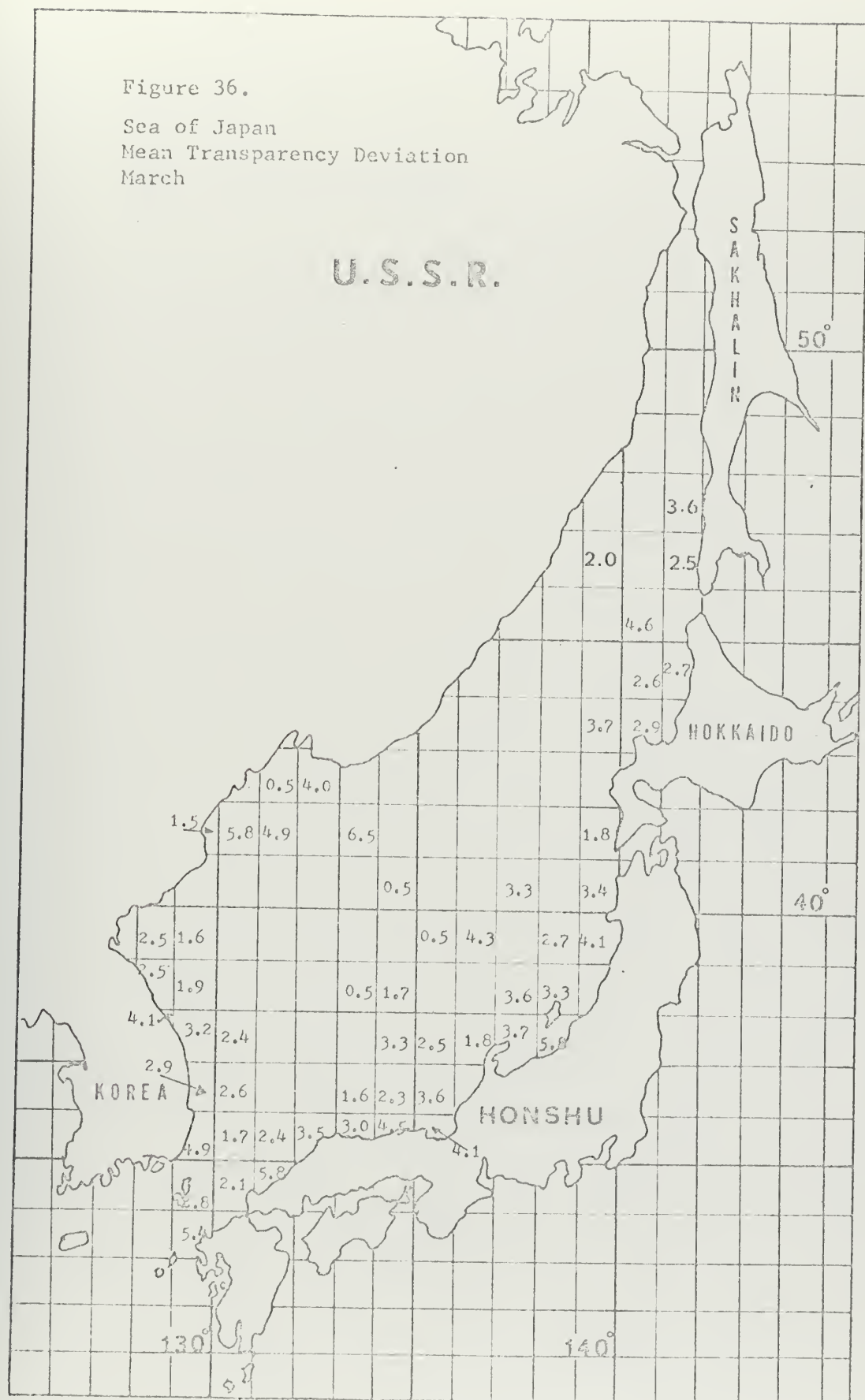


Figure 37.

Sea of Japan
Mean Transparency Deviation
April

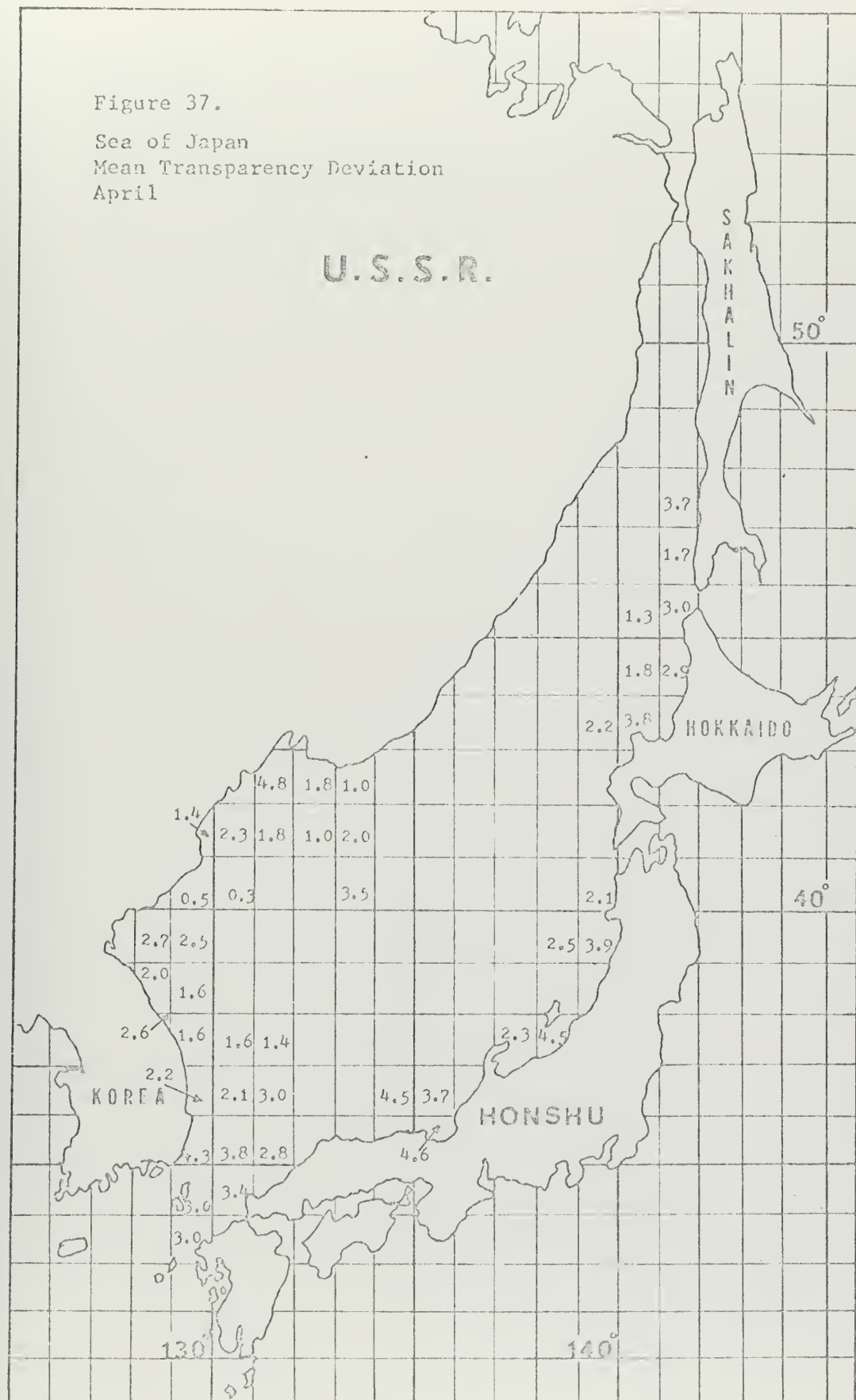


Figure 38.

Sea of Japan
Mean Transparency Deviation
May

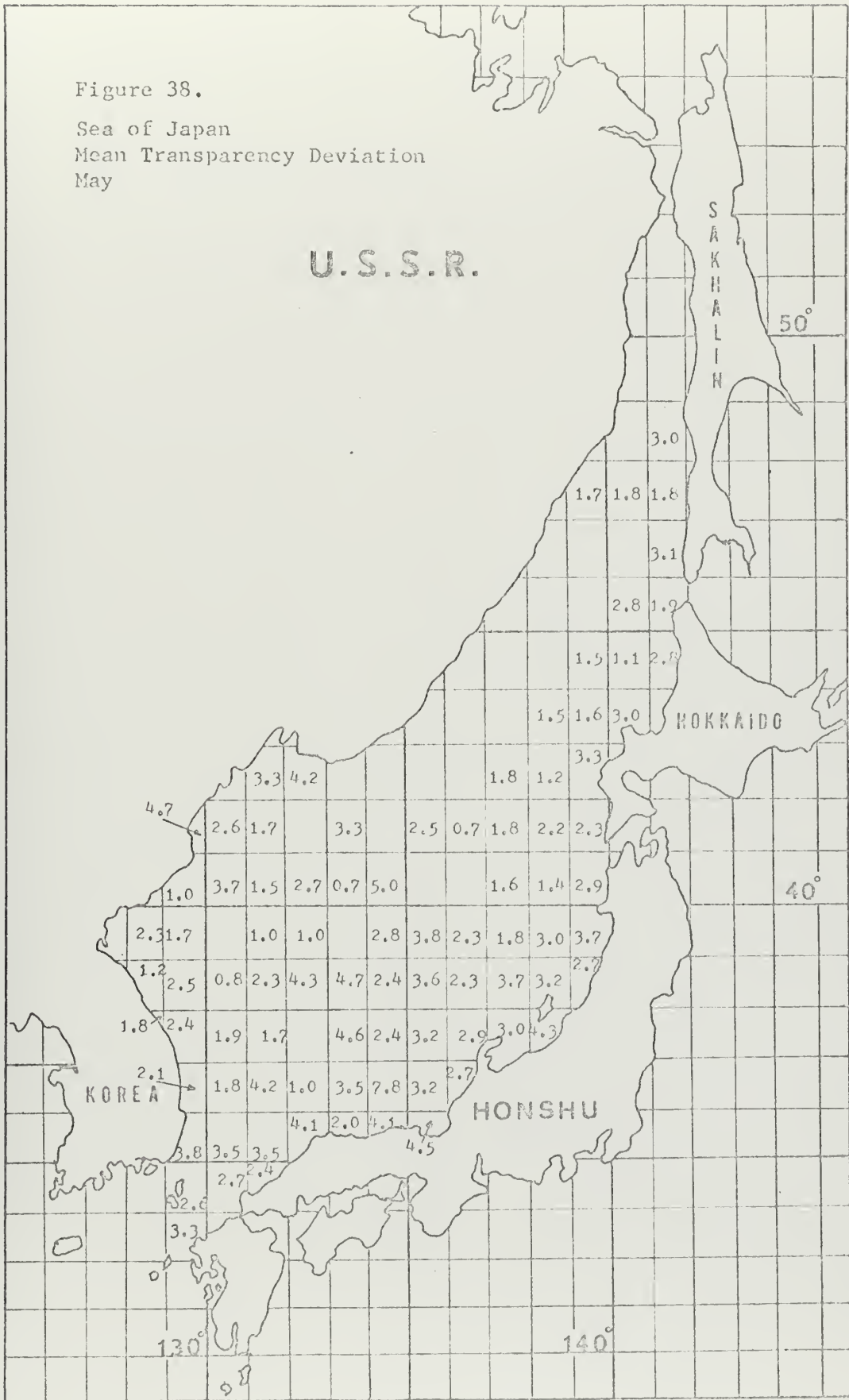


Figure 39.

Sea of Japan
Mean Transparency Deviation
June

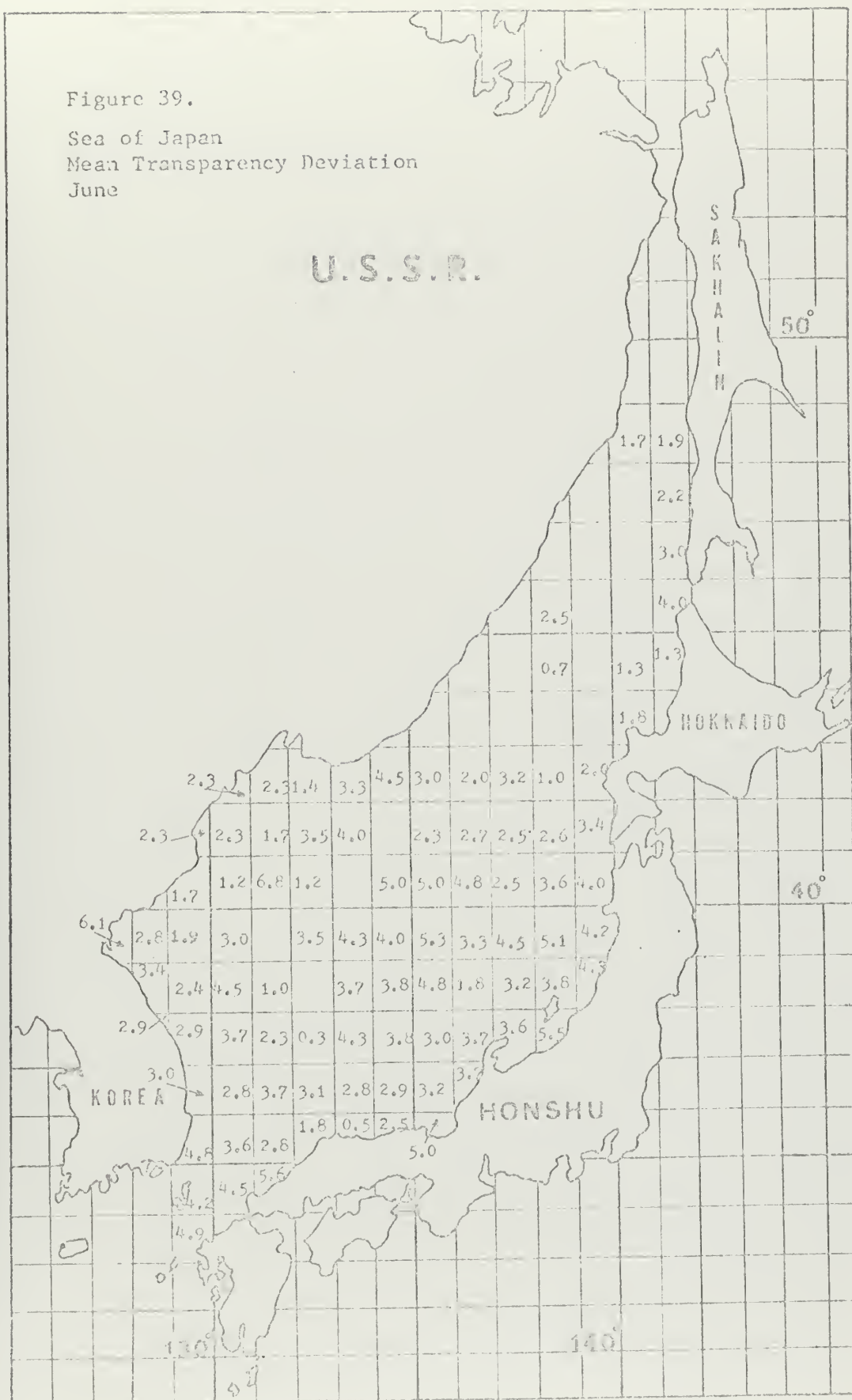


Figure 40.

Sea of Japan
Mean Transparency Deviation
July

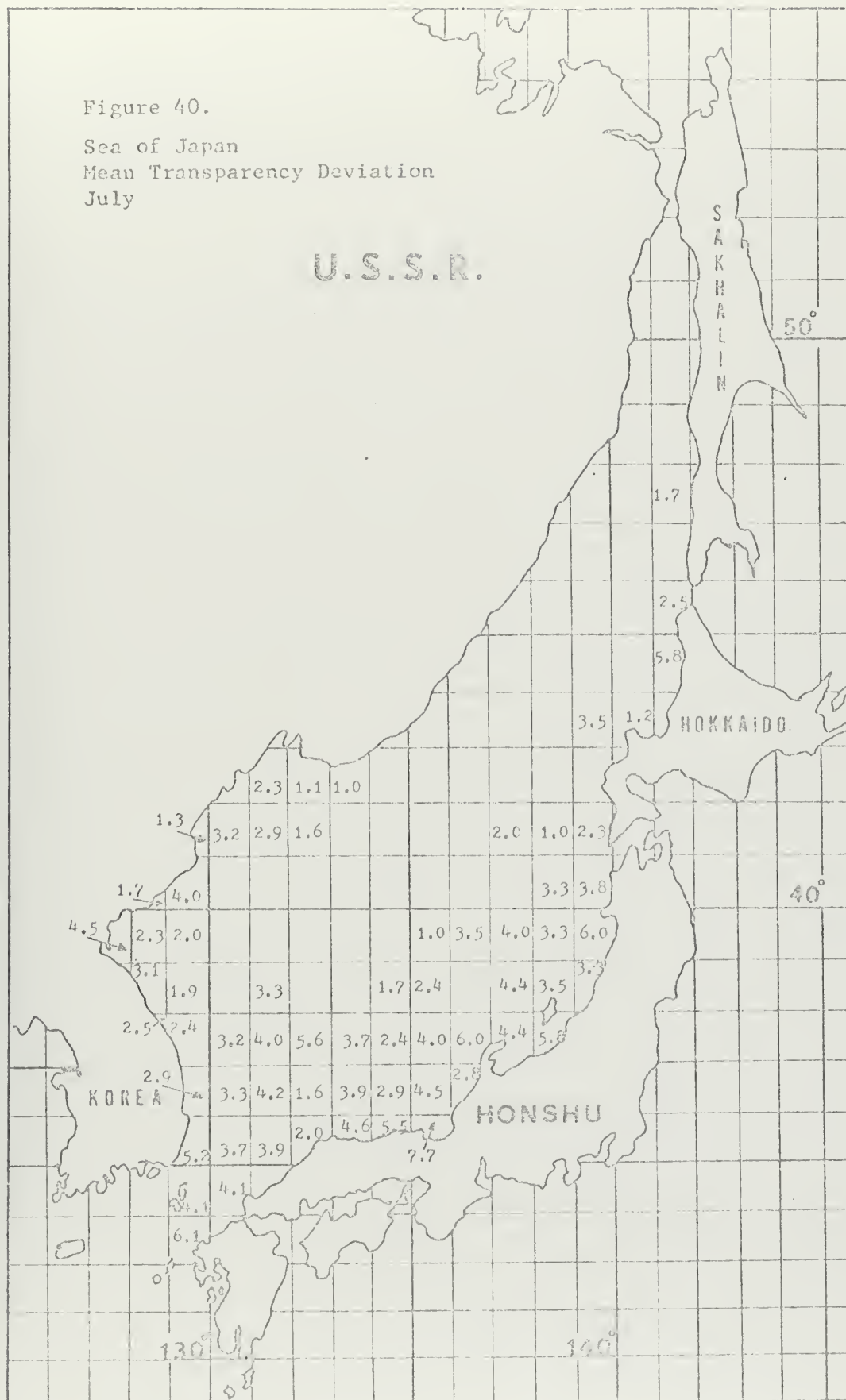


Figure 41.

Sea of Japan
Mean Transparency Deviation
August

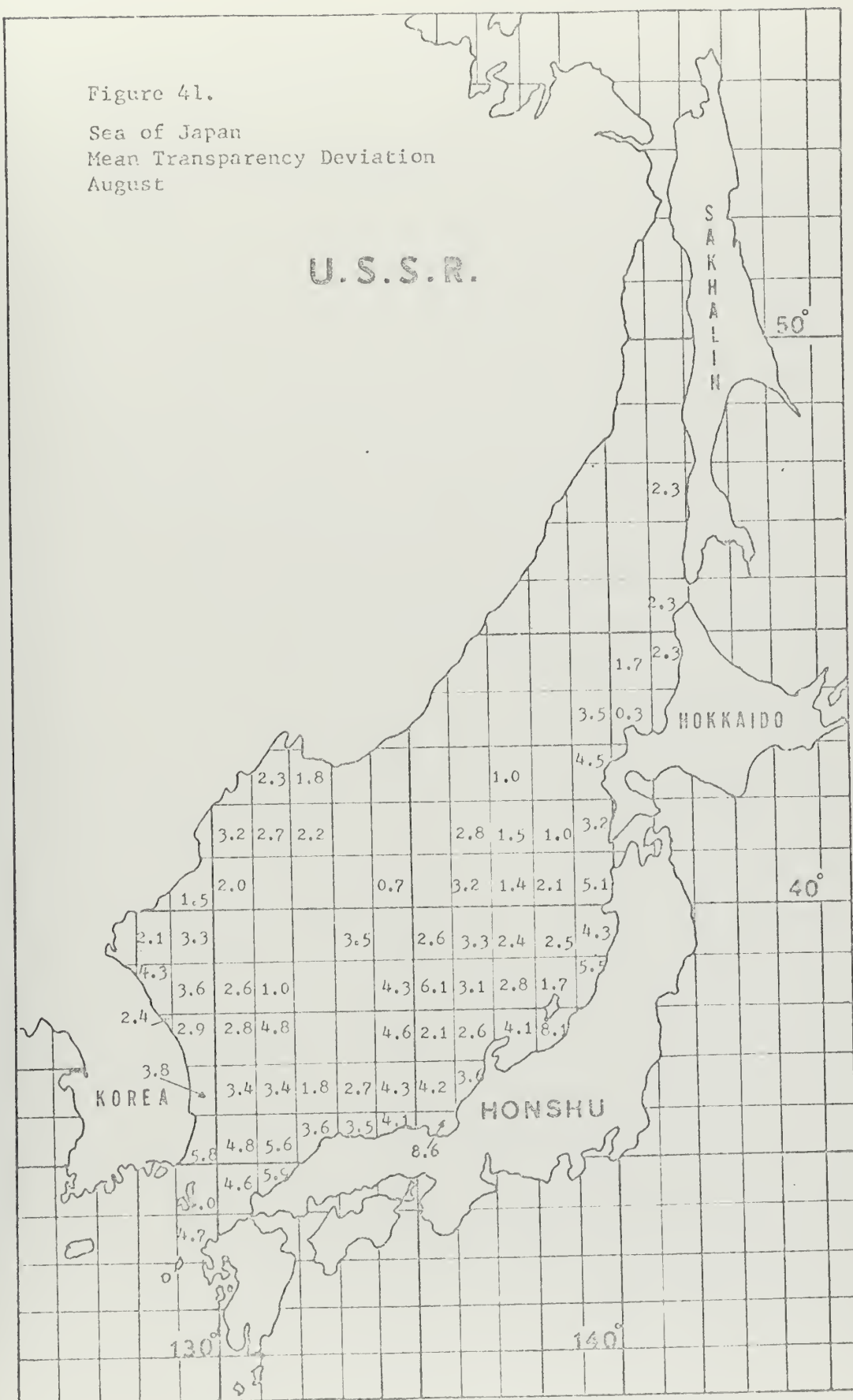


Figure 42.

Sea of Japan
Mean Transparency Deviation
September

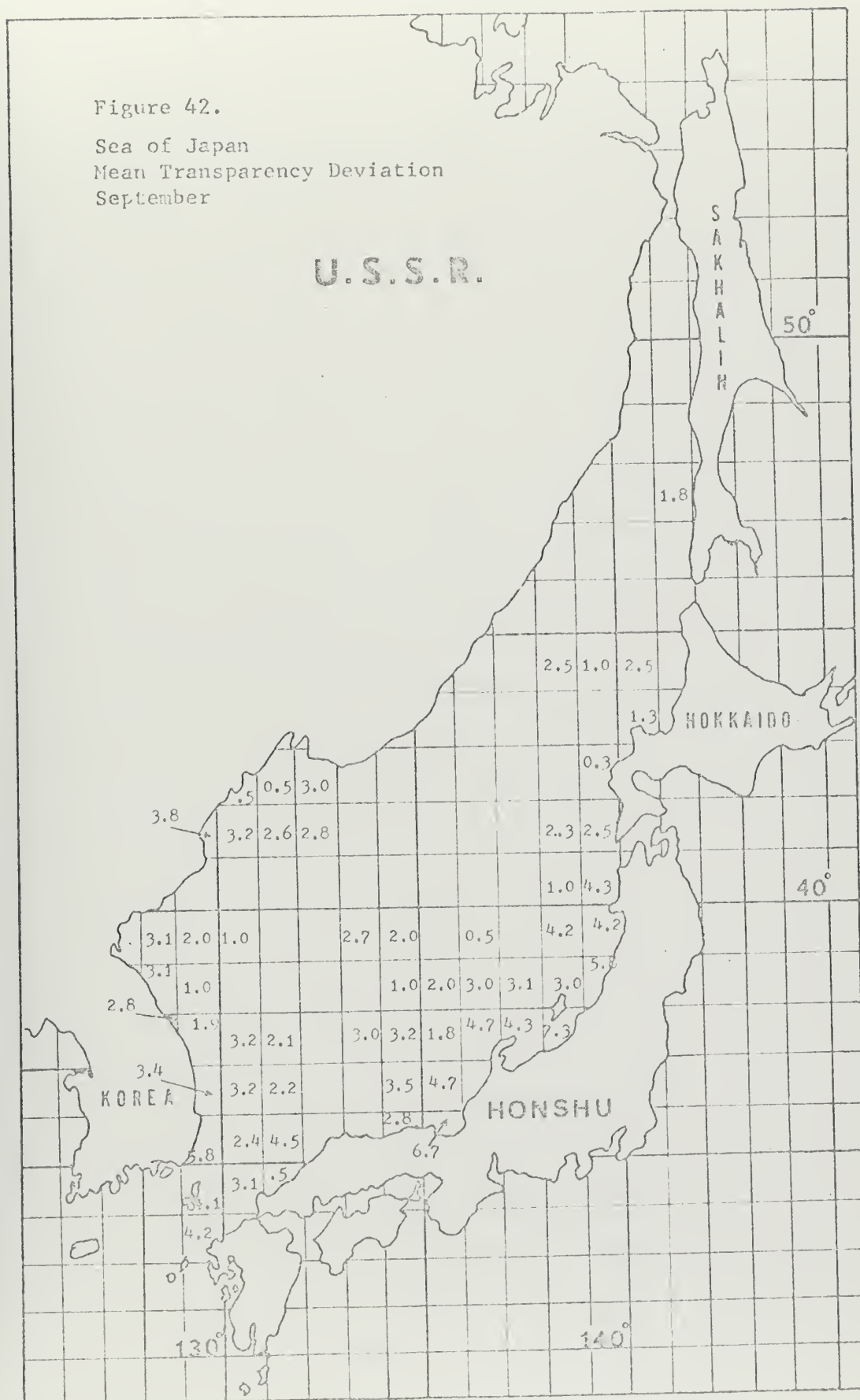


Figure 43.

Sea of Japan
Mean Transparency Deviation
October

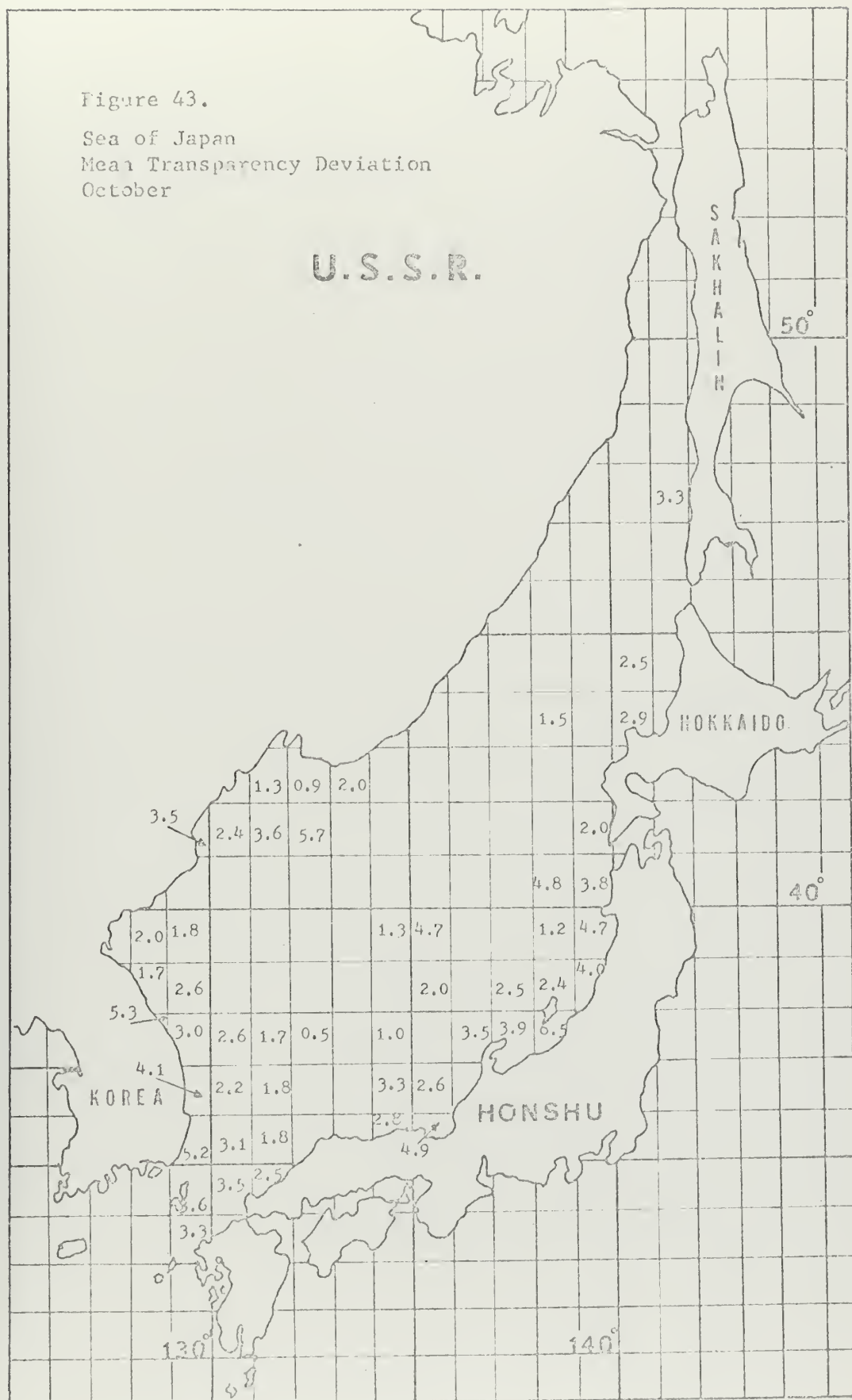


Figure 44.

Sea of Japan
Mean Transparency Deviation
November

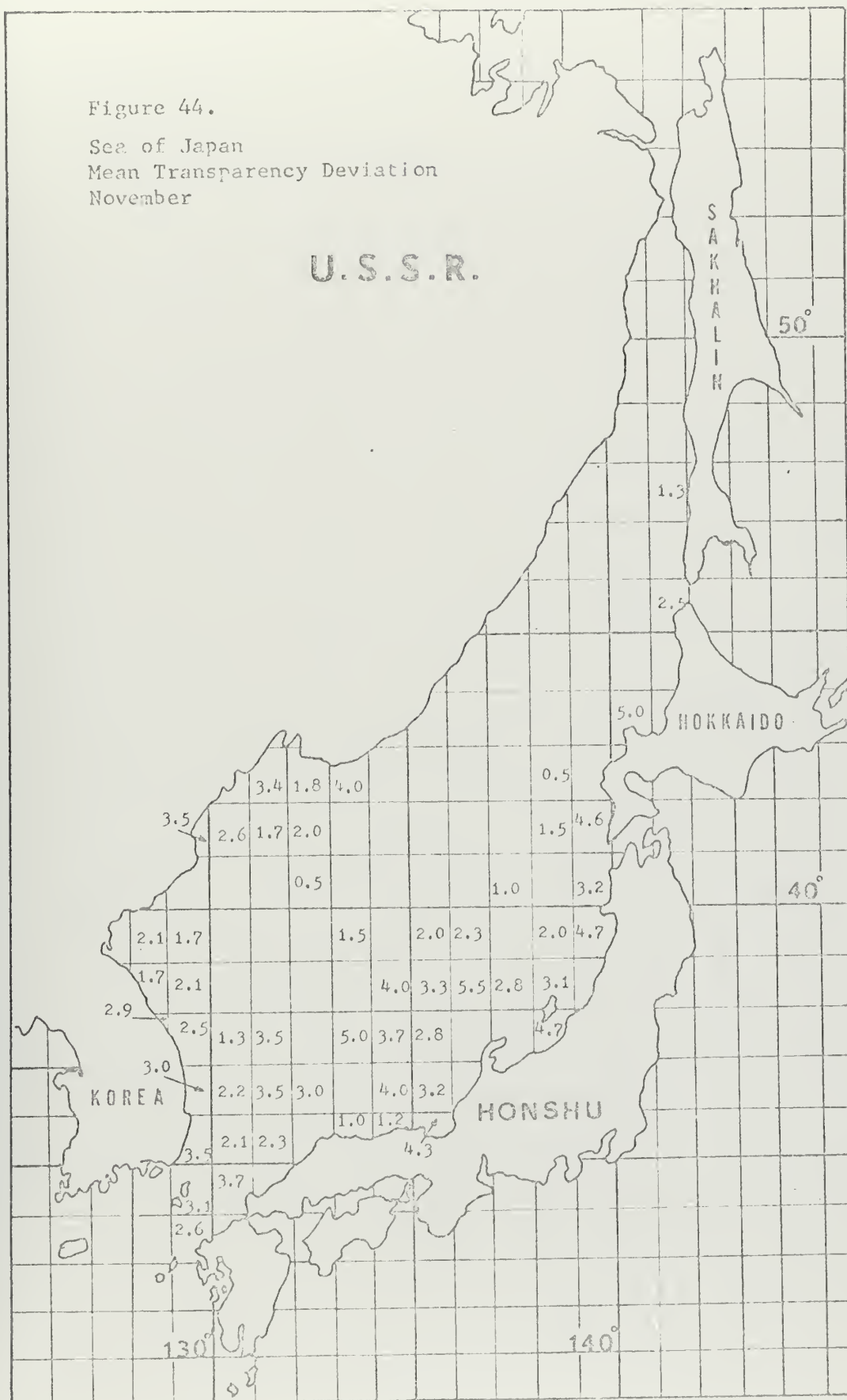


Figure 45.

Sea of Japan
Mean Transparency Deviation
December

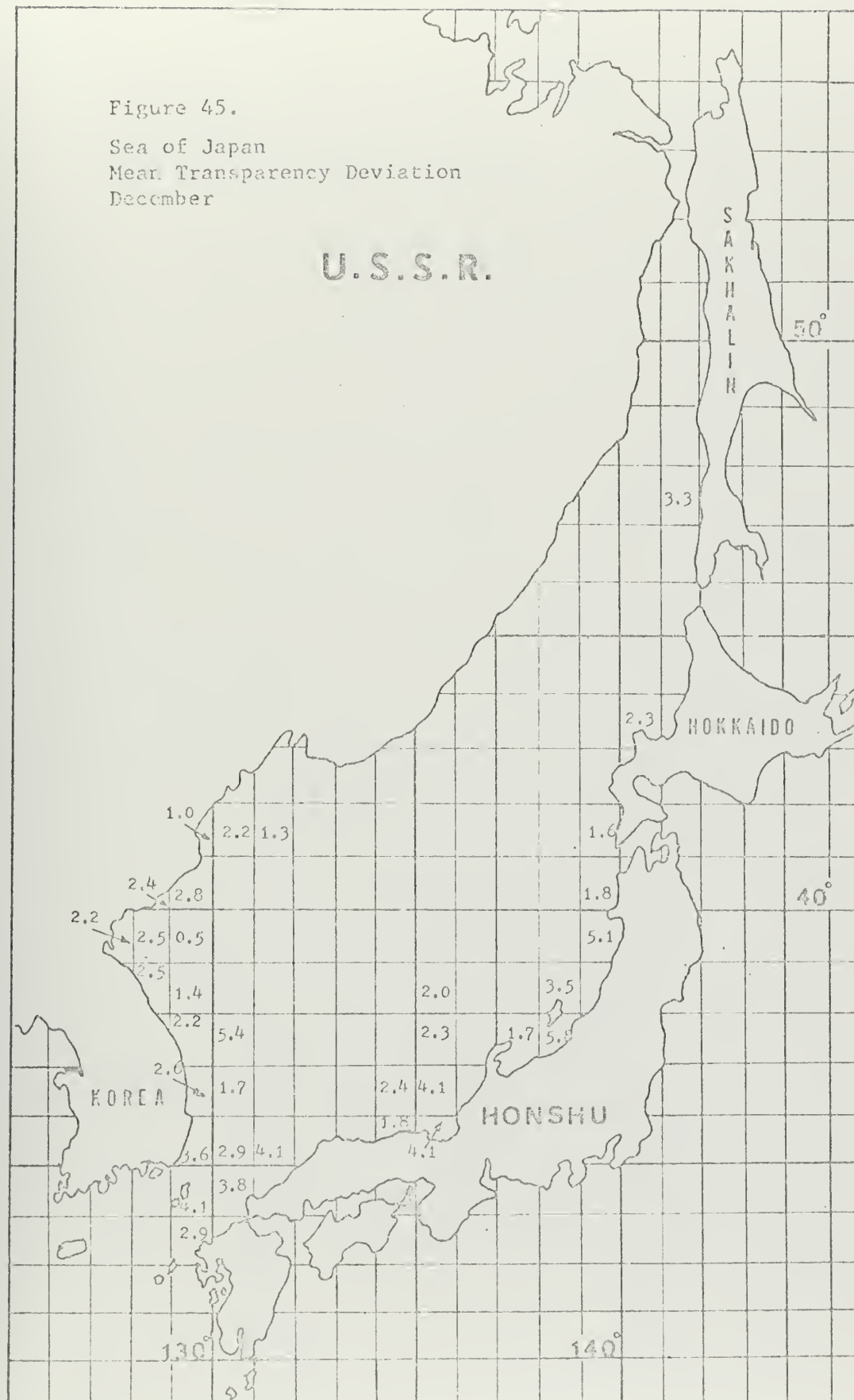


Figure 46.

Sea of Japan
Mean Deviation of all Color Data

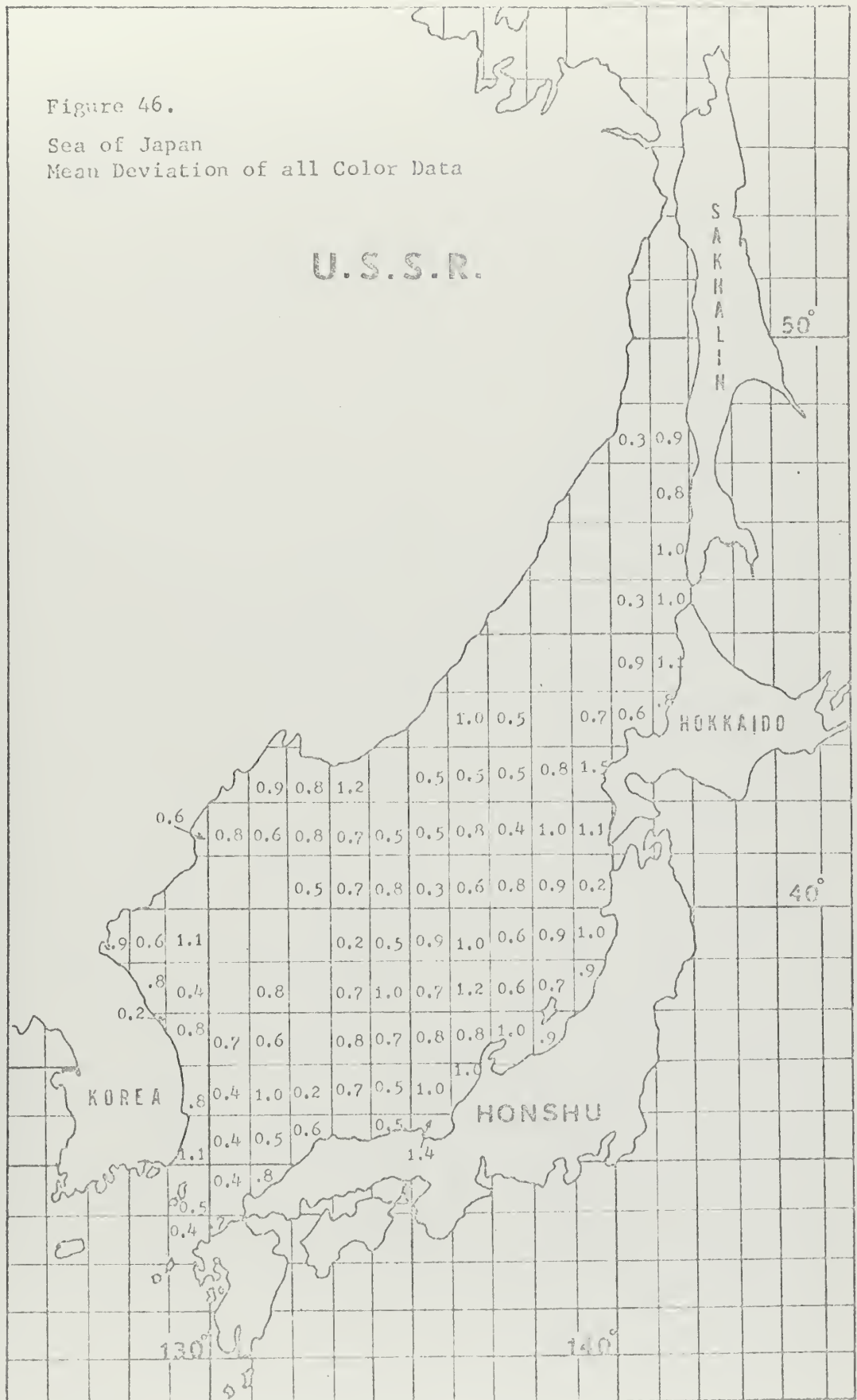
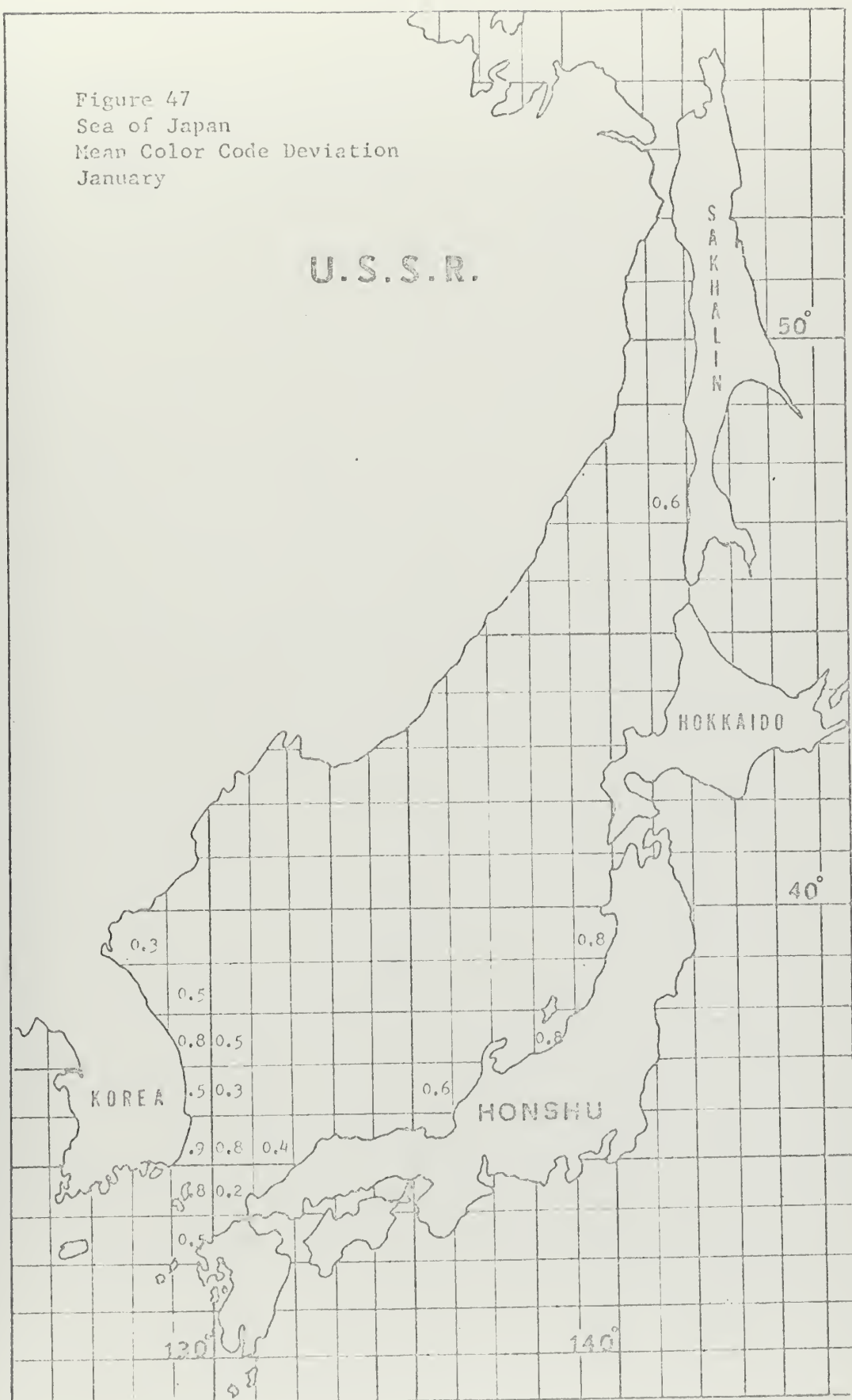


Figure 47
Sea of Japan
Mean Color Code Deviation
January



Sea of Japan
Mean Color Code Deviation
February

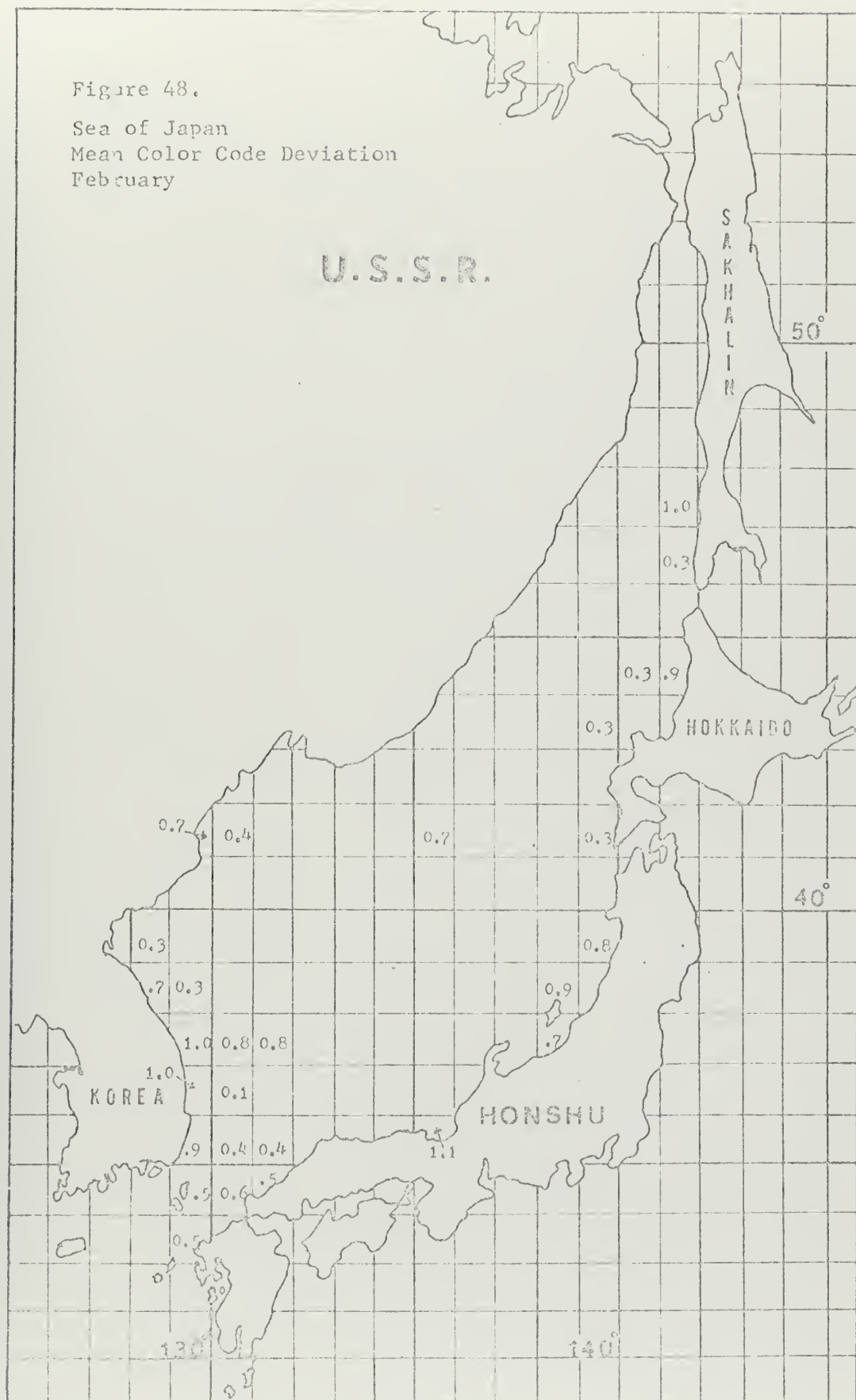


Figure 49.

Sea of Japan
Mean Color Code Deviation
March

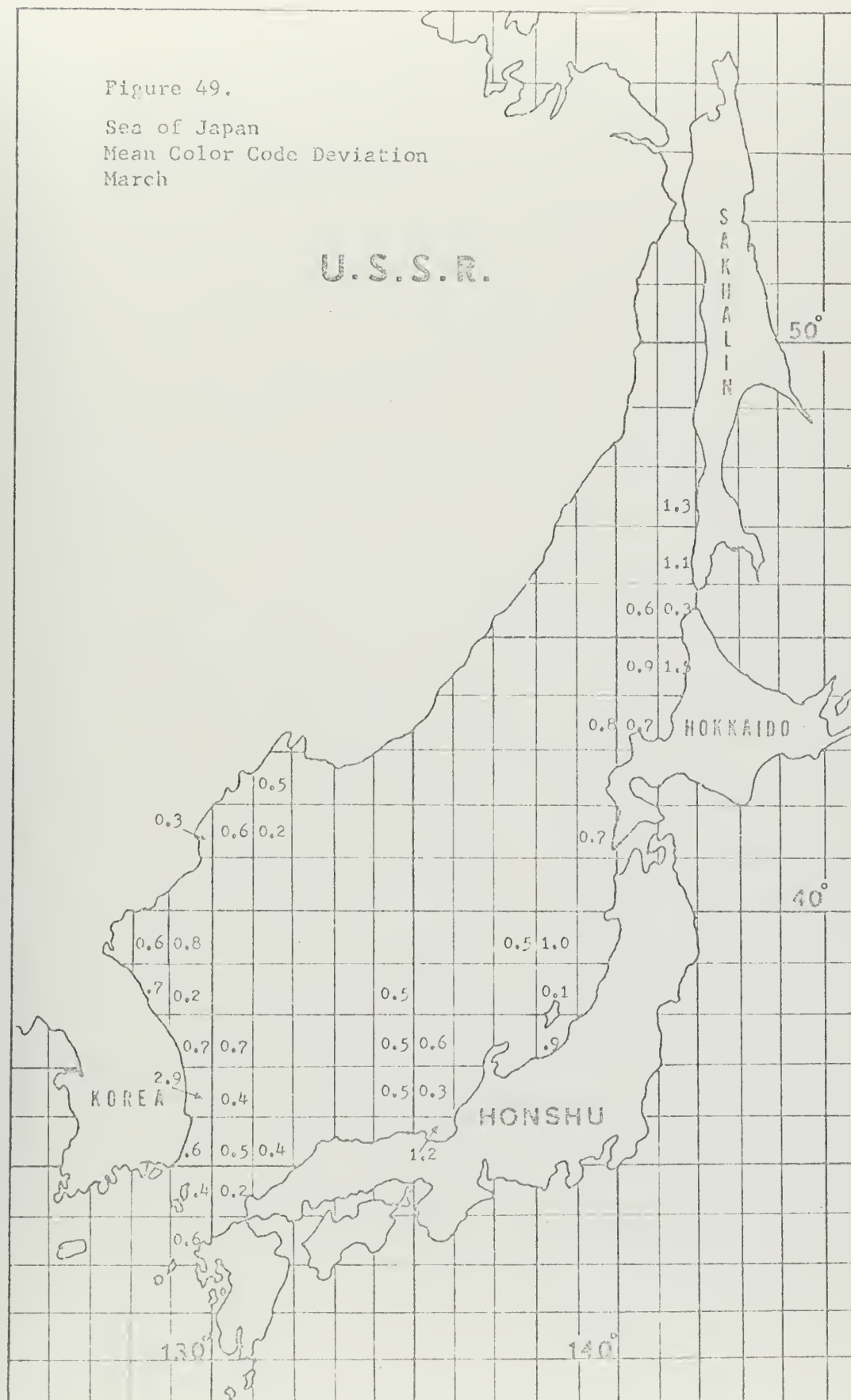


Figure 50.

Sea of Japan
Mean Color Code Deviation
April

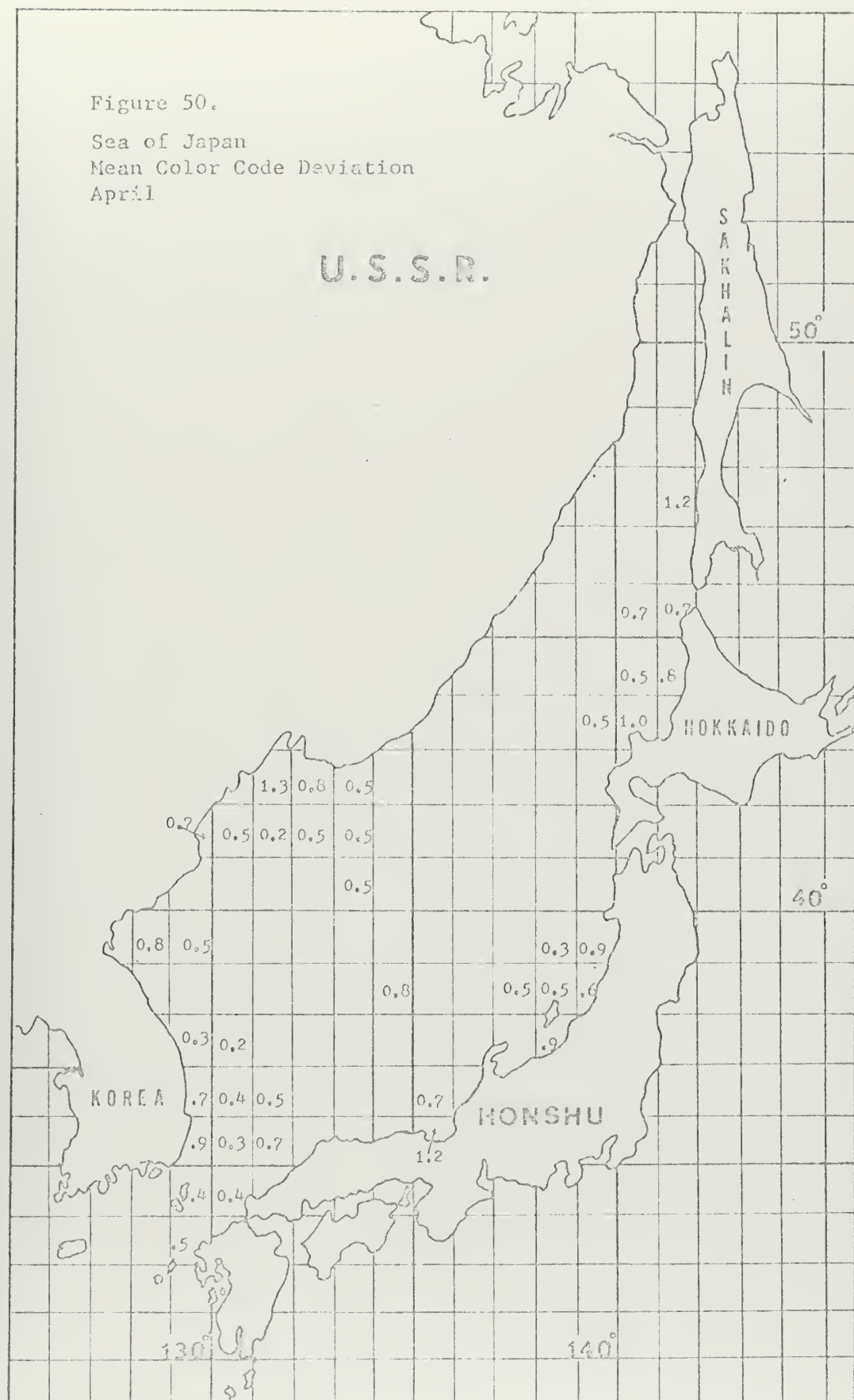


Figure 51.

Sea of Japan
Mean Color Code Deviation
May

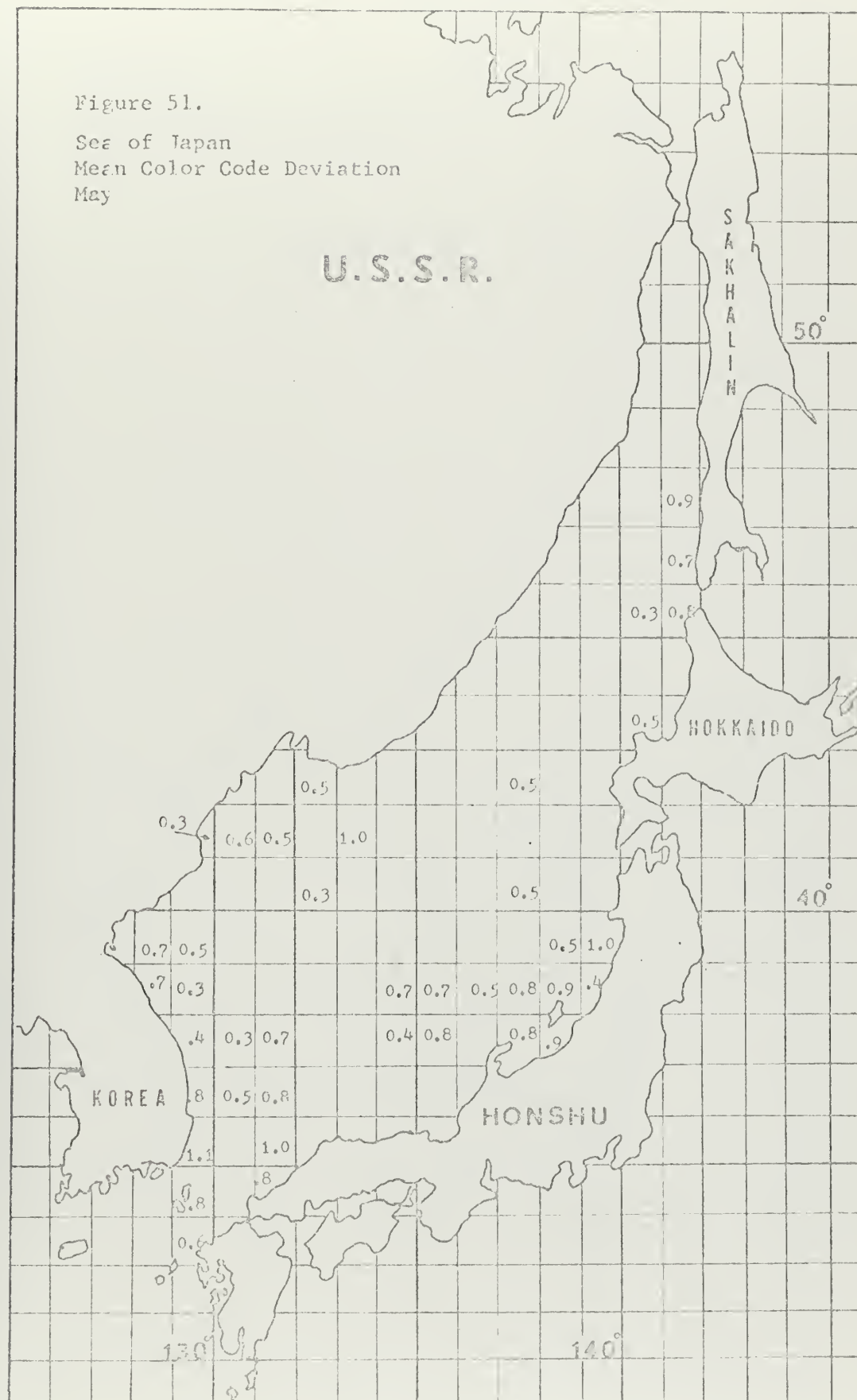


Figure 52.

Sea of Japan

Mean Color Code Deviation

June

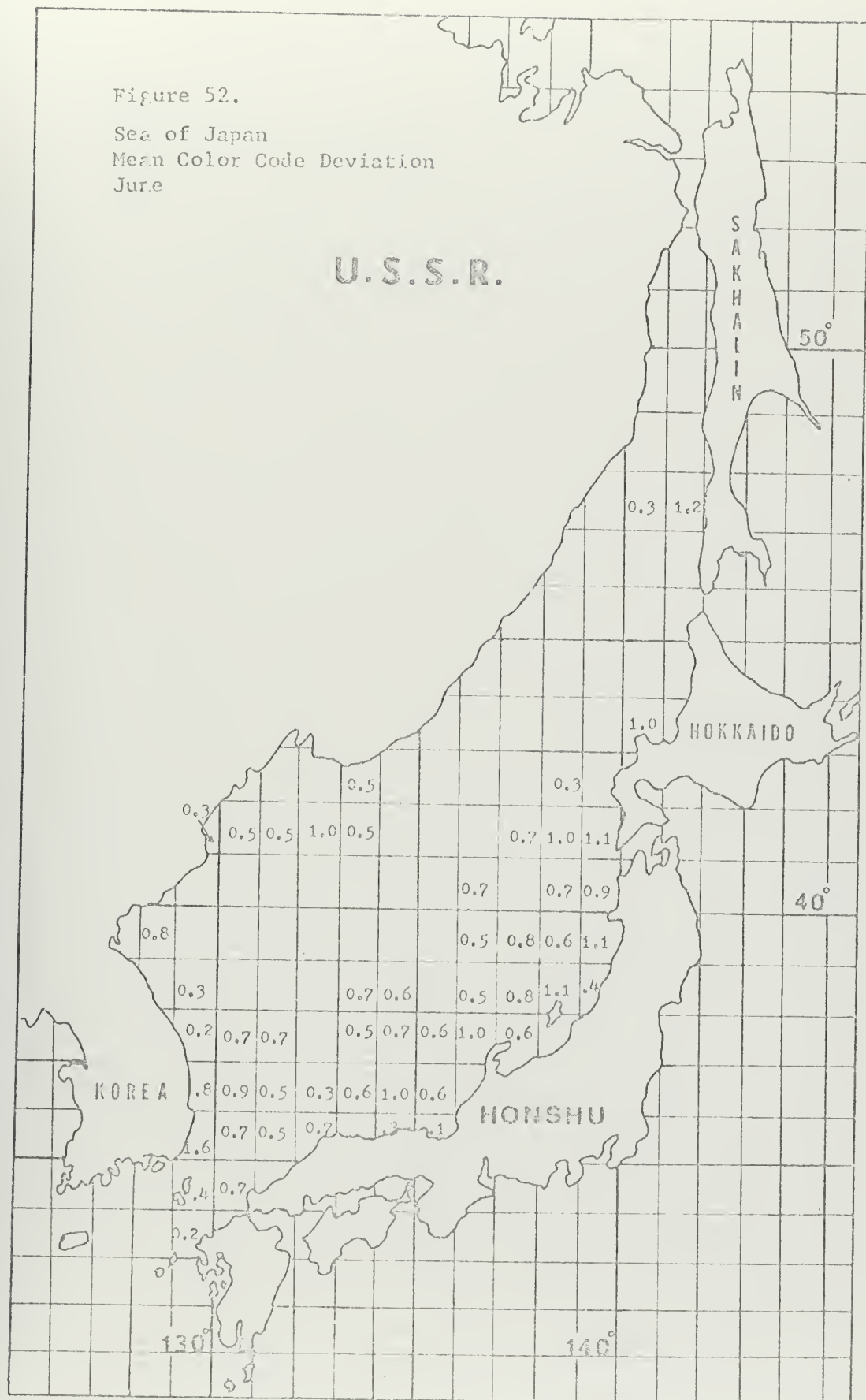


Figure 53.

Sea of Japan
Mean Color Code Deviation
July

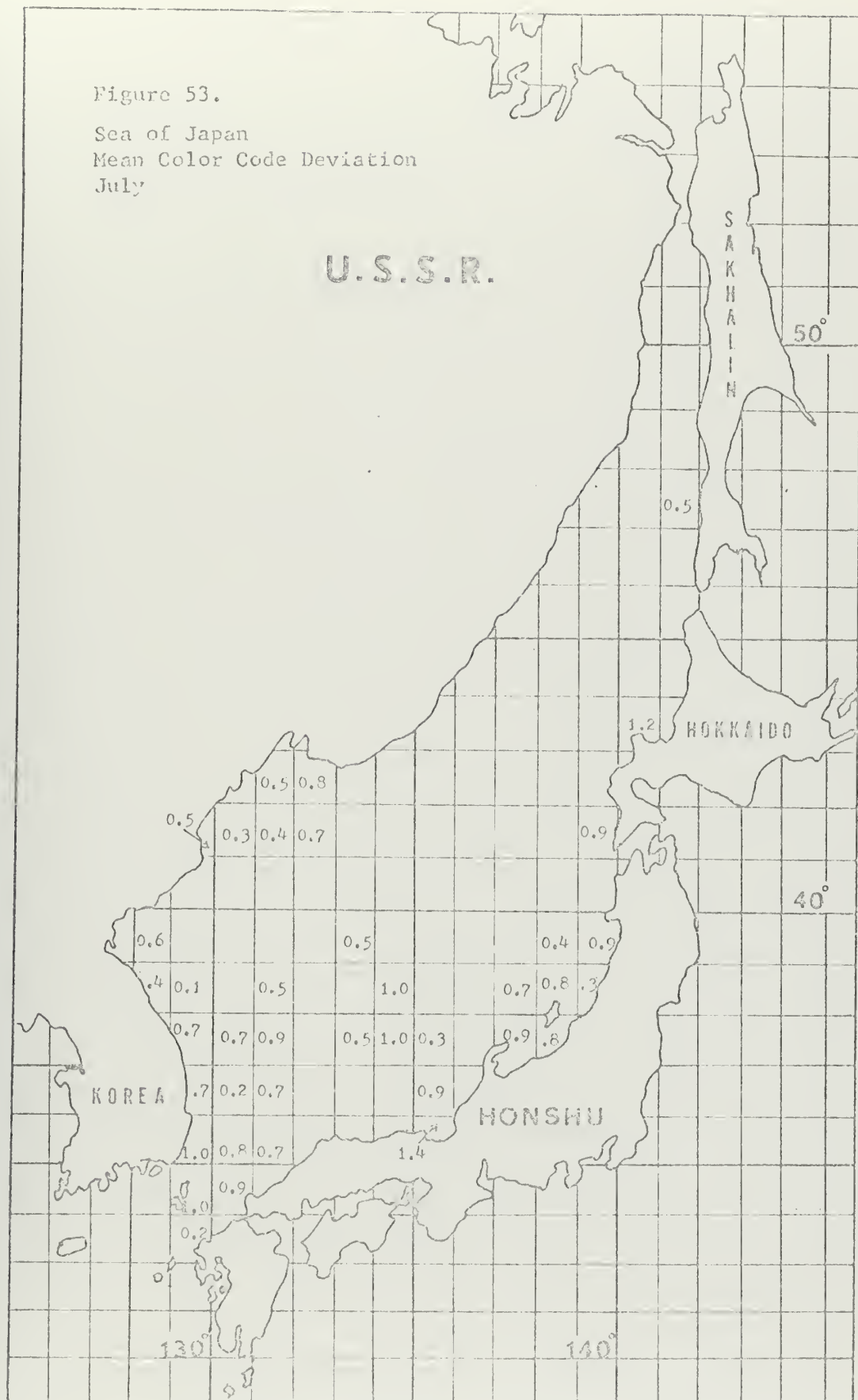


Figure 54.

Sea of Japan
Mean Color Code Deviation
August

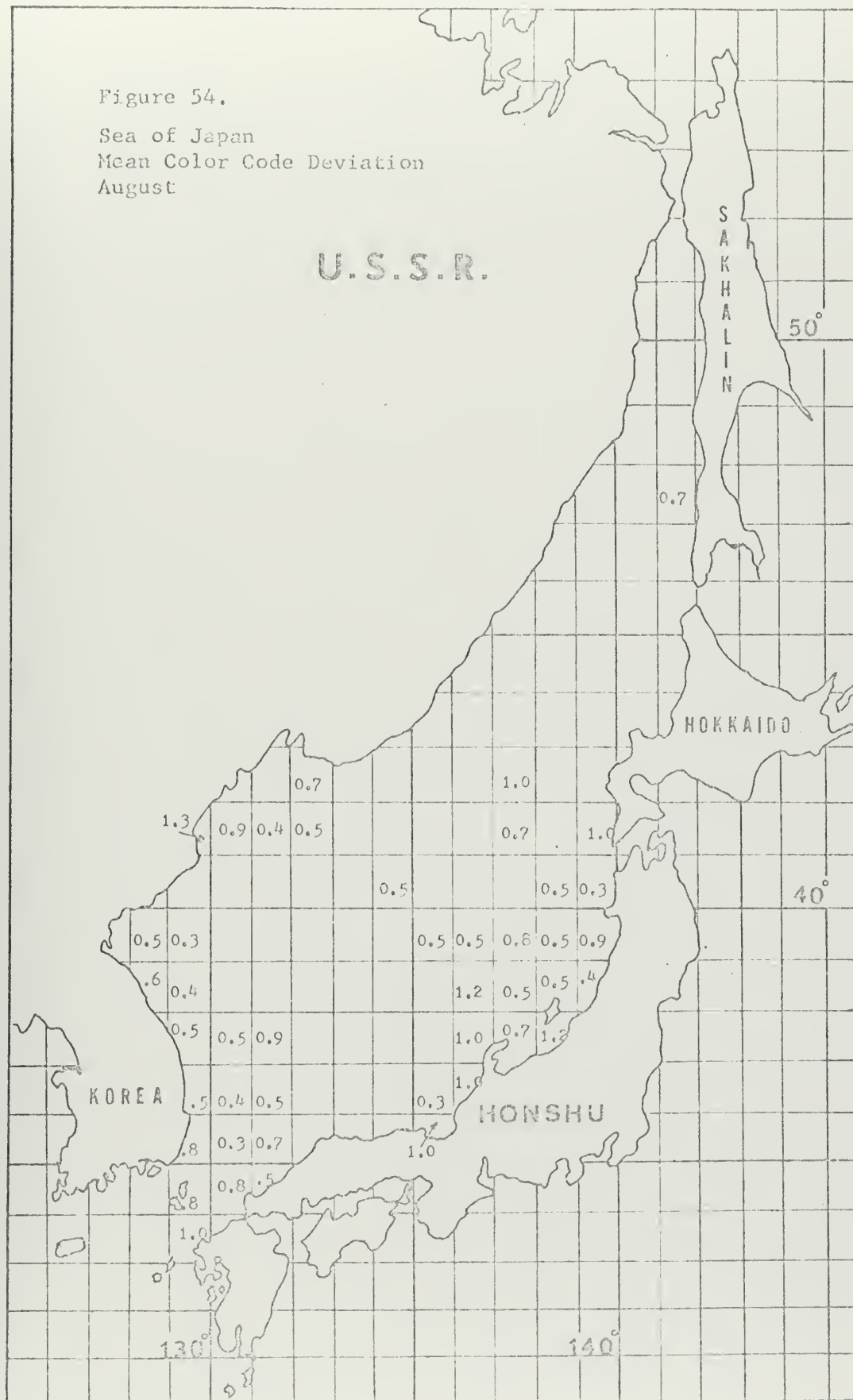


Figure 55.

Sea of Japan
Mean Color Code Deviation
September

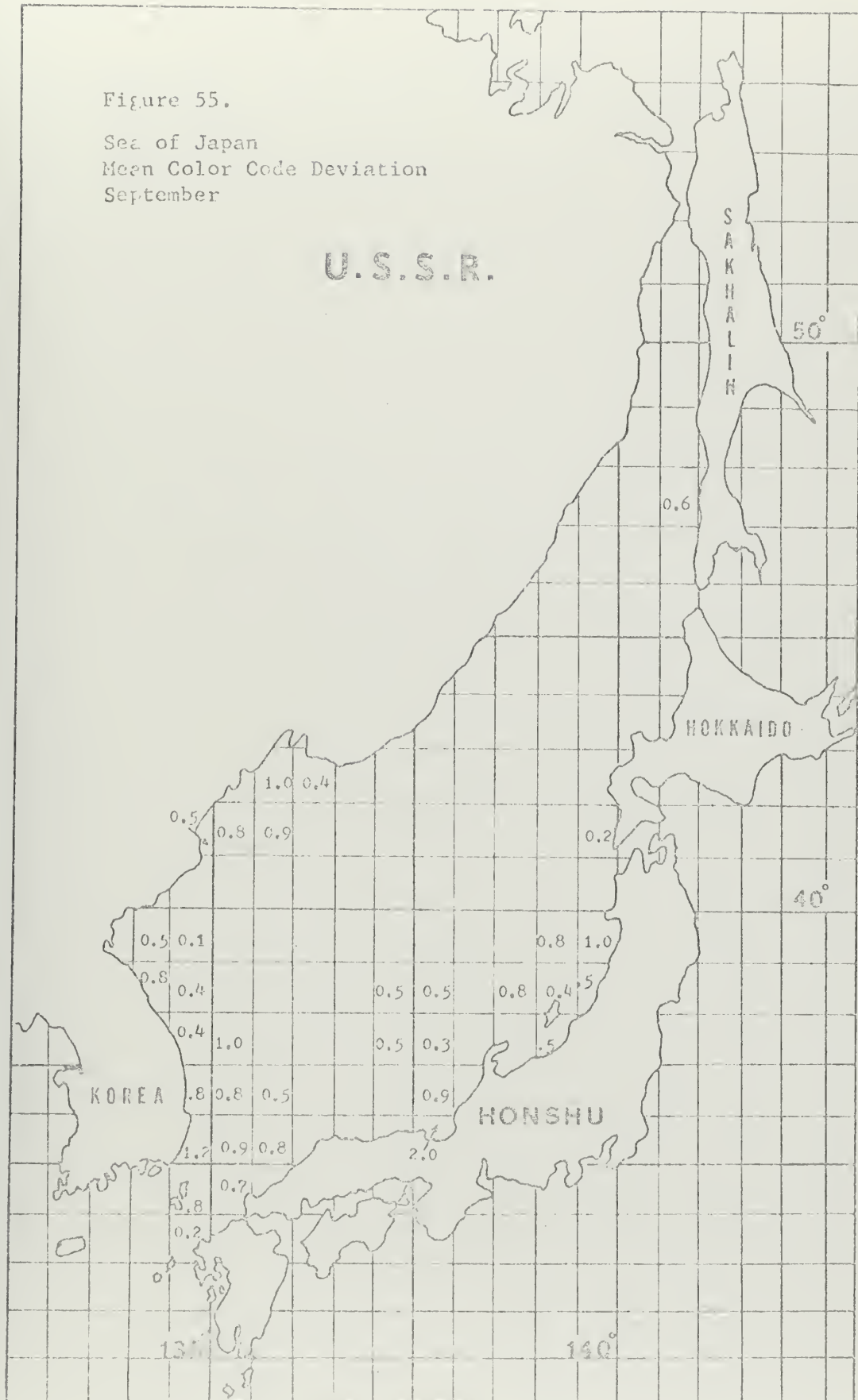


Figure 56.

Sea of Japan
Mean Color Code Deviation
October

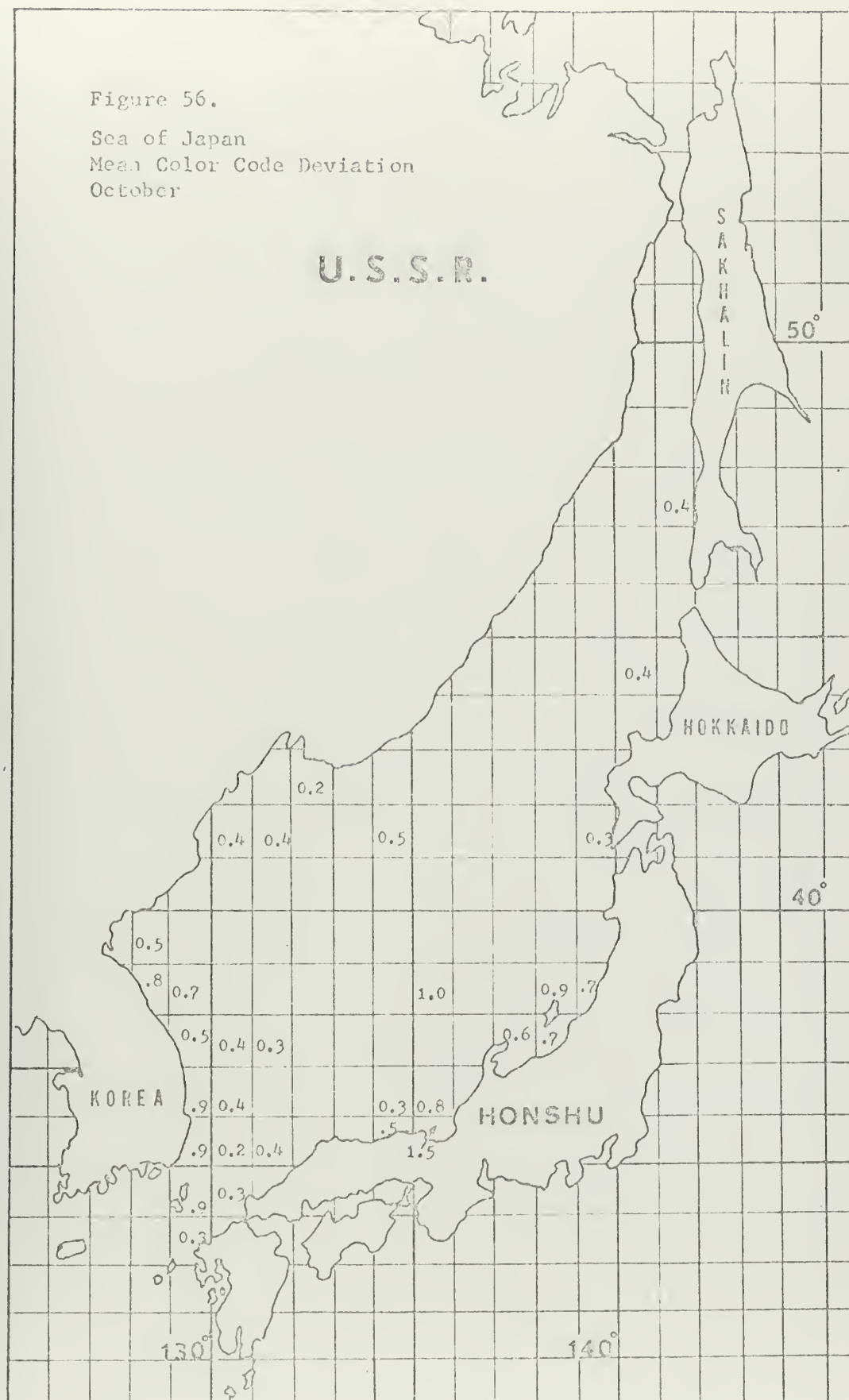


Figure 57.

Sea of Japan
Mean Color Code Deviation
November

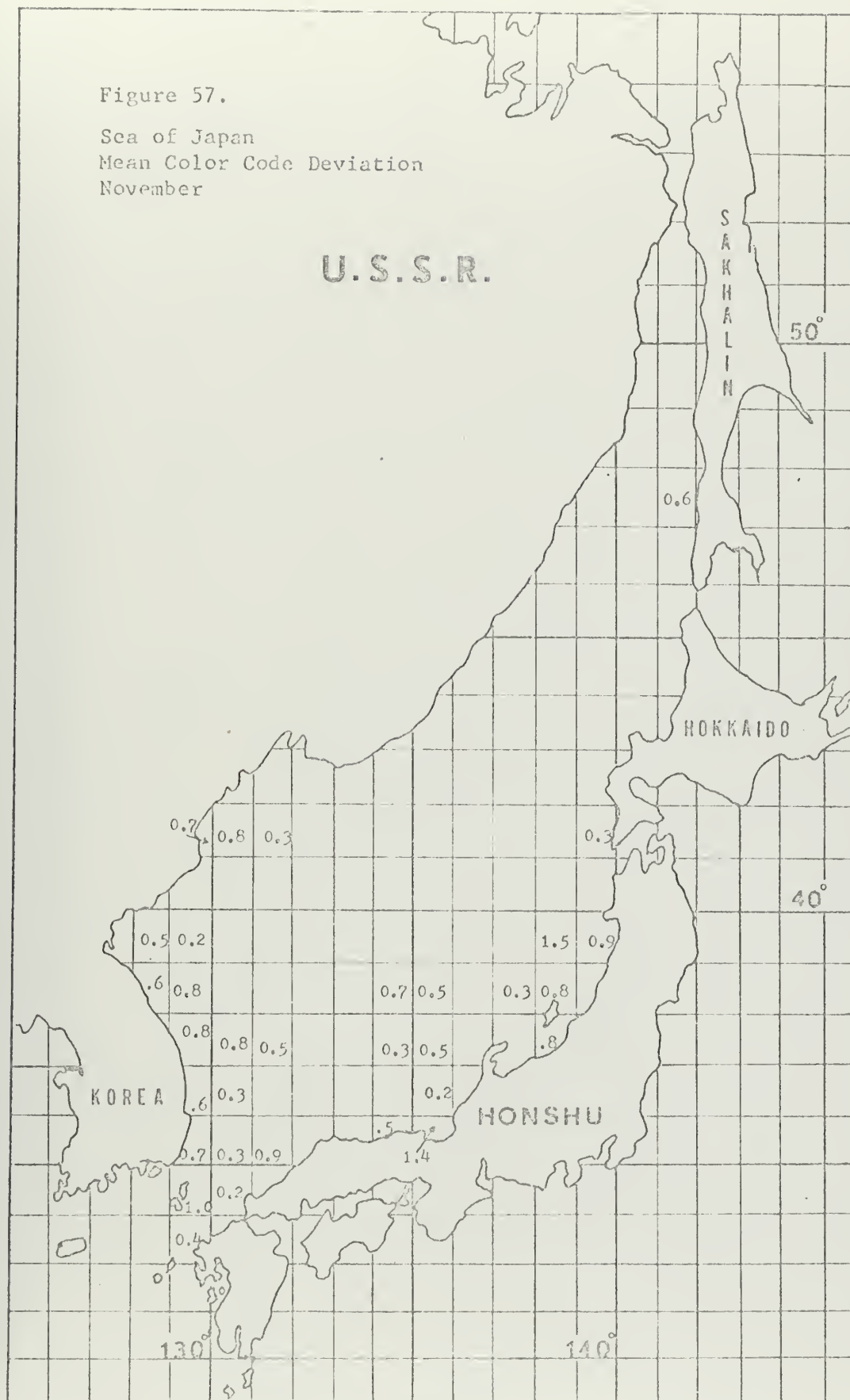


Figure 58.

Sea of Japan
Mean Color Code Deviation
December



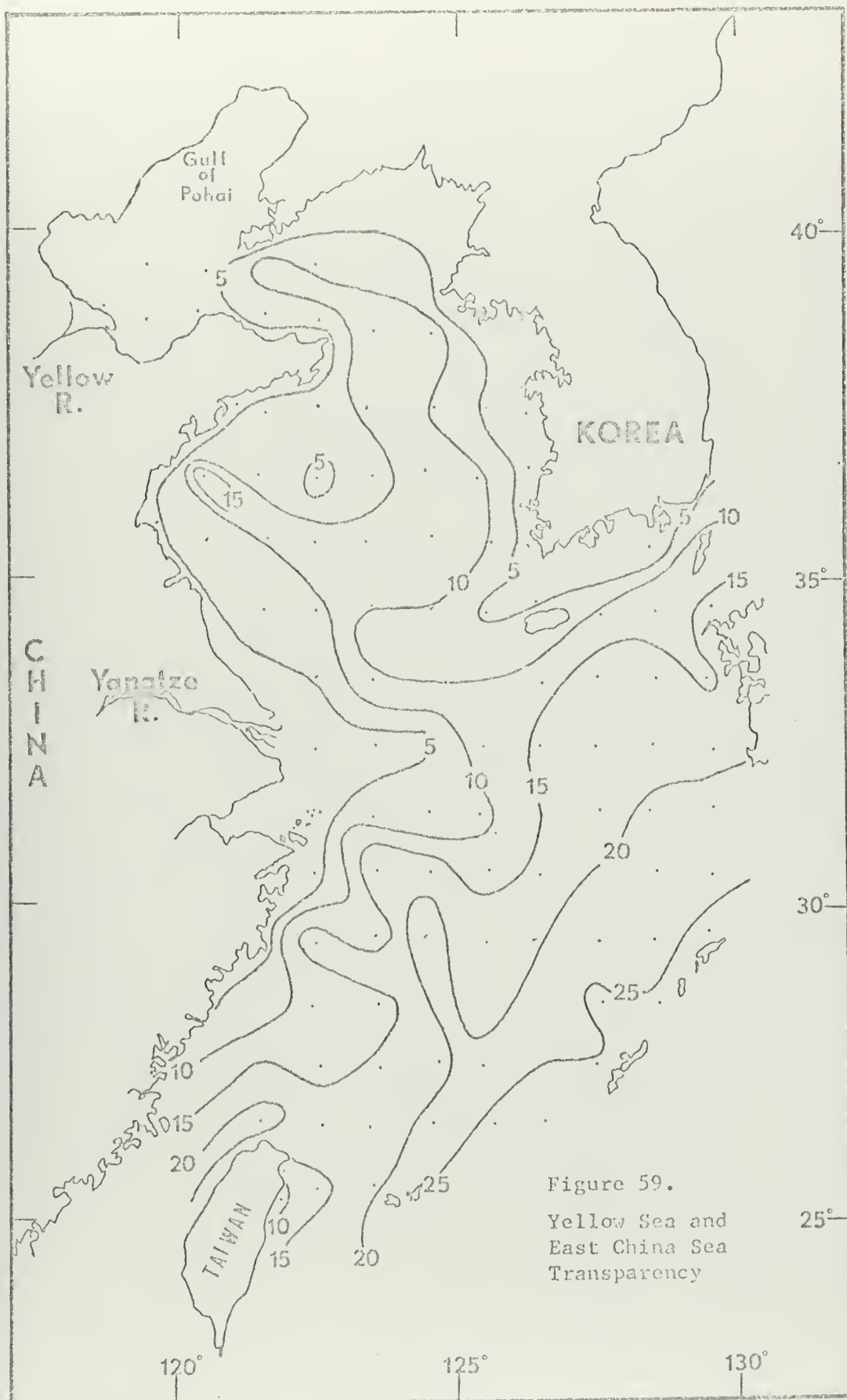


Figure 59.
Yellow Sea and
East China Sea
Transparency

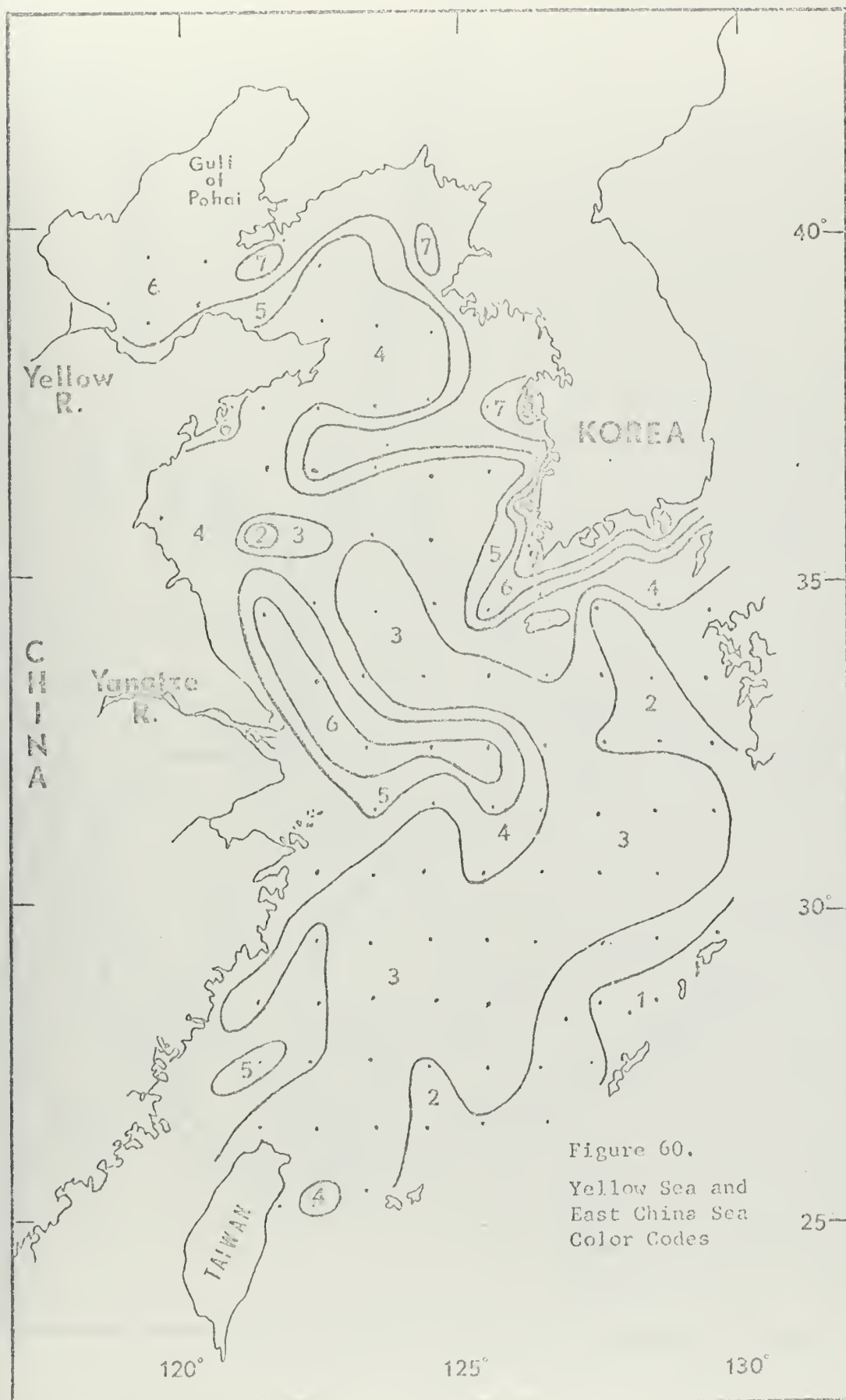


Figure 60.
Yellow Sea and
East China Sea
Color Codes

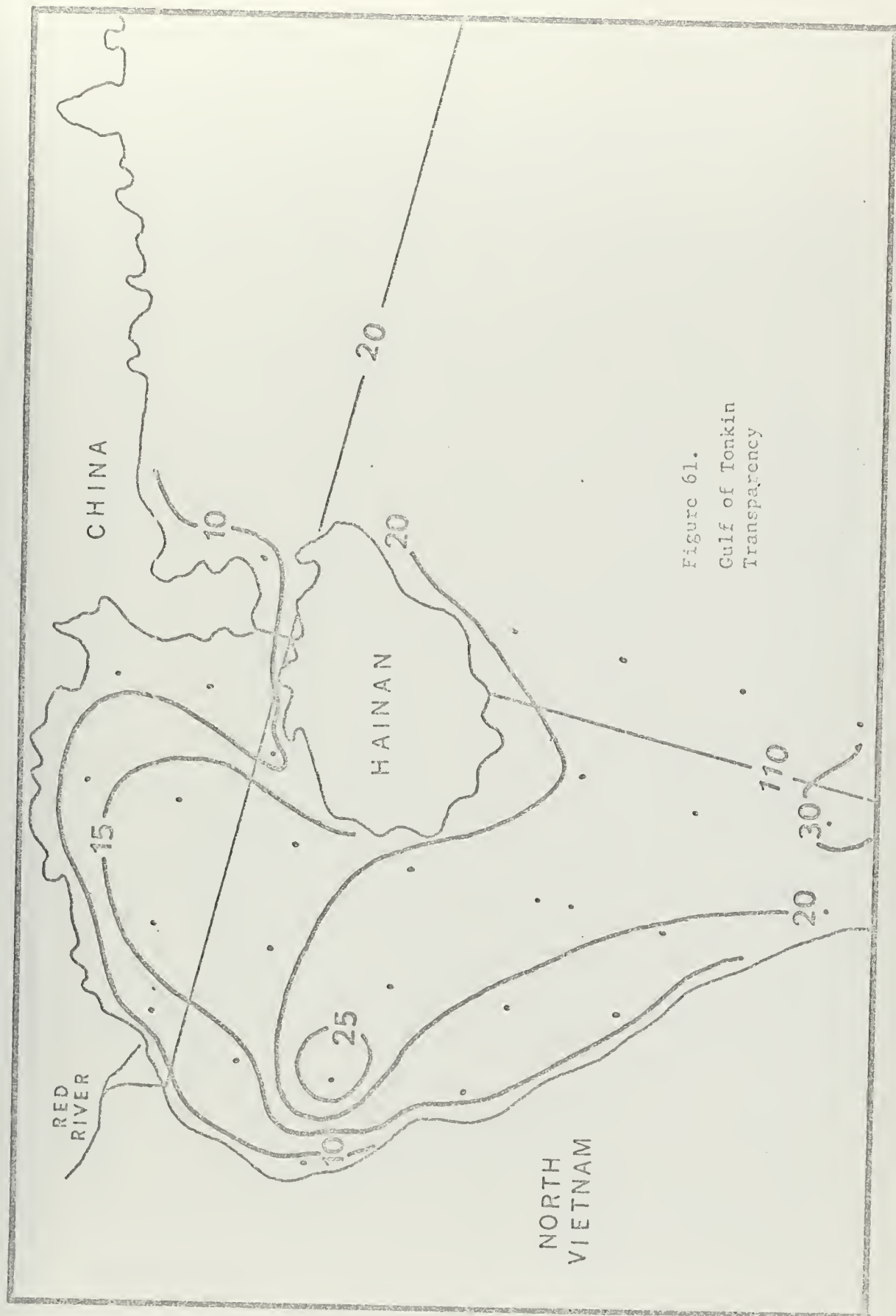


Figure 61.
Gulf of Tonkin
Transparency

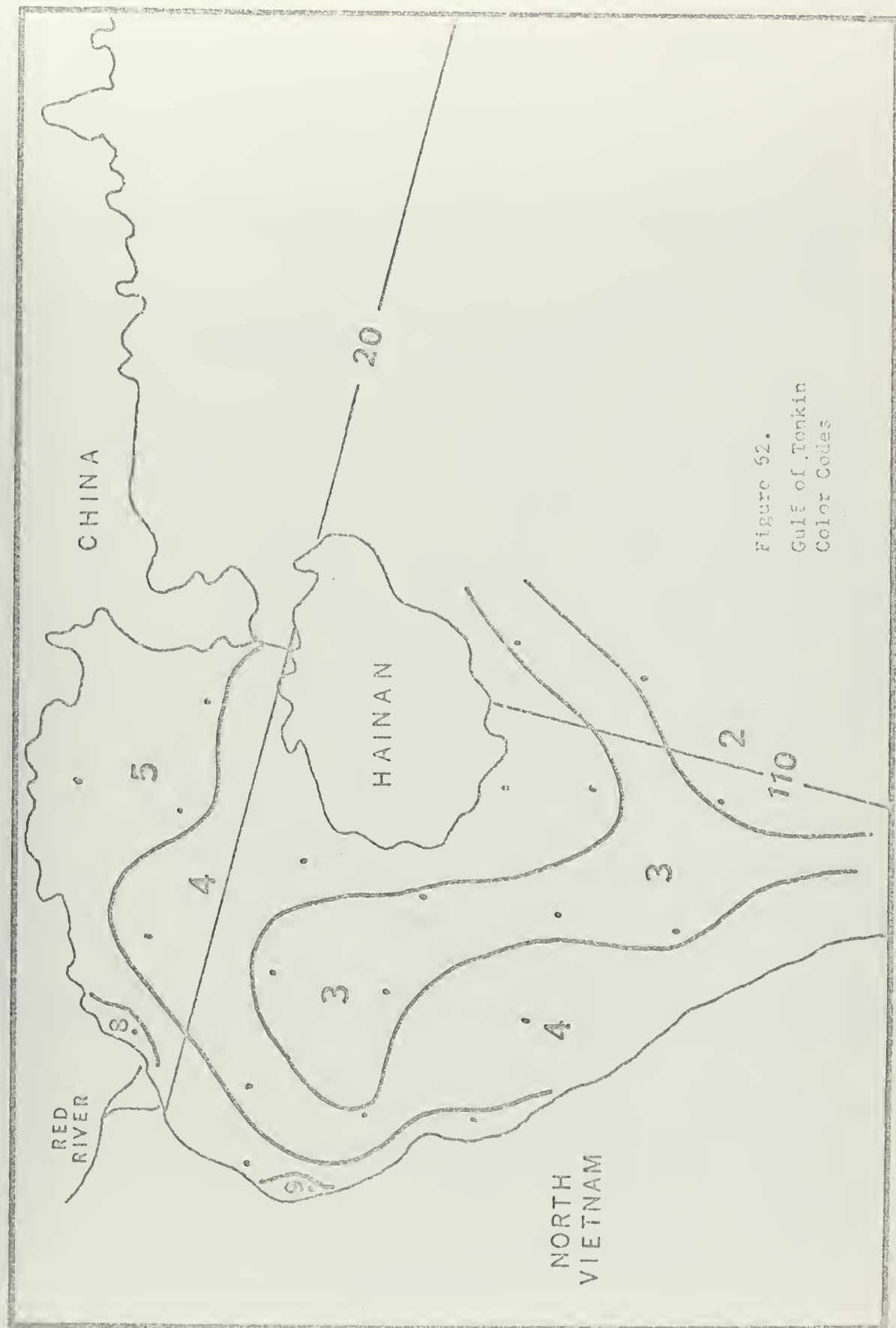


Figure 52.
Gulf of Tonkin
Color Codes

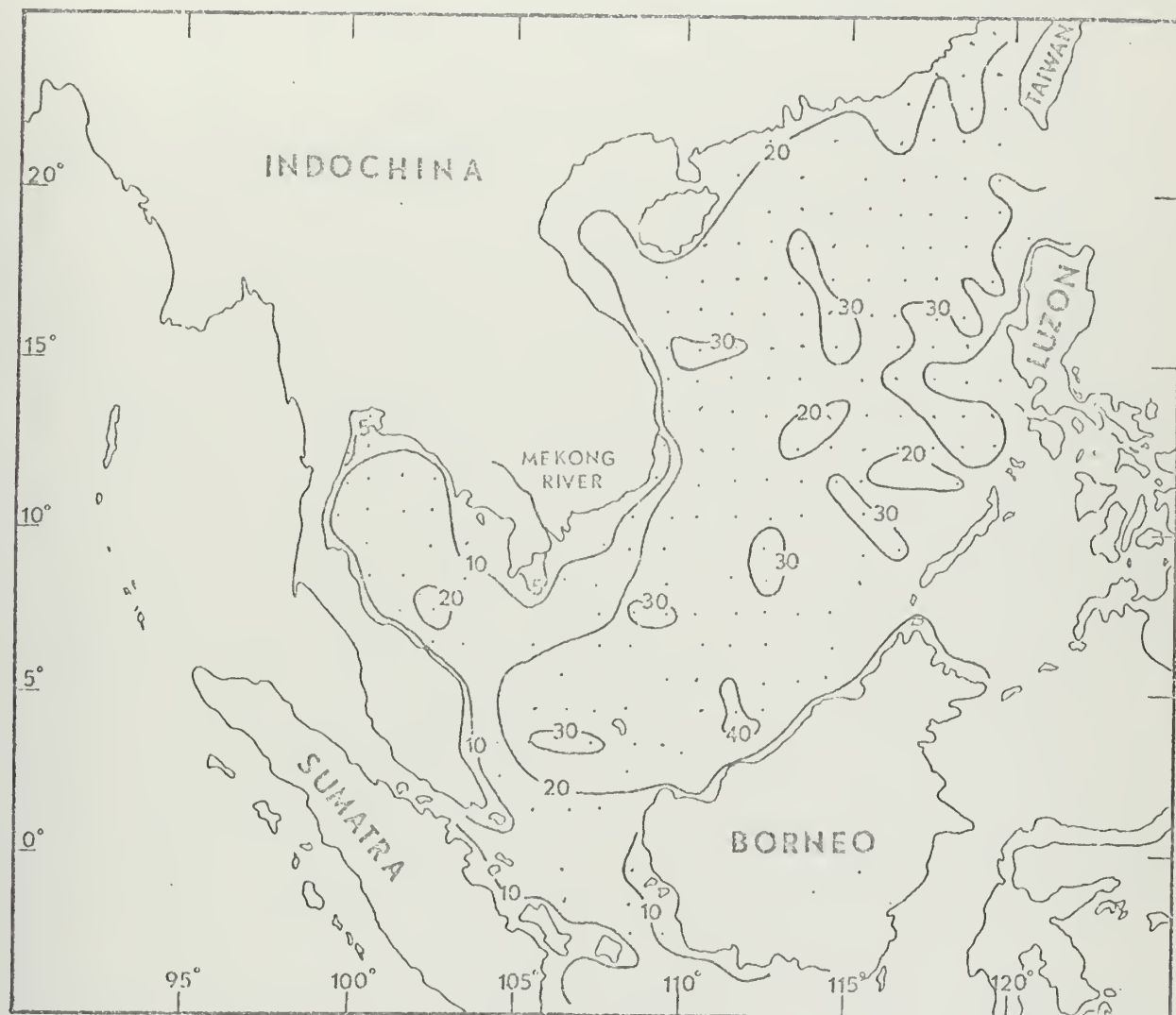


Figure 63. South China Sea and Gulf of Thailand Transparency

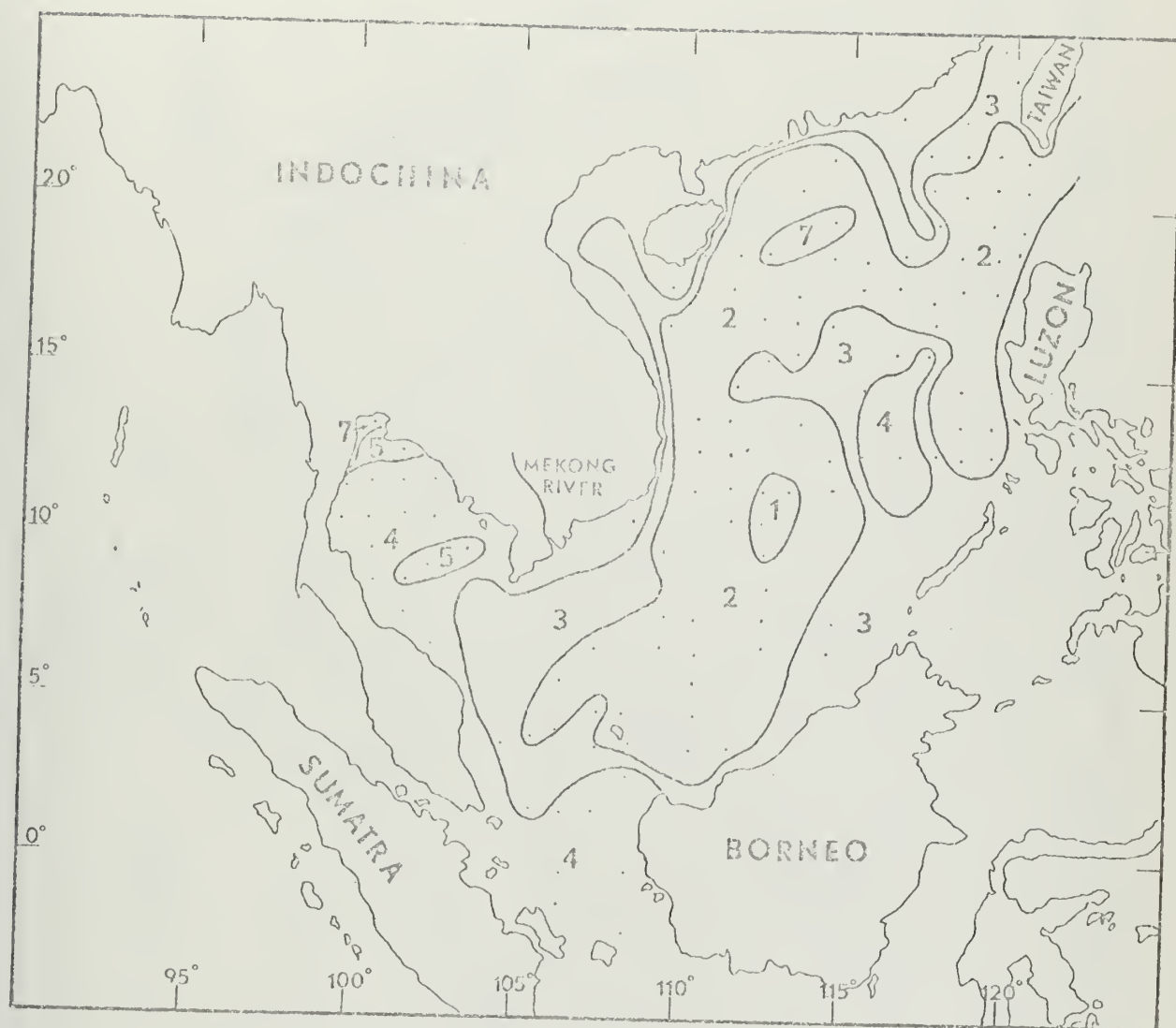


Figure 64. South China Sea and Gulf of Thailand
Color Codes

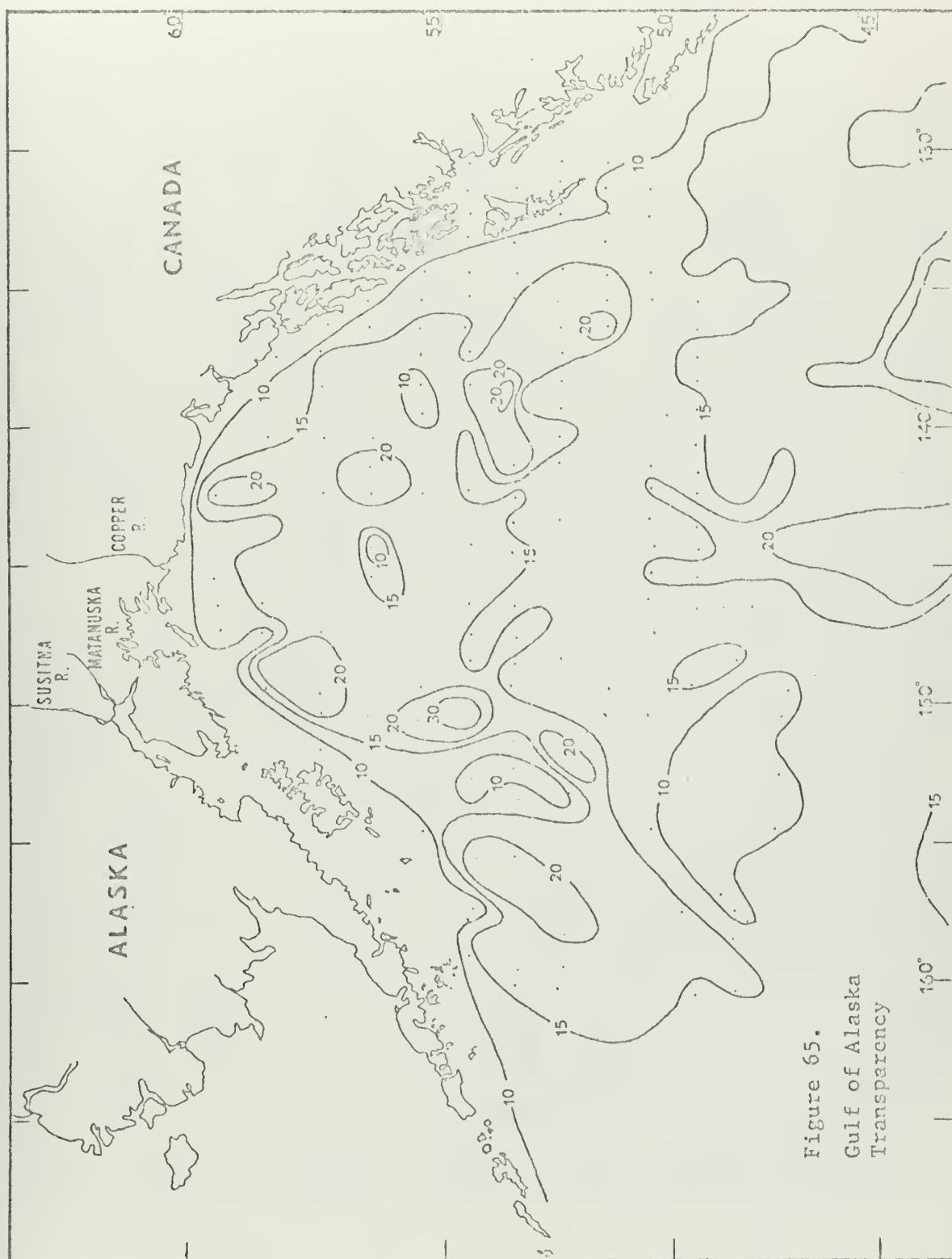
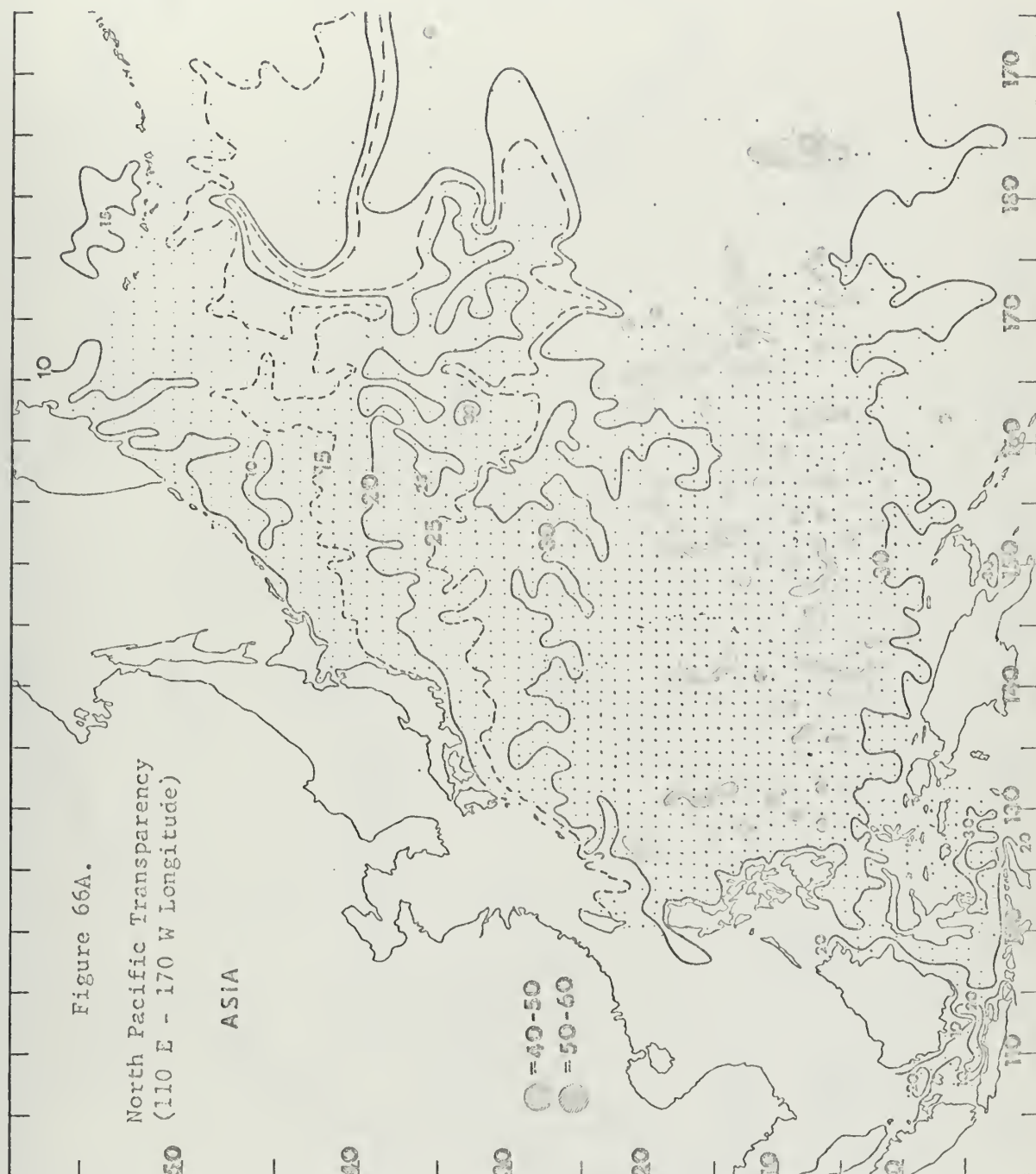
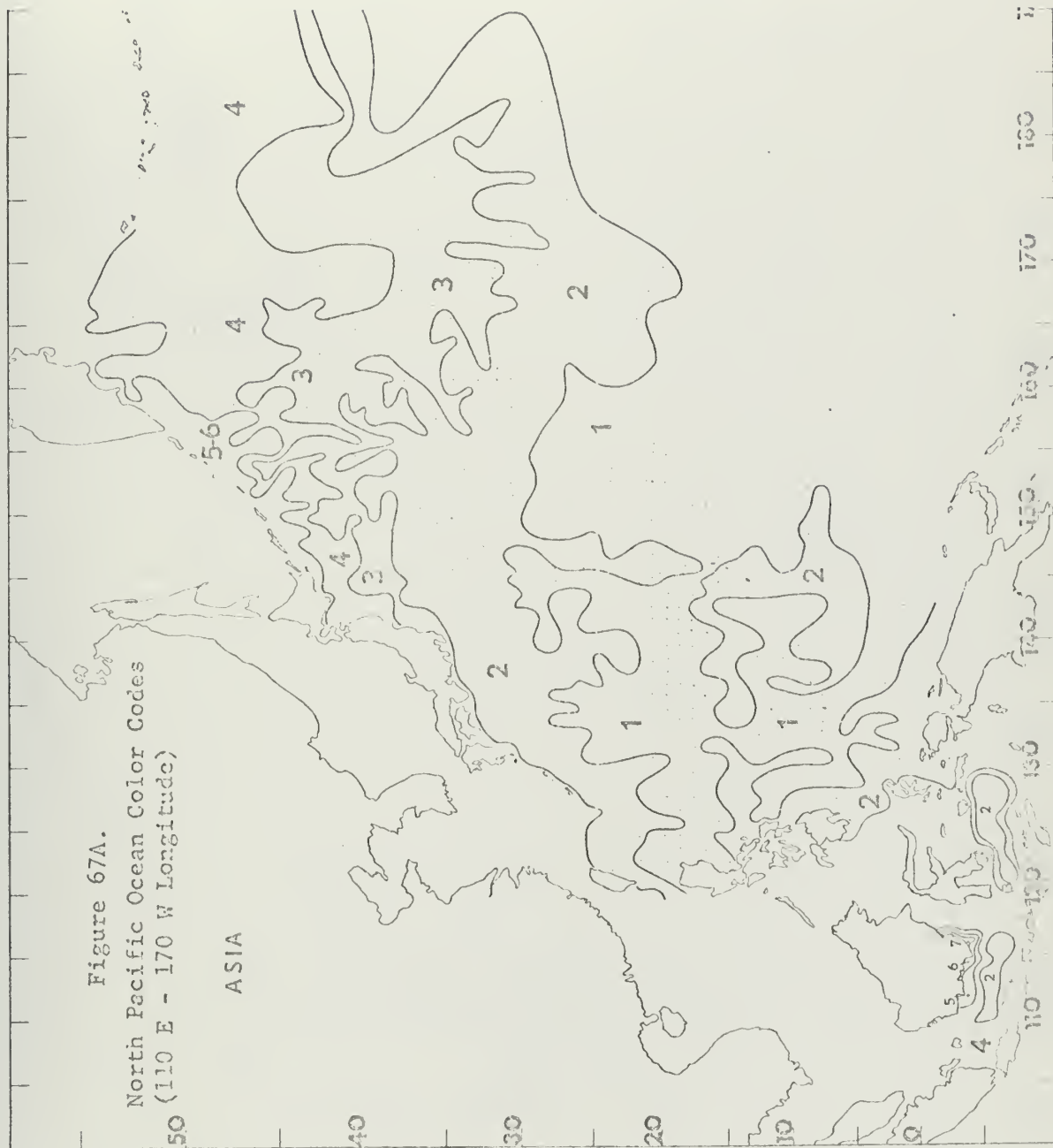
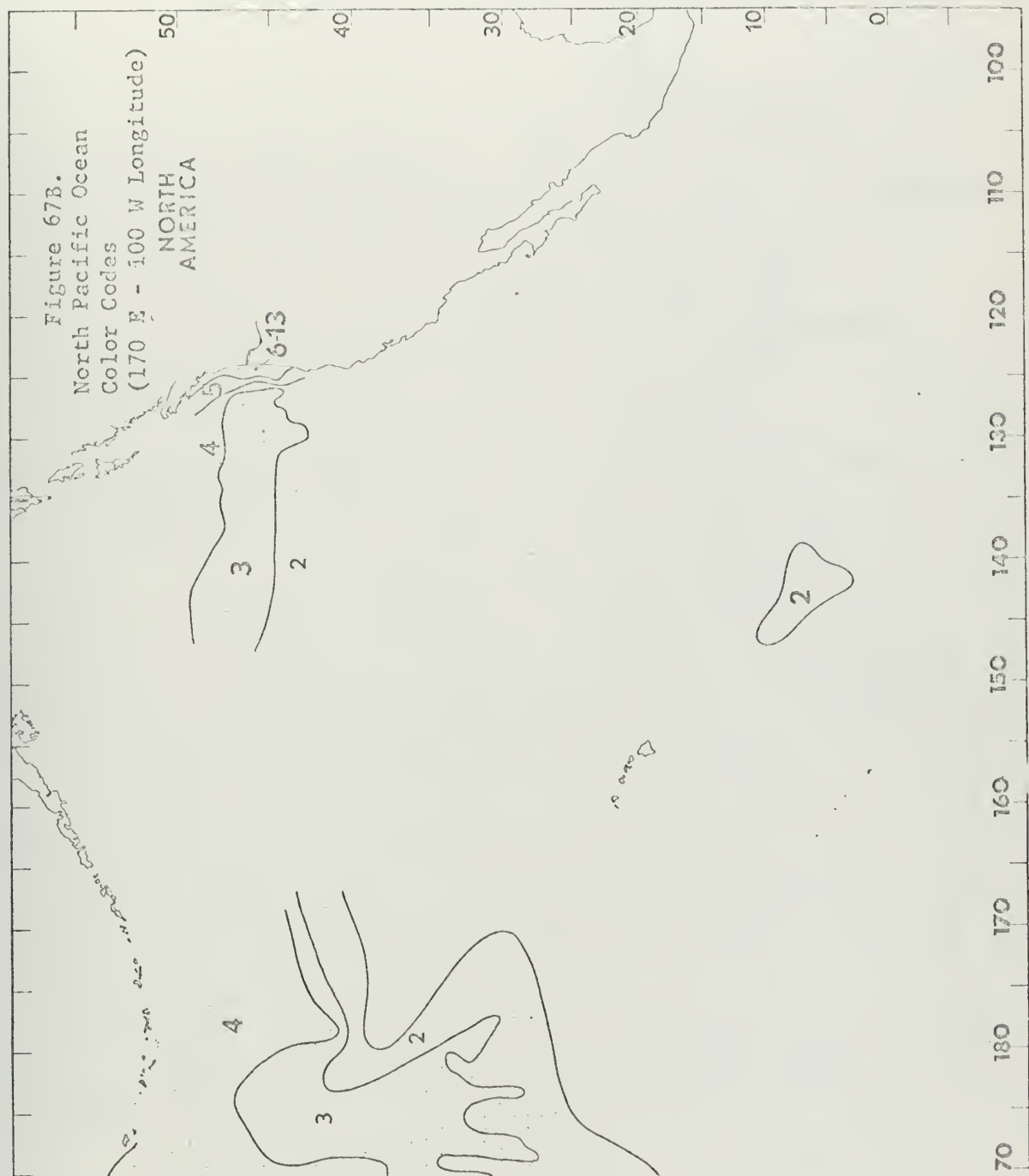


Figure 65.
Gulf of Alaska
Transparency









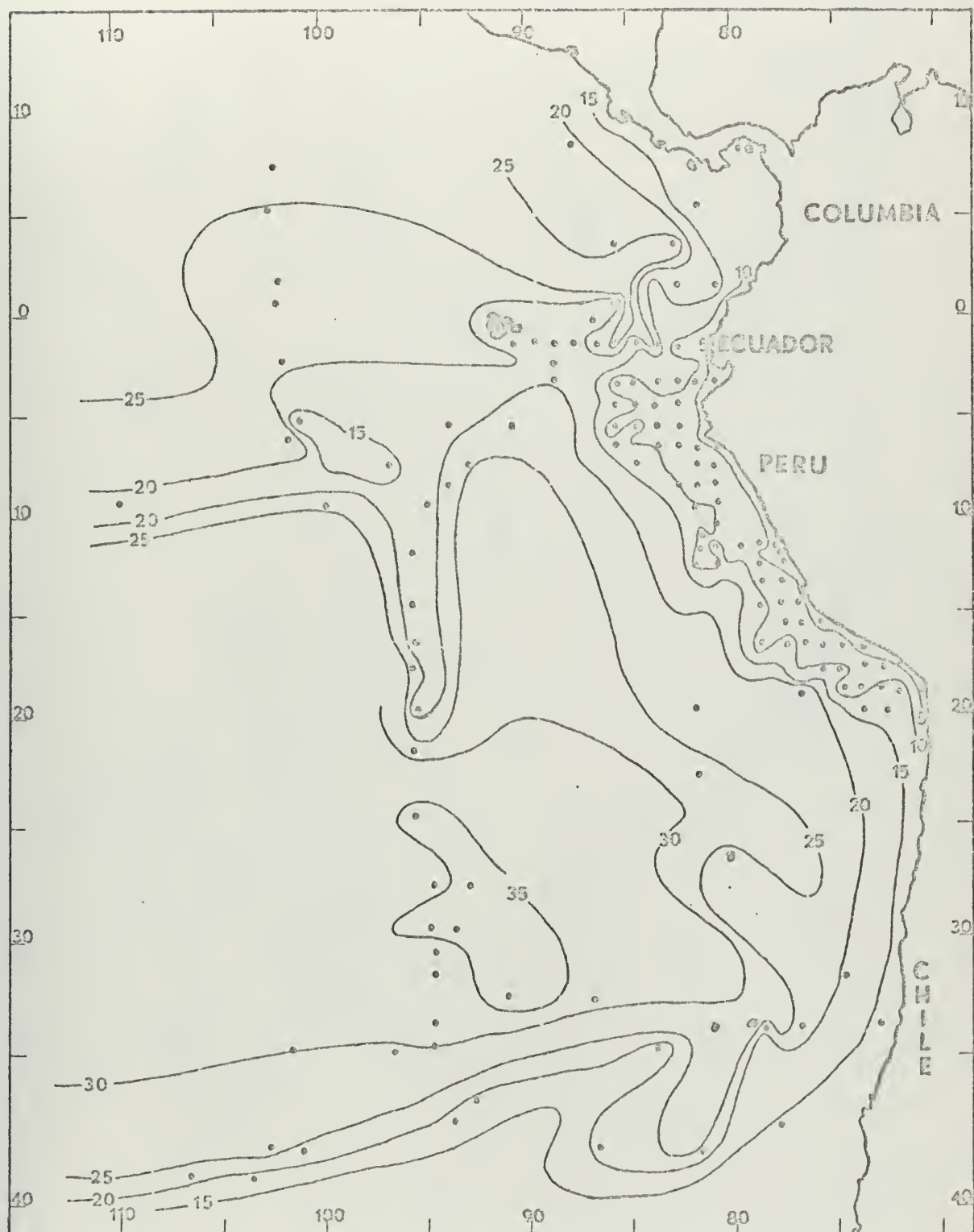


Figure 68. Eastern South Pacific Ocean Transparency

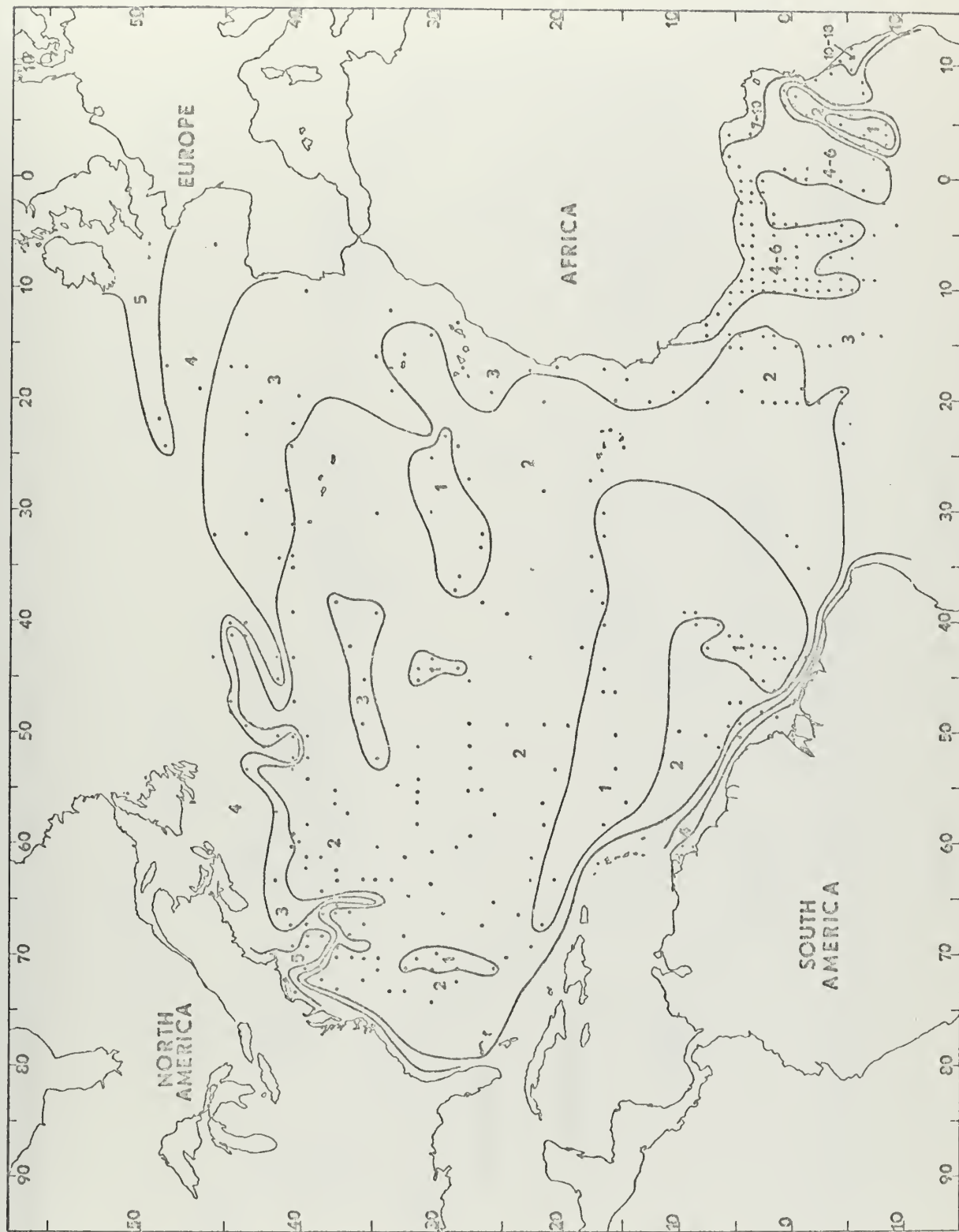


Figure 69. North Atlantic Ocean Color Codes

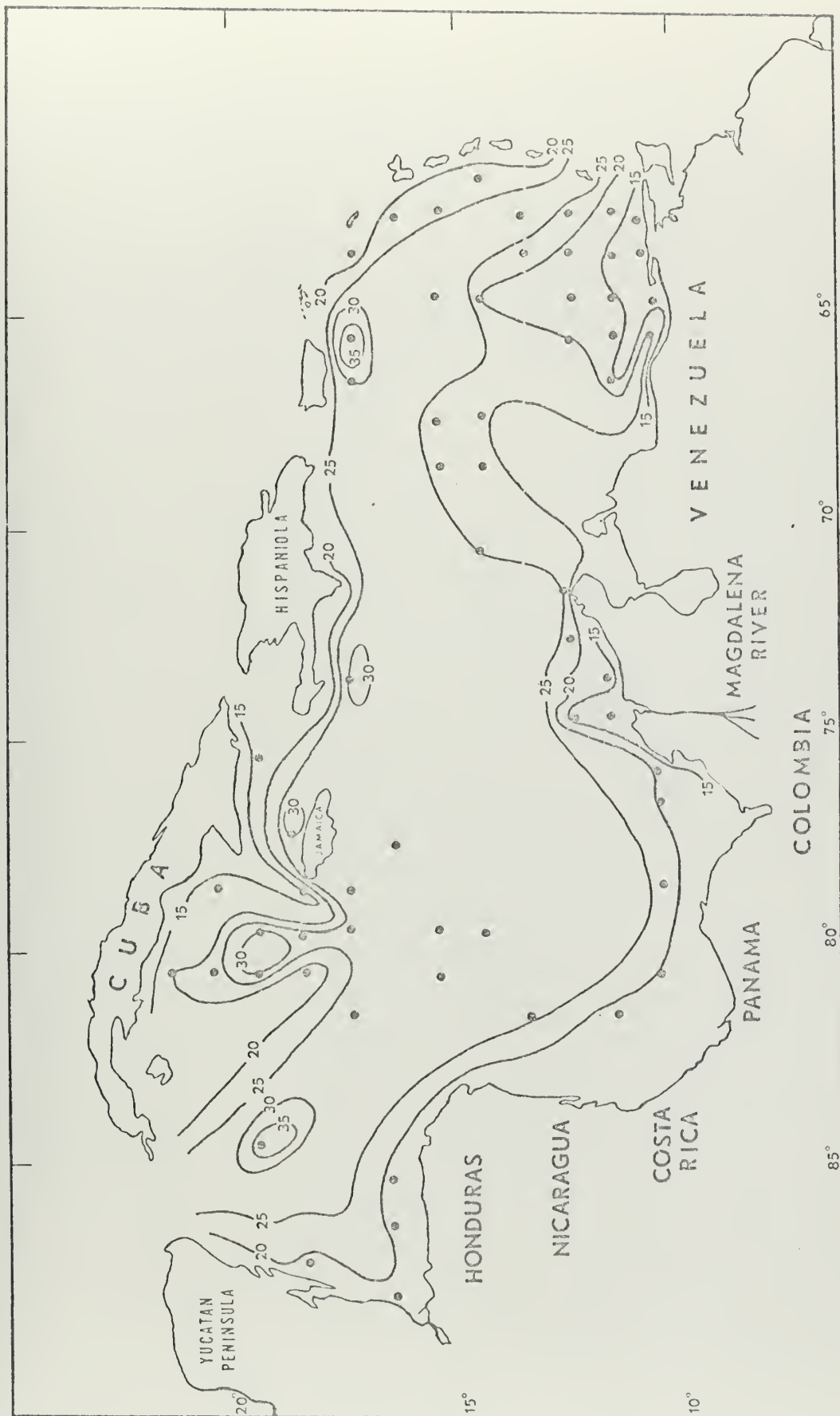


Figure 70. Caribbean Sea Transparency

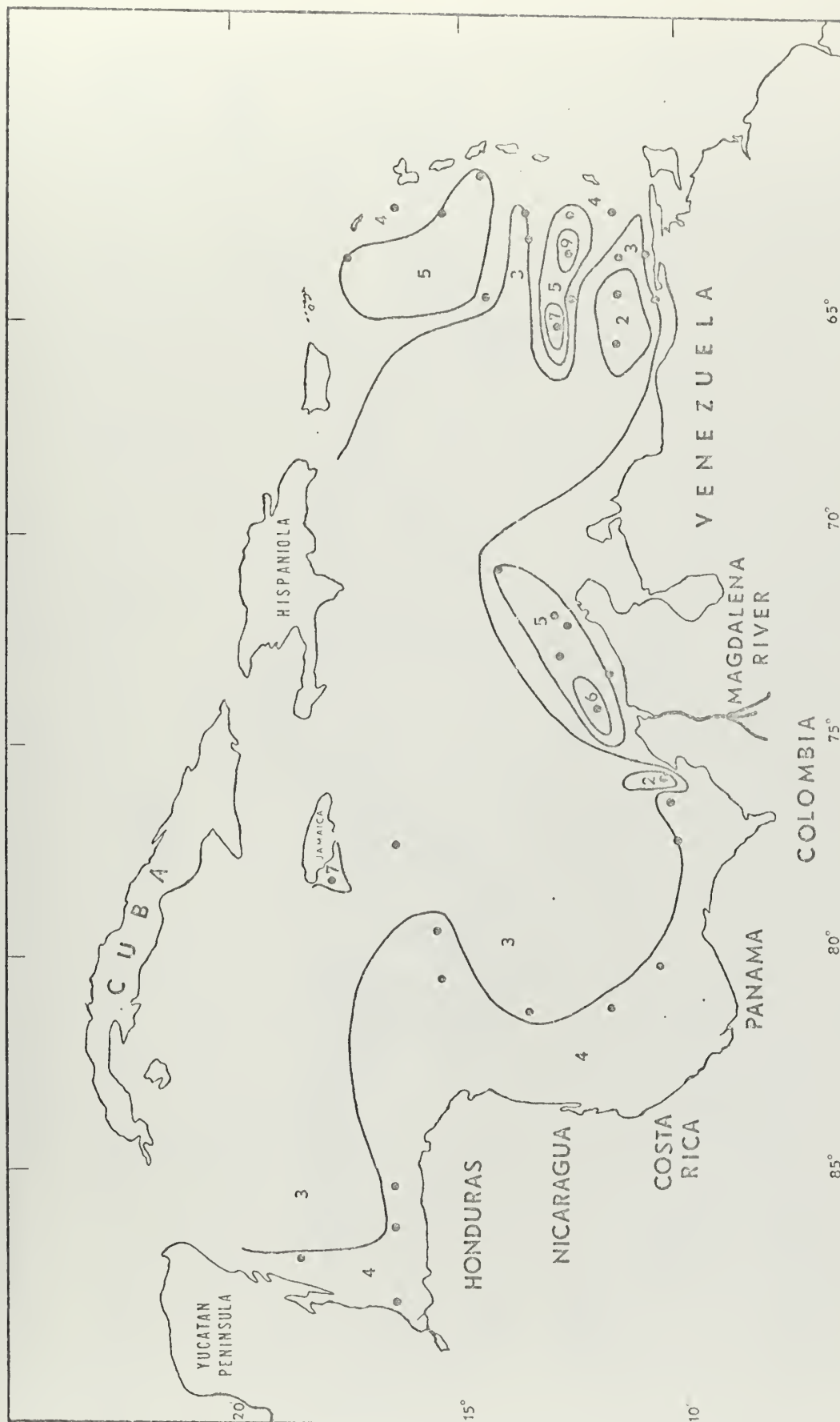


Figure 71. Caribbean Sea Color Codes

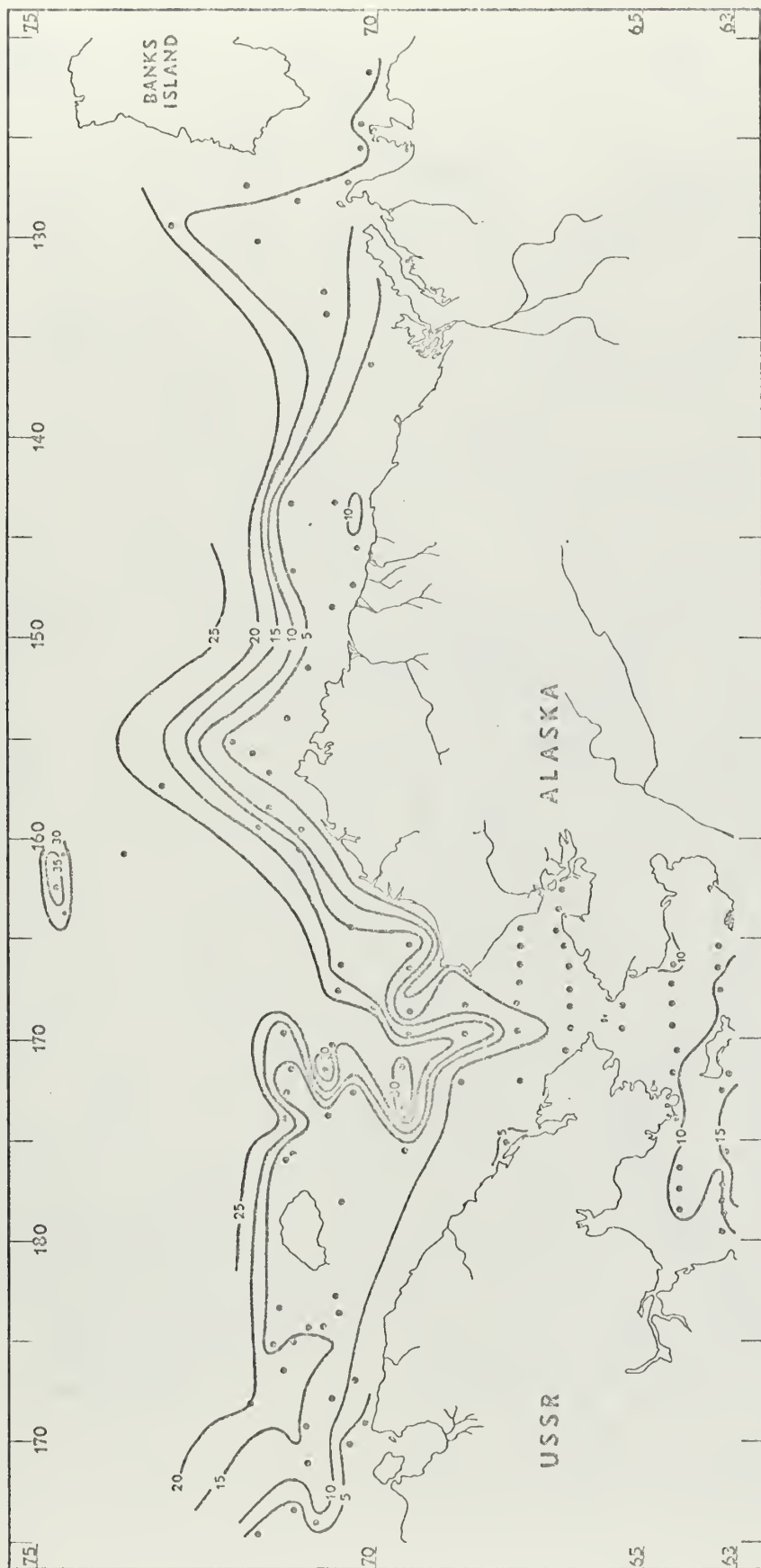


Figure 72. East Siberian, Chukchi, and Beaufort Seas Transparency

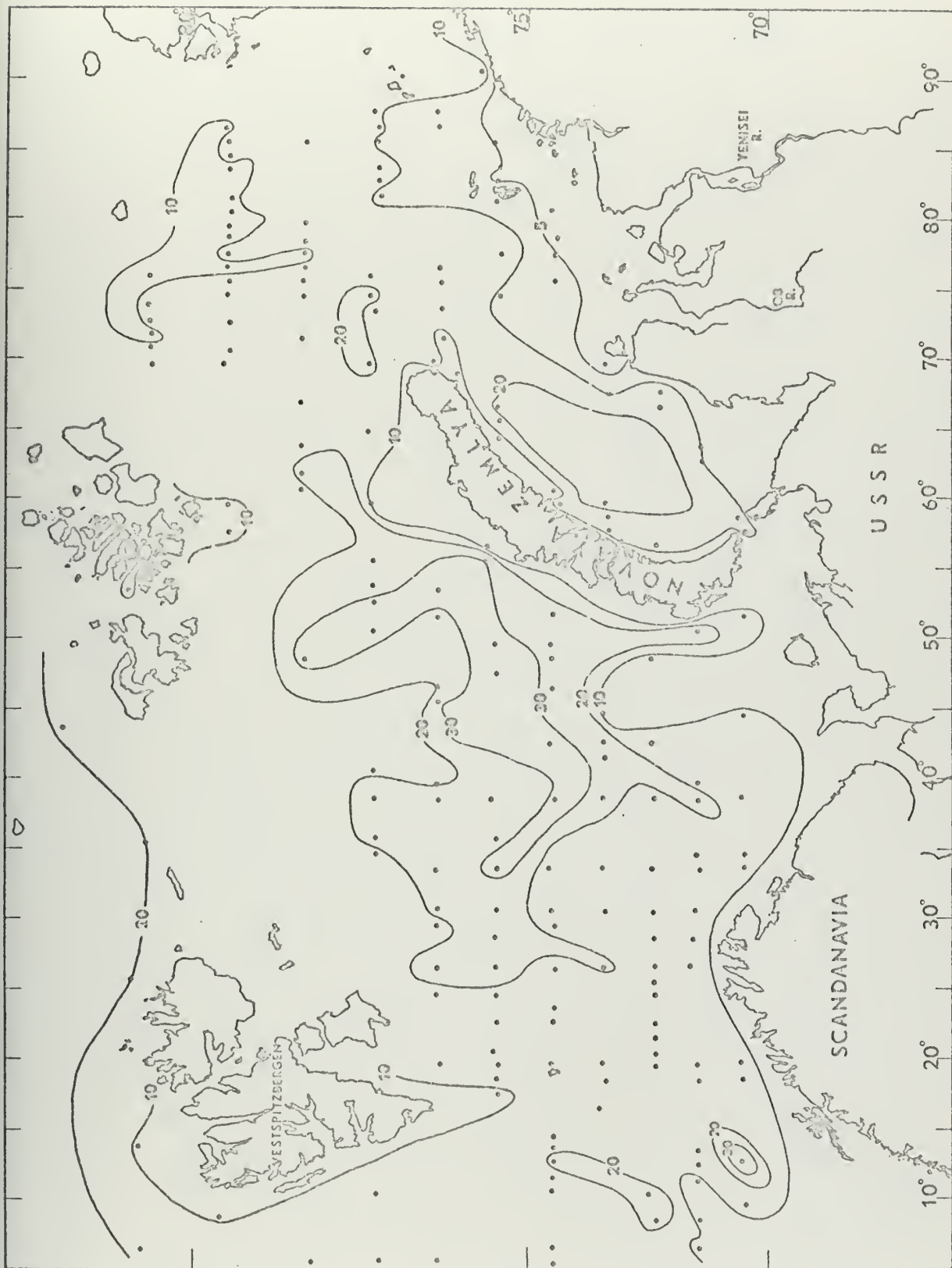


Figure 73. Barents and Kara Seas Transparency

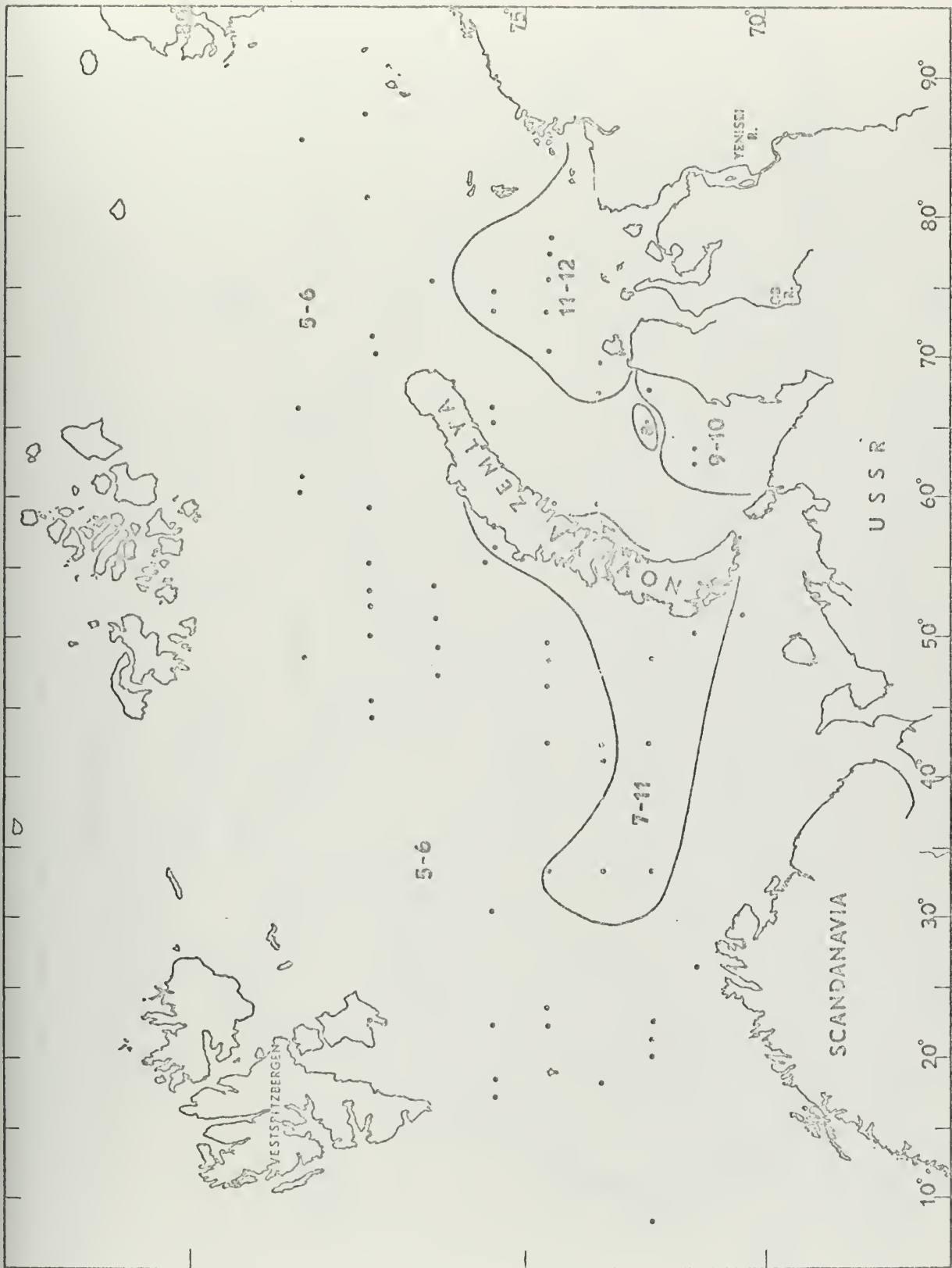


Figure 74. Barents and Kara Seas Color Codes

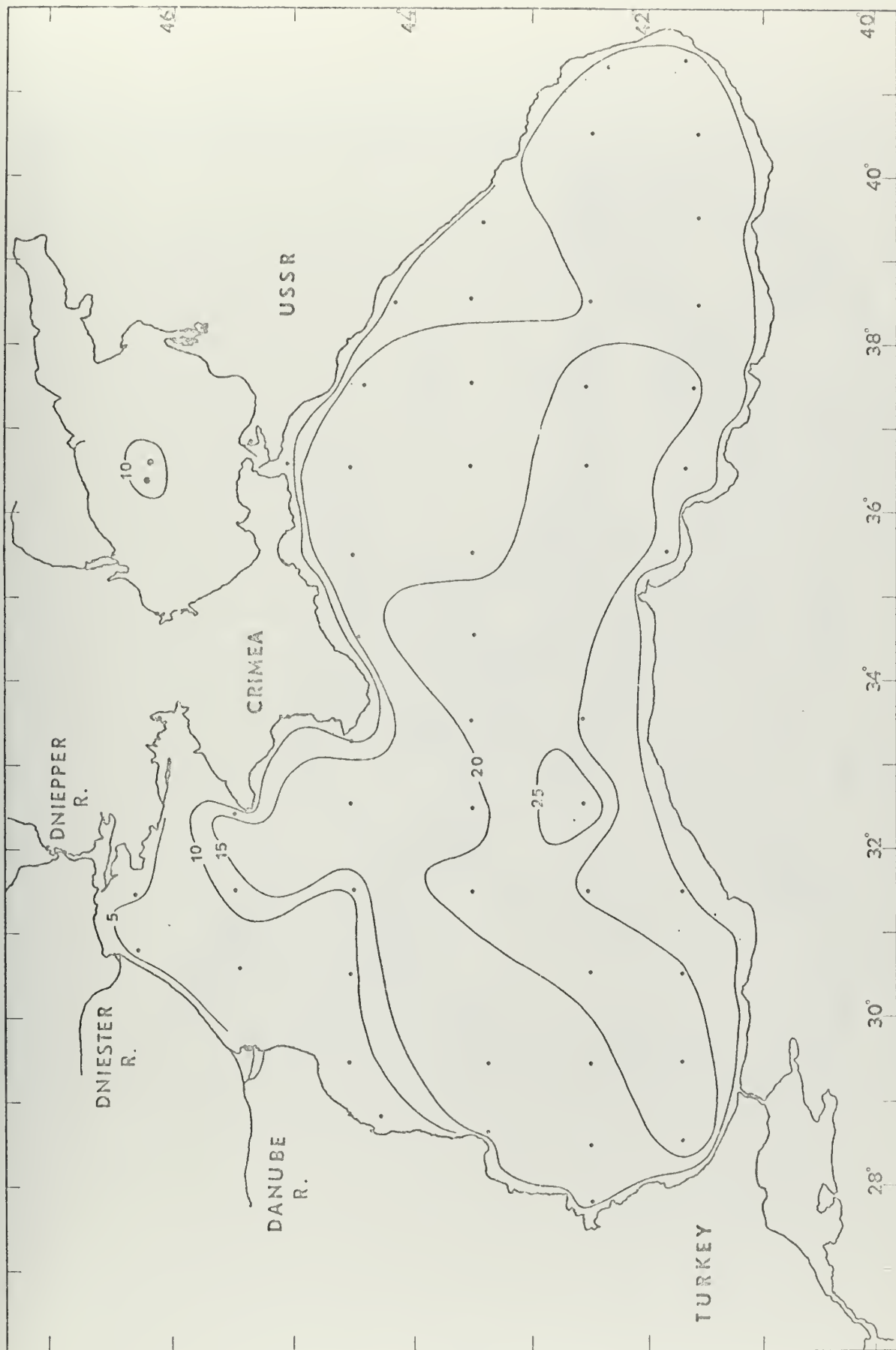


Figure 75. Black Sea Transparency



Figure 76. Mediterranean Sea - Western Basin Transparency

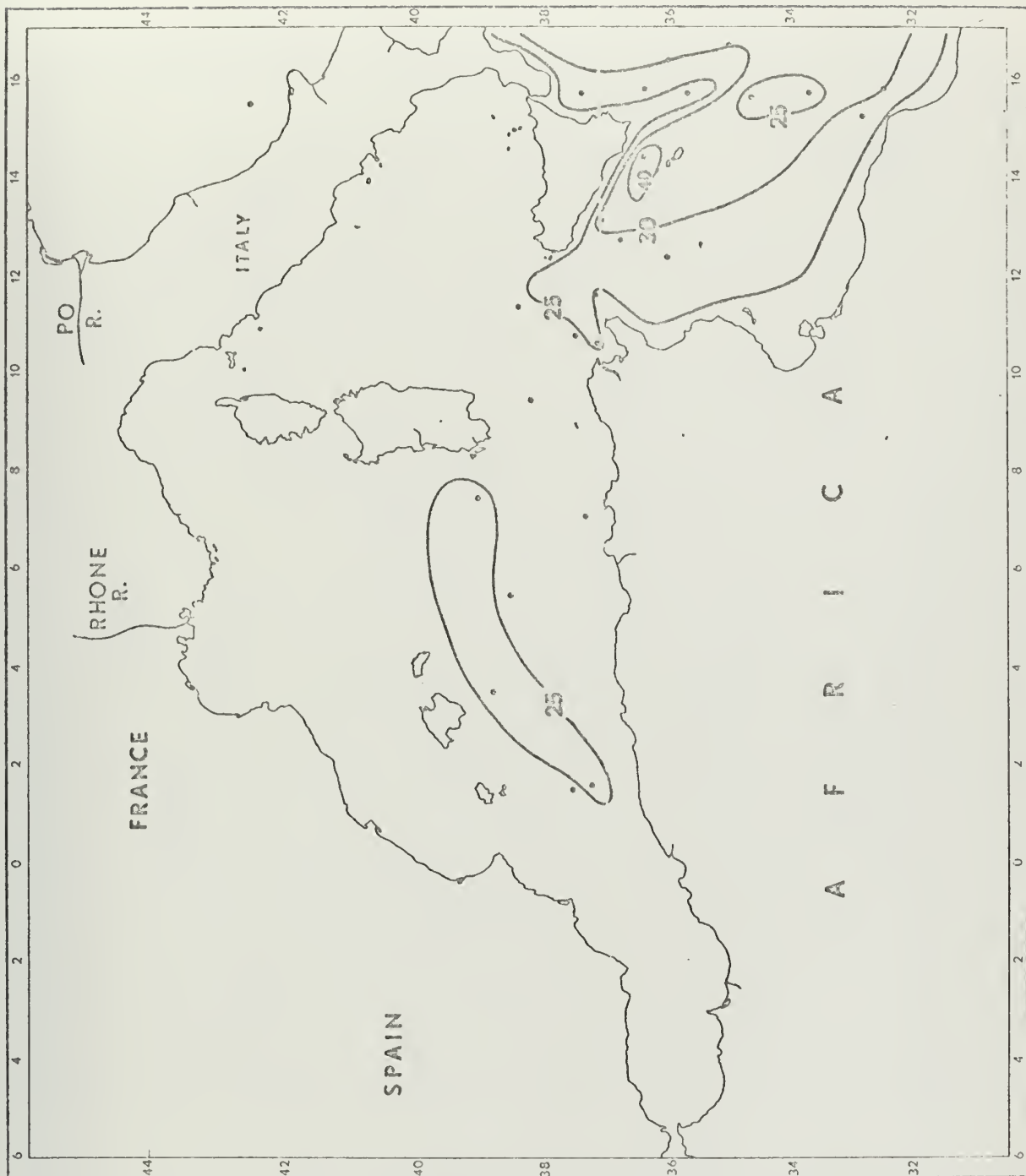


Figure 77. Mediterranean Sea - Eastern Basin Transparency

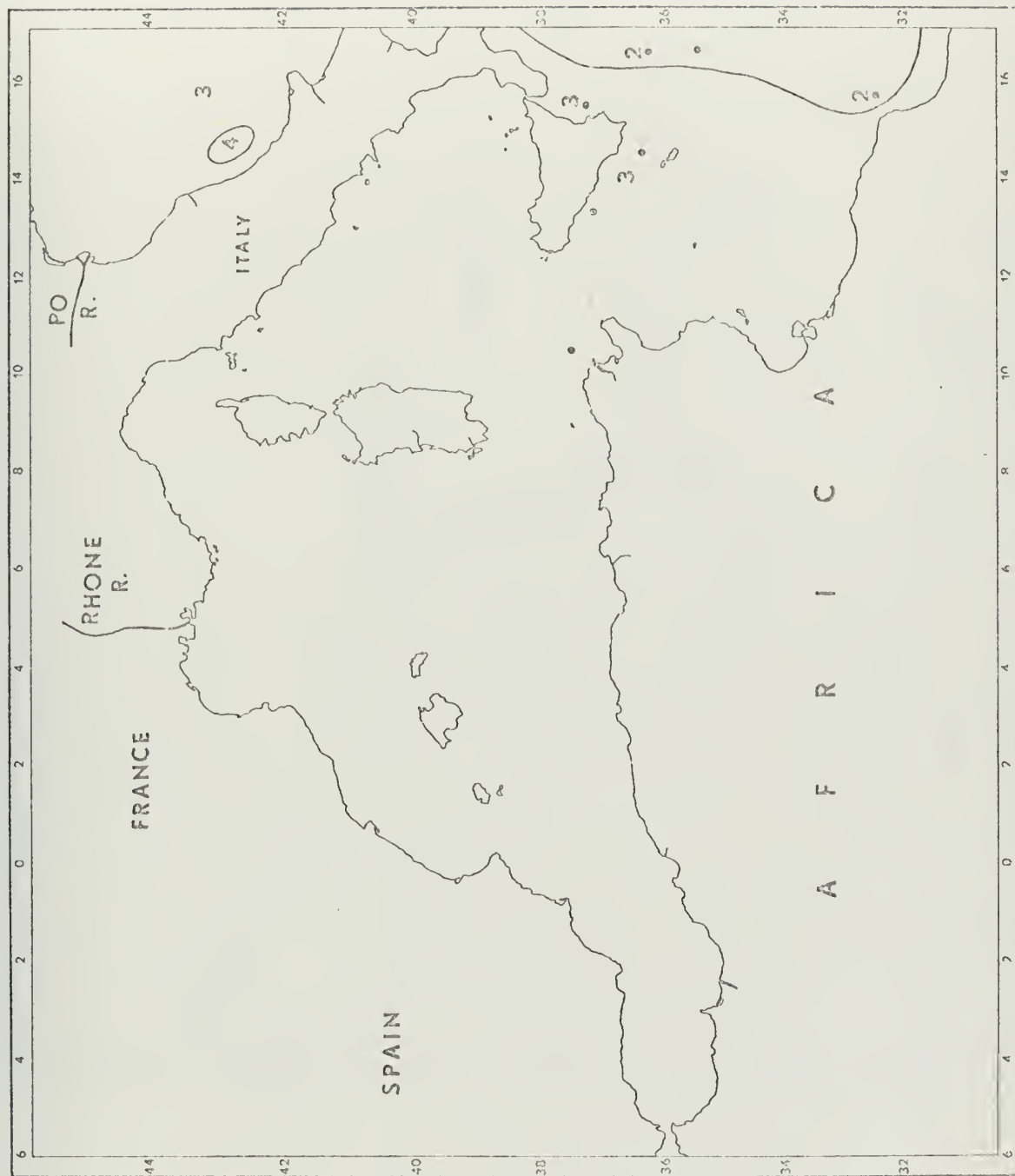


Figure 78. Mediterranean Sea - Western Basin Color Codes

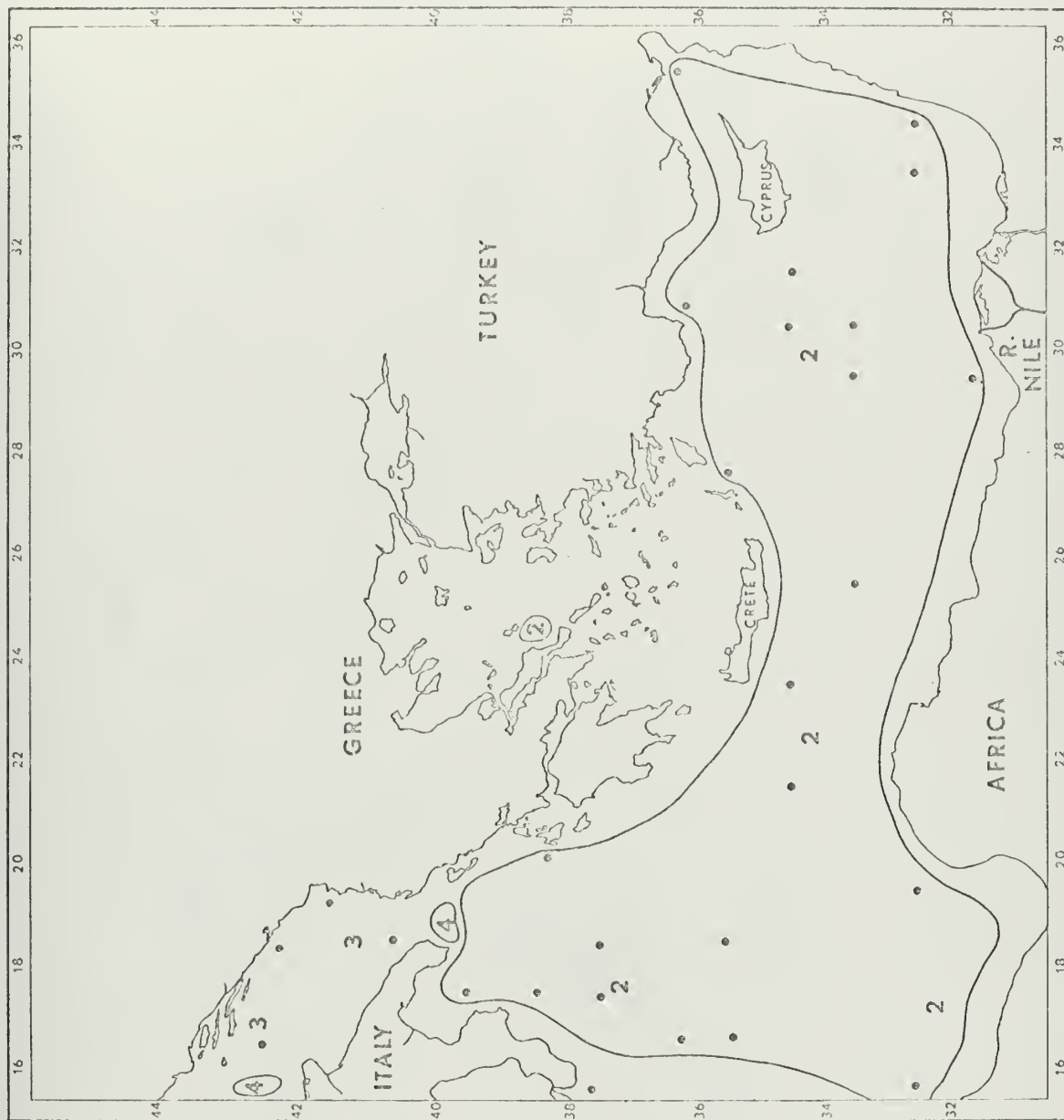


Figure 79. Mediterranean Sea - Eastern Basin Color Codes

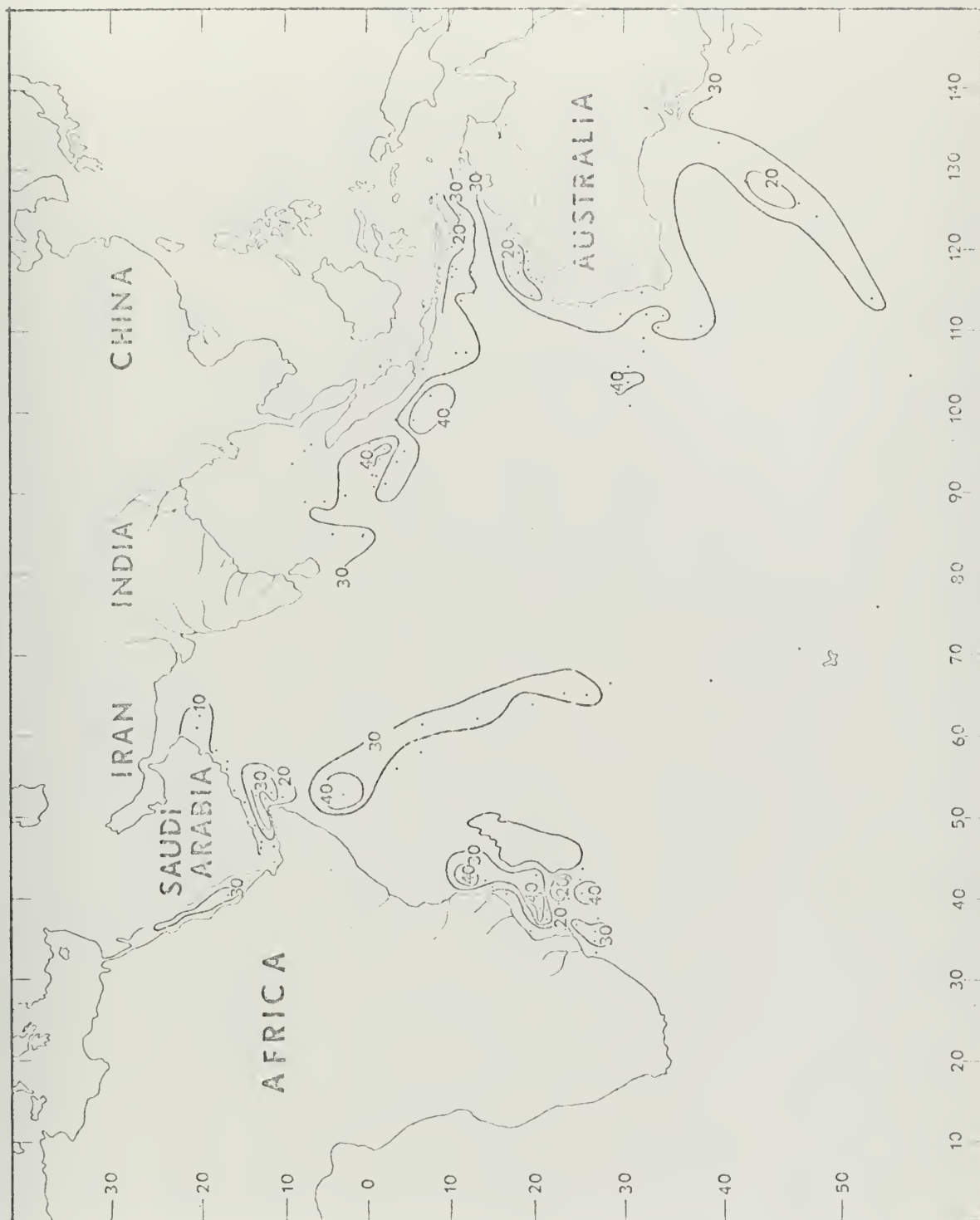


Figure 80. Indian Ocean - Summer Monsoon Season Transparency

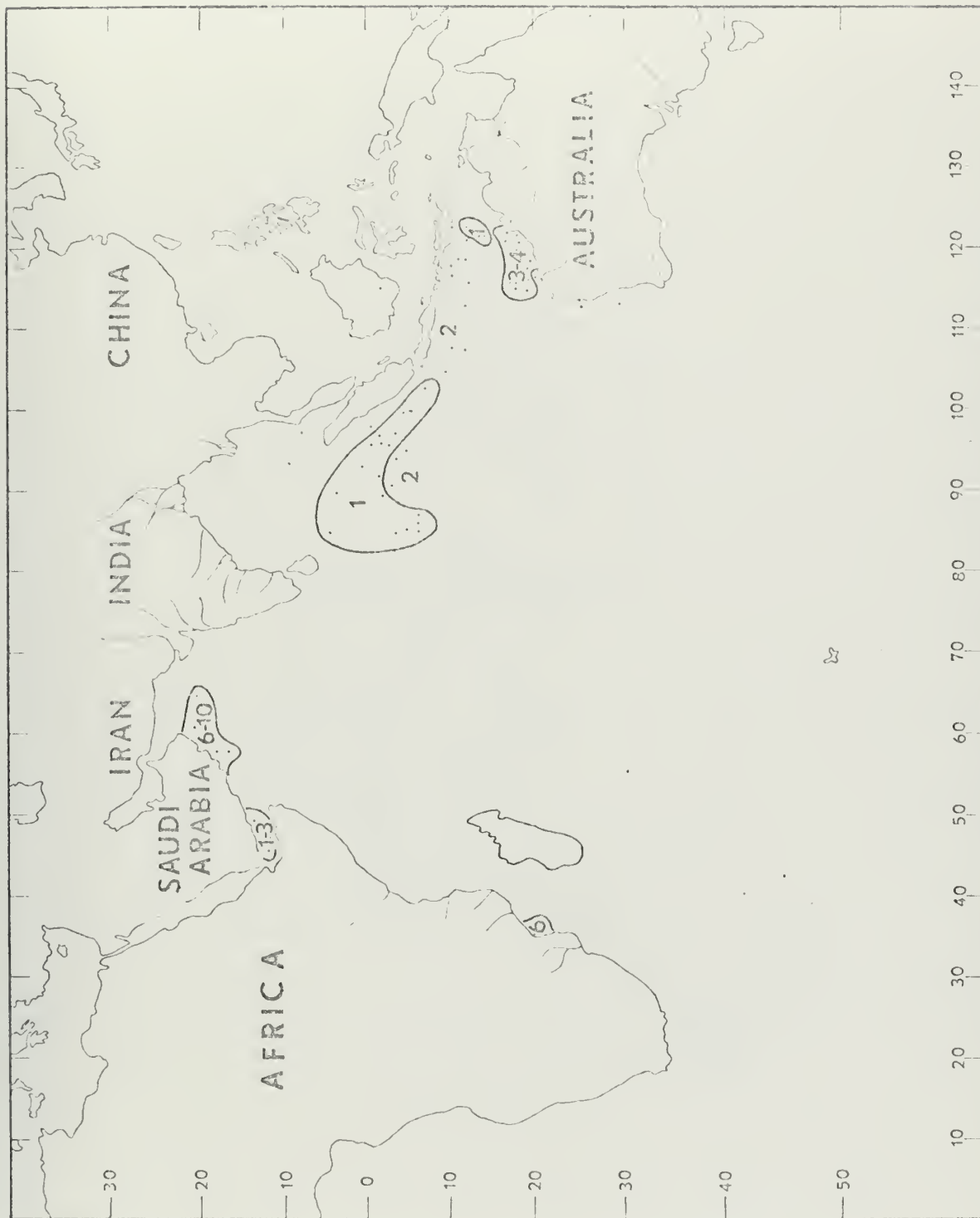


Figure 81. Indian Ocean - Summer Monsoon Season Color Code

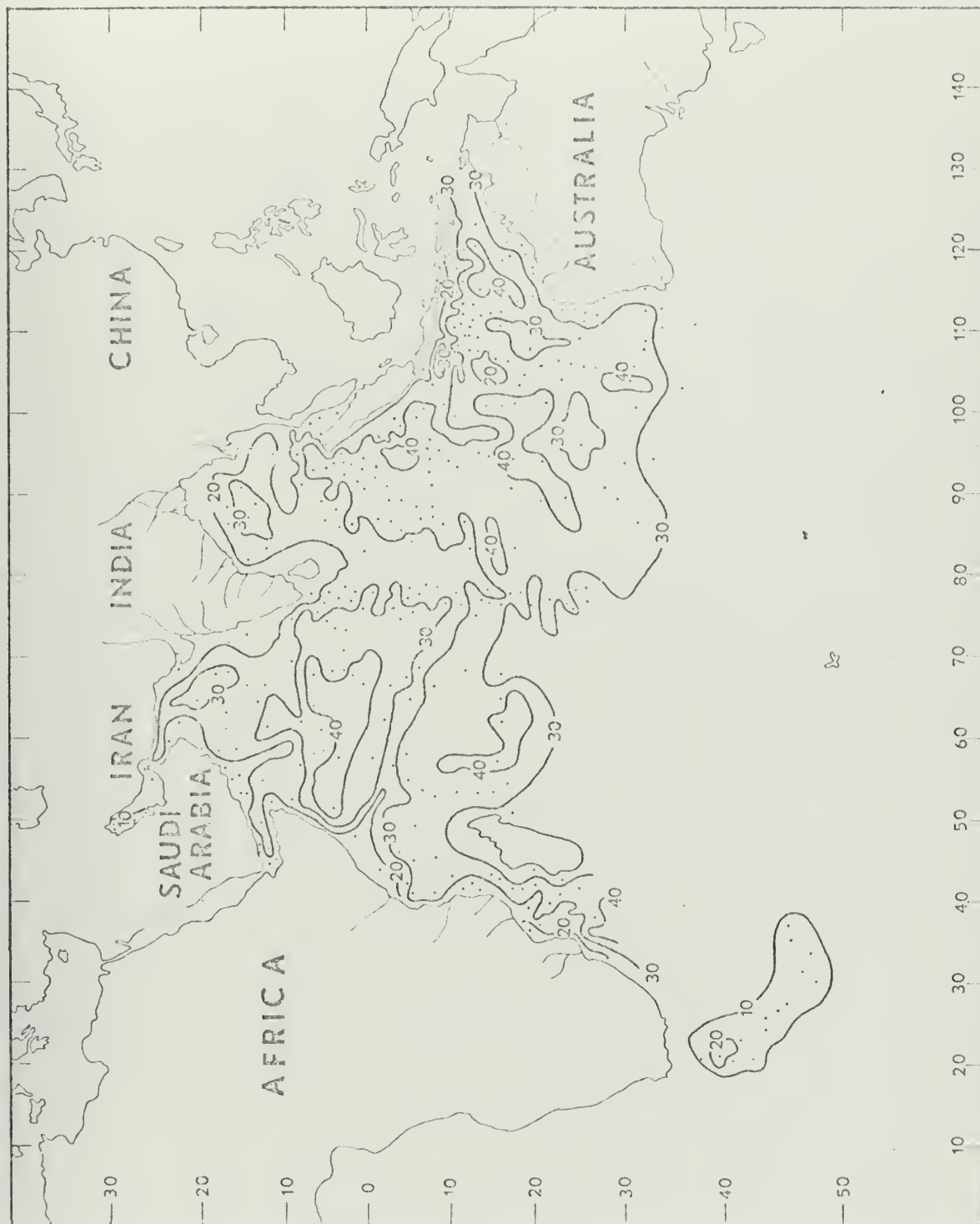


Figure 82. Indian Ocean - Winter Monsoon Season Transparency

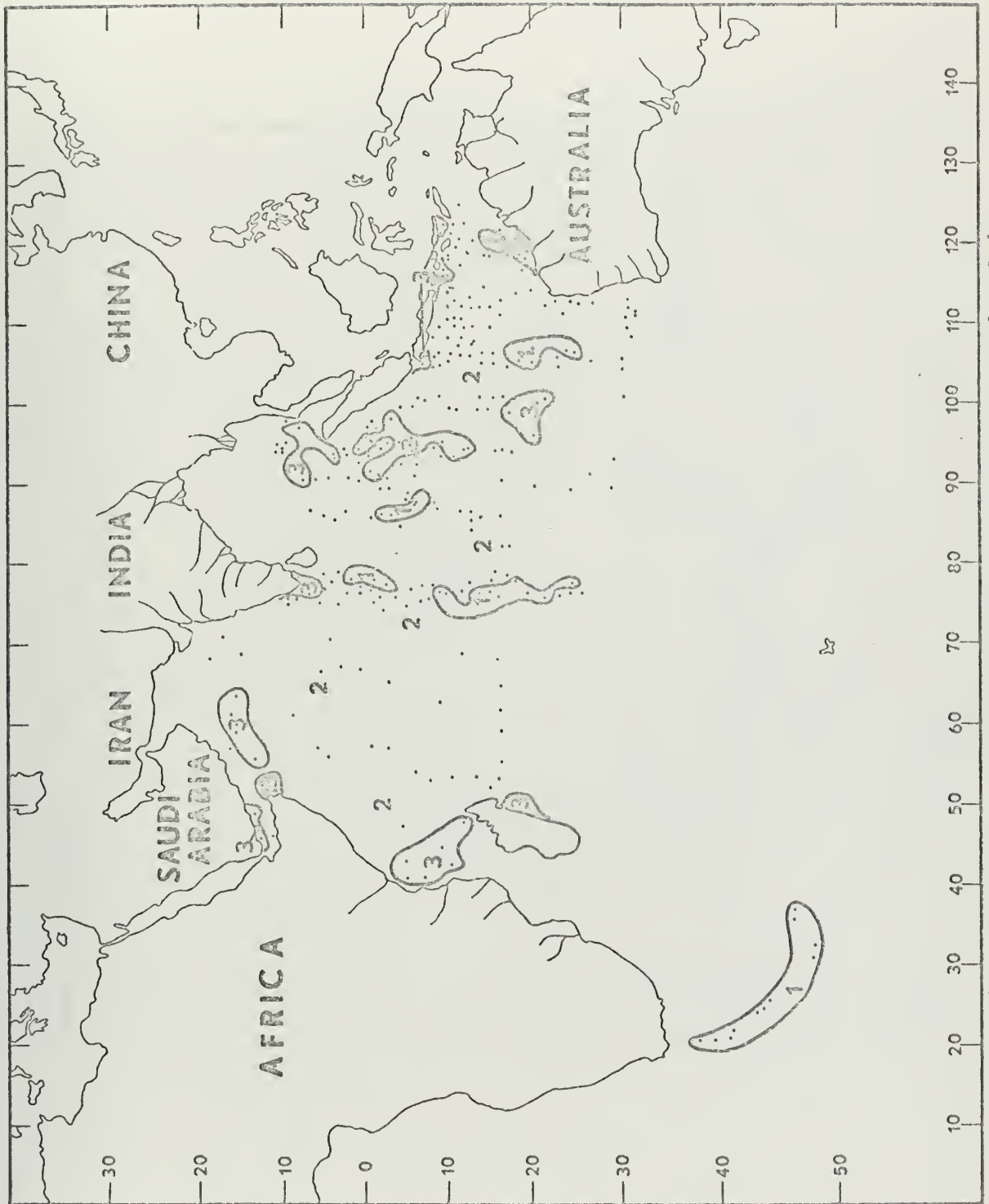


Figure 83. Indian Ocean - Winter Monsoon Season Color Codes

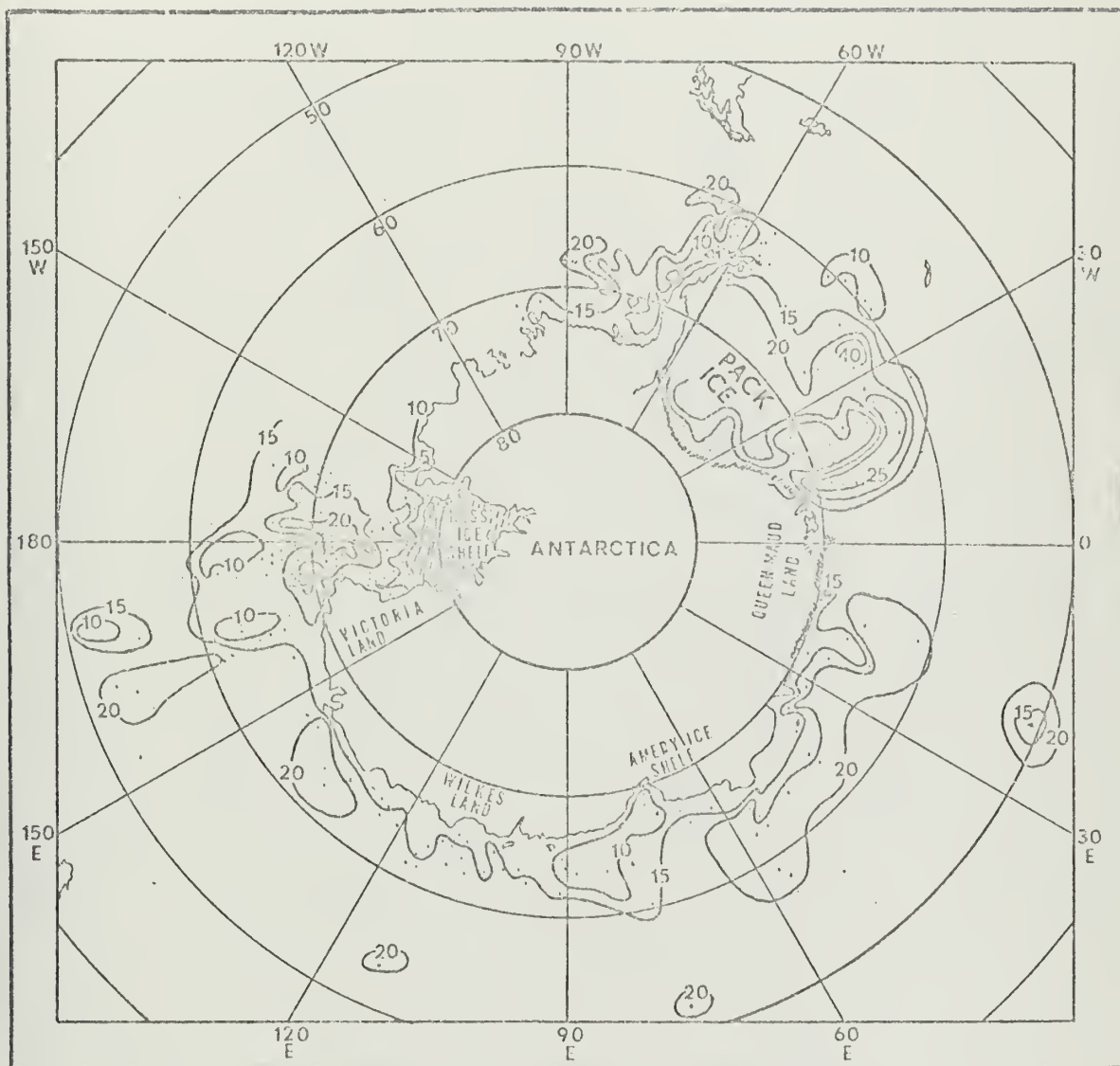


Figure 84. Southern Ocean Transparency

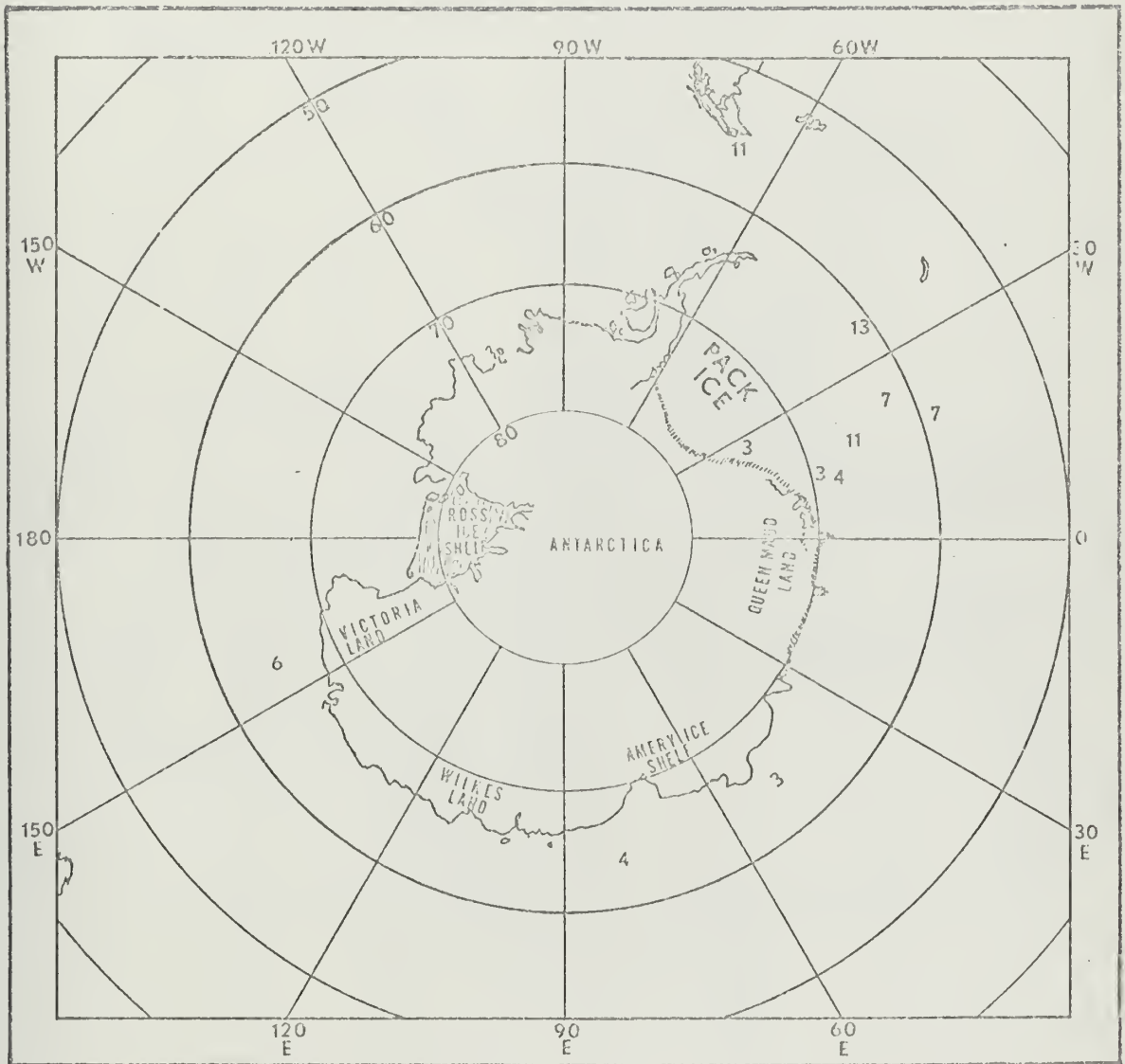


Figure 85. Southern Ocean Color Codes

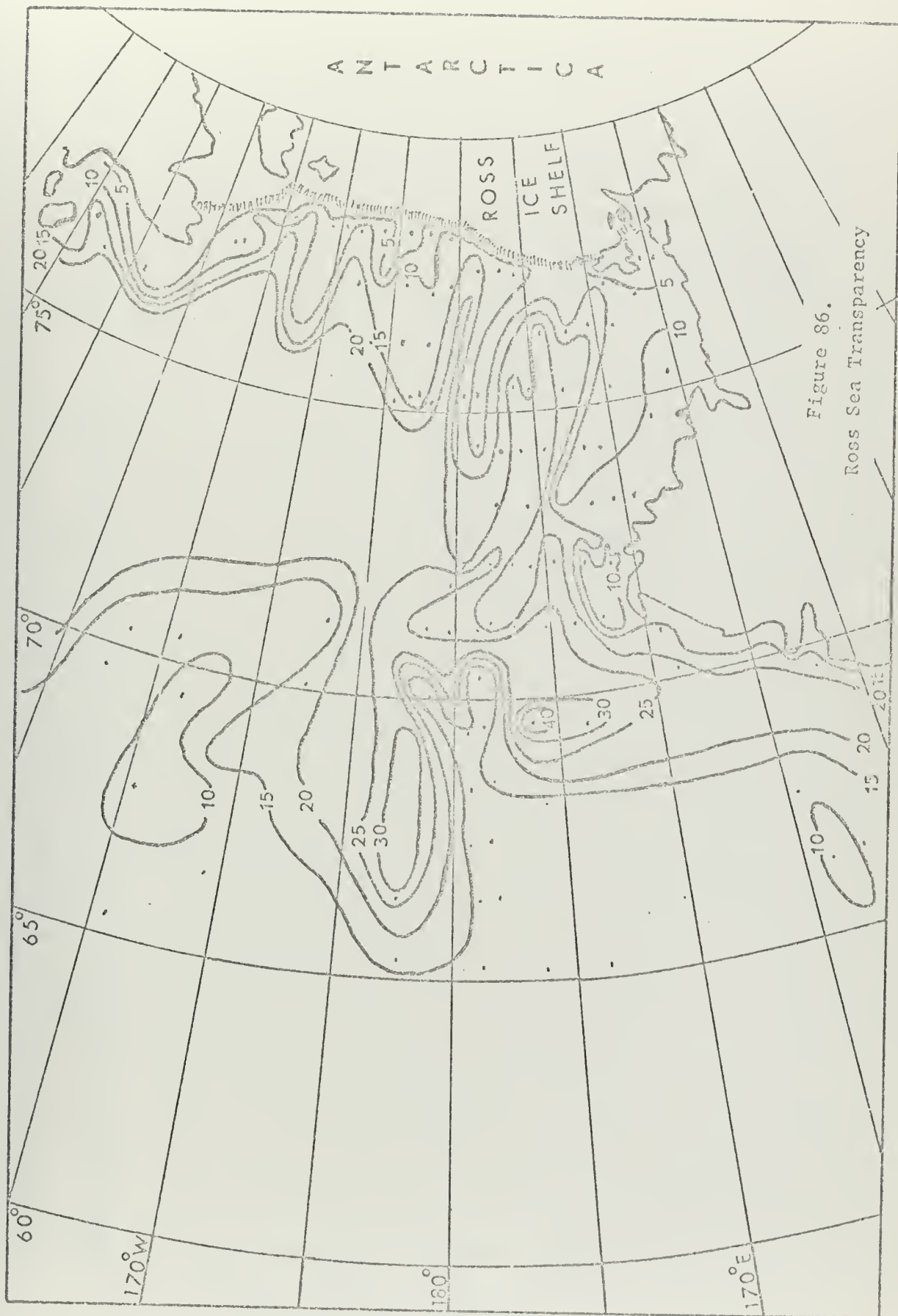


Figure 86.
Ross Sea Transparency

Figure 87.

Marsden Square 115

Latitude 30° - 40°N

Longitude 60° - 70°W

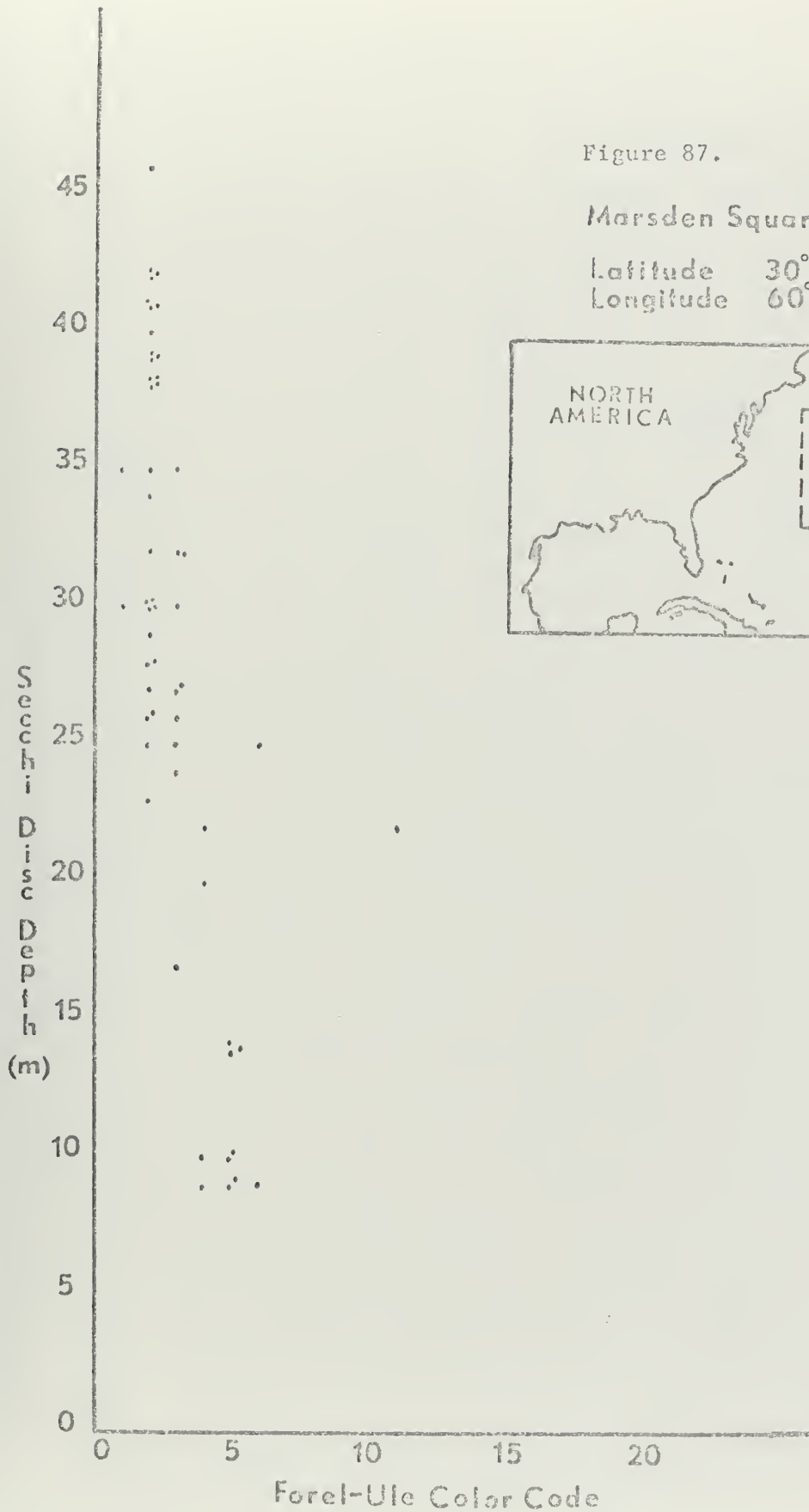
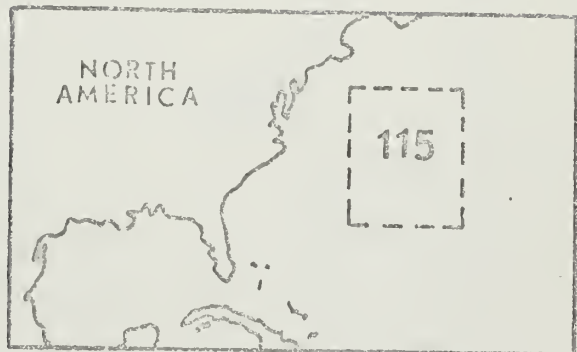


Figure 88.

Marsden Square 94

Latitude 20° - 30° N

Longitude 140° - 150° E

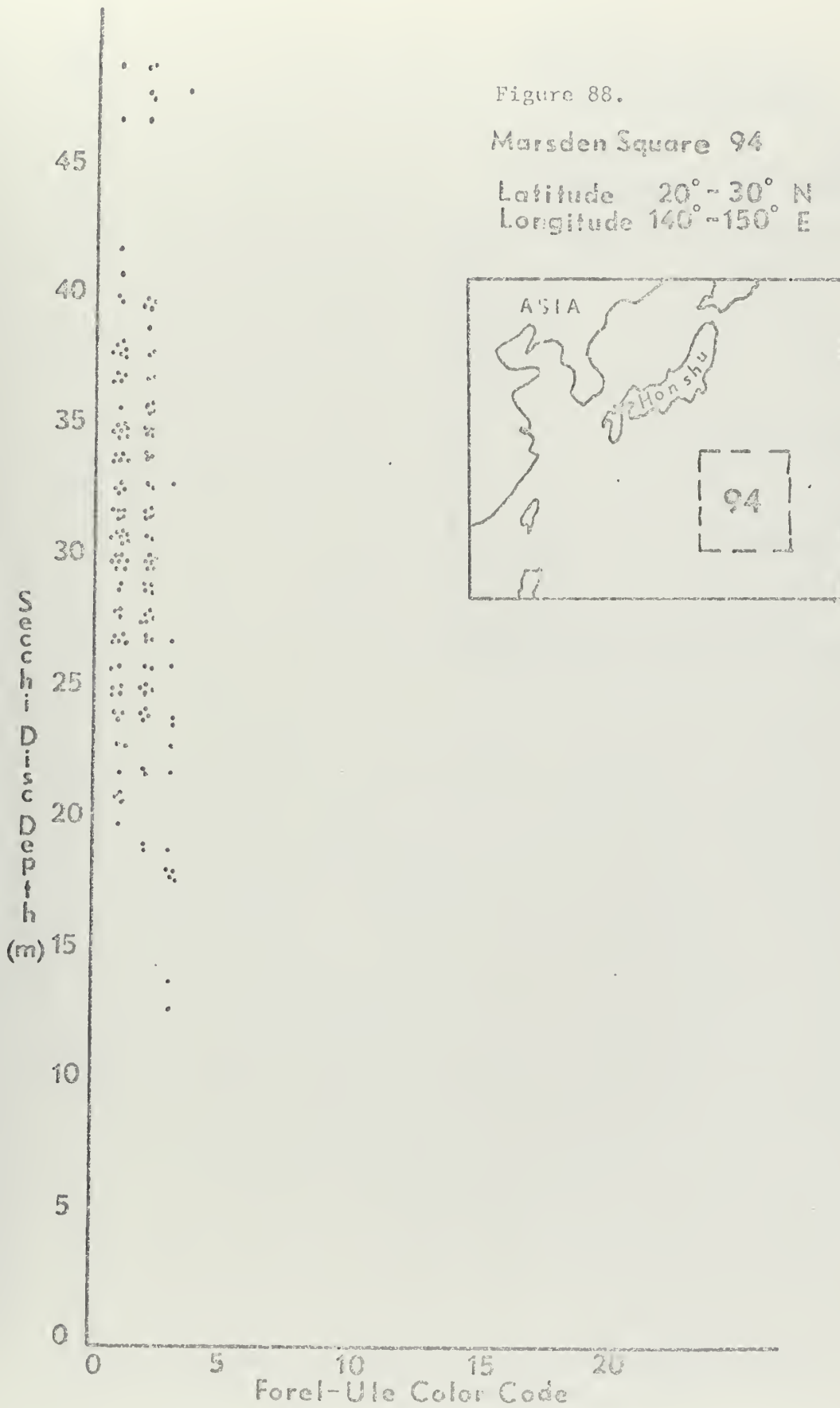


Figure 89.

Marsden Squares:
327, 328, 363 & 364

Latitude $0^{\circ} - 20^{\circ} \text{S}$
Longitude $60^{\circ} - 80^{\circ} \text{E}$

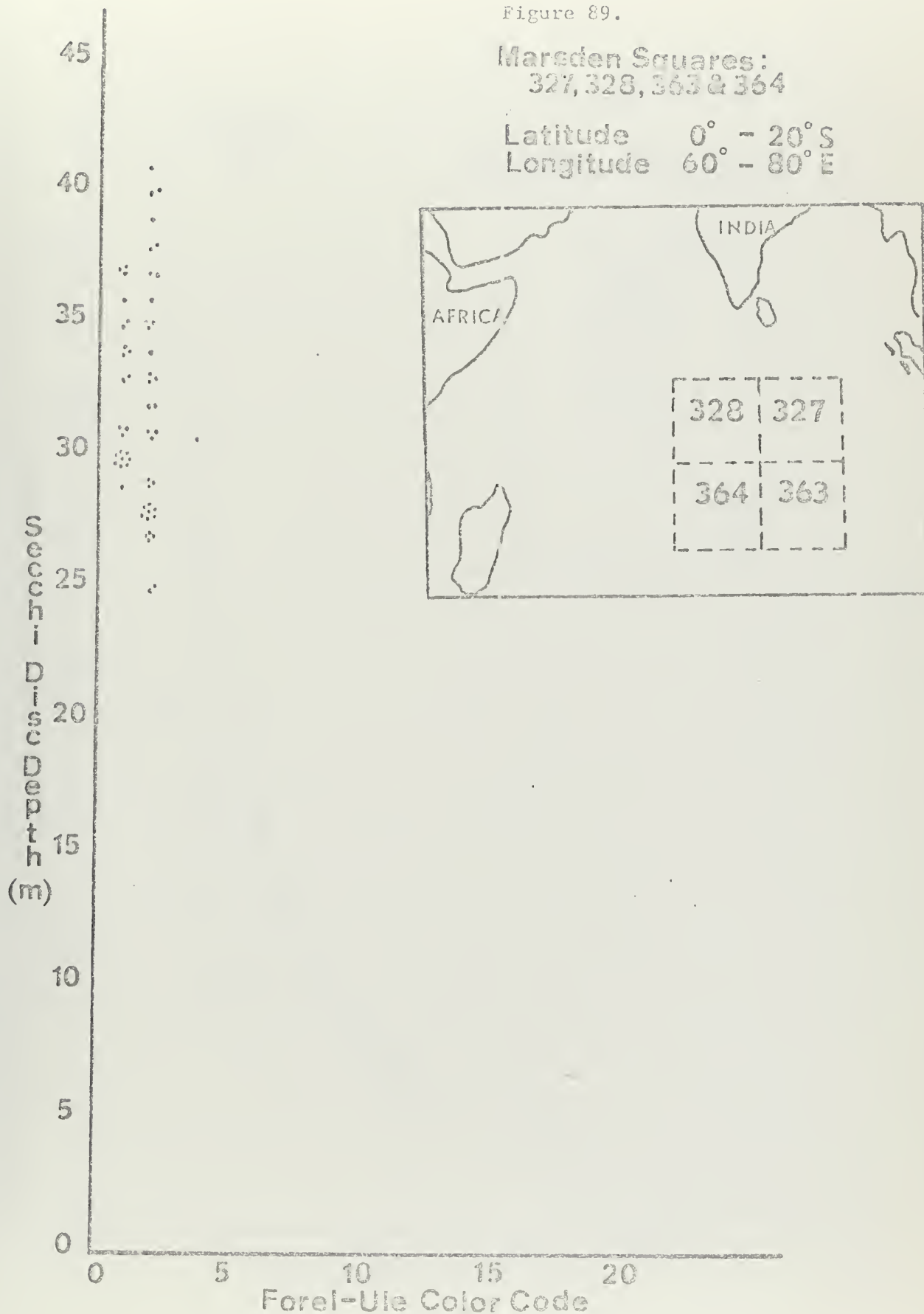
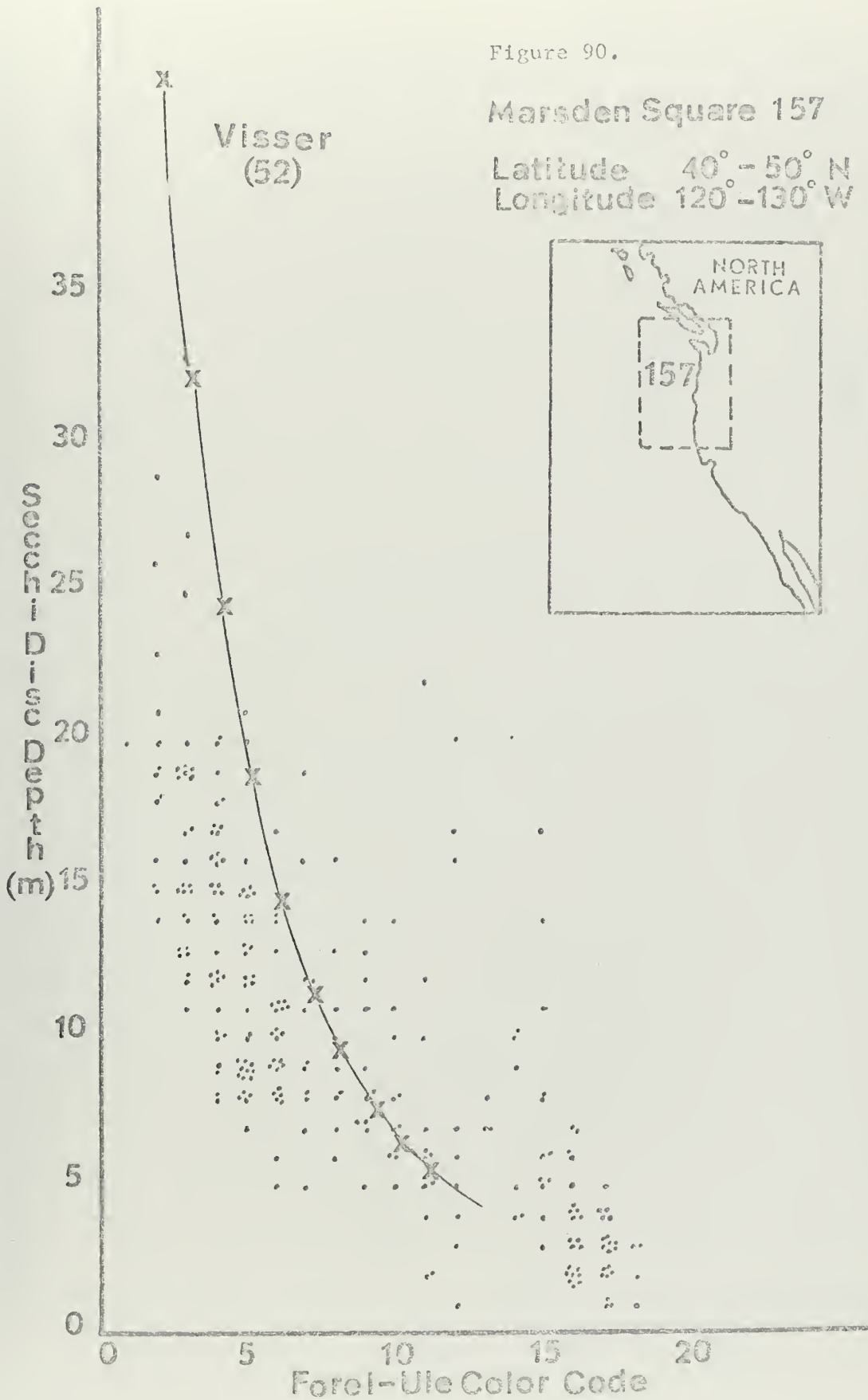


Figure 90.

Marsden Square 157

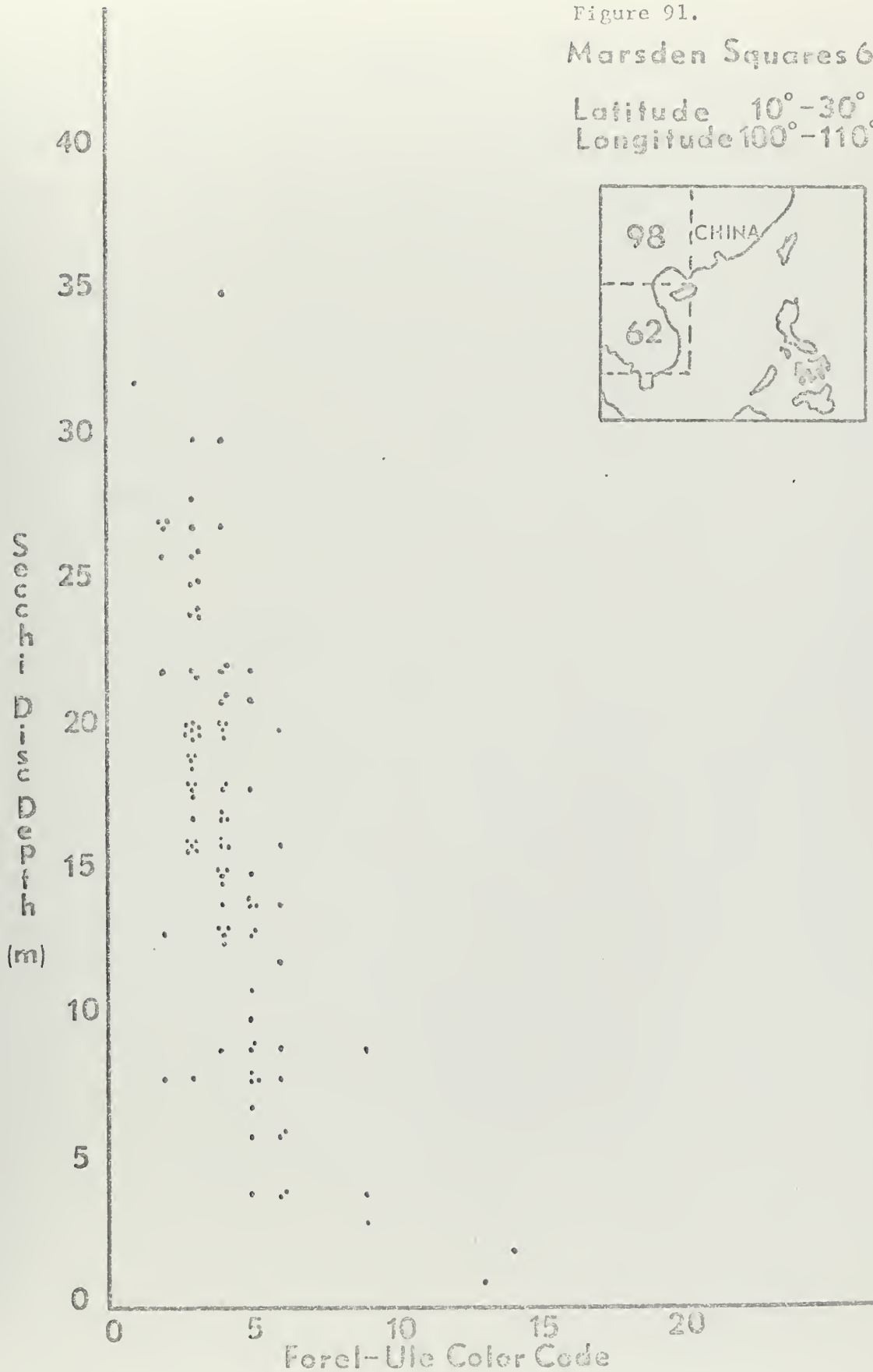
Latitude $40^{\circ}-50^{\circ}$ N

Longitude $120^{\circ}-130^{\circ}$ W



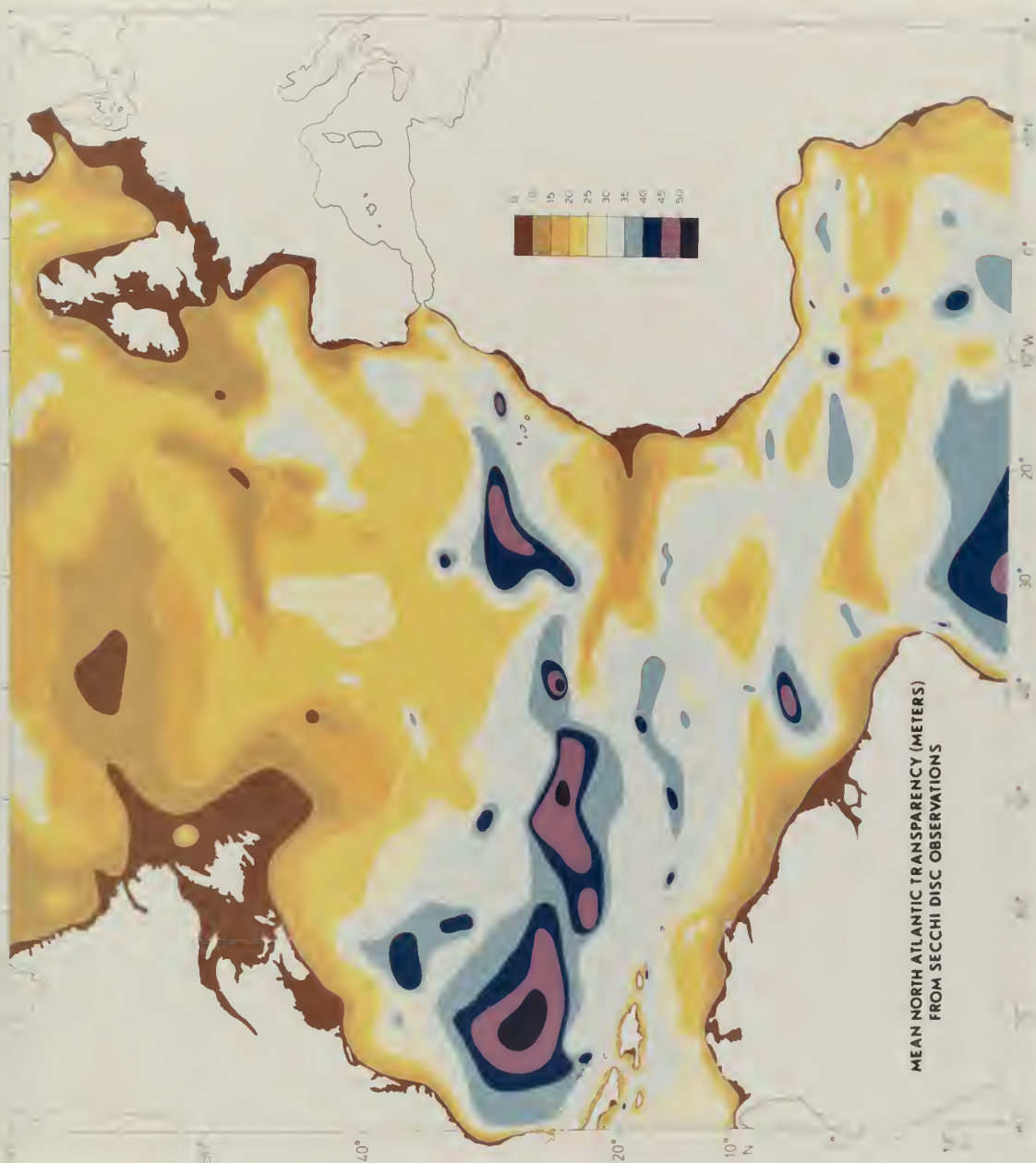
Marsden Squares 62 & 98

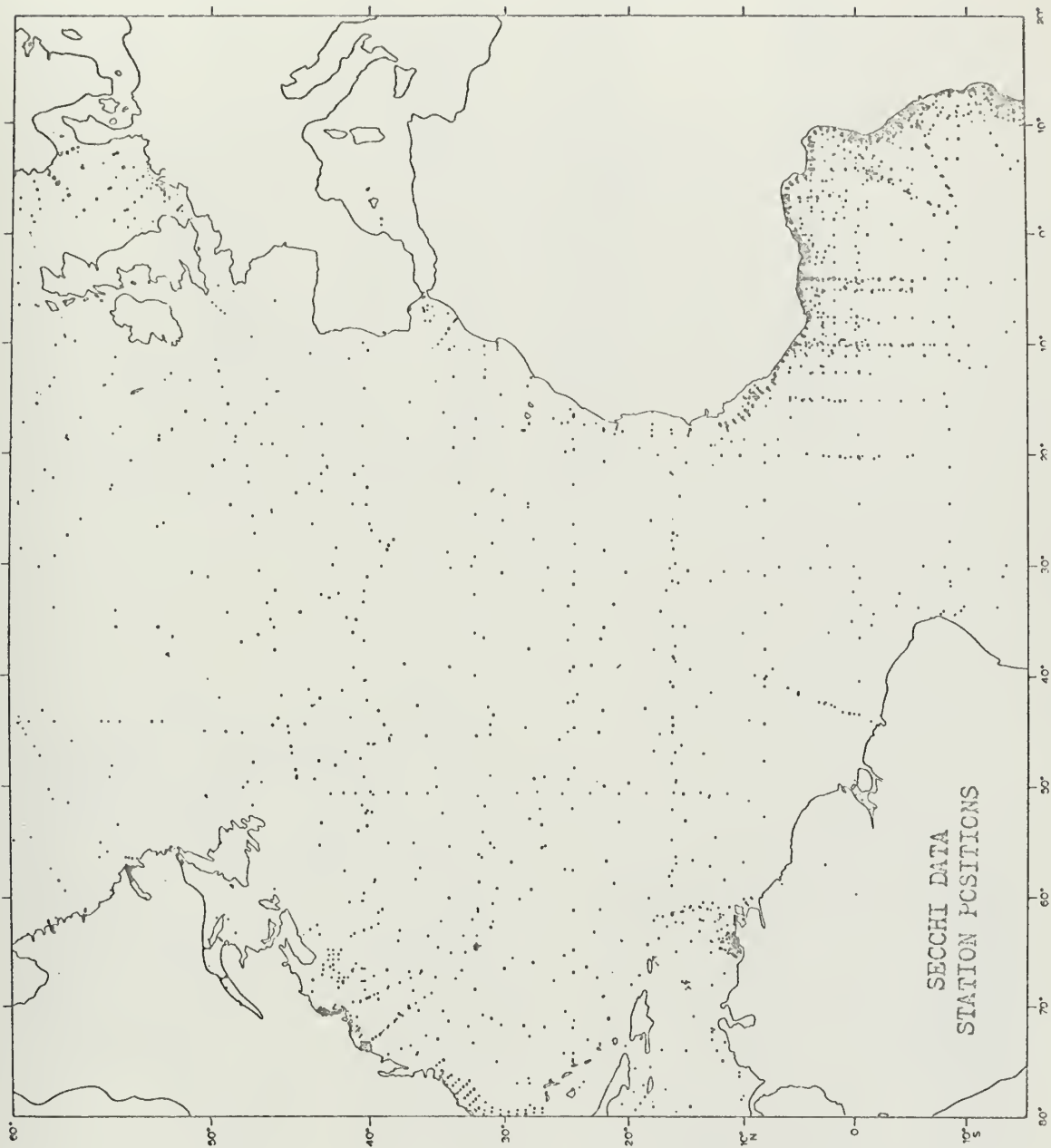
A map of East Asia and Southeast Asia. The word "CHINA" is written across the top. The number "98" is in the upper left, and "62" is in the lower left. The map shows the coastlines of China, Japan, and the Philippines.



APPENDIX A

The following chart gives the mean transparency for the North Atlantic Ocean. This chart was prepared by Dr. Robert R. Dickson of the Fisheries Laboratory, Suffolk, England and is an updated version of the chart presented in Reference 10. The NODC data for the North Atlantic, some Russian data from World Data Center B, Royal Navy/Royal Dutch Navy NAVADO Survey Data, and a limited amount of data from selected Royal Navy ships are included in this chart. Station positions for the Secchi disc data are shown on the next chart.





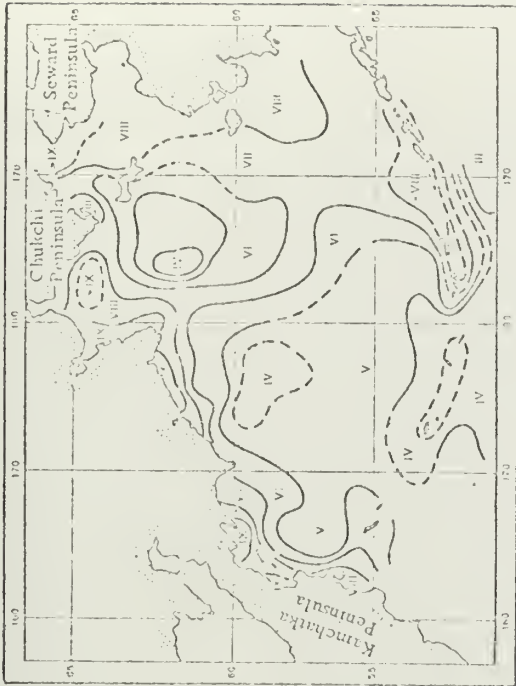


Fig. 1, b.

a) transparency of Bering Sea water (m) in the summer;
b) transparency in the summer by the standard color scale.

Transparency and color contours
from Arsen'yev and Voytov (2)

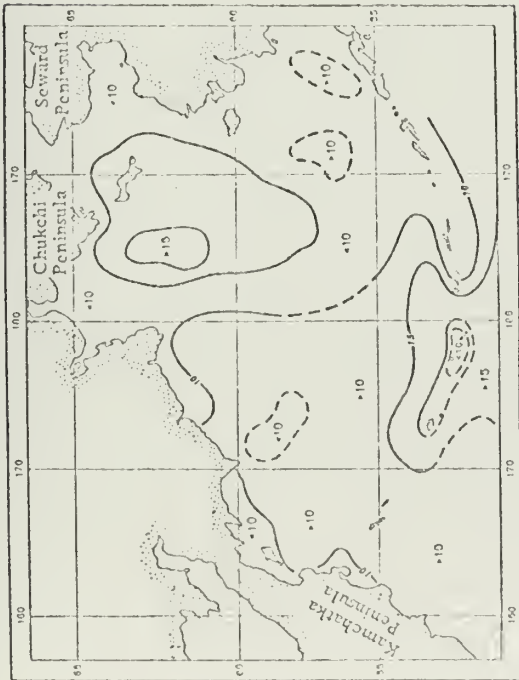


Fig. 1, a.

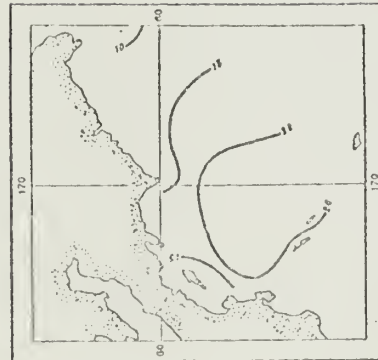
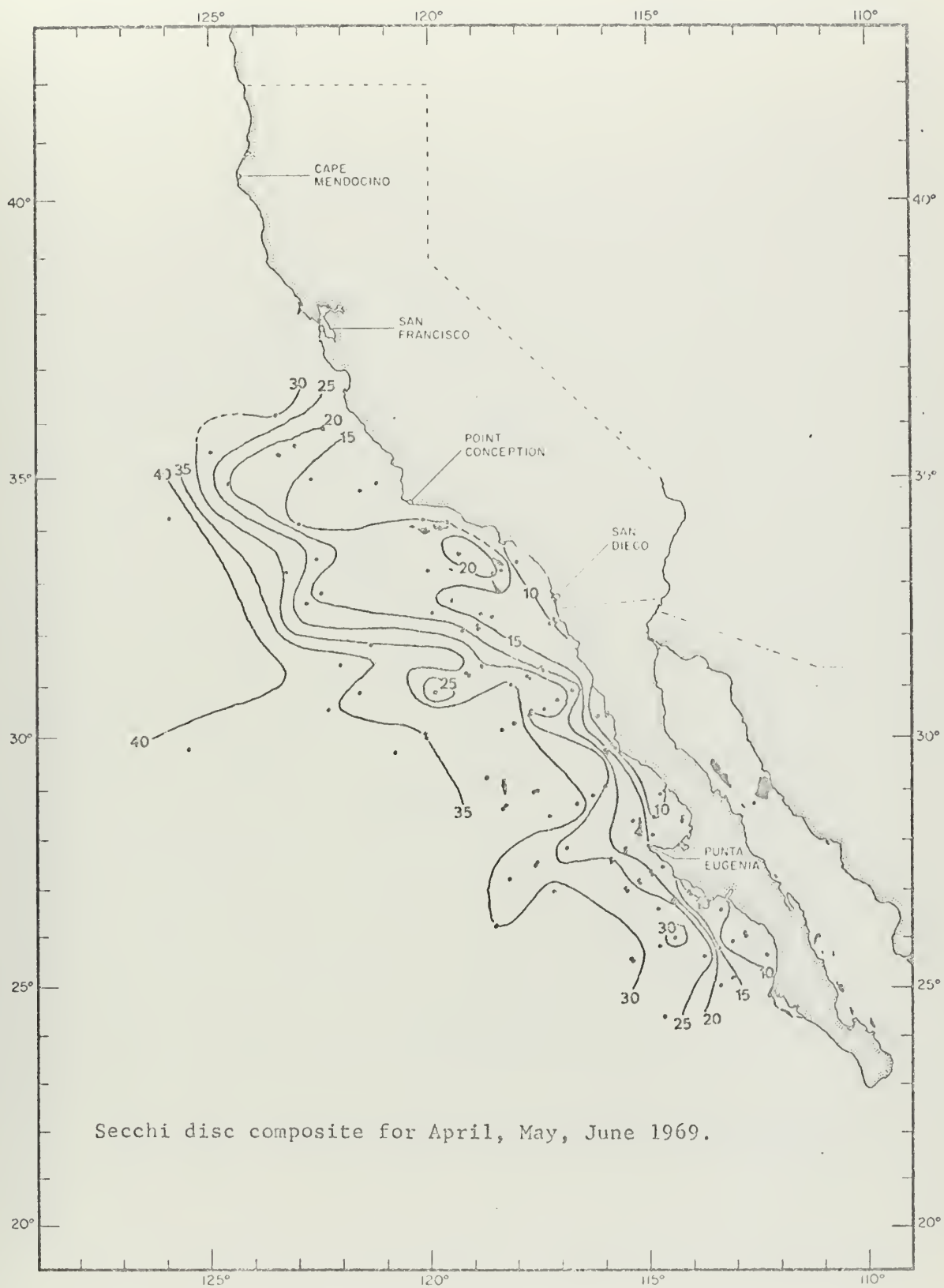


Fig. 2. Relative water transparency in the western part of the sea in the winter.

APPENDIX C

The following four charts were prepared by Robert Owen of the U. S. Bureau of Commercial Fisheries, La Jolla, California (CALCOFI). These charts are composite contours of data obtained during 1969 from CALCOFI cruises 6901, 6902, 6904-6912.





Secchi disc composite for April, May, June 1969.





Secchi disc composite for October, November, December 1969.

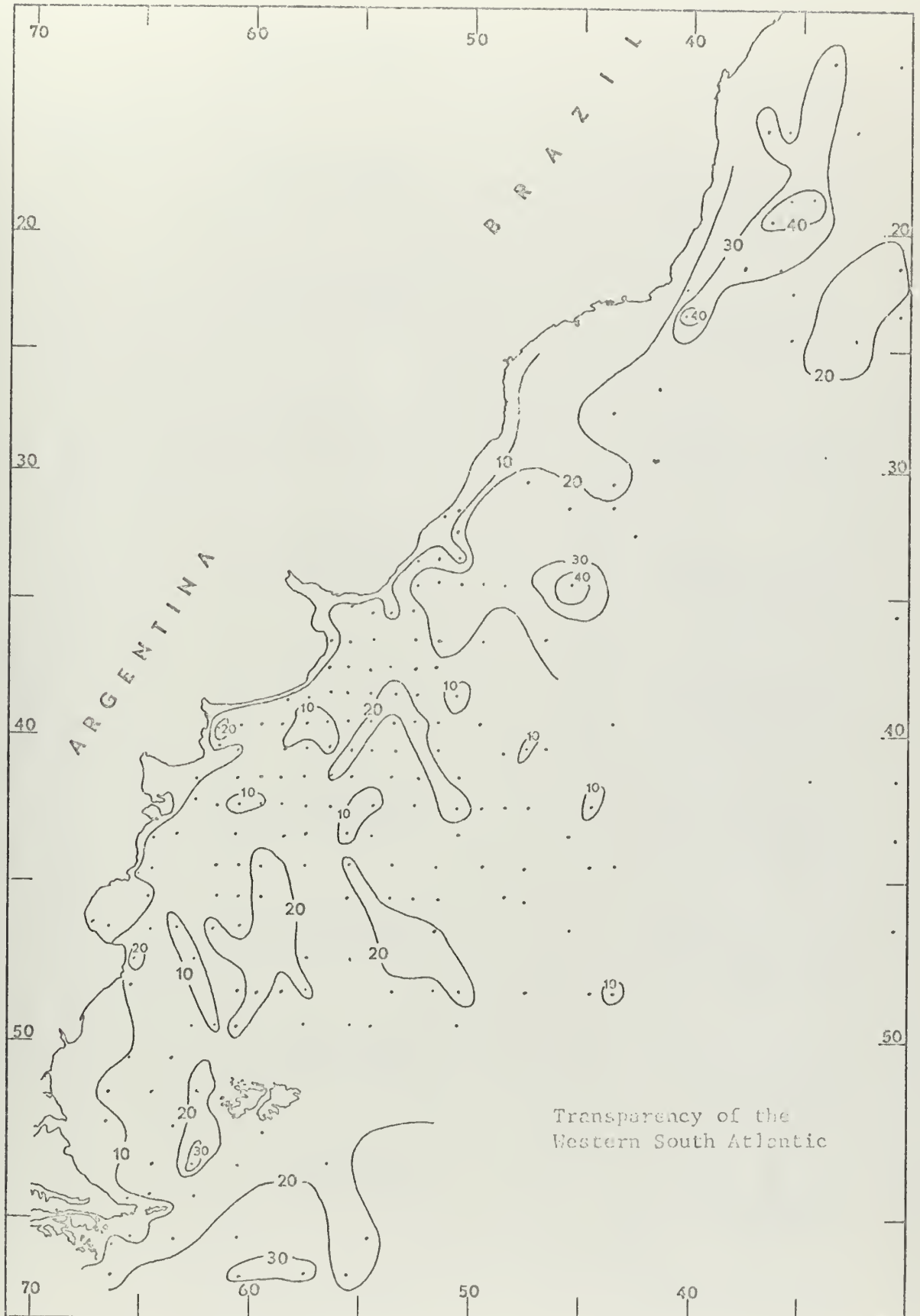


TABLE I

Vertical Extinction Coefficients and their Reciprocals Computed from Secchi Disc Depths

$$*K = \frac{1.7}{Z_s} (\text{m}^{-1})$$

$**Z_s$ (meters)	0	1	2	3	4	5	6	7	8	9
00		1.7	.85	.56	.425	.34	.283	.243	.2125	.189
10	.17	.155	.142	.131	.121	.113	.106	.100	.0944	.089
20	.0850	.0810	.0770	.0740	.0710	.068	.065	.063	.061	.059
30	.057	.055	.052	.050	.049	.049	.047	.046	.045	.044
40	.0425	.041	.040	.040	.039	.038	.037	.036	.035	.035
50	.034	.033	.033	.032	.031	.031	.030	.030	.029	.029
60	.028	.028	.027	.027	.027	.026	.026	.025	.025	.025

$$1/K = \frac{Z_s}{1.7} (\text{meters})$$

Z_s (meters)	0	1	2	3	4	5	6	7	8	9
00		.59	1.18	1.76	2.25	2.94	3.53	4.12	4.71	5.29
10	5.88	6.47	7.06	7.65	8.24	8.82	9.41	10.0	10.6	11.2
20	11.8	12.3	12.9	13.5	14.1	14.7	15.3	15.9	16.5	17.1
30	17.6	18.2	18.8	19.4	20.0	20.6	21.2	21.8	22.3	22.9
40	23.5	24.1	24.7	25.3	25.9	26.5	27.1	27.6	28.2	28.8
50	29.4	30.0	30.6	31.2	31.8	32.4	32.9	33.5	34.1	34.7
60	35.3	35.9	36.5	37.1	37.6	38.2	38.8	39.4	40.0	40.6

*K = vertical extinction coefficient

**Z_s = Secchi disc depth

TABLE II

Forel-Ule Color Scale, Proportions of Component Chemical Solutions
and Color Shades

NODC CODE	SCALE NUMBER	SOLUTION (PARTS)				COLOR
		YELLOW	BLUE	BROWN	GREEN	
01	I	0	100			Deep Blue
02	II	2	98			Blue
03	III	5	95			Greenish-Blue
04	IV	9	91			Bluish-Green
05	V	14	86			Green
06	VI	20	80			Light-Green
07	VII	27	73			Yellowish-Green
08	VIII	35	65			Yellow-Green
09	IX	44	56			Green-Yellow
10	X	54	46			Greenish-Yellow
11	XI	65	35			Yellow
11	XI			0	100	
12	XII			2	98	
13	XIII			5	95	
14	XIV			9	91	
15	XV			14	86	
16	XVI			20	80	
17	XVII			27	73	
18	XVIII			35	65	
19	XIX			44	56	
20	XX			54	46	
21	XXI			65	35	

TABLE III

SEA OF JAPAN -- MONTHLY MINIMA and MAXIMA

MONTH	MINIMUM TRANSPARENCY (METERS)	MAXIMUM TRANSPARENCY (METERS)	MINIMUM FOREL-ULE CODE	MAXIMUM FOREL-ULE CODE
January	9	20	3	6
February	7	33	2	5
March	7	29	3	5
April	8	17	3	6
May	3	19	2	6
June	8	22	2	6
July	10	27	2	4
August	10	30	1	5
September	11	31	2	6
October	9	30	2	5
November	8	30	3	5
December	9	22	3	5

PROGRAM COMPUTES THE AVERAGE VALUE OF THE TRANSPARENCY MEASUREMENTS AND FORCEL COLOR CODES REPORTED IN A ONE-DEGREE SUB-SQUARE OF A MARSDEN SQUARE. MEAN DEVIATION OF THESE MEASUREMENTS IS ALSO COMPUTED.

THE DATA USED IN THIS PROGRAM WAS PROVIDED BY THE NATIONAL OCEANOGRAPHIC DATA CENTER. THE DATA WAS RECORDED BY SUCCESSIVE MARSDEN SQUARES ON MAGNETIC TAPE.

THE FOLLOWING SECTIONS REFER TO MARSDEN SQUARE 200. THIS PROGRAM IS APPLICABLE TO ALL MARSDEN SQUARES HAVING DATA WITH NORTH LATITUDE AND EAST LONGITUDE COORDINATES. FOR DATA DESCRIBED BY A DIFFERENT SET OF SPATIAL COORDINATES, THE SECTION THAT CONSTRUCTS THE ONE-DEGREE GRID OF SUB-SQUARES MUST BE SLIGHTLY ALTERED: THE STATEMENT THAT LOCATES THE DATA POINT WITHIN A SUBSQUARE MUST ALSO BE ALTERED.

```
REAL*4      LWB, LN, LS, LE, LW
INTEGER*4    XD, XM, XTN, YD, YM, YTM, WC, TP
```

```
DIMENSION   LN(100), LS(100), LE(100), LW(100)
DIMENSION   NCMSS(100), SOMSS(100), NFMSS(100)
DIMENSION   DEVT(100), DEVF(100), ADEVT(100), ADEVF(100)
DIMENSION   WCMSS(100), SOD(100), WCC(100), MAR(2), SL(10)
```

```
DATA        LWB/159.0/, MAR/200, 201/
DATA        WCMSS/100.0, 0.0/, SOD/100.0, 0.0/, WCC/100.0, 0.0/
DATA        NCMSS/100.0, 0.0/, NFMSS/100.0, 0.0/, SOMSS/100.0, 0.0/
DATA        DEVT/100.0, 0.0/, DEVF/100.0, 0.0/, ADEVT/100.0, 0.0/
DATA        ADEVF/100.0, 0.0/
DATA        SL/50.0, 51.0, 52.0, 53.0, 54.0, 55.0, 56.0, 57.0, 58.0,
*59.0/
```

THE FOLLOWING SECTION COMPUTES THE ONE-DEGREE GRID OF SUB-SQUARES WITHIN THE GIVEN MARSDEN SQUARE. SL IS THE SOUTH LATITUDE BOUNDARY OF A SUB-SQUARE ROW. THE TERMS LS AND LN DEFINE THE SOUTH AND NORTH LATITUDE BOUNDARIES OF EACH SUB-SQUARE. THE TERMS LE AND LW DEFINE THE EAST AND WEST LONGITUDE BOUNDARIES. LWB IS THE LEFT LONGITUDE BOUNDARY OF THE MARSDEN SQUARE.

```
WRITE(6, 998)
998 FORMAT('1', 22X, 'MARSDEN SUB-SQUARE BOUNDARIES', /)
WRITE(6, 999)
999 FORMAT('0', 32X, 'LS', 8X, 'LN', 8X, 'LE', 8X, 'LW', /)
DO 1000 I=1, 10
  LS(I)=SL(1)
  LN(I)=LS(I)+1
  LW(I)=LWB+I
  LE(I)=LW(I)+1
1000 CONTINUE
DO 1001 I=11, 20
  LS(I)=SL(2)
  LN(I)=LS(I)+1
  LW(I)=LW(I-10)
  LE(I)=LW(I)+1
1001 CONTINUE
DO 1002 I=21, 30
  LS(I)=SL(3)
  LN(I)=LS(I)+1
  LW(I)=LW(I-20)
  LE(I)=LW(I)+1
1002 CONTINUE
DO 1003 I=31, 40
  LS(I)=SL(4)
  LN(I)=LS(I)+1
  LW(I)=LW(I-30)
  LE(I)=LW(I)+1
```



```

1003 CONTINUE
DO 1004 I=41,50
LS(I)=SL(5)
LN(I)=LS(I)+1
LW(I)=LW(I-40)
LF(I)=LW(I)+1
1004 CONTINUE
DO 1005 I=51,60
LS(I)=SL(6)
LN(I)=LS(I)+1
LW(I)=LW(I-50)
LF(I)=LW(I)+1
1005 CONTINUE
DO 1006 I=61,70
LS(I)=SL(7)
LN(I)=LS(I)+1
LW(I)=LW(I-60)
LF(I)=LW(I)+1
1006 CONTINUE
DO 1007 I=71,80
LS(I)=SL(8)
LN(I)=LS(I)+1
LW(I)=LW(I-70)
LF(I)=LW(I)+1
1007 CONTINUE
DO 1008 I=81,90
LS(I)=SL(9)
LN(I)=LS(I)+1
LW(I)=LW(I-80)
LF(I)=LW(I)+1
1008 CONTINUE
DO 1009 I=91,100
LS(I)=SL(10)
LN(I)=LS(I)+1
LW(I)=LW(I-90)
LF(I)=LW(I)+1
1009 CONTINUE
DO 1010 I=1,100
WRITE(4,1011) I,LS(I),LN(I),LF(I),LW(I)
1011 FORMAT(1H,25X,I3,F7.1,3F10.1)
1010 CONTINUE

```

THE FOLLOWING SECTION READS THE DATA RECORD, DETERMINES
THE APPLICABLE SUB-SQUARE AND SUMS ALL MEASURE-
MENTS REPORTED FOR ALL SUB-SQUARES WITHIN THE
GIVEN MARSDEN SQUARE.

REWIND 4

THE REWIND STATEMENT INSURES THAT WHEN THE TAPE IS
READ IT IS READ FROM THE BEGINNING OF THE LIST
OF DATA RECORDS.

```

10 READ(4,11,END=25) MS,NC
MS IS THE MARSDEN SQUARE NUMBER.
NC IS THE FIRST DIGIT OF THE CRUISE NUMBER, ALL CRUISE
NUMBERS BEGINNING WITH 8 WERE NON-PERTINENT AND
THE CRUISE DATA WAS NOT CONSIDERED.
11 FORMAT(15X,I3,53X,I1,8X)
IF(NC.EQ.8) GO TO 10
IF(MS.EQ.MAR(2)) GO TO 25
IF(MS.EQ.MAR(1)) GO TO 14
GO TO 10
14 BACKSPACE 4
READ(4,15) XD,XM,XTM,YD,YM,YTM,WC,TP
15 FORMAT(4X,I2,I2,I1,I3,I2,I1,26X,I2,I2,35X)

```

XD,XM,XTM,YD,YM,YTM ARE THE DEGREES, MINUTES, AND TENTHS
OF MINUTES OF THE LATITUDE AND LONGITUDE COORDI-
NATES RESPECTIVELY, NC IS THE FORCEL COLOR CODE
AND TP IS THE SECCHI DISC DEPTH IN METERS.


```

IF((YM, EQ, 0), AND, (YTM, EQ, 0)) YTM=YTM+1
IF((XM, EQ, 0), AND, (XTM, EQ, 0)) XTM=XTM+1
ALAT=FLOAT(XD)+(FLOAT(XI)+(FLOAT(XTM)*0.1))/60.0
ALON=FLOAT(YD)+(FLOAT(YM)+(FLOAT(YTM)*0.1))/60.0
DO 20 J=1,100
IF((ALON,GT,LW(J)), AND, (ALON,LT,LE(J)), AND, (ALAT,GT,LS
*(J)), AND, (ALAT,LT,LN(J))) GO TO 21
20 CONTINUE
21 IF((TP, EQ, 0) GO TO 22
SDMSS(J)=SDMSS(J)+FLOAT(TP)
NCMSS(J)=NCMSS(J)+1
22 IF((WC, EQ, 0) GO TO 10
WCMSS(J)=WCMSS(J)+FLOAT(WC)
NFMSS(J)=NFMSS(J)+1

```

WHERE, IN EACH MARSDEN SUB-SQUARE:
 NCMSS IS THE NUMBER OF TRANSPARENCY OBSERVATIONS,
 SDMSS IS THE TOTAL VALUE OF SECCHI DISC DEPTHS,
 WCMSS IS THE TOTAL VALUE OF FOREL COLOR CODES,
 NFMSS IS THE NUMBER OF FOREL COLOR OBSERVATIONS.

GO TO 10

THE FOLLOWING SECTION COMPUTES THE AVERAGE VALUE OF
 THE MEASUREMENTS IN EACH MARSDEN SUB-SQUARE.
 SDD AND WCC DEFINE THE AVERAGE VALUE OF TRANSPAR-
 ENCY AND FOREL COLOR RESPECTIVELY IN EACH SUB-
 SQUARE.

```

25 WRITE(6,45)
45 FORMAT('1')
WRITE(6,46) MAR(1)
46 FORMAT(1H, 25X, 'MARSDEN SQUARE', I4, //)
WRITE(6,47)
47 FORMAT(1H, 10X, 'MARSDEN', 4X, 'TRANSPARENCY', 2X, 'AVERAGE
  VALUE', 2X, 'FOREL COLOR', 2X, 'AVERAGE VALUE', /, 1H, 9X, '
  SUB-SQUARE', 2X, 'OBSERVATIONS', 3X, 'TRANSPARENCY', 3X, 'OB
  SERVATIONS', 3X, 'FOREL COLOR')
DO 50 I=1,100
IF(NCMSS(I), EQ, 0) GO TO 48
SDD(I)=SDMSS(I)/NCMSS(I)
48 IF(NFMSS(I), EQ, 0) GO TO 49
WCC(I)=WCMSS(I)/NFMSS(I)
49 WRITE(6,51) I, NCMSS(I), SDD(I), NFMSS(I), WCC(I)
51 FORMAT('0', 12X, I3, 8X, I5, 12X, F4.1, 10X, I5, 11X, F4.1)
50 CONTINUE

```

THE FOLLOWING SECTION COMPUTES THE AVERAGE DEVIATION
 OF THE REPORTED MEASUREMENTS IN EACH ONE-DEGREE
 SUB-SQUARE OF THE MARSDEN SQUARE.

THE VARIABLE NAMES DEVT, DEVF, ADEVT, ADEVF HAVE THE
 FOLLOWING DEFINITIONS:
 DEVT IS THE DEVIATION FROM THE MEAN OF THE
 INDIVIDUAL TRANSPARENCY MEASUREMENTS,
 DEVF IS THE DEVIATION FROM THE MEAN OF THE
 INDIVIDUAL FOREL COLOR CODES,
 ADEVT IS THE AVERAGE VALUE OF THE TRANSPAREN-
 CY DEVIATIONS IN EACH MARSDEN SUB-SQUARE,
 ADEVF IS THE AVERAGE VALUE OF THE FOREL COLOR
 CODE DEVIATIONS IN EACH SUB-SQUARE.

```

REWIND 4
100 READ(4,111,END=200) MS,NC
111 FORMAT(15X, I3, 53X, 11, 8X)
IF(NC, EQ, 8) GO TO 100
IF(MS, EQ, MAR(2)) GO TO 200
IF(MS, EQ, MAR(1)) GO TO 114
GO TO 100
114 BACKSPACE 4
READ(4,115) XD, XM, XTM, YD, YM, YTM, WC, TP

```



```

115 FORMAT(4X,I2,I2,I1,I2,I2,I1,2X,I2,I2,35X)
    IF((XM.EQ.0).AND.(XTM.EQ.0)) XTM=XTM+1
    IF((YM.EQ.0).AND.(YTM.EQ.0)) YTM=YTM+1
    ALAT=FLOAT(XD)+(FLOAT(XM)+(FLOAT(XTM)*.0.1))/60.0
    ALON=FLOAT(YD)+(FLOAT(YM)+(FLOAT(YTM)*.0.1))/60.0
    DO 60 J=1,100
    IF((ALON.GT.LW(J)).AND.(ALON.LT.LE(J)).AND.(ALAT.GT.LS
    Y(J)).AND.(ALAT.LT.LN(J))) GO TO 121
60 CONTINUE
121 IF(TP.EQ.0) GO TO 125
    DEVT(J)=DEVT(J)+ABS(SDD(J)-FLOAT(TP))
125 IF(WC.EQ.0) GO TO 100
    DEVF(J)=DEVF(J)+ABS(WCC(J)-FLOAT(WC))
    GO TO 100
200 WRITE(6,205)
205 FORMAT('1')
    WRITE(6,206) MAR(1)
206 FORMAT(1H,42X,'MARSDEN SQUARE',I4, '/')
    WRITE(6,207)
207 FORMAT(1H,10X,'MARSDEN',4X,'TRANSPARENCY',2X,'AVERAGE'
    *,2X,'VALUE',2X,'AVERAGE',1X,'VALUE',2X,'FOREL',3X,'COL
    *OR',2X,'AVERAGE',1X,'VALUE',2X,'AVERAGE',1X,'VALUE',/,
    *,1H,9X,'SUB-SQUARE',2X,'OBSERVATIONS',3X,'TRANSPARENCY'
    *,5X,'DEVIATION',4X,'OBSERVATIONS',3X,'FOREL',1X,'COLOR'
    *,5X,'DEVIATION')
    DO 225 I=1,100
    IF(NOMSS(I).EQ.0) GO TO 208
    ADEVT(I)=DEVT(I)/NOMSS(I)
208 IF(NEMSS(I).EQ.0) GO TO 209
    ADEVF(I)=DEVF(I)/NEMSS(I)
209 WRITE(6,210) I,NOMSS(I),SDD(I),ADEVT(I),NEMSS(I),
    WCC(I),ADEVF(I)
210 FORMAT('C',12X,I3,9X,I4,12X,F4.1,11X,F4.1,10X,I4,12X,
    F3.1,11X,F4.1)
225 CONTINUE
    REWIND 4
    STOP
    END

```


BIBLIOGRAPHY

1. American Geographical Society. Serial Atlas of the Marine Environment, Folios 1-19, 1953 to 1970.
2. Arsen'yev, V., and Voytov, V., "Relative Transparency and Color of Bering Sea Water," Oceanology, 8(1), 41-43, 1968.
3. Aruga, Y. and Monsi, M., "Primary Production in the Northwestern Part of the Pacific off Honshu, Japan," Journal of the Oceanographical Society of Japan, 18(2), 37-46, 1962.
4. Bogorov, B. G., "Biogeographical Region of the Plankton of the North-Western Pacific Ocean and their Influence on the Deep Sea," Deep Sea Research, 5(2), 149-161, 1958.
5. Bogorov, V. G. and Bass, T. S., "Fish Distribution as Related to the Location of Productive Areas of Plankton in the Indian Ocean," Oceanology, 6(6), 847-849, 1966.
6. Bumpus, D. F. and Clarke, A. H., Hydrography of the Western Atlantic: Transparency of the Coastal and Oceanic Waters of the Western Atlantic, Woods Hole Oceanographic Institution Technical Report 10, 1947.
7. Clarke, G. L. and Russell, H. D., The Transparency and Color of Ocean Waters with Special Reference to the W. Pacific, Woods Hole Oceanographic Institution (unpublished report), 1944.
8. Cialdi, A. and Secchi, P. A., "On the Transparency of the Sea," Translation by Professor Albert Collier, Limnology and Oceanography, 13, 391-394, 1968.
9. Curl, H. Jr., "Primary Production Measurements in the North Coastal Waters of South America," Deep Sea Research, 7(2), 183-189, 1960.
10. Dickson, R. R., On the Relationship between Ocean Transparency and the Depth of Sonic Scattering Layers in the North Atlantic, paper presented to the International Council for Exploration of the Sea, C.M. 1969/C:7 Hydrographic Committee, 1969.
11. Dietrich, G., General Oceanography, p. 475-549, Interscience Publishers, New York, 1963.
12. El-Sayed, S. Z., "On the Productivity of the Southwest Atlantic Ocean and the Waters West of the Antarctic Peninsula," Biology of the Antarctic Sea III, ed. by G. A. Llano and W. L. Schmitt, Antarctic Research Series, 11, 15-47, Horn-Shafer Company, Baltimore, 1967.
13. El-Sayed, S. Z., and Mandelli, E. F., "Primary Production and Standing Crop of Phytoplankton in the Weddell Sea and Drake Passage," Biology of the Antarctic Sea II, ed. by G. A. Llano, Antarctic Research Series, 5, 87-106, Garamond/Pridemark Press Inc., Baltimore, 1965.

14. Emery, K. O., "Transparency of Water off Southern California," Transactions of the American Geophysical Union, 35(2), 217-220, 1954.
15. Fairbridge, R. W., editor, The Encyclopedia of Oceanography, v. 1, Reinhold Publishing Corporation, New York, 1021 p., 1966.
16. Forel, F. A., "Couleur de l'Eau," Abstract from La Lemane (Vol. II), Lausanne, 462-487, 1895, (Translation by Jean Dutto, George Washington University, Washington, D. C.)
17. Graham, J. J., "Secchi Disc Observations and Extinction Coefficients in the Central and Eastern North Pacific Ocean," Limnology and Oceanography, 11(2), 184-190, 1966.
18. Hart, T. J., "Notes on the Relation between Transparency and Plankton Content of the Surface Water of the Southern Ocean," Deep Sea Research, 9, 109-114, 1962.
19. Holmes, R. W., "The Secchi Disc in Turbid Coastal Waters," preprint of article accepted for publication in Limnology and Oceanography.
20. Jerlov, N. G., "Optical Studies of Ocean Waters," Reports of the Swedish Deep-Sea Expedition 1947-1948, ed. by H. Pettersson, Vol. III, 1-61, Elanders Boktryckeri Aktiebolag, Sweden, 1951.
21. Jerlov, N. G., "Factors Influencing the Colour of the Oceans," Studies on Oceanography, ed. by Y. Kozo, 260-264, University of Washington Press, 1965.
22. Jerlov, N. G., Optical Oceanography, Elsevier, Amsterdam, London, New York, 194 p., 1968.
23. Joseph J., "Meeresoptik," Landolt-Bornstein Zahlenwerte und Functionen Aus Physik, Chemie, Astronomie, Geophysik und Technik, ed. by A. Eucken, Vol. III, 441-459, Springer-Verlag, Berlin, Göttingen, Heidelberg, 1952.
24. Kalle, K., "Zum Problem der Meereswasserfarbe," Ann.d.Hydrogr. und Mar. Meteor., 66, 1-13, 1938.
25. Kharchenko, A. M., "Currents and Water Masses in the East China Sea," Oceanology, 8(1), 28-36, 1968.
26. Lepley, L. K. "Coastal Water Clarity from Space Photographs," Photogrammetric Engineering, 34(7), 667-674, 1968.
27. Markerov, J. V., editor, Atlas of Temperature, Salinity and Density of Water in the Pacific Ocean, Publishing House of the Academy of Sciences of the USSR, Moscow, 119 p., 1963.
28. Manheim, F. T. and Meade, R. H., "Suspended Matter in Surface Waters of the Atlantic Continental Margin from Cape Code to the Florida Keys," Science, 167(3917), 371-376, 1970.

29. Murphy, C. I., "Effect of Water Clarity on Albacore Catches," Limnology and Oceanography, 4(1), 86-93, 1959.
30. Otto, L., "Light Attenuation in the North Sea and the Dutch Wadden Sea," Netherlands Journal of Sea Research, 3(1), 28-51, 1966.
31. Poole, H. H. and Atkins, W. R. G., "Photoelectric Measurement of Submarine Illumination throughout the Year," Journal of the Marine Biological Association of the United Kingdom, 16, 297-324, 1929.
32. Postma, H., "Suspended Matter and Secchi Disc Visibility in Coastal Waters," Netherlands Journal of Sea Research, 1(3), 359-390, 1961.
33. Redfield, A. C., Ketchum, B. H. and Richards, F. A., "The Influence of Organisms on the Composition of Sea Water," The Sea, ed. by M. N. Hill, 2, 26-77, Interscience Publishers, New York, 1963.
34. Russell, H. D. and Clarke, G. L., The Transparency of East Indian Waters and Adjacent Area, Woods Hole Oceanographic Institution Report 2, 1944.
35. Russell, H. D. and Clarke, G. L., Transparency of Icelandic, North and Central American, West Indian, Hawaiian Territory and Fiji Island Waters, Woods Hole Oceanographic Institution Report 3, 1944.
36. Ryther, J. H. and Yentsch C. S., "The Estimation of Phytoplankton Production in the Ocean from Chlorophyll and Light Data," Limnology and Oceanography, 2(3), 281-286, 1957.
37. Ryther, J. H., Hall, J. R., Pease, A. K., Bakum, A. and Jones, M. M., "Primary Organic Production in Relation to the Chemistry and Hydrography of the Western Indian Ocean," Limnology and Oceanography, 11(3), 371-380, 1966.
38. Schott, G., Geographie des Atlantischen Oceans, Verlag von C. Boysen, Hamburg, 3rd edition, 1942.
39. Shoulejkin, W., "On the Color of the Sea," Physical Review, 22(1), 85-100, 1923.
40. Sower, L. A., The Forel Scale and its Modifications, U. S. Navy Hydrographic Office Informal Oceanographic Manuscripts No. 35-60, Unpublished Manuscript, 1960.
41. Tyler, J. E., "Colour of the Sea," Nature, 202(4939), 1262-1264, 1964.
42. Tyler, J. E., "The Secchi Disc," Limnology and Oceanography, 13(1), 1-6, 1968.

43. Uda, M., "Hydrographical Studies based on Simultaneous Oceanographical Surveys Made in the Japan Sea," Records of Oceanographical Works of Japan, 6, 19-107, 1934.
44. Uda, M., "Oceanography of the Subarctic Pacific Ocean," Journal of the Fisheries Research Board of Canada, 20(1), 119-179, 1963.
45. Ule, W., "Determination of Water Color in the Sea," Petermanns Mitteilungen aus Justus Perthus Geographischer Anstalt, v. 38, 70-71, Gotha, 1892.
46. U. S. Navy Hydrographic Office Publication No. 705, Oceanographic Atlas of the Polar Seas, Part II, Arctic, 1958.
47. U. S. Navy Hydrographic Office Publication No. 752, Marine Geography of Korean Waters, 8-9, 1951.
48. U. S. Navy Hydrographic Office Publication No. 754, Marine Geography of Indochinese Waters, p. 36, 1951.
49. U. S. Navy Hydrographic Office Publication No. 757, Marine Geography of the Sea of Japan, 48-50, 1951.
50. U. S. Navy Hydrographic Office Study No. 27, Transparency of the Water off Japan, 1943.
51. U. S. Navy Hydrographic Office Chart H. O. Misc 15222, Transparency Chart of the North Atlantic Ocean.
52. Visser, M. P., "Secchi Disc and Sea Colour Observations in the North Atlantic Ocean during the Navado III Cruise, 1964-1965, Aboard H. Neth. M.S. 'Snellius' (Royal Netherlands Navy)," Netherlands Journal of Sea Research, 3(4), 553-563, 1967.
53. Wyrski, K., "The Upwelling in the Region Between Java and Australia during the South-East Monsoon," Australia Journal of Marine and Freshwater Research, 13(3), 217-225, 1962.
54. Zenkevitch, L., Biology of the Seas of the U.S.S.R., Translated by S. Botcharskaya, Interscience Publishers, New York, 955 p., 1963.
55. Voytov, V. I., and M. G. Dement'yeva, Oceanology (Acad. Sci. USSR) 10(1), 35-37, 1970. (English trans.).

INITIAL DISTRIBUTION LIST

	No. Copies
1. Defense Documentation Center Cameron Station Alexandria, Virginia 22314	2
2. Library, Code 0212 Naval Postgraduate School Monterey, California 93940	2
3. Department of Oceanography Naval Postgraduate School Monterey, California 93940	3
4. Naval Weather Service Command Washington Navy Yard Washington, D. C. 20390	1
5. Officer in Charge Fleet Numerical Weather Facility Naval Postgraduate School Monterey, California 93940	1
6. Commanding Officer and Director Naval Undersea Research & Development Center Attn: Code 2230 San Diego, California 92152	1
7. Director, Naval Research Laboratory Attn: Tech. Services Info. Officer Washington, D. C. 20390	1
8. Office of Naval Research Department of the Navy Washington, D. C. 20360	1
9. Commander, Air Weather Service Military Airlift Command U. S. Air Force Scott Air Force Base, Illinois 62226	2
10. Department of Commerce, ESSA Weather Bureau Washington, D. C. 20235	2
11. Oceanographer of the Navy The Madison Building 732 N. Washington Street Alexandria, Virginia 22314	1

12. Naval Oceanographic Office 1
Attn: Library
Washington, D. C. 20390
13. National Oceanographic Data Center 1
Washington, D. C. 20390
14. Mission Bay Research Foundation 1
7730 Herschel Avenue
La Jolla, California 92038
15. Director, Maury Center for Ocean Sciences 1
Naval Research Laboratory
Washington, D. C. 20390
16. Mr. Roswell W. Austin 1
Visibility Laboratory
Scripps Institution of Oceanography
La Jolla, California 92037
17. Mr. Thomas E. Bailey 1
Central Coastal Regional Water Quality Control Board
1108 Garden Street
San Luis Obispo, California 93401
18. Dr. George F. Beardsley 2
Department of Oceanography
Oregon State University
Corvallis, Oregon 97331
19. Dr. Wayne V. Burt 1
Department of Oceanography
Oregon State University
Corvallis, Oregon 97331
20. Dr. Peyton Cunningham 6
Department of Physics
Naval Postgraduate School
Monterey, California 93940
21. Dr. Seibert Q. Duntley 1
Visibility Laboratory
Scripps Institution of Oceanography
La Jolla, California 92037
22. Mr. George Eck 1
Naval Air Development Center
Johnsville, Warminster, Pennsylvania 18974
23. Mr. Gary Gilbert 1
Stanford Research Institute
Menlo Park, California

24. Dr. Eugene C. Haderlie 1
 Department of Oceanography
 Naval Postgraduate School
 Monterey, California 93940

25. Dr. R. C. Honey 1
 Stanford Research Institute
 Menlo Park, California

26. Professor Alexandre Ivanoff 1
 Laboratoire d'Océanographie Physique
 de la Faculté des Sciences de Paris
 9, Quai Saint-Bernard
 Paris (V^e), France

27. Dr. N. G. Jerlov 1
 Institute for Physical Oceanography
 Solvgade 83K
 Copenhagen, K, Denmark

28. Mr. Kenneth V. Mackenzie 1
 Ocean Sciences Department Code D503
 Naval Undersea Research & Development Center
 San Diego Division
 San Diego, California 92152

29. Dr. Robert E. Morrison 1
 AEL
 Office of Environmental Systems
 ESSA
 6010 Executive Blvd.,
 Rockville, Maryland 20852

30. Mr. Jerry Norton 1
 Oceanography Department
 Naval Postgraduate School
 Monterey, California 93940

31. Mr. Larry Ott 6
 Naval Air Development Center
 Johnsville, Warminster, Pennsylvania 18974

32. Mr. Robert Owen 3
 U. S. Bureau of Commercial Fisheries
 La Jolla, California

33. Dr. John H. Phillips 2
 Hopkins Marine Station
 Pacific Grove, California 93950

34. Mr. James Reese 1
 Ocean Sciences Department - Code D503
 Naval Undersea Research & Development Center
 San Diego Division
 San Diego, California 92152

35. Mr. Thomas J. Shopple 1
Naval Air Development Center
Johnsville, Warminster, Pennsylvania 13974

36. Dr. Warren Thompson 1
Department of Oceanography
Naval Postgraduate School
Monterey, California 93940

37. Mr. S. P. Tucker 6
Department of Oceanography
Naval Postgraduate School
Monterey, California 93940

38. Mr. John E. Tyler 1
Visibility Laboratory
Scripps Institution of Oceanography
La Jolla, California 92037.

39. Mr. Lowell Van Billiard 1
Naval Ships Engineering Center
Prince Georges Center
Hyattsville, Maryland 20782

40. LCDR Lanny A. Yeske 1
USS BAYA
% FPO San Francisco 96601

41. Dr. Paul Titterton 1
Sylvania Electronic Systems - Western Division
P.O. Box 188
Mountain View, California 94040

42. Mr. Alan Baldridge, Librarian 1
Hopkins Marine Station
Pacific Grove, California 93950

43. Mr. Ted Petzold 1
Visibility Laboratory
Scripps Institution of Oceanography
La Jolla, California 92037

44. Director, Moss Landing Marine Laboratories 1
Moss Landing, California 95039

45. Mrs. Elsie F. DuPre 1
Oceanography Branch, Optical Sciences Division
Naval Research Laboratory
Washington, D. C. 20390

46. Dr. Rudolph W. Preisendorfer 1
Department of Mathematics
Naval Postgraduate School
Monterey, California 93940

47. Mr. W. J. Stachnik 1
Optical Systems
U. S. Navy Underwater Sound Laboratory
Fort Trumbull
New London, Connecticut 06320
48. Mr. Raymond N. Vranicar 2
Code AIR-370D
Naval Air Systems Command
Washington, D. C. 20360
49. Mr. Irvin H. Gatzke 2
Code AIR-370
Naval Air Systems Command
Washington, D. C. 20360
50. Dr. H. R. Gordon 1
Institute of Marine Sciences
University of Miami
10 Rickenbacher Causeway
Miami, Florida 33149
51. Dr. Robert W. Holmes 2
Marine Science Institute
University of California
Santa Barbara, California 93106
52. Dr. Robert Andrews 2
Department of Oceanography, Code 58Ad
Naval Postgraduate School
Monterey, California 93940
53. Professor Glenn H. Jung, Code 58Jg 1
Department of Oceanography
Naval Postgraduate School
Monterey, California 93940
54. Mr. Clarence Gilliam 1
Naval Ammunition Depot
Crane, Indiana 47522
55. LT Margaret Anne Frederick, USN 4
Fleet Numerical Weather Central
Monterey, California 93940
56. Dr. R. R. Dickson 2
Ministry of Agriculture, Fisheries & Food
Fisheries Laboratory
Lowestoft
Suffolk, England
57. Dr. M. P. Visser 1
Royal Netherlands Meteorological Institute
De Bilt, Netherlands

58. Mr. Henry Odum 3
Oceanographers Services Branch
National Oceanographic Data Center
Washington, D. C. 20390
59. Dr. T. Laevastu 1
Fleet Numerical Weather Facility
Monterey, California 93940
60. LCDR R. J. Wilson, USN 1
Box 31
FPO New York 09540
61. Mr. Charles J. Robinove 1
Associate Program Manager, EROS
U. S. Department of the Interior
Geological Survey
Washington, D. C. 20242
62. Dr. Klaus Wyrski 1
Department of Oceanography
University of Hawaii
Honolulu, Hawaii 96822
63. Mr. Sargun Tont 1
T-28
Scripps Institution of Oceanography
La Jolla, California 92037
64. Mr. Walter B. Fowler 1
Code 625
National Aeronautics & Space Administration
Goddard Space Flight Center
Greenbelt, Maryland 20771

DOCUMENT CONTROL DATA - R & D

Security classification of title, body of abstract and indexing annotation must be entered when the overall report is classified

1. ORIGINATING ACTIVITY (Corporate author)

Naval Postgraduate School
Monterey, California 93940

2a. REPORT SECURITY CLASSIFICATION

Unclassified

2b. GROUP

3. REPORT TITLE

An Atlas of Secchi Disc Transparency Measurements and Forel-Ule Color Codes for
the Oceans of the World

4. DESCRIPTIVE NOTES (Type of report and, inclusive dates)

Master's Thesis; September 1970

5. AUTHOR(S) (First name, middle initial, last name)

Margaret Anne Frederick

6. REPORT DATE

September 1970

7a. TOTAL NO. OF PAGES

177

7b. NO. OF REFS

54

8a. CONTRACT OR GRANT NO.

b. PROJECT NO

c.

d.

9a. ORIGINATOR'S REPORT NUMBER(S)

9b. OTHER REPORT NO(S) (Any other numbers that may be assigned
this report)

10. DISTRIBUTION STATEMENT

This document has been approved for public release and sale; its distribution is
unlimited.

11. SUPPLEMENTARY NOTES

12. SPONSORING MILITARY ACTIVITY

Naval Postgraduate School
Monterey, California 93940

13. ABSTRACT

An investigation was made of the global distribution of Secchi disc water transparency measurements and Forel-Ule water color codes which were on file at the National Oceanographic Data Center prior to June 1969. Charts were constructed for 17 major areas of the world's oceans to show the horizontal distributions of transparency and/or color. Data generally were presented as mean distributions. Charts were prepared showing the overall mean transparency and Forel-Ule color distribution for all of the data considered, except for the Sea of Japan, for which monthly mean charts were constructed. Plots of transparency measurements against the corresponding color codes were also drawn for five selected areas.

Transparency showed marked variations in each area considered. Generally it is greater in the central basins and decreases in coastal regions. Reduced transparency readings and discolored waters were noted for areas affected by river runoff, for areas of high organic productivity, and where standing plankton crops were found. Seasonal variations in transparency and color were not noted except for the Sea of Japan and the Indian Ocean (winter and summer). No simple relation between transparency and color was apparent.

14 KEY WORDS	LINK A		LINK B		LINK C	
	ROLE	WT	ROLE	WT	ROLE	WT
Transparency						
Sea Water Transparency						
Sea Water Color						
Forel Color						
Forel-Ule Color						
Secchi Disc Transparency Distribution						
Forel-Ule Color Distribution						
Secchi Depths						
Ocean Transparency						
Ocean Color						
Atlas of Ocean Transparency						
Atlas of Ocean Color						
Transparency and Color of the World's Ocean						
Hydrological Optics						
Optical Properties of Sea Water						

DUDLEY KNOX LIBRARY
NAVAL POSTGRADUATE SCHOOL
MONTEREY, CA 93943

DUDLEY KNOX LIBRARY
NAVAL POSTGRADUATE SCHOOL
MONTEREY, CALIFORNIA 93943

Thesis 124644
F7871 Frederick
c.1 An atlas of Secchi
disc transparency
measurements and Forel-
Ule color codes for
the oceans of the
world.

15 FEB 74 22464
10 MAR 74 22464
10 JUL 79 22670
10 JUL 79 S10712
28 OCT 80 7966
26849

Thesis 124644
F7871 Frederick
c.1 An atlas of Secchi
disc transparency
measurements and Forel-
Ule color codes for
the oceans of the
world.

thesF7871

An atlas of Secchi disc transparency mea



3 2768 001 95999 2

DUDLEY KNOX LIBRARY